Universidad de Concepción
Dirección de Postgrado
Facultad de Ciencias Físicas y Matemáticas
Programa de Doctorado en Ciencias Aplicadas
con Mención en Ingeniería Matemática

SPATIO-TEMPORAL DYNAMICS OF SELECTED MULTISPECIES SYSTEMS: MULTICLASS TRAFFIC AND PREDATOR-PREY-TAXIS MODELS

Tesis para optar al grado de Doctor en Ciencias
Aplicadas con mención en Ingeniería Matemática

Rafael Enrique Ordoñez Cardales

concepción-chile
2020

Profesor Guía: Dr. Raimund Bürger
CI^{2}MA y Departamento de Ingeniería Matemática
Universidad de Concepción, Chile

Cotutor: Dr. Luis Miguel Villada Osorio
GIMNAP–DMAT Universidad del Bío-Bío
y CI^{2}MA Universidad de Concepción, Chile

Cotutor: Dr. Christophe Chalons
Laboratoire de Mathématiques de Versailles
Université Versailles Saint-Quentin-en-Yvelines, Versailles, France

Spatio-temporal dynamics of selected multispecies systems: multiclass traffic and predator-prey-taxis models

Rafael Enrique Ordoñez Cardales

Directores de Tesis: Raimund Bürger, Universidad de Concepción, Chile.
Luis Miguel Villada, Universidad del Bío-Bío, Chile.
Christophe Chalons, Université Versailles Saint-Quentin-en-Yvelines, Versailles, France.

Director de Programa: Raimund Bürger, Universidad de Concepción, Chile.

Comisión evaluadora

Prof.

Prof.

Prof.

Prof.

Comisión examinadora

Firma: _____
Prof. Raimund Bürger, Universidad de Concepción, Chile.

Firma: _____
Prof.

Firma: _____
Prof.

Firma: _____
Prof. Luis Miguel Villada, Universidad del Bío-Bío, Chile.

Calificación: _____

Concepción,

Abstract

This thesis deals with the mathematical and numerical analysis of two models that describe the behavior of multiple species from partial differential equations. In particular, a system of conservation laws with a discontinuous flow function and a reaction-diffusion system coupled with elliptic equations are considered, modeling traffic flow problems that distinguish between free-congested flow and the dynamics of populations that interact with chemotaxis. The main contents of this thesis is structured as follows:

In **Chapter** 1, we construct a numerical scheme that is similar to the one proposed by [J.D. Towers, A splitting algorithm for LWR traffic models with flux discontinuities in the unknown, *J. Comput. Phys.*, **421** (2020), article 109722], by decomposing the discontinuous velocity function into a Lipschitz continuous function plus a Heaviside function and designing a corresponding splitting scheme. The part of the scheme related to the discontinuous flux is handled by a semi-implicit step that does, however, not involve the solution of systems of linear or nonlinear equations. It is proved that the whole scheme converges to a weak solution in the scalar case. The scheme can in a straightforward manner be extended to the multiclass LWR (MCLWR) model, which is defined by a hyperbolic system of N conservation laws for N driver classes that are distinguished by their preferential velocities. It is shown that the multiclass scheme satisfies an invariant region principle, that is, all densities are nonnegative and their sum does not exceed a maximum value. In the scalar and multiclass cases no flux regularization or Riemann solver is involved, and the CFL condition is not more restrictive than for an explicit scheme for the continuous part of the flux. Numerical tests for the scalar and multiclass cases are presented.

In **Chapter** 2, we formulate a reaction-diffusion system to describe three interacting species within the Hastings-Powell (HP) food chain structure with chemotaxis produced by three chemicals. We construct a finite volume (FV) scheme for this system, and in combination with the non-negativity and a priori estimates for the discrete solution, the existence of a discrete solution of the FV scheme is proved. It is shown that the scheme converges to the corresponding weak solution of the model. The convergence proof uses two ingredients of interest for various applications, namely the discrete Sobolev embedding inequalities with general boundary conditions and a space-time L^1 compactness argument. Finally, numerical tests illustrate the model and the behavior of the FV scheme.

In **Chapter** 3, we consider a mathematical model for the spatio-temporal evolution of three biological species in a food chain model consisting of two competitive preys and one predator with intra-specific competition. The species move toward higher concentrations of a chemical substance which is produced by themselves. The resulting reaction-diffusion system consists of three parabolic equations along with three elliptic equations describing the behavior of the chemical substance. First, the local existence of nonnegative solutions is proved, then we provide uniform estimates in Lebesgue spaces which lead to boundedness and the global well-posedness for the system. Finally we report and discuss some numerical simulation.

Resumen

Esta tesis trata del análisis matemático y numérico de dos modelos que describen el comportamiento de múltiples especies a partir de ecuaciones diferenciales parciales. En particular, se considera un sistema de leyes de conservación con función de flujo discontinuo y un sistema de reacción-difusión acoplado a ecuaciones elípticas, modelando problemas de flujo de tránsito que distinguen entre flujo libre y congestionado, y la dinámica de poblaciones que interactúan con quimiotaxis.

Los contenidos principales de la tesis se estructuran como sigue:

En el **Capítulo** 1, Construimos un esquema numérico, que es similar a uno propuesto por [J.D. Towers, A splitting algorithm for LWR traffic models with flux discontinuities in the unknown, *J. Comput. Phys.*, **421** (2020), article 109722], descomponiendo la funciíon de velocidad discontinua en una funciíon continua de Lipschitz más una función de Heaviside y disear un esquema el cuál es dividido en las dos partes en las que se descompuso la función de velocidad. La parte del esquema relacionada con la función de flujo discontinuo se maneja mediante un paso semi-implícito que, sin embargo, no involucra la solución de sistemas de ecuaciones lineales o no lineales. Se prueba que todo el esquema converge a una solución débil en el caso escalar. El esquema puede extenderse de manera sencilla al modelo LWR multiclase (MCLWR), que se define por un sistema hiperbólico de N leyes de conservación para N clases de conductores que se distinguen por sus velocidades. Se muestra que el esquema multiclase satisface un principio de región invariante, es decir, todas las densidades son no negativas y su suma no excede un valor máximo. En los casos escalar y multiclase, no se involucra la regularización de flujo ni el resolvedor de Riemann, y la condición CFL no es ms restrictiva que para un esquema explícito para la parte continua del flujo. Se presentan ejemplos numéricos para los casos escalares y multiclase.

En el **Capítulo** 2 formulamos un sistema de reacción-difusión para describir tres especies que interactúan dentro de la estructura de la cadena alimenticia de Hastings-Powell (HP) con quimiotaxis producida por tres sustancias químicas. Construimos un esquema de volumenes finitos (FV) para este sistema, y en combinación con la no negatividad y las estimaciones a priori para la solución discreta, se demuestra la existencia de una solución discreta del FV esquema. Se muestra que el esquema converge a la correspondiente solución débil del modelo. La prueba de convergencia utiliza dos ingredientes de interés para varias aplicaciones, a saber,

las desigualdades de inclusión de Sobolev discretas con condiciones de contorno generales y un argumento de compacidad espacio-tiempo en L^1. Finalmente, los ejemplos numéricos ilustran el modelo y el comportamiento del FV esquema.

En el **Capítulo** 3 consideramos un modelo matemático para la evolución espacio temporal de tres especies biológicas en un modelo de cadena alimenticia que consta de dos presas competitivas entre sí y un depredador con competencia intra-específica. Las especies se mueven hacia o en contra de concentraciones más altas de una sustancia química la cuál es producida por ellas mismas. El sistema de reacción-difusión resultante consta de tres ecuaciones parabólicas junto de las tres ecuaciones elípticas que describen el comportamiento de las sustancias químicas. Primero se prueba la existencia local de soluciones no negativas, luego proporcionamos estimaciones uniformes en los espacios de Lebesgue que conducen a la acotación y al buen planteamiento global del sistema. Finalmente reportamos y discutimos algunas simulaciones numéricas.

Agradecimientos

En primer lugar, quiero agradecer de manera muy especial a Elizabeth Martínez, mi esposa y compañera, quien por casi 5 años estuvo a mi lado esperando pacientemente a que culminara mis estudios. Gracias por todo Amor. A mi hija Juliana, "*mi chiquitolina*" cuyas sonrisas y locuras penetraban en lo más profundo de mi ser motivándome a seguir adelante. A ustedes, que son mi razón de ser les quiero decir que ojala el tiempo sea benevolente conmigo para poder compartir y disfrutar juntos.

A mis padres, Enivia y Miguel quienes siempre creyeron en mi, ellos que siempre me inspiraron a ser mejor tanto en lo profesional como en lo personal. Mama y Papa ustedes han sido mi ejemplo de vida enseñandome a seguir hacia adelante con responsabilidad y mesura. A mis hermanos Miguel, Sofia, Daniel, Berena, Luis, Jorge, Jairo, Enith y Liliana quienes a su modo han contribuido para mi crecimiento personal y profesional. A mis primos, tíos y sobrinos a los cuales siempre tuvieron fe en mi. A la abuela Caracol, Maria Helena, a Roxana, Eduardo y Sofia quienes me recibieron en el valle y han estado pendiente de mi esposa e hija mientras yo culminaba mis estudios.

Quiero agradecer a mi director de tesis, profesor Raimund Bürger, a quien admiro y respeto mucho, muchas gracias por su gestión y apoyo como profesor, director de programa y luego como director de tesis. De igual manera agradezco al profesor Luis Miguel Villada quien siempre estuvo allí incondicionalmente. A ustedes que aún sabiendo que yo era una persona un poco complicada, aunque tuviéramos dificultades siempre me recibían con amabilidad y con entusiasmo para seguir trabajando estuvieron. Para ustedes mi gratitud infinita.

Agradezco a todos los profesores de mi programa, en especial manera a los profesores: Rodolfo Araya, Raimund Bürger, Leonardo Figueroa, Rodolfo Rodriguez, Mauricio Sepúlveda por sus enseanzas. Al igual que los profesores Pep Mulet, Christophe Chalons, Paola Goatin quienes me recibieron en mis visitas a España y Francia respectivamente. Al centro de Investigación en Ingeniería Matemática (CI^2MA) de la Universidad de Concepción, por sus cómodas instalaciones que me acogieron durante todo este tiempo. A la señora Lorena, por su calidez y amabilidad.

A mis compaeros del doctorado por las charlas, cafés, almuerzos y por todas los cosas que vivimos durante mi estancia en el programa. Quiero mencionar de manera muy especial a mis compaeros de generacin: Bryan, Cristian, Paul, Willian, gracias por su amistad, por las

comelonas y por su apoyo.

A mis compatriotas Alberth, Andres, Astrid, Brayan, Diana, Eduardo, Harold, Ivan, Juan, Mauricio, Luis, Liliana, Saul, Pedro, Ruben, Wilbert con quienes compartí muchos buenos momentos. A los hermanos de otra madre Stick Alvarez, Derwin Barrios, Pedro Gomez, Victor Jaraba, Rodolfo Marquez, Andres Osorio, Aljeandro Palacios y Fredis Valencia quienes a pesar de la distancia siempre han creído en mí. De manera muy especial a mis hermanos Alejandro Fraija, Victor Ramos, Deivinson Villa y Jesus Vellojin, con quienes cultivé mi amor por las matemáticas.

Agradezco también a la Universidad de Cartagena donde empece a forjar este camino, a la Universidad del Norte donde pude continuar este camino. Agradecer además a todas las instituciones que permitieron realizar este trabajo: Al departamento de Ingenería Matemática; al Centro de Recursos Hídrico para la Agricultura y Minería (CRHIAM); a INRIA Associate Team “Efficient numerical schemes for non-local transport phenomena” (NOLOCO; 2018-2020).

Rafael Enrique Ordoñez Cardales

Contents

List of Tables

List of Figures

Introduction

Many fields of science and engineering involve the multispecies flow models, such as fluid mechanics [15,59,78,105], heat and mass transfer [83,84,98], ecology [34,57,58,67], and numerous other applications [9, 23, 24, 38, 49, 56, 66, 69, 82, 89]. For such flows, a correct mathematical model describing the interactions between different species is of the utmost importance. A variety of models have been developed to describe such interactions.

The aim of this thesis work is the mathematical and numerical analysis of two models describing multispecies behavior based on partial differential equations. Among the applications mentioned, those that motivated the development of this thesis are mainly related to those that give rise to a system of conservation laws with discontinuous flux function and reaction-diffusion system coupled with elliptic equations. Challenges in these mathematical problems concern to the treatment of discontinuous flux function and the strong nonlinearities involved in the reaction-diffusion system. We begin by studying conservation laws with discontinuous flux function through Multiclass Lighthill-Whitham-Richards (MCLWR) traffic model with discontinuous velocity function. We remark that this model its of interest because present a transition between free and congested flow regimes that can be described by a velocity function that has a discontinuity at a determined density. Reaction-diffusion system is studying through predator-prey models with chemotaxis. The novelty in this model is that each species secretes a chemical substance of corresponding concentration and is able to orient its movement towards a higher concentration of this chemical substance or away from it.

Let us introduce the two problems to work in this thesis, and then give a description to solve each.

Chapter 1, is concerned with the conservation laws whose flux is a discontinuous function of the unknowns. This kind of problem arises in many physical applications including flow in porous media [48], sedimentation [25,42], and the LWR traffic model [64,94]. We are particularly interest in the multiclass Lighthill-Whitham-Richards (MCLWR) traffic model

$$\partial_t \phi_i + \partial_x\big(\phi_i v_i(\phi)\big) = 0, \quad i = 1, \dots, N; \quad x \in \mathbb{R}, \quad t \geqslant 0.$$

Here $\phi_i = \phi(x,t)$ represent the densities of vehicles of class i, $i = 1, \dots, N$, and $\phi = \phi_1 + \cdots + \phi_N$ denotes the total density of vehicles. The velocity function v_i is assumed to depend on ϕ, where

we assume that

$$v_i(\phi) = v_i^{\max} V(\phi), \quad i = 1, \dots, N,$$

where $v_1^{\max} < v_2^{\max} < \ldots < v_N^{\max}$ are the maximum velocities of the N classes of vehicles and V is a hindrance function that models the drivers' attitude to reduce speed in the presence of other cars. The MCLWR model has been studied intensively in recent years. The system has some interesting properties and in particular admits a separable entropy function for an arbitrary number of driver classes. We refer to [12, 13, 20, 22, 24, 26, 28, 43, 44, 96, 100, 101, 101–104] for numerical and analytical treatments and emphasize that to our knowledge a velocity function discontinuous in the unknowns has not been considered so far for the MCLWR model. The purpose of **Chapter** 1 is to present a numerical treatment for the MCLWR model with a discontinuous velocity function that has one decreasing jump at a density value $\phi^* \in (0, \phi_{\max})$, that is

$$\begin{aligned} &V(\phi) = \begin{cases} V_{\mathrm{f}}(\phi) & \text{for } 0 \leqslant \phi \leqslant \phi^*, \\ V_{\mathrm{c}}(\phi) & \text{for } \phi^* < \phi \leqslant \phi_{\max}, \end{cases} \qquad V_{\mathrm{f}} \in C^1[0, \phi^*], \quad V_{\mathrm{c}} \in C^1[\phi^*, \phi_{\max}], \\ &V_{\mathrm{f}}(0) = 1, \quad V_{\mathrm{f}}'(\phi) \leqslant 0 \text{ on } [0, \phi^*], \quad V_{\mathrm{c}}'(\phi) \leqslant 0 \text{ on } [\phi^*, \phi_{\max}], \quad V_{\mathrm{f}}(\phi_{\max}) = 0, \\ &\alpha_V := V_{\mathrm{f}}(\phi^*) - V_{\mathrm{c}}(\phi^*) > 0, \end{aligned}$$

where V_{f} and V_{c} denote the branches of V used for the free (f) and congested (c) regimes, respectively. Then, we introduce a numerical scheme for the scalar case $N = 1$, which is based on the numerical scheme given in [90] but with slight differences. Then, after imposing the appropriate CFL condition we prove the well-known L^∞ and total variation diminishing (TVD) properties. We prove additional time continuity estimate to show that the numerical solutions converge to weak solution when the spatial and temporal mesh widths tend to zero. The most important novelty is the extension of the method to a generate a model with $N \geqslant 1$ of driver classes.

The second problem, which motivates **Chapter** 2, is related to a predator-prey model which incorporates chemotaxis phenomena. Here, we recall that chemotaxis is the is the ability of a biological species to orient its movement towards high concentrations of a chemical substance or away from it. In particular, in **Chapter** 2 we consider a reaction-diffusion system describing three interacting species with respective density u_i, $i = 1, 2, 3$, in the Hastings-Powell (HP) food chain structure [52, 71], where each species secretes a chemical substance of corresponding concentration y_i, $i = 1, 2, 3$. The resulting model is a strongly coupled nonlinear system of six PDEs with chemotactic terms, namely three parabolic equations describing the evolution of the densities u_i coupled with three elliptic equations for the concentrations y_i, $i = 1, 2, 3$.

$$\begin{aligned} \partial_t u_1 - D_1 \Delta u_1 + \chi_1 \operatorname{div}(u_1 \nabla y_2) &= F_1(\boldsymbol{u}), \\ \partial_t u_2 - D_2 \Delta u_2 + \chi_2 \operatorname{div}\big(u_2 \nabla (y_1 - y_3)\big) &= F_2(\boldsymbol{u}), \\ \partial_t u_3 - D_3 \Delta u_3 + \chi_3 \operatorname{div}(u_3 \nabla y_2) &= F_3(\boldsymbol{u}), \\ -\mathcal{D}_i \Delta y_i + \theta_i y_i &= \delta_i u_i, \quad i = 1, 2, 3 \quad (\boldsymbol{x}, t) \in \Omega \times (0, T]. \end{aligned}$$

The interaction due to competition between the species is specified by the functional responses

$$
\begin{aligned}
F_1(\boldsymbol{u}) &:= \left(1-\frac{u_1}{k}\right)u_1 - \frac{L_2M_2u_1u_2}{R_0+u_1},\\
F_2(\boldsymbol{u}) &:= \frac{L_2M_2u_1u_2}{R_0+u_1} - L_2u_2 - \frac{L_3M_3u_2u_3}{C_0+u_2},\\
F_3(\boldsymbol{u}) &:= \frac{L_3M_3u_2u_3}{C_0+u_2} - L_3u_3.
\end{aligned}
$$

Our propose in this chapter is present a convergent finite volume finite for the previous system and prove that the limit of the discrete solution constitutes a weak solution for the system previously mentioned.

We recall that in the **Chapter** 2 we conduct numerical experiments whose results suggest that a solution to the problem indeed exists. Then, we wonder whether it is possible to prove the existence of the weak solution to our problem from an analytical point of view. Thus, **Chapter** 3 is motivated in order to answer this question. In this chapter we discuss the existence of the solution from on the point of view of mathematical analysis, simplified system analysis parabolic-elliptic with logistic terms was studied in [86]. The model problem is similar to that of **Chapter** 2 but with slight differences. The model of chapter 3 is given by the following PDEs system.

$$
\begin{aligned}
\partial_t u_1 - D_1\Delta u_1 - \chi_1 \mathrm{div}(u_1\nabla y_3) &= F_1(\boldsymbol{u}),\\
\partial_t u_2 - D_2\Delta u_2 - \chi_2 \mathrm{div}(u_2\nabla y_3) &= F_2(\boldsymbol{u}),\\
\partial_t u_3 - D_3\Delta u_3 + \chi_3 \mathrm{div}(u_3\nabla (y_1+y_2)) &= F_3(\boldsymbol{u}),\\
-\mathcal{D}_1\Delta y_1 + \theta_1 y_1 &= \delta_1 u_1,\\
-\mathcal{D}_2\Delta y_2 + \theta_2 y_2 &= \delta_2 u_2,\\
-\mathcal{D}_3\Delta y_3 + \theta_3 y_3 &= \delta_3 u_3, \quad (\boldsymbol{x},t)\in\Omega\times(0,T],
\end{aligned}
$$

where Holling-type II functional responses F_i, $i=1,2,3$ are given by

$$
\begin{aligned}
F_1(\boldsymbol{u}) &:= r_1u_1\left(1-\frac{u_1}{k_1}\right) - \sigma_1u_1u_2 - \frac{M_1u_1}{A_1+u_1}u_3,\\
F_2(\boldsymbol{u}) &:= r_2u_2\left(1-\frac{u_2}{k_2}\right) - \sigma_2u_1u_2 - \frac{M_2u_2}{A_2+u_2}u_3,\\
F_3(\boldsymbol{u}) &:= \gamma_1\frac{M_1u_1}{A_1+u_1}u_3 + \gamma_2\frac{M_2u_2}{A_2+u_2}u_3 - Lu_3 - Hu_3^2.
\end{aligned}
$$

Herein, $u_1(\boldsymbol{x},t)$ and $u_2(\boldsymbol{x},t)$ represent the total density of the preys at position $\boldsymbol{x}$ at time t meanwhile $u_3(\boldsymbol{x},t)$ represent the total density of predator. Notice, that here the system of six PDEs describes a in a food chain model consisting of two competitive preys, furthermore the predator is in intra-specific competition.

Contribution of this thesis

In **Chapter** 1 we introduce a numerical scheme for the MCLWR model with discontinuous flux that is based on the available treatment [90] of the scalar model. The scalar version of the scheme slightly differs from that of [90] but we prove that it produces approximations that also converge to a weak solution. Numerical experiments provide evidence that it approximates the same solutions as the scheme of [90]. In the multiclass case we prove satisfaction of an invariant region principle, that is, numerical solutions assume values in

$$\mathcal{D} := \left\{(\phi_1, \ldots, \phi_N)^{\mathrm{T}} \in \mathbb{R}^N : \phi_1 \geqslant 0, \ldots, \phi_N \geqslant 0,\ \phi = \phi_1 + \cdots + \phi_N \leqslant \phi_{\max}\right\}$$

under corresponding assumptions on the initial and boundary data.

The contents of this chapter correspond to the article:

- R. Bürger, C. Chalons, R. Ordoñez, L.M. Villada, A Multiclass Lighthill-Whitham-Richards traffic model with a discontinuous velocity function, *Netw. Heterog. Media* (Accepted).

In **Chapter** 2 we prove the existence of weak solutions of the system of six PDEs with chemotactic terms, consisting in three parabolic equations describing the evolution of the biological species coupled with three elliptic equations for the chemical substance. In order to prove that, we propose a convergent finite volume (FV) method for their numerical approximation and we prove that the limit of the discrete solutions constitutes a weak solution. In addition, we will illustrate numerically the chemotactic movement and the importance of the chemotactic coefficients in the movement of each species, either towards higher concentrations or towards low concentrations. Finally, we show that with the specified numerical parameters, this model exhibits spatial-temporal oscillatory behavior.

The contents of this chapter correspond to the article [27]:

- R. Bürger, R. Ordoñez, M. Sepulveda, L.M. Villada, Numerical analysis of a three-species chemotaxis model, *Comput. Math. Appl* 80 (2020) 183–203.

In **Chapter** 3 we prove the global classical solutions of the system of six PDEs describing a predator-prey model in a food chain model consisting of two competitive preys and predator is in intra-specific competition. First, the local existence of a non-negative solution is proved using the Banach-fixed-point theorem and the properties of the heat semigroup. In addition, we show that the solution of problem satisfy the L^α-integrability property. Then, using the local existence of the solution and the L^α-integrability we prove existence of a global classical solution. Our goal is to construct a weak solution as the limit of global classical solutions of appropriately regularized problems. In order to prove this, first we prove a stability result

for the classical solutions, then we define a sequence of classical $(\boldsymbol{u}^k, \boldsymbol{y}^k)$ and prove some k-independent estimates. Therefore we can invoke the Aubin-Lions Lemma to guarantees the existence of the limit function that is a weak solution of our problem. Finally we report some numerical simulations.

The contents of this chapter correspond to ongoing research:

- P. Amorim, R. Bürger, R. Ordoñez, L.M. Villada, Global existence in a food chain model consisting of two competitive preys, one predator and chemotaxis, *(In preparation)*.

Introducción

Muchos campos de la ciencia y la ingeniería involucran los modelos de flujo de múltiples especies, tal como la mecánica de fluidos [15, 59, 78, 105], transferencia de calor y masa [83, 84, 98], ecología [34, 57, 58, 67], y muchas otras aplicaciones [9, 23, 24, 38, 49, 56, 66, 69, 82, 89]. Para tales flujos, un modelo matemático correcto que describa las interacciones entre diferentes especies es de suma importancia. Se han desarrollado una variedad de modelos para describir tales interacciones.

El objetivo de este trabajo de tesis es el análisis matemático y numérico de dos modelos que describen el comportamiento multiespecie basado en ecuaciones diferenciales parciales. Entre las aplicaciones mencionadas, las que motivaron el desarrollo de esta tesis están relacionadas principalmente con las que dan lugar a un sistema de leyes de conservación con función de flujo discontinuo y sitemas de reacción-difusión acoplados con ecuaciones elípticas. Los desafíos en estos problemas matemáticos se refieren al tratamiento de la función de flujo discontinuo y las fuertes no linealidades involucradas en el sistema de reacción-difusión. Comenzamos estudiando las leyes de conservación con función de flujo discontinuo a través del modelo de tráfico Multiclass Lighthill-Whitham-Richards (MCLWR) con función de velocidad discontinua. Observamos que este modelo es de interés porque presenta una transición entre regímenes de flujo libre y congestionado que puede ser descrito por una función de velocidad que tiene una discontinuidad en una densidad determinada. Se estudia el sistema de reacción-difusión a través de modelos depredador-presa con quimiotaxis. La novedad de este modelo es que cada especie segrega una sustancia química de concentración correspondiente y es capaz de orientar su movimiento hacia una concentración mayor de esta sustancia química o alejarse de ella.

Introducimos los dos problemas a trabajar en esta tesis, y luego damos una descripción para resolver estos problemas.

El **Capítulo** 1, es acerca de leyes de conservación con flujo discontinuo sobre la variable de estudio. Este tipo de problemas surge en muchas aplicaciones físicas incluyendo flujo en medios porosos [48], sedimentación [25, 42], y el modelo de tráfico vehicular LWR [64, 94]. Estamos particularmente interesados en el modelo multiclase de tráfico vehicular MCLWR

$$\partial_t \phi_i + \partial_x \big(\phi_i v_i(\phi)\big) = 0, \quad i = 1, \dots, N.$$

Aquí $\phi_i = \phi(x,t)$ representa las densidades de los vehiculos de la clase i, $i = 1, \dots, N$, y $\phi = \phi_1 + \cdots + \phi_N$ denota la densidad total de los vehiculos. La función de velocidad v_i es

asumida dependiente de ϕ, donde asumimos que

$$v_i(\phi) = v_i^{\max} V(\phi), \quad i = 1, \ldots, N,$$

donde $v_1^{\max} < v_2^{\max} < \ldots < v_N^{\max}$ son las velocidades máximas de las N clases de vehiculos y V es una función de obstáculo que modela la actitud de los conductores para reducir la velocidad en presencia de otros coches. Este modelo ha sido exaustivamente estudiado en los últimos aos. El sistema posee algunas propiedades de interés y en particular admite una función de entropía separable para un número arbitrario de clases de vehículos. Nos referimos a [12, 13, 20, 22, 24, 26, 28, 43, 44, 96, 100, 101, 101–104] para el tratamiento numérico y analítico y enfatizamos que hasta donde sabemos una función de velocidad discontinua sobre la variable de estudio no ha sido considerada hasta ahora para el modelo MCLWR. El proposito del **Capítulo** 1 es presentar un tratamiento numérico para el modelo MCLWR con función de velocidad discontinua con un salto decreciente en un valor de densidad $\phi^* \in (0, \phi_{\max})$, es decir

$$V(\phi) = \begin{cases} V_{\mathrm{f}}(\phi) & \text{for } 0 \leqslant \phi \leqslant \phi^*, \\ V_{\mathrm{c}}(\phi) & \text{for } \phi^* < \phi \leqslant \phi_{\max}, \end{cases} \qquad V_{\mathrm{f}} \in C^1[0, \phi^*], \quad V_{\mathrm{c}} \in C^1[\phi^*, \phi_{\max}],$$
$$V_{\mathrm{f}}(0) = 1, \quad V_{\mathrm{f}}'(\phi) \leqslant 0 \text{ on } [0, \phi^*], \quad V_{\mathrm{c}}'(\phi) \leqslant 0 \text{ on } [\phi^*, \phi_{\max}], \quad V_{\mathrm{f}}(\phi_{\max}) = 0,$$
$$\alpha_V := V_{\mathrm{f}}(\phi^*) - V_{\mathrm{c}}(\phi^*) > 0.$$

donde V_{f} y V_{c} denotan las partes de V usadas para los regímenes libre (f) y congestionado (c), respectivamente. Entonces introducimos un esquema numérico para el caso escalar $N = 1$, el cual está basado en el esquema numérico dado en [90] pero con una ligera diferencia. Entonces, después de imponer una apropiada condición CFL probamos las ya conocidas propiedades L^∞ y variación total acotada (TVD). Probamos estimaciones adicionales de continuidad en el tiempo para mostrar que las soluciones numéricas convergen a la solución debil cuando los tamaos de las mallas en espacio y tiempo tienden a cero. La novedad más importante es la extensión del método para generar un modelo con $N \geqslant 1$ de clases de conductores.

El segundo problema, el cual motiva el **Capítulo** 2, trata sobre el modelo de depredador-presa que incorpora fenómenos de quimiotaxis. Recordar que la quimiotaxis es la capacidad de una especie biológica para orientar su movimiento hacia grandes concentraciones de una sustancia química o alejarse de ella. En particular, en el **Chapter** 2 consideramos un sistema de reacción-difusión que describe tres especies que interactúan con densidad respectiva u_i, $i = 1, 2, 3$, en la estructura de la cadena alimentacia de Hastings-Powell (HP) [52, 71], donde cada especie secreta una sustancia química de concentración y_i, $i = 1, 2, 3$. El modelo resultante es un sistema no lineal fuertemente acoplado de seis PDEs con términos quimiotácticos, a saber, tres ecuaciones parabólicas que describen la evolución de las densidades u_i junto con tres ecuaciones elípticas

para las concentraciones y_i, $i = 1, 2, 3$.

$$\begin{aligned}
\partial_t u_1 - D_1 \Delta u_1 + \chi_1 \operatorname{div}(u_1 \nabla y_2) &= F_1(\boldsymbol{u}),\\
\partial_t u_2 - D_2 \Delta u_2 + \chi_2 \operatorname{div}\big(u_2 \nabla (y_1 - y_3)\big) &= F_2(\boldsymbol{u}),\\
\partial_t u_3 - D_3 \Delta u_3 + \chi_3 \operatorname{div}(u_3 \nabla y_2) &= F_3(\boldsymbol{u}),\\
-\mathcal{D}_i \Delta y_i + \theta_i y_i &= \delta_i u_i, \quad i = 1, 2, 3 \quad (\boldsymbol{x}, t) \in \Omega \times (0, T].
\end{aligned}$$

La interacción debida a la competetición entre las especies está especificada por las respuestas funcionales

$$\begin{aligned}
F_1(\boldsymbol{u}) &\coloneqq \left(1 - \frac{u_1}{k}\right) u_1 - \frac{L_2 M_2 u_1 u_2}{R_0 + u_1},\\
F_2(\boldsymbol{u}) &\coloneqq \frac{L_2 M_2 u_1 u_2}{R_0 + u_1} - L_2 u_2 - \frac{L_3 M_3 u_2 u_3}{C_0 + u_2},\\
F_3(\boldsymbol{u}) &\coloneqq \frac{L_3 M_3 u_2 u_3}{C_0 + u_2} - L_3 u_3.
\end{aligned}$$

Nuestra proposito en este capítulo es presentar un esquema de volúmenes finitos convergente para el sistema anterior y demostrar que el límite de la solución discreta constituye una solución débil para el sistema antes mencionado.

Recordamos que en el **Capítulo** 2 realizamos experimentos numéricos cuyos resultados sugieren que existe una solución al problema en estudio. Entonces, nos preguntamos si es posible probar la existencia de la solución débil de nuestro problema desde un punto de vista analítico. Así, el **Capítulo** 3 está motivado en orden a dar una respuesta a esta pregunta, en este capítulo discutimos la existencia de la solución del problema desde el punto de vista del análisis mateático, El análisis del sistema simplificado, parabólico-elíptico con término logístico fue estudiado en [86]. El problema modelo es similar al problema visto en el **Capítulo** 2 pero con ligeras diferencias. El modelo del capítulo 3 está dado el siguiente sistema PDEs.

$$\begin{aligned}
\partial_t u_1 - D_1 \Delta u_1 - \chi_1 \operatorname{div}(u_1 \nabla y_3) &= F_1(\boldsymbol{u}),\\
\partial_t u_2 - D_2 \Delta u_2 - \chi_2 \operatorname{div}(u_2 \nabla y_3) &= F_2(\boldsymbol{u}),\\
\partial_t u_3 - D_3 \Delta u_3 + \chi_3 \operatorname{div}(u_3 \nabla (y_1 + y_2)) &= F_3(\boldsymbol{u}),\\
-\mathcal{D}_1 \Delta y_1 + \theta_1 y_1 &= \delta_1 u_1,\\
-\mathcal{D}_2 \Delta y_2 + \theta_2 y_2 &= \delta_2 u_2,\\
-\mathcal{D}_3 \Delta y_3 + \theta_3 y_3 &= \delta_3 u_3, \quad (\boldsymbol{x}, t) \in \Omega \times (0, T],
\end{aligned}$$

donde las respuestas funcionales Holling tipo II F_i, $i = 1, 2, 3$ están dadas por

$$\begin{aligned}
F_1(\boldsymbol{u}) &\coloneqq r_1 u_1 \left(1 - \frac{u_1}{k_1}\right) - \sigma_1 u_1 u_2 - \frac{M_1 u_1}{A_1 + u_1} u_3,\\
F_2(\boldsymbol{u}) &\coloneqq r_2 u_2 \left(1 - \frac{u_2}{k_2}\right) - \sigma_2 u_1 u_2 - \frac{M_2 u_2}{A_2 + u_2} u_3,\\
F_3(\boldsymbol{u}) &\coloneqq \gamma_1 \frac{M_1 u_1}{A_1 + u_1} u_3 + \gamma_2 \frac{M_2 u_2}{A_2 + u_2} u_3 - L u_3 - H u_3^2.
\end{aligned}$$

Aquí $u_1(\boldsymbol{x},t)$ y $u_2(\boldsymbol{x},t)$ denotan la densidad total de las presas 1 y 2 en la posición $\boldsymbol{x}$ y tiempo t mientras que $u_3(\boldsymbol{x},t)$ denota la densidad total del depredator en la posición $\boldsymbol{x}$ y tiempo t. Tenga en cuenta que aquí el sistema de seis PDEs describe un modelo en una cadena alimenticia que consta de dos presas competitivas y un depredador, además, el depredador presenta competencia intra-específica.

Contribuciones de esta tesis

En el **Capítulo** 1 presentamos un esquema numérico para el modelo MCLWR con flujo discontinuo que se basa en el tratamiento disponible [90] del modelo escalar. La versión escalar del esquema difiere ligeramente de la de [90] pero demostramos que produce aproximaciones que también convergen a la solución débil. Los experimentos numéricos proporcionan evidencia de que nuestra solución numérica del esquema se aproxima a la misma solución numérica que el esquema de [90]. En el caso multiclase, probamos la satisfacción de un principio de región invariante, es decir, las soluciones numéricas asumen valores en

$$\mathcal{D} := \left\{(\phi_1,\dots,\phi_N)^{\mathrm{T}} \in \mathbb{R}^N : \phi_1 \geqslant 0,\dots,\phi_N \geqslant 0,\ \phi = \phi_1 + \cdots + \phi_N \leqslant \phi_{\max}\right\}$$

bajo correspondientes supuestos de la condición incicial y las condiciones de borde.

Los contenidos de este capítulo corresponden a la siguiente publicación:

- R. Bürger, C. Chalons, R. Ordoñez, L.M. Villada, A Multiclass Lighthill-Whitham-Richards traffic model with a discontinuous velocity function, *Netw. Heterog. Media* (Aceptado).

En el **Capítulo** 2 demostramos la existencia de soluciones débiles del sistema de seis PDEs con términos quimiotácticos, que consisten en tres ecuaciones parabólicas que describen la evolución de las especies biológica junto con tres ecuaciones elípticas para la sustancia química. Para demostrarlo, proponemos un método de volumenes finitos (FV) convergente para su aproximación numérica y demostramos que el límite de las soluciones discretas constituye una solución débil. Además, ilustraremos numéricamente el movimiento quimiotáctico y la importancia de los coeficientes quimiotácticos en el movimiento de cada especie, ya sea hacia concentraciones mayores o hacia concentraciones bajas. Finalmente, mostramos que con los parámetros numéricos específicos, este modelo exhibe un comportamiento oscilatorio espacio-temporal.

Los contenidos de este capítulo corresponden a la publicación [27]:

- R. Bürger, R. Ordoñez, M. Sepulveda, L.M. Villada, Numerical analysis of a three-species chemotaxis model, *Comput. Math. Appl* 80 (2020) 183–203.

En el **Capítulo** 3 probamos la existencia de soluciones clásicas globales del sistema de seis PDEs que describen un modelo de depredador-presa en una cadena alimenticia que consta

de dos presas competitivas y un depredador con competencia intra-específica. Primero, se demuestra la existencia local de una solución no-negativa usando el teorema del punto fijo de Banach y las propiedades del semigrupo de la ecuación del calor. Además, mostramos que la solución del problema satisface la propiedad de L^α integrabilidad. Luego, utilizando la existencia local de la solucin y la L^α integrabilidad, se prueba la solución clásica global. Nuesto objetivo es construir una solución débil como límite de soluciones clásicas globales de un apropiado problema regularizado. Primero, probamos un resultado de estabilidad para las soluciones clásicas globales. Luego defnimos una sucesión de soluciones clásicas $(\boldsymbol{u}^k, \boldsymbol{y}^k)$ y probamos algunas estimaciones que son independientes de k. Por lo tanto, podemos invocar el Lema de Aubin-Lions para garantizar la existencia de la función límite, la cual es una solucin débil de nuestro problema. Finalmente reportamos algunas simulaciones numérica.

Los contenidos de este capítulo corresponde a la investigación:

- P. Amorin, R. Bürger, R. Ordoñez, L.M. Villada, Global existence in a food chain model consisting of two competitive preys, one predator and chemotaxis, *(In preparation)*.

CHAPTER 1

A multiclass Lighthill-Whitham-Richards traffic model with a discontinuous velocity function

1.1 Introduction

1.1.1 Scope

The multiclass Lighthill-Whitham-Richards (MCLWR) model is a generalization of the well-known Lighthill-Whitham-Richards (LWR) model [61,80] to multiple classes of drivers and was formulated independently by Wong and Wong [96] and Benzoni-Gavage and Colombo [12]. The model is given by the following system of conservation laws in one space dimension, where the sought unknowns are the densities $\phi_i = \phi_i(x,t)$ of vehicles of class i, $i = 1,\dots,N$, as a function of distance x and time t [12,96]:

$$\partial_t \phi_i + \partial_x\big(\phi_i v_i(\phi)\big) = 0, \quad i = 1,\dots,N. \tag{1.1}$$

Here $\phi = \phi_1 + \cdots + \phi_N$ denotes the total density of vehicles. The velocity function v_i is assumed to depend on ϕ, where we assume that

$$v_i(\phi) = v_i^{\max} V(\phi), \quad i = 1,\dots,N, \tag{1.2}$$

where $v_1^{\max} < v_2^{\max} < \ldots < v_N^{\max}$ are the maximum velocities of the N classes of vehicles and V is a hindrance function that models the drivers' attitude to reduce speed in the presence of other cars. This function is usually assumed to be continuous and piecewise smooth on an interval $[0,\phi_{\max}]$, where $\phi_{\max} > 0$ denotes a maximum vehicle density, with

$$V(0) = 1, \quad V'(\phi) < 0, \quad V(\phi_{\max}) = 0.$$

The simplest function having all these properties is the linear interpolation $V(\phi) = 1 - \phi/\phi_{\max}$. However, equation (1.1) is studied herein under the assumption that V is piecewise continuous

with one decreasing jump at a density value $\phi^* \in (0, \phi_{\max})$, that is

$$\begin{aligned} V(\phi) &= \begin{cases} V_{\mathrm{f}}(\phi) & \text{for } 0 \leqslant \phi \leqslant \phi^*, \\ V_{\mathrm{c}}(\phi) & \text{for } \phi^* < \phi \leqslant \phi_{\max}, \end{cases} \qquad V_{\mathrm{f}} \in C^1[0, \phi^*], \quad V_{\mathrm{c}} \in C^1[\phi^*, \phi_{\max}], \\ & V_{\mathrm{f}}(0) = 1, \quad V_{\mathrm{f}}'(\phi) \leqslant 0 \text{ on } [0, \phi^*], \quad V_{\mathrm{c}}'(\phi) \leqslant 0 \text{ on } [\phi^*, \phi_{\max}], \quad V_{\mathrm{f}}(\phi_{\max}) = 0, \\ & \alpha_V := V_{\mathrm{f}}(\phi^*) - V_{\mathrm{c}}(\phi^*) > 0. \end{aligned} \tag{1.3}$$

We consider (1.1) on the domain $\Pi_T := (-L, L) \times (0, T)$, where $L > 0$ and $T > 0$, along with the initial and boundary conditions

$$\begin{aligned} \phi_i(x, 0) = \phi_{i,0}(x) \in [0, \phi_{\max}], \quad x \in (-L, L), \\ \phi_i(-L, t) = r_i(t) \in [0, \phi_{\max}], \quad t \in (0, T), \\ \phi_i(L, t) = s_i(t) \in [0, \phi_{\max}], \quad t \in (0, T), \quad i = 1, \ldots, N; \end{aligned} \tag{1.4a}$$

$$\boldsymbol{\mathcal{F}}(t) \in (\boldsymbol{v}^{\max})^{\mathrm{T}} \boldsymbol{s}(t) \tilde{V}\big(s(t)\big), \quad t \in (0, T); \quad \boldsymbol{v}^{\max} := (v_1^{\max}, \ldots, v_N^{\max})^{\mathrm{T}}. \tag{1.4b}$$

The non-standard boundary condition (1.4b) on the total density is required in case that $s(t) = \phi^*$, where $\boldsymbol{s}(t) := (s_1(t), \ldots, s_N(t))^{\mathrm{T}}$ and $s(t) = s_1(t) + \cdots + s_N(t)$. This implies that we assign values to $\boldsymbol{\mathcal{F}}(t)$ according to

$$\boldsymbol{\mathcal{F}}(t) = \begin{cases} (\boldsymbol{v}^{\max})^{\mathrm{T}} \boldsymbol{s}(t) V(\phi^*-) & \text{if the traffic ahead of } x = L \text{ is free-flowing,} \\ (\boldsymbol{v}^{\max})^{\mathrm{T}} \boldsymbol{s}(t) V(\phi^*+) & \text{if the traffic ahead of } x = L \text{ is congested.} \end{cases} \tag{1.5}$$

This assumption is motivated in a wider sense by models of phase transitions between free and congested traffic flow regimes [32, 36], and more specifically by treatments of the single-class scalar version of (1.1)–(1.4). In the scalar case the model can be formulated following initial-boundary value problem for a scalar conservation law defined on Π_T:

$$\begin{aligned} \partial_t \phi + \partial_x f(\phi) = 0, \quad (x, t) \in \Pi_T \quad f(\phi) = v^{\max} \phi V(\phi), \\ \phi(x, 0) = \phi_0(x) \in [0, \phi_{\max}], \quad x \in (-L, L), \\ \phi(-L, t) = r(t) \in [0, \phi_{\max}], \quad t \in (0, T), \\ \phi(L, t) = s(t) \in [0, \phi_{\max}], \quad \mathcal{F}(t) \in \tilde{f}\big(s(t)\big) \quad t \in (0, T), \end{aligned} \tag{1.6}$$

with a jump in $V(\phi)$ or equivalently, in the flux $f(\phi)$, see [90, 94], where $\tilde{f}$ denotes the multi-valued version of f and $\mathcal{F}(t) \in \tilde{f}(s(t))$ represents the non-standard boundary condition of the flux discontinuity, see [90].

1.1.2 Related work

Conservation laws with discontinuous flux function arise in many physical applications including flow in porous media [48], sedimentation [25, 42], and the LWR traffic model [64, 94]. Here we limit the discussion to analyses where the flux is a discontinuous function of the unknown (as

opposed to the more widely studied discontinuous dependence on spatial position). This property implies that standard numerical methods cannot be applied directly due to the presence of waves that travel at infinite speed, namely so-called zero waves. These waves carry information about the flux but this value is transported instantaneously, which excludes applying explicit schemes due to the lack of regularity of the flux. Gimse [47] was the first to present a solution to this problem. He studied a conservation law where the flux function has a single jump. He discussed the existence of the zero wave, generalized the method of convex hull construction, and solved the Riemann problem using a front tracking algorithm.

Carrillo [31] studied conservation laws with a discontinuous flux function where the flux is allowed to have discontinuities on a finite subset of real numbers. The proof of existence of solutions is based on the comparison principle and an entropy inequality involving a version of semi-Kružkov entropies. Dias and Figueira [39] studied a related problem by using a mollification technique to smooth out discontinuities. They showed that solutions to a suitably regularized problem converge to solutions of the original problem in the limit. They also defined the notions of weak solution and weak entropy solution. The mollification technique was implemented in [40,41]. Moreover, Dias and Figueira [40] proposed a numerical scheme for Riemann problem. Specifically, they introduced a procedure to obtain a new Lipschitz continuous flux function with the same lower convex envelope of the original flux, and then a standard Lax-Friedrichs method is employed.

Martin and Vovelle [68] considered the problem of numerical approximation in the Cauchy-Dirichlet problem for a scalar conservation law with a flux function having finitely many discontinuities. The well-posedness of this problem had been proved by Carrillo. An implicit finite volume scheme is constructed in [68] and Newton's method is employed to solve the resulting system of nonlinear equations. Furthermore, convergence to the unique entropy solution is shown.

Lu et al. [64] explicitly constructed the entropy solutions for the LWR traffic flow model with a piecewise quadratic flow-density relationship. Their approach is based on constructions of entropy solutions to a sequence of approximate problems in which the flow-density relationship is continuous but tends to the discontinuous flux when a small parameter in this sequence tends to zero.

Bulíček et al. [18] introduced new concepts of entropy weak and measure-valued solutions that are consistent with the standard ones if the flux is continuous. They identified a given discontinuous flux function with a continuous curve that consists of the graph of this flux and abscissae that fill the jumps. Consequently, instead of a discontinuous flux function of the unknown, they deal with an implicit relation that represents a curve. One has one degree of freedom to set up the "optimal" unknown (independent variable). These ideas are combined in [19], where the authors treat the case of a flux function discontinuous in spatial position and the unknown. Through appropriate estimates for entropy measure-valued solutions well-posedness is shown.

Wiens et al. [94] applied Dias and Figueira's mollification approach to solving a conservation law with a piecewise linear flux function in which there is a single discontinuity at a critical point. They introduced a mollified function and then the analytical solution to the corresponding Riemann problem is derived in the limit. Furthermore they constructed a Riemann solver that forms the basis for a high-resolution finite volume scheme of Godunov type and used an alternate approach that eliminates the severe CFL constraint by incorporating the effect of zero waves directly into the local Riemann solver.

Towers [90] presented a finite difference scheme that implements a splitting consistent with the decomposition the flux $f(u) = p(u) + g(u)$, where p is a Lipschitz continuous function and g is a function of Heaviside type that includes the jumps of f. The scheme has the form (see [90, Eq. (3.11)])

$$\begin{cases} \begin{cases} U_j^{n+1/2} = \tilde{G}^{-1}\big(U_j^n - \lambda g_{j+1}^{n+1/2}\big), \quad j = M, M-1, \dots, 1, \\ g_j^{n+1/2} = \big(U_j^{n+1/2} - U_j^n + \lambda g_{j+1}^{n+1/2}\big)/\lambda, \quad j = M, M-1, \dots, 1, \end{cases} \\ U_j^{n+1} = U_j^{n+1/2} - \lambda \Delta_- \tilde{p}\big(U_{j+1}^{n+1/2} - U_j^{n+1/2}\big), \quad j = 1, \dots, M, \end{cases} \tag{1.7}$$

which can be written in conservation form as follows:

$$\begin{aligned} U_j^{n+1/2} &= U_j^n - \lambda\big(g_{j+1}^{n+1/2} - g_j^{n+1/2}\big), \\ U^{n+1} &= U_j^{n+1/2} - \lambda \Delta_- \tilde{p}\big(U_{j+1}^{n+1/2}, U_j^{n+1/2}\big). \end{aligned}$$

The first part of the scheme is implicit and consistent with $u_t + g(u)_x = 0$, but the resulting equations can be solved by evaluation of a piecewise linear function. Hence, an iterative solver like Newton's method is not required. The second part of the scheme is consistent with $u_t + p(u)_x = 0$ and is explicit, and can be solved by any scheme suitable for a scalar conservation law with Lipschitz continuous flux. Towers [90] focused on the Godunov flux for the explicit part but also presented a simple flux-limited Lax-Wendroff-type modification to the Godunov scheme.

1.1.3 Outline

The remainder of this chapter is organized as follows. In Section 1.2 we present a numerical scheme for the LWR traffic flow model. We first introduce some assumptions and the notion of weak solution in Section 1.2.1. Next, Section 1.2.2 is devoted to the presentation of our scheme for the scalar case ($N = 1$) and we imposed the appropriate CFL condition. Then, in Section 1.2.3, we prove that under the CFL condition it satisfies uniform L^∞ and TVD properties. Moreover we prove some kind time continuity estimates and to the end this section we prove the convergence of our numerical solution converge to weak solution in sense of Definition 1.1. In Section 1.3 we extend the algorithm to the multiclass case ($N > 1$) and prove that the scheme preserves the invariant region $\mathcal{D}$. In Section 1.4 we present several numerical examples to confirm all the results mentioned before. Section 3.6.1 collects some conclusions.

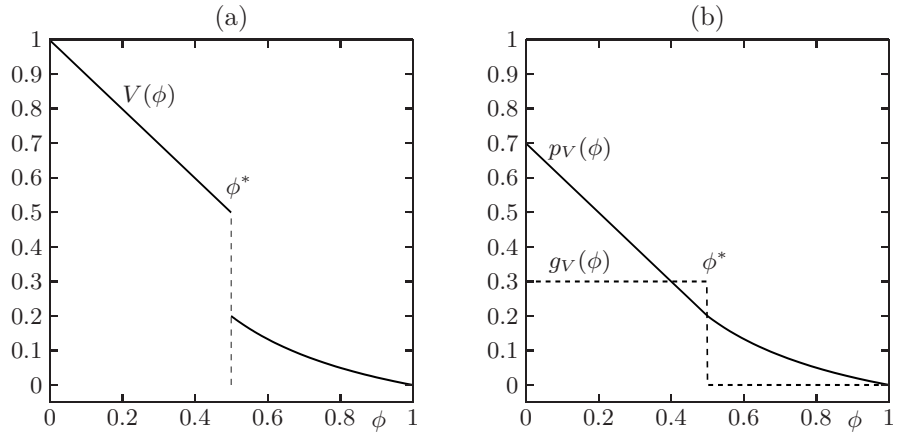

Figure 1.1: (a) Piecewise continuous velocity function $V(\phi)$ with discontinuity at $\phi = \phi^*$, (b) continuous and discontinuous portions $p_V(\phi)$ (solid line) and $g_V(\phi)$ (dashed line).

1.2 Construction of the numerical scheme in the scalar case

Before describing the numerical scheme we introduce some assumptions and the definition of weak solutions proposed in [40], which is employed herein.

1.2.1 Preliminaries

To outline the basic idea, and to make the comparison with [90] transparent, we define the functions

$$g_V(\phi) := \alpha_V H(\phi^* - \phi), \quad p_V(\phi) := V(\phi) - g_V(\phi), \tag{1.8}$$

where p_V is a Lipschitz continuous, piecewise smooth and decreasing function, while $g_V(\phi)$ is a non-negative and decreasing function, see Figure 1.1. Furthermore, as in [90], we can equivalently specify

$$\mathcal{G}(t) \in \tilde{g}_V\big(s(t)\big), \tag{1.9}$$

where $\tilde{g}_V$ denotes the multivalued version of g_V. With respect to the initial and boundary data we assume that the initial density function ϕ_0 satisfies

$$\phi_0(x) \in [0, \phi_{\max}] \quad \text{for } x \in (-L, L), \quad \phi_0 \in BV([-L, L]), \quad g_V(\phi_0) \in BV([-L, L]).$$

The boundary functions r and s are assumed to satisfy

$$r(t), s(t) \in [0, \phi_{\max}] \quad \text{for } t \in [0, T], \quad r, s \in BV([0, T]).$$

We also assume that $\mathcal{G}(t) \in [0, \alpha_V]$ for all $t \in [0, T]$, and $\mathcal{G} \in BV([0, T])$.

Definition 1.1 (Weak solution [40]). *A function $\phi \in L^\infty(\Pi_T)$ is said to be a* weak solution *to the initial-boundary value problem (1.6) if there exists a function $q \in L^\infty(\Pi_T)$ satisfying $q(x,t) \in \tilde{f}(\phi(x,t))$ a.e. such that for all test functions $\psi \in C_0^1([-L,L]\times[0,T))$,*

$$\int_0^T \int_{-L}^{L} \big(\phi\psi_t + q\psi_x\big)\,\mathrm{d}x\,\mathrm{d}t + \int_{-L}^{L} \phi_0(x)\psi(x,0)\,\mathrm{d}x = 0.$$

1.2.2 Numerical scheme

The domain Π_T is discretized as follows. We choose a partition $\{I_j\}_{j=1}^M$ of $[-L,L]$ composed of uniform cells $I_j = [x_{j-1/2}, x_{j+1/2})$, where $x_{j+1/2} = x_j + \Delta x/2$, that are centered in x_j and have length $|I_j| = \Delta x = 2L/M$. Then, for $\Delta t > 0$, we let $t^n = n\Delta t$ for $n = 0,\dots,\mathcal{N}$, where $\mathcal{N}$ is an integer such that $T \in [t^{\mathcal{N}}, t^{\mathcal{N}} + \Delta t)$. The unknowns ϕ_j^n approximate the cell average of the exact solution $\phi(\cdot,t^n)$ in the cell I_j. The initial condition is discretized by

$$\phi_j^0 = \frac{1}{\Delta x}\int_{I_j} \phi_0(x)\,\mathrm{d}x, \quad j = 1,\dots,M,$$

and the boundary conditions with $\mathcal{F}(t) \in \tilde{f}(s)$ are discretized as follows:

$$\begin{aligned}
&\phi_0^{n+1/2} = \phi_0^n = r(t^n) = t^n, \quad \phi_{M+1}^{n+1/2} = \phi_{M+1}^n = s(t^n) = s^n,\\
&r^n \in [0,\phi_{\max}], \quad s^n \in [0,\phi_{\max}], \quad g_{M+1}^{n+1/2} \in [0,\alpha_V],\\
&g_{M+1}^{n+1/2} = g_{M+1}^n = \mathcal{G}(s^n) = \begin{cases} \alpha_V & \text{if } s^n < \phi^*,\\ \alpha_V & \text{if } s^n = \phi^* \text{ and traffic ahead of } x = L \text{ is free-flowing},\\ 0 & \text{if } s^n = \phi^* \text{ and traffic ahead of } x = L \text{ is congested},\\ 0 & \text{if } s^n > \phi^*. \end{cases}
\end{aligned} \tag{1.10}$$

Before proposing our scheme we recall that the basic idea of a splitting scheme consists in solving within each time step, first the PDE

$$\partial_t\phi + \partial_x\big(v^{\max}\phi g_V(\phi)\big) = 0, \tag{1.11}$$

followed by the solution of the conservation law with continuous flux

$$\partial_t\phi + \partial_x\big(v^{\max}\phi p_V(\phi)\big) = 0. \tag{1.12}$$

Note that in the scalar case the constant $v^{\max}$ is immaterial. For the remainder of the analysis of the scalar case we assume that t or x are rescaled so that $v^{\max} = 1$.

Based on the form of the flux function of equations (1.11) and (1.12) and the properties of the functions g_V and p_V, we may write a numerical scheme for (1.6) that is motivated by Scheme 4 of [23] in the following form:

$$\begin{aligned}
\phi_j^{n+1/2} &= \phi_j^n - \lambda\big(\phi_j^n g_{V,j+1}^{n+1/2} - \phi_{j-1}^n g_{V,j}^{n+1/2}\big),\\
\phi_j^{n+1} &= \phi_j^{n+1/2} - \lambda\big(\phi_j^{n+1/2} p_V\big(\phi_{j+1}^{n+1/2}\big) - \phi_{j-1}^{n+1/2} p_V\big(\phi_j^{n+1/2}\big)\big), \quad j = 1,\dots,M.
\end{aligned} \tag{1.13}$$

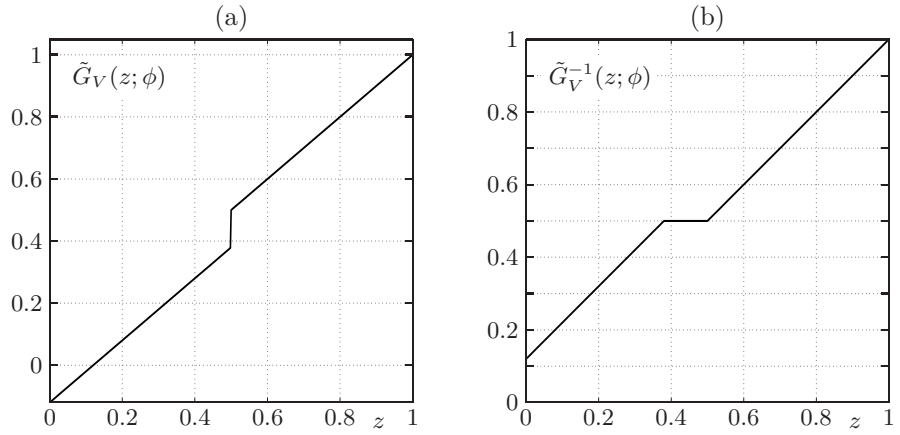

Figure 1.2: (a) function $z \mapsto \tilde{G}_V(z;\phi)$ given by (1.16a) with $\lambda v^{\max} = 1/2$, $\alpha_V = 0.3$, and $\phi = 0.8$, (b) its inverse $z \mapsto \tilde{G}_V^{-1}(z;\phi)$ given by (1.16b).

The first half-step in (1.13) is semi-implicit and is consistent with (1.11) whereas the second half-step is explicit and consistent with (1.12).

In order to evaluate the first line in (1.13), we start by computing the values $g_{V,j}^{n+1/2}$ from $j = M+1$ to $j = 1$ (in decreasing order). This is motivated by the following argument, where we start from the semi-implicit equation

$$\phi_j^{n+1/2} = \phi_j^n - \lambda\big(\phi_j^n g_V\big(\phi_{j+1}^{n+1/2}\big) - \phi_{j-1}^n g_V\big(\phi_j^{n+1/2}\big)\big) \tag{1.14}$$

along with a known value $\mathcal{G}(\phi_{M+1}^{n+1/2})$ arising from the boundary condition. Next, we write $g_V(\phi_{j+1}^{n+1/2})$ as $g_{V,j+1}^{n+1/2}$ and then rearrange (1.14) as

$$\phi_j^{n+1/2} - \lambda\phi_{j-1}^n g_V\big(\phi_j^{n+1/2}\big) = \phi_j^n - \lambda\phi_j^n g_{V,j+1}^{n+1/2}. \tag{1.15}$$

Let us now define the function

$$G_V(z;\phi) := z - \lambda\phi g_V(z), \quad z,\phi \in [0,\phi_{\max}]$$

along with its multivalued version (with respect to z) $\tilde{G}_V(\cdot;\phi)$. Then $\tilde{G}_V$ is strictly increasing and has a unique inverse $z \mapsto \tilde{G}_V^{-1}(z;\phi)$, see Figure 1.2. Explicitly, we get

$$\tilde{G}_V\big(z;\phi\big) := \begin{cases} z - \lambda\alpha_V\phi & \text{for } z \in [0,\phi^*), \\ [\phi^* - \lambda\alpha_V\phi, \phi^*] & \text{for } \phi = \phi^*, \\ z & \text{for } z \in [\phi^*,\phi_{\max}], \end{cases} \tag{1.16a}$$

$$\tilde{G}_V^{-1}\big(z;\phi\big) := \begin{cases} z + \lambda\alpha_V\phi & \text{for } z \in [-\lambda\alpha_V\phi, \phi^* - \lambda\alpha_V\phi), \\ \phi^* & \text{for } z \in [\phi^* - \lambda\alpha_V\phi, \phi^*], \\ z & \text{for } z \in [\phi^*,\phi_{\max}]. \end{cases} \tag{1.16b}$$

Consequently, we may express (1.15) as

$$\tilde{G}_V\big(\phi_j^{n+1/2};\phi_{j-1}^n\big)=\phi_j^n-\lambda\phi_j^n g_{V,j+1}^{n+1/2},$$

which allows us to obtain $\phi_j^{n+1/2}$ by applying $\tilde{G}_V^{-1}(z;\phi)$ to both sides, that is

$$\phi_j^{n+1/2}=\tilde{G}_V^{-1}\big(\phi_j^n-\lambda\phi_j^n g_{V,j+1}^{n+1/2};\phi_{j-1}^n\big). \tag{1.17}$$

Now that $\phi_j^{n+1/2}$ is available, we solve for $g_{V,j}^{n+1/2}$ the equation

$$\phi_j^{n+1/2}=\phi_j^n-\lambda\big(\phi_j^n g_{V,j+1}^{n+1/2}-\phi_{j-1}^n g_{V,j}^{n+1/2}\big), \tag{1.18}$$

provided that $\phi_{j-1}^n>0$. If $\phi_{j-1}^n=0$, we define directly

$$g_{V,j}^{n+1/2}=g_V\big(\phi_j^{n+1/2}\big).$$

The numerical scheme can be summarized in Algorithm 1.1:

Algorithm 1.1 (BCOV scheme, scalar case)**.**

Input: approximate solution vector $\{\phi_j^n\}_{j=1}^M$ for $t=t^n$

$g_{V,M+1}^{n+1/2}\leftarrow\mathcal{G}(\phi_{M+1}^{n+1/2})$ *(using* (1.10)*)*

do $j=M,M-1,\dots,1$

$\phi_j^{n+1/2}\leftarrow\tilde{G}_V^{-1}\big(\phi_j^n-\lambda\phi_j^n g_{V,j+1}^{n+1/2};\phi_{j-1}^n\big)$

if $\phi_{j-1}^n\neq 0$ **then**

$$g_{V,j}^{n+1/2}\leftarrow\frac{\phi_j^{n+1/2}-\phi_j^n+\lambda g_{V,j+1}^{n+1/2}\phi_j^n}{\lambda\phi_{j-1}^n}$$

else

$g_{V,j}^{n+1/2}\leftarrow g_V(\phi_j^{n+1/2})$

endif

enddo

do $j=1,2,\dots,M$

$\phi_j^{n+1}\leftarrow\phi_j^{n+1/2}-\lambda\big(\phi_j^{n+1/2}p_V\big(\phi_{j+1}^{n+1/2}\big)-\phi_{j-1}^{n+1/2}p_V\big(\phi_j^{n+1/2}\big)\big)$

enddo

Output: approximate solution vector $\{\phi_j^{n+1}\}_{j=1}^M$ for $t=t^{n+1}=t^n+\Delta t$

Next, we demonstrate that the numerical scheme (1.18) is consistent with (1.11).

Lemma 1.1. *Assume that* $\phi_j^{n+1/2} \in [0, \phi_{\max}]$ *for all* j. *Then* $g_{V,j}^{n+1/2} \in \tilde{g}_V(\phi_j^{n+1/2})$ *for all* j. *In particular* $g_{V,j}^{n+1/2} \in [0, \alpha_V]$ *for all* j.

Proof. Let us first assume that $\phi_{j-1} = 0$. Then the result follows from the definition of the function $g_V(z)$ and the corresponding assignment to $g_{V,j}^{n+1/2}$ in Algorithm 1.1. If $\phi_{j-1} \neq 0$, then (1.17) and (1.16) imply that

$$\phi_j^{n+1/2} - \lambda \phi_{j-1}^n g_{V,j}^{n+1/2} \in \tilde{G}_V\big(\phi_j^{n+1/2}; \phi_{j-1}^n\big).$$

Therefore, by a straightforward case-by-case study (of the cases arising in (1.16)) we conclude that $g_{V,j}^{n+1/2} \in \tilde{g}_V(\phi_j^{n+1/2})$. □

Now, to derive CFL conditions, we write the scheme (1.13) in incremental form

$$\phi_j^{n+1/2} = \phi_j^n + C_{g,j+1/2}^{n+1/2} \Delta_+ \phi_j^{n+1/2} - D_{g,j-1/2}^{n+1/2} \Delta_- \phi_j^n, \tag{1.19a}$$

$$\phi_j^{n+1} = \phi_j^{n+1/2} + C_{p,j+1/2}^{n+1/2} \Delta_+ \phi_j^{n+1/2} - D_{p,j-1/2}^{n+1/2} \Delta_- \phi_j^{n+1/2} \tag{1.19b}$$

with the spatial difference operators $\Delta_+ V_j := V_{j+1} - V_j$ and $\Delta_- V_j := V_j - V_{j-1}$ and the incremental coefficients

$$C_{g,j+1/2}^{n+1/2} := \begin{cases} \lambda \phi_j^n \dfrac{g_V(\phi_j^{n+1/2}) - g_V(\phi_{j+1}^{n+1/2})}{\phi_{j+1}^{n+1/2} - \phi_j^{n+1/2}} & \text{if } \phi_{j+1}^{n+1/2} \neq \phi_j^{n+1/2}, \\ 0 & \text{otherwise,} \end{cases}$$

$$D_{g,j-1/2}^{n+1/2} := \lambda g_V(\phi_j^{n+1/2}),$$

$$C_{p,j+1/2}^{n+1/2} := \begin{cases} \lambda \phi_j^{n+1/2} \dfrac{p_V(\phi_j^{n+1/2}) - p_V(\phi_{j+1}^{n+1/2})}{\phi_{j+1}^{n+1/2} - \phi_j^{n+1/2}} & \text{if } \phi_{j+1}^{n+1/2} \neq \phi_j^{n+1/2}, \\ 0 & \text{otherwise,} \end{cases}$$

$$D_{p,j-1/2}^{n+1/2} := \lambda p_V(\phi_j^{n+1/2}).$$

To have an L^∞ estimate (Lemma 1.2 below) and the Total Variation Diminishing (TVD) property (Lemma 1.3 below) sufficient conditions are

$$0 \leqslant D_{p,j-1/2}^{n+1/2}, C_{p,j+1/2}^{n+1/2} \leqslant \frac{1}{2}, \quad C_{g,j+1/2}^{n+1/2} \geqslant 0, \quad 0 \leqslant D_{g,j-1/2}^{n+1/2} \leqslant 1 \quad \text{for all } j.$$

First, we observe the following fact about $\tilde{g}_V$. If $z_1, z_2 \in [0, \phi_{\max}]$ and $z_1 \neq z_2$, then

$$g_{V,1} \in \tilde{g}_V(z_1),\ g_{V,2} \in \tilde{g}_V(z_2) \Longrightarrow \frac{g_{V,2} - g_{V,1}}{z_2 - z_1} \leqslant 0. \tag{1.20}$$

This property and Lemma 1.1 imply that

$$D_{g,j-1/2}^{n+1/2}, C_{g,j+1/2}^{n+1/2} \geqslant 0 \quad \text{for all } j.$$

Next, the properties of the function p_V ensure that

$$C_{p,j+1/2}^{n+1/2},\ D_{p,j-1/2}^{n+1/2} \geqslant 0 \quad \text{for all } j.$$

Finally, to enforce the inequalities

$$D_{p,j-1/2}^{n+1/2},\ C_{p,j+1/2} \leqslant \frac{1}{2} \quad \text{and} \quad D_{g,j-1/2}^{n+1/2} \leqslant 1 \quad \text{for all } j,$$

we impose the CFL conditions

$$\lambda\Big(\phi_{\max} \max_{1\leqslant j\leqslant M}\big|p_V'(\phi_j)\big| + \max_{1\leqslant j\leqslant M} p_V(\phi_j)\Big) \leqslant \frac{1}{2}, \qquad \lambda\alpha_V \leqslant 1. \tag{1.21}$$

1.2.3 Convergence of the scalar scheme

The goal is to prove convergence of approximate solution to a weak solution of (1.6). The discrete solutions $\{\phi_j^{n+1/2}\}$ constructed via the scheme (1.13) are extended to the whole domain Π_T by defining the piecewise constant function

$$\phi^{\Delta}(x,t) = \sum_{n=0}^{\mathcal{N}}\sum_{j=1}^{M} \chi_j(x)\chi^n(t)\phi_j^{n+1/2} \tag{1.22}$$

where $\Delta = (\Delta x, \Delta t)$ and $\chi_j(x)$ and $\chi^n(t)$ are the characteristic functions of cell I_j and the time interval $[t^n, t^n + \Delta t)$, respectively. The ratio $\lambda = \Delta t/\Delta x$ is always kept constant, so the limits $\Delta t \to 0$, $\Delta x \to 0$, and $\Delta \to \mathbf{0}$ are equivalent.

We start by proving an L^∞ estimate on ϕ^Δ. In the remainder of this section it is always assumed that the CFL condition (1.21) is in effect.

Lemma 1.2. *If $\phi_j^0 \in [0, \phi_{\max}]$ for $j = 1, \dots, M$, then*

$$\phi_j^n, \phi_j^{n+1/2} \in [0, \phi_{\max}] \quad \text{for all } j = 1, \dots, M \text{ and } n = 1, \dots, \mathcal{N}. \tag{1.23}$$

Proof. Taking $n = 0$ and $j = M$ in (1.17) yields

$$\phi_M^{1/2} = \tilde{G}_V^{-1}\big(\phi_M^0 - \lambda\phi_M^0 g_{V,M+1}^{1/2}; \phi_{M-1}^0\big). \tag{1.24}$$

The boundary condition $g_{V,M+1}^{1/2} = \mathcal{G}(t^0) \subseteq [0, \alpha_V]$ together with the assumption implies that

$$-\lambda\alpha_V\phi_M^0 \leqslant \phi_M^0 - \lambda\phi_M^0 g_{V,M+1}^{1/2} \leqslant \phi_{\max}.$$

Since $\tilde{G}_V^{-1}(\cdot;\phi)$ is a nondecreasing function and maps $[-\lambda\alpha_V\phi, \phi_{\max}]$ onto $[0, \phi_{\max}]$, (1.24) implies that $\phi_M^{1/2} \in [0, \phi_{\max}]$. It follows from (1.1) that $g_{V,M}^{1/2} \in [0, \alpha_V]$. Reasoning in this way for $j = M-1, M-2, \dots, 1$ yields $\phi_j^{1/2} \in [0, \phi_{\max}]$ for $j = 1, \dots, M$. Since $\phi_0^{1/2}, \phi_{M+1}^{1/2} \in [0, \phi_{\max}]$ by (1.10), and taking into account (1.19), we find that ϕ_j^1 is a convex combination of $\phi_{j-1}^{1/2}$, $\phi_j^{1/2}$ and $\phi_{j+1}^{1/2}$. Thus, $\phi_j^1 \in [0, \phi_{\max}]$ for $j = 1, \dots, M$. Repeating this argument inductively for $n = 1, \dots, \mathcal{N}$ we obtain (1.23). □

Lemma 1.3. *The discrete approximate solutions generated by the scheme (1.19) satisfy the following spatial variation bounds:*

$$\begin{aligned}\sum_{j=0}^{M}\left|\phi_{j+1}^{n}-\phi_{j}^{n}\right| &\leqslant \mathrm{TV}(\phi_0)+\mathrm{TV}(r)+\mathrm{TV}(s),\\ \sum_{j=0}^{M}\left|\phi_{j+1}^{n+1/2}-\phi_{j}^{n+1/2}\right| &\leqslant \mathrm{TV}(\phi_0)+\mathrm{TV}(r)+\mathrm{TV}(s).\end{aligned} \tag{1.25}$$

Proof. Applying the operator Δ_+ to (1.19a) and rearranging yields

$$\left(1+C_{g,j+1/2}^{n+1/2}\right)\Delta_+\phi_j^{n+1/2}=\left(1-D_{g,j+1/2}^{n+1/2}\right)\Delta_+\phi_j^{n}+C_{g,j+3/2}^{n+1/2}\Delta_+\phi_{j+1}^{n+1/2}+D_{g,j-1/2}^{n+1/2}\Delta_+\phi_{j-1}^{n}.$$

Taking absolute values, summing over $j=1,\dots,M-1$ and using (1.21) we get

$$\begin{aligned}\sum_{j=1}^{M-1}\left(1+C_{g,j+1/2}^{n+1/2}\right)\left|\Delta_+\phi_j^{n+1/2}\right| \leqslant{}& \sum_{j=1}^{M-1}\left(1-D_{g,j+1/2}^{n+1/2}\right)\left|\Delta_+\phi_j^{n}\right|+\sum_{j=1}^{M-1}C_{g,j+3/2}^{n+1/2}\left|\Delta_+\phi_{j+1}^{n+1/2}\right|\\ &+\sum_{j=1}^{M-1}D_{g,j-1/2}^{n+1/2}\left|\Delta_+\phi_{j-1}^{n}\right|.\end{aligned}$$

Cancelling telescoping terms we obtain

$$\begin{aligned}\sum_{j=1}^{M-1}\left|\Delta_+\phi_j^{n+1/2}\right|+C_{g,3/2}^{n+1/2}\left|\Delta_+\phi_1^{n+1/2}\right| \leqslant{}& \sum_{j=1}^{M-1}\left|\Delta_+\phi_j^{n}\right|-D_{g,M-1/2}^{n+1/2}\left|\Delta_+\phi_{M-1}^{n}\right|+C_{g,M+1/2}^{n+1/2}\left|\Delta_+\phi_M^{n+1/2}\right|\\ &+D_{g,1/2}^{n+1/2}\left|\Delta_+\phi_0^{n+1/2}\right|.\end{aligned} \tag{1.26}$$

The boundary condition implies

$$\begin{aligned}\Delta_+\phi_0^{n+1/2}&=\left(1-D_{g,1/2}^{n+1/2}\right)\Delta_+\phi_0^{n}+C_{g,3/2}^{n+1/2}\Delta_+\phi_1^{n+1/2},\\ \left(1+C_{g,M+1/2}^{n+1/2}\right)\Delta_+\phi_M^{n+1/2}&=\Delta_+\phi_M^{n}+D_{g,M-1/2}^{n+1/2}\Delta_+\phi_1^{n+1/2}.\end{aligned}$$

After taking absolute values in the two previous equations, we get

$$\begin{aligned}\left|\Delta_+\phi_0^{n+1/2}\right| &\leqslant \left(1-D_{g,1/2}^{n+1/2}\right)\left|\Delta_+\phi_0^{n}\right|+C_{g,3/2}^{n+1/2}\left|\Delta_+\phi_1^{n+1/2}\right|,\\ \left(1+C_{g,M+1/2}^{n+1/2}\right)\left|\Delta_+\phi_M^{n+1/2}\right| &\leqslant \left|\Delta_+\phi_M^{n}\right|+D_{g,M-1/2}^{n+1/2}\left|\Delta_+\phi_{M-1}^{n+1/2}\right|.\end{aligned} \tag{1.27}$$

From (1.26) and (1.27)

$$\sum_{j=0}^{M}\left|\Delta_+\phi_j^{n+1/2}\right| \leqslant \sum_{j=0}^{M}\left|\Delta_+\phi_j^{n}\right|. \tag{1.28}$$

Reasoning in the same way as the proof of Lemma 5.2 in [90] we find that

$$\sum_{j=0}^{M}\left|\Delta_+\phi_j^{n+1}\right| \leqslant \sum_{j=0}^{M}\left|\Delta_+\phi_j^{n}\right|+\left|r^{n+1}-r^{n}\right|+\left|s^{n+1}-s^{n}\right|.$$

It follows by induction that

$$\sum_{j=0}^{M}\left|\phi_{j+1}^{n}-\phi_{j}^{n}\right| \leqslant \mathrm{TV}(\phi_0)+\mathrm{TV}(r)+\mathrm{TV}(s). \tag{1.29}$$

From (1.28) and (1.29) we get (1.25). □

Now, we prove some time continuity estimates. The proof of the first of them is very similar to that of [90, Lemma 5.5], so we omit the details.

Lemma 1.4. *The following discrete L^1 time continuity estimate holds for $n \geqslant 0$:*

$$\sum_{j=0}^{M+1}|\phi_j^{n+1}-\phi_j^{n+1/2}| \leqslant \Omega_1, \quad \Omega_1 := \mathrm{TV}(\phi_0)+\mathrm{TV}(r)+\mathrm{TV}(s)+2\phi_{\max}.$$

Lemma 1.5. *The following estimate holds:*

$$\sum_{j=1}^{M}\left|\phi_j^{1/2}-\phi_j^0\right| \leqslant \Omega_2, \quad \Omega_2 := \sum_{j=1}^{M}\left|g_V\left(\phi_{j+1}^0\right)-g_V\left(\phi_j^0\right)\right|+\mathrm{TV}(\phi_0)+\phi_{\max}. \tag{1.30}$$

Proof. We define $g_{V,j}^0 = g_V(\phi_j^0)$. The first equation in (1.13) with $n=0$ implies

$$\phi_j^{1/2}-\phi_j^0 = \lambda\phi_{j-1}^0\left(g_{V,j}^{1/2}-g_{V,j}^0\right)-\lambda\phi_j^0\left(g_{V,j+1}^{1/2}-g_{V,j+1}^0\right)-\lambda\phi_j^0\left(\Delta_+ g_{V,j}^0\right)-\lambda g_{V,j}^0\left(\Delta_+\phi_{j-1}^0\right).$$

Thus

$$\phi_j^{1/2}-\phi_j^0-\lambda\phi_{j-1}^0\left(g_{V,j}^{1/2}-g_{V,j}^0\right) = \lambda\phi_j^0\left(g_{V,j+1}^{1/2}-g_{V,j+1}^0\right)-\lambda\left(\phi_j^0\Delta_+ g_{V,j}^0+g_{V,j}^0\Delta_+\phi_{j-1}^0\right). \tag{1.31}$$

Taking absolute values in (1.31) and using (1.20) we find that

$$\left|\phi_j^{1/2}-\phi_j^0\right|+\lambda\phi_{j-1}^0\left|g_{V,j}^{1/2}-g_{V,j}^0\right| \leqslant \lambda\phi_j^0\left|g_{V,j+1}^{1/2}-g_{V,j+1}^0\right|+\lambda\phi_j^0\left|\Delta_+ g_{V,j}^0\right|+\lambda g_{V,j}^0\left|\Delta_+\phi_{j-1}^0\right|.$$

Summing over $j=1,\dots,M$ and cancelling telescoping terms yields

$$\begin{aligned}\sum_{j=1}^{M}\left|\phi_j^{1/2}-\phi_j^0\right|+\lambda\phi_0^0\left|g_{V,1}^{1/2}-g_{V,1}^0\right| &\leqslant \lambda\phi_M^0\left|g_{V,M+1}^{1/2}-g_{V,M+1}^0\right| \\ &\quad +\lambda\sum_{j=1}^{M}\phi_j^0\left|\Delta_+ g_{V,j}^0\right|+\lambda\sum_{j=1}^{M}g_{V,j}^0\left|\Delta_+\phi_{j-1}^0\right|.\end{aligned} \tag{1.32}$$

Applying the boundary condition in (1.32), Lemmas 1.1, 1.2, and the CFL condition (1.21) we get (1.30). □

Lemma 1.6. *There exists a constant Ω_3 that is independent of Δ such that the following time continuity estimate holds:*

$$\sum_{j=0}^{M+1}\left|\phi_j^{n+1/2}-\phi_j^{n-1/2}\right| \leqslant \Omega_3 \quad \text{for } n \geqslant 1. \tag{1.33}$$

Proof. For $n \geqslant 2$ and subtracting from the first half-step of (1.13) the corresponding formula for $\phi_j^{n-1/2}$ and rearranging terms we get

$$\begin{aligned}&\phi_j^{n+1/2} - \phi_j^{n-1/2} - \lambda\phi_{j-1}^{n-1}\big(g_{V,j}^{n+1/2} - g_{V,j}^{n-1/2}\big)\\ &= \big(1 - \lambda g_{V,j+1}^{n+1/2}\big)\big(\phi_j^n - \phi_j^{n-1}\big) + \lambda g_{V,j}^{n+1/2}\big(\phi_{j-1}^n - \phi_{j-1}^{n-1}\big) - \lambda\phi_j^{n-1}\big(g_{V,j+1}^{n+1/2} - g_{V,j+1}^{n-1/2}\big).\end{aligned}$$

Taking absolute values and applying the CFL condition (1.21) yields

$$\begin{aligned}&\big|\phi_j^{n+1/2} - \phi_j^{n-1/2} - \lambda\phi_{j-1}^{n-1}\big(g_{V,j}^{n+1/2} - g_{V,j}^{n-1/2}\big)\big|\\ &\leqslant \big(1 - \lambda g_{V,j+1}^{n+1/2}\big)\big|\phi_j^n - \phi_j^{n-1}\big| + \lambda g_{V,j}^{n+1/2}\big|\phi_{j-1}^n - \phi_{j-1}^{n-1}\big|\\ &\quad + \big|\lambda\phi_j^{n-1}\big(g_{V,j+1}^{n+1/2} - g_{V,j+1}^{n-1/2}\big)\big|.\end{aligned}$$

From (1.20) we get

$$\begin{aligned}&\big|\phi_j^{n+1/2} - \phi_j^{n-1/2}\big| + \big|\lambda\phi_{j-1}^{n-1}\big(g_{V,j}^{n+1/2} - g_{V,j}^{n-1/2}\big)\big|\\ &\leqslant \big(1 - \lambda g_{V,j+1}^{n+1/2}\big)\big|\phi_j^n - \phi_j^{n-1}\big| + \lambda g_{V,j}^{n+1/2}\big|\phi_{j-1}^n - \phi_{j-1}^{n-1}\big|\\ &\quad + \big|\lambda\phi_j^{n-1}\big(g_{V,j+1}^{n+1/2} - g_{V,j+1}^{n-1/2}\big)\big|.\end{aligned} \tag{1.34}$$

Summing over j and cancelling telescoping terms we obtain

$$\begin{aligned}\sum_{j=1}^M\big|\phi_j^{n+1/2} - \phi_j^{n-1/2}\big| \leqslant \sum_{j=1}^M\big|\phi_j^n - \phi_j^{n-1}\big| &+ \lambda g_{V,1}^{n+1/2}\big|\phi_0^n - \phi_0^{n-1}\big| + \lambda\phi_M^{n-1}\big|g_{V,M+1}^{n+1/2} - g_{V,M+1}^{n-1/2}\big|\\ &- \lambda g_{V,M+1}^{n+1/2}\big|\phi_M^n - \phi_M^{n-1}\big|.\end{aligned}$$

The last inequality implies

$$\sum_{j=1}^M\big|\phi_j^{n+1/2} - \phi_j^{n-1/2}\big| \leqslant \sum_{j=1}^M\big|\phi_j^n - \phi_j^{n-1}\big| + \big|r^n - r^{n-1}\big| + \big|\mathcal{G}(t^n) - \mathcal{G}(t^{n-1})\big|.$$

We observe that

$$\begin{aligned}\phi_j^n - \phi_j^{n-1} = \big(1 - B_{j+1/2}^{n-1} - A_{j-1/2}^{n-1}\big)\big(\phi_j^{n-1/2} - \phi_j^{n-3/2}\big)&\\ + A_{j+1/2}^{n-1}\big(\phi_{j+1}^{n-1/2} - \phi_{j+1}^{n-3/2}\big) + B_{j-1/2}^{n-1}\big(\phi_{j-1}^{n-1/2} - \phi_{j-1}^{n-3/2}\big),&\end{aligned} \tag{1.35}$$

where

$$\begin{aligned}A_{j+1/2}^{n-1} &= -\lambda\int_0^1 \partial_1\varphi\big(\theta\phi_{j+1}^{n-1/2} + (1-\theta)\theta\phi_{j+1}^{n-3/2}, \theta\phi_{j+1}^{n-1/2} + (1-\theta)\theta\phi_{j+1}^{n-3/2}\big)\,\mathrm{d}\theta,\\ B_{j+1/2}^{n-1} &= \lambda\int_0^1 \partial_2\varphi\big(\theta\phi_{j+1}^{n-1/2} + (1-\theta)\theta\phi_{j+1}^{n-3/2}, \theta\phi_{j+1}^{n-1/2} + (1-\theta)\theta\phi_{j+1}^{n-3/2}\big)\,\mathrm{d}\theta.\end{aligned}$$

Herein $\varphi(\phi_{j+1}, \phi_j) = \phi_j p_V(\phi_{j+1})$ and $\partial_i\varphi$ denotes the partial derivative of φ with respect to the i-th argument ($i = 1, 2$). Since $\phi, p_V(\phi) \geqslant 0$ and $p_V'(\phi) \leqslant 0$, the function $\varphi(\phi_{j+1}, \phi_j)$ is nonincreasing with respect to ϕ_{j+1} and nondecreasing with respect to ϕ_j. This implies (together with the CFL condition)

$$0 \leqslant A_{j+1/2}^{n-1}, B_{j+1/2}^{n-1} \leqslant \frac{1}{2}. \tag{1.36}$$

The remainder of the proof is similar to the proof of Lemma 5.6 in [90]. Details are omitted. □

Now, we are ready to prove the convergence of ϕ^Δ as $\Delta \to \mathbf{0}$.

Lemma 1.7. *The functions ϕ^Δ defined by (1.22) converge in $L^1(\Pi_T)$ and boundedly a.e. a along subsequence to a limit function $\phi \in C([0,T], L^1(-L,L)) \cap L^\infty(\Pi_T))$.*

Proof. The proof is a standard argument using the L^∞ estimate (Lemma 1.2), the uniform spatial variation bound (Lemma 1.3), and the L^1 Lipschitz continuity in time estimate (Lemma 1.6). □

In order to show that the limit function ϕ identified in Lemma 1.7 is a weak solution in the sense of Definition 1.1, we must also prove the convergence of the flux approximations. Instead of showing that the approximations $\{g_{V,j}^{n+1/2}\}$ converge we show that the approximations $\{h_j^{n+1/2}\}$ converge, where we define

$$h_j^{n+1/2} := \phi_j^{n+1/2} g_{V,j}^{n+1/2} \quad \text{for all } j = 1, \dots, M \text{ and } n = 0, \dots, \mathcal{N},$$

and extend these quantities to functions defined on Π_T by

$$h^\Delta(x,t) := \sum_{n=0}^{\mathcal{N}} \sum_{j=1}^{M} \chi_j(x) \chi^n(t) h_j^{n+1/2}.$$

Now, we require additional time continuity estimates, which is the contents of the following lemma. Its proof is very similar to that of Lemmas 5.8 and 5.9 in [90], and is therefore omitted.

Lemma 1.8. *The following uniform estimates hold for $n \geqslant 1$, where the constant Ω_4 is independent of Δ:*

$$\sum_{j=1}^{M} \left| \phi_j^{n+1} - \phi_j^n \right| \leqslant \Omega_4, \qquad \Omega_4 := \Omega_2 + \mathrm{TV}(s) + \mathrm{TV}(r), \tag{1.37}$$

$$\sum_{j=1}^{M} \left| \phi_j^{n+1/2} - \phi_j^n \right| \leqslant \Omega_1 + \Omega_4. \tag{1.38}$$

The following lemma is needed to establish a spatial variation bound on the approximations $h_j^{n+1/2}$.

Lemma 1.9. *There exists a constant Ω_5 that is independent of Δ such that*

$$\sum_{j=1}^{M} \phi_j^n \left| \Delta_+ g_{V,j}^{n+1/2} \right| \leqslant \Omega_5.$$

Proof. From the first half-step of the scheme we get

$$\phi_j^{n+1/2} - \phi_j^n = -\lambda \big(\phi_j^n \Delta_+ g_{V,j}^{n+1/2} + g_{V,j}^{n+1/2} \Delta_+ \phi_{j-1}^n \big),$$

which can be rerranged as

$$\lambda\phi_j^n\Delta_+ g_{V,j}^{n+1/2} = -\big(\phi_j^{n+1/2} - \phi_j^n\big) - \lambda g_{V,j}^{n+1/2}\Delta_+\phi_{j-1}^n.$$

Taking absolute values and summing over $j = 1, \dots, M$ we get

$$\lambda\sum_{j=1}^{M}\phi_j^n\big|\Delta_+ g_{V,j}^{n+1/2}\big| \leqslant \sum_{j=1}^{M}\big|\phi_j^{n+1/2} - \phi_j^n\big| + \lambda\sum_{j=1}^{M} g_{V,j}^{n+1/2}\big|\Delta_+\phi_{j-1}^n\big|.$$

From Lemma 1.1 and the CFL condition (1.21) we have

$$\sum_{j=1}^{M}\phi_j^n\big|\Delta_+ g_{V,j}^{n+1/2}\big| \leqslant \frac{1}{\lambda}\sum_{j=1}^{M}\big|\phi_j^{n+1/2} - \phi_j^n\big| + \sum_{j=1}^{M}\big|\Delta_+\phi_{j-1}^n\big|.$$

The result is obtained from (1.38) in Lemma 1.8 and Lemma 1.3. □

We are now ready to bound the spatial variation of the approximations $h_j^{n+1/2}$.

Lemma 1.10. *There exists a constant Ω_6 that is independent of Δ such that*

$$\sum_{j=1}^{M}|h_{j+1}^{n+1/2} - h_j^{n+1/2}| \leqslant \Omega_6. \tag{1.39}$$

Proof. The first part of scheme (1.13) can be written as

$$\phi_j^{n+1/2} = \phi_j^n - \lambda\big(\phi_j^n g_{V,j+1}^{n+1/2} + g_{V,j}^{n+1/2}\big(\phi_j^{n+1/2} - \phi_{j-1}^n\big)\big) + \lambda\phi_j^{n+1/2} g_{V,j}^{n+1/2}.$$

Applying the spatial difference operator to the above equation we get

$$\begin{aligned}\Delta_+\phi_j^{n+1/2} = {} & \big(1 - \lambda g_{V,j+1}^{n+1/2}\big)\Delta_+\phi_j^n + \lambda\Delta_+ h_j^{n+1/2} - \lambda\phi_{j+1}^n\Delta_+ g_{V,j+1}^{n+1/2} \\ & - \lambda\Delta_+ g_{V,j}^{n+1/2}\big(\phi_j^{n+1/2} - \phi_j^n\big) + \lambda g_{V,j}^{n+1/2}\Delta_+\phi_{j-1}^n - \lambda g_{V,j+1}^{n+1/2}\Delta_+\phi_j^{n+1/2}.\end{aligned}$$

Thus

$$\begin{aligned}\lambda\Delta_+ h_j^{n+1/2} = {} & \Delta_+\phi_j^{n+1/2} - \big(1 - \lambda g_{V,j+1}^{n+1/2}\big)\Delta_+\phi_j^n + \lambda\phi_{j+1}^n\Delta_+ g_{V,j+1}^{n+1/2} \\ & + \lambda\Delta_+ g_{V,j}^{n+1/2}\big(\phi_j^{n+1/2} - \phi_j^n\big) + \lambda g_{V,j}^{n+1/2}\Delta_+\phi_{j-1}^n + \lambda g_{V,j+1}^{n+1/2}\Delta_+\phi_j^{n+1/2}.\end{aligned}$$

After taking absolute values and using $|\Delta_+ g_{V,j}^{n+1/2}| \leqslant \alpha_V$, Lemma 1.1 and the CFL condition (1.21) we get

$$\begin{aligned}&\lambda\big|\Delta_+ h_j^{n+1/2}\big| \\ &\leqslant 2\big|\Delta_+\phi_j^{n+1/2}\big| + \big|\Delta_+\phi_j^n\big| + \lambda\phi_{j+1}^n\big|\Delta_+ g_{V,j+1}^{n+1/2}\big| + \big|\phi_j^{n+1/2} - \phi_j^n\big| + \big|\Delta_+\phi_{j-1}^n\big|.\end{aligned}$$

Summing over $j = 1, \dots, M$ we get

$$\sum_{j=1}^{M}\big|\Delta_+ h_j^{n+1/2}\big| \leqslant \frac{2}{\lambda}\sum_{j=1}^{M}\big|\Delta_+\phi_j^{n+1/2}\big| + \frac{2}{\lambda}\sum_{j=1}^{M}\big|\Delta_+\phi_j^n\big| + \frac{1}{\lambda}\sum_{j=1}^{M}\big|\phi_j^{n+1/2} - \phi_j^n\big| + \sum_{j=1}^{M}\phi_{j+1}^n\big|\Delta_+ g_{V,j+1}^{n+1/2}\big|.$$

Finally, the result follows from Lemma 1.3, (1.38) in Lemma 1.8, and Lemma 1.9. □

The following lemma is required to prove the L^1 Lipschitz continuity in time and spatial variation bounds on $\{h_j^{n+1/2}\}$.

Lemma 1.11. *There exists a constant Ω_7 that is independent of Δ such that*

$$\Delta x \sum_{j=1}^{M}\sum_{n=1}^{\mathcal{N}} \phi_j^{n-1}\left|g_{V,j+1}^{n+1/2}-g_{V,j+1}^{n-1/2}\right| \leqslant \Omega_7. \tag{1.40}$$

Proof. From (1.34) we get

$$\begin{aligned}\lambda\phi_j^{n-1}\left|g_{V,j+1}^{n+1/2}-g_{V,j+1}^{n-1/2}\right| \leqslant \left(1-\lambda g_{V,j+2}^{n+1/2}\right)\left|\phi_{j+1}^{n}-\phi_{j+1}^{n-1}\right| + \lambda g_{V,j+1}^{n+1/2}\left|\phi_j^n-\phi_j^{n-1}\right| \\ -\left|\phi_{j+1}^{n+1/2}-\phi_{j+1}^{n-1/2}\right| + \lambda\phi_{j+1}^{n-1}\left|g_{V,j+2}^{n+1/2}-g_{V,j+2}^{n-1/2}\right|.\end{aligned}$$

By induction we obtain

$$\begin{aligned}\lambda\phi_j^{n-1}\left|g_{V,j+1}^{n+1/2}-g_{V,j+1}^{n-1/2}\right| \leqslant \sum_{k=j+1}^{M}\left|\phi_k^n-\phi_k^{n-1}\right| + \left|g_{V,M+1}^{n+1/2}-g_{V,M+1}^{n-1/2}\right| \\ -\sum_{k=j+1}^{M}\left|\phi_k^{n+1/2}-\phi_k^{n-1/2}\right| + \left|\phi_j^n-\phi_j^{n-1}\right|.\end{aligned} \tag{1.41}$$

Recalling (1.35) we have

$$\begin{aligned}\sum_{k=j+1}^{M}\left|\phi_k^n-\phi_k^{n-1}\right| \leqslant \sum_{k=j+1}^{M}\left(1-B_{k+1/2}^{n-1}-A_{k-1/2}^{n-1}\right)\left|\phi_k^{n-1/2}-\phi_k^{n-3/2}\right| \\ +\sum_{k=j+1}^{M}A_{k+1/2}^{n-1}\left|\phi_{k+1}^{n-1/2}-\phi_{k+1}^{n-3/2}\right| + \sum_{k=j+1}^{M}B_{k-1/2}^{n-1}\left|\phi_{k-1}^{n-1/2}-\phi_{k-1}^{n-3/2}\right|.\end{aligned}$$

Cancelling telescoping terms and applying (1.36) yields

$$\sum_{k=j+1}^{M}\left|\phi_k^n-\phi_k^{n-1}\right| \leqslant \sum_{k=j+1}^{M}\left|\phi_k^{n-1/2}-\phi_k^{n-3/2}\right| + \frac{1}{2}\left|\phi_{M+1}^{n-1/2}-\phi_{M+1}^{n-3/2}\right| + \frac{1}{2}\left|\phi_j^{n-1/2}-\phi_j^{n-3/2}\right|.$$

Then (1.41) becomes

$$\begin{aligned}&\lambda\phi_j^{n-1}\left|g_{V,j+1}^{n+1/2}-g_{V,j+1}^{n-1/2}\right| \\ &\leqslant \sum_{k=j+1}^{M}\left|\phi_k^{n-1/2}-\phi_k^{n-3/2}\right| - \sum_{k=j+1}^{M}\left|\phi_k^{n+1/2}-\phi_k^{n-1/2}\right| + \frac{1}{2}\left|\phi_{M+1}^{n-1/2}-\phi_{M+1}^{n-3/2}\right| \\ &\quad + \frac{1}{2}\left|\phi_j^{n-1/2}-\phi_j^{n-3/2}\right| + \left|\phi_j^n-\phi_j^{n-1}\right| + \left|g_{V,M+1}^{n+1/2}-g_{V,M+1}^{n-1/2}\right|.\end{aligned}$$

Summing over $n \geqslant 2$ and $j = 1, \dots, M$, cancelling telescoping terms and multiplying the result by Δx we get

$$\Delta x \sum_{j=1}^{M} \sum_{n=2}^{\mathcal{N}} \phi_j^{n-1} \big| g_{V,j+1}^{n+1/2} - g_{V,j+1}^{n-1/2} \big| \leqslant S_1 + \cdots + S_5,$$

where we define

$$\begin{aligned}
S_1 &:= \frac{2L}{\lambda} \sum_{j=1}^{M} \big| \phi_j^{3/2} - \phi_j^{1/2} \big|, \quad S_2 := \frac{L}{\lambda} \sum_{n=2}^{\mathcal{N}} \big| s^{n-1/2} - s^{n-3/2} \big|, \\
S_3 &:= \frac{\Delta x}{\lambda} \sum_{j=1}^{M} \sum_{n=2}^{\mathcal{N}} \big| \phi_j^{n} - \phi_j^{n-1} \big|, \quad S_4 := \frac{2L}{\lambda} \sum_{n=2}^{\mathcal{N}} \big| g_{V,M+1}^{n+1/2} - g_{V,M+1}^{n-1/2} \big|, \\
S_5 &:= \frac{\Delta x}{2\lambda} \sum_{j=1}^{M} \sum_{n=2}^{\mathcal{N}} \big| \phi_j^{n-1/2} - \phi_j^{n-3/2} \big|.
\end{aligned}$$

In view of the bounds established so far, there holds

$$S_1 \leqslant \frac{2L}{\lambda} \Omega_3, \quad S_2 \leqslant \frac{L}{\lambda} \mathrm{TV}(s), \quad S_3 \leqslant \Omega_4 T, \quad S_4 \leqslant \frac{2L}{\lambda} \mathrm{TV}(\mathcal{G}), \quad S_5 \leqslant \frac{\Omega_3}{2} T.$$

These bounds in conjunction with $|g_{V,j}^{3/2} - g_{V,j}^{1/2}| \leqslant \alpha_V$ imply that there exists a constant Ω_7 such that (1.40) is valid. □

Lemma 1.12. *There exists a constant Ω_8 that is independent of Δ such that*

$$\Delta t \sum_{n=0}^{\mathcal{N}} \sum_{j=1}^{M} \big| h_{j+1}^{n+1/2} - h_j^{n+1/2} \big| + \Delta x \sum_{n=1}^{\mathcal{N}} \sum_{j=1}^{M} \big| h_j^{n+1/2} - h_j^{n-1/2} \big| \leqslant \Omega_8. \tag{1.42}$$

Proof. In light of the spatial variation bound (1.39) we find that

$$\Delta t \sum_{n=0}^{\mathcal{N}} \sum_{j=1}^{M} \big| h_{j+1}^{n+1/2} - h_j^{n+1/2} \big| \leqslant \Omega_6 T.$$

The first part of (1.13) implies

$$\begin{aligned}
\phi_j^{n+1/2} - \phi_j^{n-1/2} &= \big(1 - \lambda g_{V,j+1}^{n+1/2}\big)\big(\phi_j^n - \phi_j^{n-1}\big) + \lambda\big(h_j^{n+1/2} - h_j^{n-1/2}\big) - \lambda g_{V,j}^{n+1/2}\big(\phi_j^{n+1/2} - \phi_{j-1}^n\big) \\
&\quad + \lambda g_{V,j}^{n-1/2}\big(\phi_j^{n-1/2} - \phi_{j-1}^{n-1}\big) - \lambda \phi_j^{n-1}\big(g_{V,j+1}^{n+1/2} - g_{V,j+1}^{n-1/2}\big) \\
&= \big(1 - \lambda g_{V,j+1}^{n+1/2}\big)\big(\phi_j^n - \phi_j^{n-1}\big) + \lambda\big(h_j^{n+1/2} - h_j^{n-1/2}\big) - \lambda g_{V,j}^{n+1/2}\big(\phi_j^{n+1/2} - \phi_j^n\big) \\
&\quad - \lambda g_{V,j}^{n+1/2} \Delta_+ \phi_{j-1}^n + \lambda g_{V,j}^{n-1/2} \Delta_+ \phi_{j-1}^{n-1} + \lambda g_{V,j}^{n-1/2}\big(\phi_j^{n-1/2} - \phi_j^{n-1}\big) \\
&\quad - \lambda \phi_j^{n-1}\big(g_{V,j+1}^{n+1/2} - g_{V,j+1}^{n-1/2}\big).
\end{aligned}$$

Consequently,

$$\begin{aligned}\lambda\big(h_j^{n+1/2}-h_j^{n-1/2}\big) &= \big(\phi_j^{n+1/2}-\phi_j^{n-1/2}\big)-\big(1-\lambda g_{V,j+1}^{n+1/2}\big)\big(\phi_j^n-\phi_j^{n-1}\big)+\lambda g_{V,j}^{n+1/2}\big(\phi_j^{n+1/2}-\phi_j^n\big)\\ &\quad+\lambda g_{V,j}^{n+1/2}\Delta_+\phi_{j-1}^n-\lambda g_{V,j}^{n-1/2}\Delta_+\phi_{j-1}^{n-1}-\lambda g_{V,j}^{n-1/2}\big(\phi_j^{n-1/2}-\phi_j^{n-1}\big)\\ &\quad+\lambda\phi_j^{n-1}\big(g_{V,j+1}^{n+1/2}-g_{V,j+1}^{n-1/2}\big).\end{aligned}$$

Taking absolute values and using the CFL condition (1.21) we get

$$\begin{aligned}\lambda\big|h_j^{n+1/2}-h_j^{n-1/2}\big| &\leqslant \big|\phi_j^{n+1/2}-\phi_j^{n-1/2}\big|+\big|\phi_j^n-\phi_j^{n-1}\big|+\big|\Delta_+\phi_{j-1}^n\big|+\big|\Delta_+\phi_{j-1}^{n-1}\big|\\ &\quad+\big|\phi_j^{n+1/2}-\phi_j^n\big|+\big|\phi_j^{n-1/2}-\phi_j^{n-1}\big|+\lambda\phi_j^{n-1}\big|g_{V,j+1}^{n+1/2}-g_{V,j+1}^{n-1/2}\big|.\end{aligned}$$

Multiplying this inequality by Δx and summing over j and n we get

$$\Delta x\sum_{n=1}^{\mathcal{N}}\sum_{j=1}^{M}\big|h_j^{n+1/2}-h_j^{n-1/2}\big|\leqslant U_1+\cdots+U_5,$$

where we define

$$\begin{aligned}U_1&:=\frac{\Delta x}{\lambda}\sum_{n=1}^{\mathcal{N}}\sum_{j=1}^{M}\big|\phi_j^{n+1/2}-\phi_j^{n-1/2}\big|,\quad U_2:=\frac{\Delta x}{\lambda}\sum_{n=1}^{\mathcal{N}}\sum_{j=1}^{M}\big|\phi_j^n-\phi_j^{n-1}\big|,\\ U_3&:=\frac{2\Delta x}{\lambda}\sum_{n=1}^{\mathcal{N}}\sum_{j=1}^{M}\big|\Delta_+\phi_{j-1}^n\big|,\quad U_4:=\frac{2\Delta x}{\lambda}\sum_{n=1}^{\mathcal{N}}\sum_{j=1}^{M}\big|\phi_j^{n+1/2}-\phi_j^n\big|,\\ U_5&:=\Delta x\sum_{n=1}^{\mathcal{N}}\sum_{j=1}^{M}\phi_j^{n-1}\big|g_{V,j+1}^{n+1/2}-g_{V,j+1}^{n-1/2}\big|.\end{aligned}$$

From (1.25), (1.33), (1.37), (1.38) and (1.40) we have

$$\begin{aligned}&U_1\leqslant\Omega_3T,\quad U_2\leqslant\Omega_4T,\quad U_3\leqslant 2\big(\mathrm{TV}(\phi_0)+\mathrm{TV}(s)+\mathrm{TV}(r)\big)T,\\ &U_4\leqslant 2\big(\Omega_1+\Omega_4\big)T,\quad U_5\leqslant\Omega_7.\end{aligned}$$

Combining these bounds we see that there exists a constant Ω_8 that is independent of Δ such that (1.42) is valid. □

Lemma 1.13. *The functions h^Δ converge in $L^1(\Pi_T)$ and boundedly a.e. along subsequence to some limit function $w\in L^1(-L,L)\cap L^\infty(-L,L)$. Moreover, by a suitable choice of a subsequence, we have $w(x,t)\in\tilde{Q}(\phi(x,t))$ a.e. in Π_T, where $\phi(x,t)$ is the limit of Lemma 1.7.*

Proof. We observe that $|h_j^{n+1/2}|\leqslant\phi_{\max}\alpha_V$. Then by Helly's theorem [54] there exists a function $w\in L^1(\Pi_T)$ such that $h^\Delta\to w$ along a subsequence in $L^1(\Pi_T)$ and boundedly a.e. in Π_T. To prove the second assertion, we define $Q(\phi):=\phi g_V(\phi)$ and $\tilde{Q}$ denote the multivalued version of Q. Assume (by extracting further subsequences if necessary) that $\phi^\Delta\to\phi$, $h^\Delta\to w$ in $L^1(\Pi_T)$ and fix a point $(x,t)\in\Pi_T$ where $\phi^\Delta(x,t)\to\phi(x,t)$ and $h^\Delta(x,t)\to w(x,t)$ as $\Delta\to\mathbf{0}$. First,

we consider the case $\phi(x,t) = \phi^*$. Lemma 1.1 implies that $0 \leqslant h^\Delta(x,t) \leqslant \alpha_V \phi^\Delta(x,t)$. Then passing to the limit in the above inequality we obtain

$$w(x,t) \in [0, \alpha_V \phi^*] = \tilde{Q}(\phi^*).$$

In case $\phi(x,t) \neq \phi^*$ first we consider $\phi(x,t) < \phi^*$, then $\tilde{Q}(\phi(x,t)) = \alpha_V \phi(x,t)$. For sufficiently small Δ the inequality $\phi^\Delta(x,t) < \phi^*$ implies that $\phi_j^{n+1/2} < \phi^*$ and $\tilde{g}_V(\phi_j^{n+1/2}) = \{\alpha_V\}$. Then, by Lemma 1.1 we get

$$h^\Delta(x,t) = \sum_{n=0}^{\mathcal{N}} \sum_{j=1}^{M} \chi_j(x)\chi^n(t) h_j^{n+1/2} = \alpha_V \sum_{n=0}^{\mathcal{N}} \sum_{j=1}^{M} \chi_j(x)\chi^n(t)\phi_j^{n+1/2} = \alpha_V \phi^\Delta(x,t).$$

Thus $w(x,t) = \lim h^\Delta(x,t) = \alpha_V \lim \phi^\Delta(x,t) = \alpha_V \phi(x,t) = \tilde{Q}(\phi(x,t))$.

In the case $\phi(x,t) > \phi^*$ there holds $\tilde{Q}(\phi(x,t)) = 0$. In this case it is necessary extend $\{g_{V,j}^{n+1/2}\}$ to functions defined on Π_T by

$$g_V^\Delta(x,t) = \sum_{n=0}^{\mathcal{N}} \sum_{j=1}^{M} \chi_j(x)\chi^n(t) g_{V,j}^{n+1/2},$$

and we need to utilize the following consequence of Lemma 1.1:

$$g_V^\Delta(x,t) \in \tilde{g}_V(\phi^\Delta(x,t)), \quad (x,t) \in \Pi_T.$$

For sufficiently small Δ, $\phi^\Delta(x,t) > \phi^*$ implies that $\tilde{g}_V(\phi^\Delta(x,t)) = \{0\}$, hence $g_V^\Delta(x,t) = 0$. Finally observe that $0 \leqslant h^\Delta(x,t) \leqslant \phi^\Delta(x,t) \cdot g_V^\Delta(x,t) = 0$ for sufficiently small Δ. Hence $w(x,t) = \tilde{Q}(\phi(x,t)) = 0$. □

Theorem 1.1 (Main result)**.** *The functions ϕ^Δ converge in $L^1(\Pi_T)$ and boundedly a.e. along subsequence to some $\phi \in C([0,T], L^1(-L,L)) \cap L^\infty(\Pi_T)$. The limit function $\phi(x,t)$ is a weak solution in sense of Definition 1.1.*

Proof. The convergence is ensured by Lemma 1.7. It remains to prove that the limit ϕ is a weak solution. Let us fix a point $(x,t) \in \Pi_T$, then Lemma 1.13 implies that $w(x,t) \in \tilde{Q}(\phi(x,t))$ a.e. in Π_T. If $\phi(x,t) \neq \phi^*$, then $\tilde{Q}(\phi(x,t)) = Q(\phi(x,t))$. Thus $w(x,t) = Q(\phi(x,t))$, then we define $q(x,t) = \phi p_V(\phi) + Q(\phi(x,t)) = f(\phi(x,t))$. In the case where $\phi(x,t) = \phi^*$ we take $w(x,t) \in [0, \alpha_V \phi^*]$ and define

$$q(x,t) = \phi^* p_V(\phi^*) + w(x,t) \in [\phi^* p_V(\phi^*), \phi^* p_V(\phi^*) + \alpha_V \phi^*] = \tilde{f}(\phi^*).$$

In either case $q(x,t) \in \tilde{f}(\phi(x,t))$.

We note that the two steps of (1.13) imply

$$\phi_j^{n+1} - \phi_j^n + \lambda\big(\phi_j^n g_{V,j+1}^{n+1/2} - \phi_{j-1}^n g_{V,j}^{n+1/2} + \phi_j^{n+1/2} p_{V,j+1}^{n+1/2} - \phi_{j-1}^{n+1/2} p_{V,j}^{n+1/2}\big) = 0. \tag{1.43}$$

We now choose a test function $\psi \in C_0^1((-L,L)\times[0,T))$ and define $\psi_j^n := \psi(x_j,t^n)$. Multiplying (1.43) by $\Delta x \psi_j^n$ and summing the result over j and n yields

$$\Delta x\Delta t\sum_{n=0}^{\mathcal{N}}\sum_{j=1}^{M}\frac{\phi_j^{n+1}-\phi_j^n}{\Delta t}\psi_j^n+\Delta x\Delta t\sum_{n=0}^{\mathcal{N}}\sum_{j=1}^{M}\frac{\phi_j^n g_{V,j+1}^{n+1/2}-\phi_{j-1}^n g_{V,j}^{n+1/2}}{\Delta x}\psi_j^n$$
$$+\Delta x\Delta t\sum_{n=0}^{\mathcal{N}}\sum_{j=1}^{M}\frac{\phi_j^{n+1/2}p_{V,j+1}^{n+1/2}-\phi_{j-1}^{n+1/2}p_{V,j}^{n+1/2}}{\Delta x}\psi_j^n=0.$$

A summation by parts yields

$$\Delta x\Delta t\sum_{n=0}^{\mathcal{N}}\sum_{j=1}^{M}\phi_j^{n+1}\frac{\psi_j^{n+1}-\psi_j^n}{\Delta t}+\Delta x\sum_{j=1}^{M}\phi_j^0\psi_j^0+\Delta x\Delta t\sum_{n=0}^{\mathcal{N}}\sum_{j=1}^{M}\frac{\psi_{j+1}^n-\psi_j^n}{\Delta x}\phi_j^n g_{V,j+1}^{n+1/2}$$
$$+\Delta x\Delta t\sum_{n=0}^{\mathcal{N}}\sum_{j=1}^{M}\frac{\psi_{j+1}^n-\psi_j^n}{\Delta x}\phi_j^{n+1/2}p_{V,j+1}^{n+1/2}=0. \tag{1.44}$$

An application of (1.19) yields, as $\Delta x,\Delta t\to 0$,

$$\Delta x\Delta t\sum_{n=0}^{\mathcal{N}}\sum_{j=1}^{M}\phi_j^{n+1}\frac{\psi_j^{n+1}-\psi_j^n}{\Delta t}=\Delta x\Delta t\sum_{n=0}^{\mathcal{N}}\sum_{j=1}^{M}\phi_j^{n+1/2}\frac{\psi_j^{n+1}-\psi_j^n}{\Delta t}+\mathcal{O}(\Delta x).$$

This equation and Lemma 1.2.3 imply that the two first sums in (1.44) converge to

$$\int_0^T\int_{-L}^{L}\phi\psi_t\,\mathrm{d}x\,\mathrm{d}t+\int_{-L}^{L}\phi_0(x)\psi(x,0)\,\mathrm{d}x\,\mathrm{d}t$$

Concerning the last term in (1.44), we get

$$\Delta x\Delta t\sum_{n=0}^{\mathcal{N}}\sum_{j=1}^{M}\frac{\psi_{j+1}^n-\psi_j^n}{\Delta x}\phi_j^{n+1/2}p_{V,j+1}^{n+1/2}$$
$$=\Delta x\Delta t\sum_{n=0}^{\mathcal{N}}\sum_{j=1}^{M}\frac{\psi_{j+1}^n-\psi_j^n}{\Delta x}\phi_j^{n+1/2}p_{V,j}^{n+1/2}$$
$$+\Delta x\Delta t\sum_{n=0}^{\mathcal{N}}\sum_{j=1}^{M}\frac{\psi_{j+1}^n-\psi_j^n}{\Delta x}\big(\phi_j^{n+1/2}p_{V,j+1}^{n+1/2}-\phi_j^{n+1/2}p_{V,j}^{n+1/2}\big).$$

By properties of the function p_V we get the estimate

$$\phi_j^{n+1/2}p_{V,j+1}^{n+1/2}-\phi_j^{n+1/2}p_{V,j}^{n+1/2}=\phi_j^{n+1/2}\big(p_{V,j+1}^{n+1/2}-p_{V,j}^{n+1/2}\big)\leqslant\phi_{\max}\|p_V'\|_\infty\Delta x.$$

Thus

$$\left|\Delta x\Delta t\sum_{n=0}^{\mathcal{N}}\sum_{j=1}^{M}\frac{\big(\psi_{j+1}^n-\psi_j^n\big)}{\Delta x}\big(\phi_j^{n+1/2}p_{V,j+1}^{n+1/2}-\phi_j^{n+1/2}p_{V,j}^{n+1/2}\big)\right|$$
$$\leqslant 2MT\phi_{\max}\Delta x\|\partial_t\psi\|_\infty\|p_V'\|_\infty,$$

which goes to zero as $\Delta x \to 0$. Therefore the last term in (1.44) converges to

$$\int_0^T \int_{-L}^{L} \phi p_V(\phi) \psi_x \,\mathrm{d}x \,\mathrm{d}t$$

as $\Delta x \to 0$. The second term in (1.44) can be written as

$$\begin{aligned}
&\Delta x \Delta t \sum_{n=0}^{\mathcal{N}} \sum_{j=1}^{M} \frac{\psi_{j+1}^n - \psi_j^n}{\Delta x} \phi_j^n g_{V,j+1}^{n+1/2} \\
&= \Delta x \Delta t \sum_{n=0}^{\mathcal{N}} \sum_{j=1}^{M} \frac{\psi_{j+1}^n - \psi_j^n}{\Delta x} \phi_j^{n+1/2} g_{V,j}^{n+1/2} + \Delta x \Delta t \sum_{n=0}^{\mathcal{N}} \sum_{j=1}^{M} \frac{\psi_{j+1}^n - \psi_j^n}{\Delta x} \phi_j^n \Delta_+ g_{V,j}^{n+1/2} \\
&\quad + \Delta x \Delta t \sum_{n=0}^{\mathcal{N}} \sum_{j=1}^{M} \frac{\psi_{j+1}^n - \psi_j^n}{\Delta x} g_{V,j}^{n+1/2} \big(\phi_j^n - \phi_j^{n+1/2}\big).
\end{aligned}$$

Using Lemmas 1.9, 1.1, and 1.8 we get

$$\begin{aligned}
\left| \Delta x \Delta t \sum_{n=0}^{\mathcal{N}} \sum_{j=1}^{M} \frac{\psi_{j+1}^n - \psi_j^n}{\Delta x} \phi_j^n \Delta_+ g_{V,j}^{n+1/2} \right| &\leqslant \Delta x \|\partial_x \psi\|_\infty \Omega_5 T, \\
\left| \Delta x \Delta t \sum_{n=0}^{\mathcal{N}} \sum_{j=1}^{M} \frac{\psi_{j+1}^n - \psi_j^n}{\Delta x} g_{V,j}^{n+1/2} \big(\phi_j^n - \phi_j^{n+1/2}\big) \right| &\leqslant \alpha_V \Delta x \|\partial_x \psi\|_\infty \big(\Omega_1 + \Omega_4\big) T.
\end{aligned}$$

Consequently, as $\Delta x \to 0$,

$$\begin{aligned}
\Delta x \Delta t \sum_{n=0}^{\mathcal{N}} \sum_{j=1}^{M} \frac{\psi_{j+1}^n - \psi_j^n}{\Delta x} \phi_j^n \Delta_+ g_{V,j}^{n+1/2} &\to 0, \\
\Delta x \Delta t \sum_{n=0}^{\mathcal{N}} \sum_{j=1}^{M} \frac{\psi_{j+1}^n - \psi_j^n}{\Delta x} g_{V,j}^{n+1/2} \big(\phi_j^n - \phi_j^{n+1/2}\big) &\to 0.
\end{aligned}$$

Then substituting $g_V^{\Delta}(x_j, t^n) = g_{V,j}^{n+1/2}$ and applying the dominated convergence theorem we obtain that the second term in (1.44) converges to

$$\int_0^T \int_{-L}^{L} w \psi_x \,\mathrm{d}x \,\mathrm{d}t.$$

Collecting the previous results we get

$$\int_0^T \int_{-L}^{L} (\phi \psi_t + q \psi_x) \,\mathrm{d}x \,\mathrm{d}t + \int_{-L}^{L} \phi_0(x) \psi(x, 0) \,\mathrm{d}x = 0,$$

so ϕ is a weak solution in sense of Definition 1.1. □

1.3 Extension to the MCLWR model

Algorithm 1.1 cannot be applied directly in a component-wise manner for each class i in the multiclass case (1.1)–(1.4), but we can first solve for the total density ϕ and then update the densities $\phi_1, \dots, \phi_N$ for each class. The multiclass version of the scalar scheme (1.6) can be written as

$$\begin{aligned} \phi_{i,j}^{n+1/2} &= \phi_{i,j}^{n} - \lambda v_i^{\max}\big(\phi_{i,j}^{n} g_V\big(\phi_{j+1}^{n+1/2}\big) - \phi_{i,j-1}^{n} g_V\big(\phi_{j}^{n+1/2}\big)\big), \\ \phi_{i,j}^{n+1} &= \phi_{i,j}^{n+1/2} - \lambda v_i^{\max}\big(\phi_{i,j}^{n+1/2} p_V\big(\phi_{j+1}^{n+1/2}\big) - \phi_{i,j-1}^{n+1/2} p_V\big(\phi_{j}^{n+1/2}\big)\big), \\ & i = 1, \dots, N, \quad j = 1, \dots, M, \end{aligned} \tag{1.45}$$

where the following quantity is an approximate value of the total density ϕ:

$$\phi_j^{n+1/2} := \phi_{1,j}^{n+1/2} + \cdots + \phi_{N,j}^{n+1/2}.$$

In order to solve (1.45), we need to impose the non-standard boundary condition (1.4b). Recalling that $V(\phi) = g_V(\phi) + p_V(\phi)$ we can equivalently specify for the multiclass case the condition (1.9). The correspondence when $s(t) = \phi^*$ is

$$\begin{aligned} \boldsymbol{\mathcal{F}}(t) &= (\boldsymbol{v}^{\max})^{\mathrm{T}} \boldsymbol{s}(t) V(\phi^* -) \Leftrightarrow \mathcal{G}(t) = \alpha_V, \\ \boldsymbol{\mathcal{F}}(t) &= (\boldsymbol{v}^{\max})^{\mathrm{T}} \boldsymbol{s}(t) V(\phi^* +) \Leftrightarrow \mathcal{G}(t) = 0. \end{aligned} \tag{1.46}$$

Coming back to (1.45), we define $\Phi_j^n := (\phi_{1,j}^n, \dots, \phi_{N,j}^n)^{\mathrm{T}}$. Summing over $i = 1, \dots, N$, assuming that g_V is evaluated at the new time step, and replacing $g_V(\phi_{j+1}^{n+1/2})$ by $g_{V,j+1}^{n+1/2}$, we get

$$\phi_j^{n+1/2} = \phi_j^n - \lambda (\boldsymbol{v}^{\max})^{\mathrm{T}} \big(g_{V,j+1}^{n+1/2} \Phi_j^n - g_V\big(\phi_j^{n+1/2}\big) \Phi_{j-1}^n\big). \tag{1.47}$$

This can be rearranged as

$$\phi_j^{n+1/2} - \lambda (\boldsymbol{v}^{\max})^{\mathrm{T}} \Phi_{j-1}^n g_V\big(\phi_j^{n+1/2}\big) = \phi_j^n - \lambda (\boldsymbol{v}^{\max})^{\mathrm{T}} \Phi_j^n g_{V,j+1}^{n+1/2}. \tag{1.48}$$

Let us now define the function

$$G_V(z; \Phi) := z - \lambda (\boldsymbol{v}^{\max})^{\mathrm{T}} \Phi g_V(z)$$

and denote by $\tilde{G}_V(\cdot; \Phi)$ its multivalued version (with respect to z). Then $\tilde{G}$ is strictly increasing and has a unique inverse $z \mapsto \tilde{G}_V^{-1}(z; \Phi)$. Expressing (1.48) as

$$\tilde{G}_V\big(\phi_j^{n+1/2}; \Phi_{j-1}^n\big) = \phi_j^n - \lambda (\boldsymbol{v}^{\max})^{\mathrm{T}} \Phi_j^n g_{V,j+1}^{n+1/2} \tag{1.49}$$

which allows us to obtain $\phi_j^{n+1/2}$ by applying $\tilde{G}_V^{-1}(z; \Phi)$ to both sides, that is

$$\phi_j^{n+1/2} = \tilde{G}_V^{-1}\big(\phi_j^n - \lambda (\boldsymbol{v}^{\max})^{\mathrm{T}} \Phi_j^n g_{V,j+1}^{n+1/2}; \Phi_{j-1}^n\big).$$

Now that $\phi_j^{n+1/2}$ is available, we solve for $g_{V,j}^{n+1/2}$ the equation

$$\phi_j^{n+1/2} = \phi_j^n - \lambda(\boldsymbol{v}^{\max})^{\mathrm{T}}\big(g_{V,j+1}^{n+1/2}\Phi_j^n - g_{V,j}^{n+1/2}\Phi_{j-1}^n\big)$$

(cf. (1.47)). This yields

$$g_{V,j}^{n+1/2} = \frac{\phi_j^{n+1/2} - \phi_j^n + \lambda g_{V,j+1}^{n+1/2}(\boldsymbol{v}^{\max})^{\mathrm{T}}\Phi_j^n}{\lambda(\boldsymbol{v}^{\max})^{\mathrm{T}}\Phi_{j-1}^n},$$

provided that $\Phi_{j-1}^n \neq \mathbf{0}$. If $\Phi_{j-1}^n = \mathbf{0}$ then we set $g_{V,j}^{n+1/2} = g_V(\phi_j^{n+1/2})$. The numerical scheme for the multiclass model can be summarized in the following algorithm.

Algorithm 1.2 (BCOV scheme, multiclass case)**.**

Input: approximate solution vector $\{\phi_{i,j}^n\}_{j=1}^M$, $i = 1, \ldots, N$ for $t = t^n$

$g_{V,M+1}^{n+1/2} \leftarrow \mathcal{G}(\phi_{M+1}^{n+1/2})$ *(using (1.10) and (1.46))*

do $j = M, M-1, \ldots, 1$

$\phi_j^{n+1/2} \leftarrow \tilde{G}_V^{-1}\big(\phi_j^n - \lambda g_{V,j+1}^{n+1/2}(\boldsymbol{v}^{\max})^{\mathrm{T}}\Phi_j^n; \Phi_{j-1}^n\big)$

if $\Phi_{j-1}^n \neq \mathbf{0}$ **then**

$$g_{V,j}^{n+1/2} \leftarrow \frac{\phi_j^{n+1/2} - \phi_j^n + \lambda g_{V,j+1}^{n+1/2}(\boldsymbol{v}^{\max})^{\mathrm{T}}\Phi_j^n}{\lambda(\boldsymbol{v}^{\max})^{\mathrm{T}}\Phi_{j-1}^n}$$

else

$g_{V,j}^{n+1/2} \leftarrow g_V(\phi_j^{n+1/2})$

endif

enddo

do $j = 1, \ldots, M$

do $i = 1, \ldots, N$

$\phi_{i,j}^{n+1/2} \leftarrow \phi_{i,j}^n - \lambda v_i^{\max}\big(\phi_{i,j}^n g_{V,j+1}^{n+1/2} - \phi_{i,j-1}^n g_{V,j}^{n+1/2}\big)$

enddo

enddo

do $j = 1, \ldots, M$

do $i = 1, \ldots, N$

$\phi_{i,j}^{n+1} \leftarrow \phi_{i,j}^{n+1/2} - \lambda v_i^{\max}\big(\phi_{i,j}^{n+1/2} p_V\big(\phi_{j+1}^{n+1/2}\big) - \phi_{i,j-1}^{n+1/2} p_V\big(\phi_j^{n+1/2}\big)\big)$

enddo

enddo

Output: approximate solution vectors $\{\phi_{i,j}^{n+1}\}_{j=1}^{M}$, $i = 1, \ldots, N$ for $t = t^{n+1} = t^n + \Delta t$

Remark 1.1. *We recall that the boundary condition* $g_{V,M+1}^{n+1/2} = \mathcal{G}(\phi_{M+1}^{n+1/2})$ *that appears in Algorithm 1.2 is defined using (1.10) for the total density* $\phi_{M+1}^{n+1/2}$. *We illustrate this boundary condition in Section 1.4.5.*

The problem of interest to us is to show that $\mathcal{D}$ is an invariant region of the scheme. To this end we first consider the evolution of the total density ϕ. Summing over $i = 1, \ldots, N$ the second equation in (1.45) yields

$$\phi_j^{n+1} = \phi_j^{n+1/2} - \lambda(\boldsymbol{v}^{\max})^{\mathrm{T}}\big(p_V\big(\phi_{j+1}^{n+1/2}\big)^{n+1/2}\Phi_j^{n+1/2} - p_V\big(\phi_j^{n+1/2}\big)\Phi_{j-1}^{n}\big).$$

The above equation can be written in incremental form as

$$\phi_j^{n+1} = \phi_j^{n+1/2} + C_{j+1/2}^{n+1/2}\Delta_+\phi_j^{n+1/2} - D_{j-1/2}^{n+1/2}\Delta_-\phi_j^{n+1/2}, \tag{1.50}$$

where we define

$$C_{j+1/2}^{n+1/2} := \begin{cases} \lambda(\boldsymbol{v}^{\max})^{\mathrm{T}}\Phi_j^{n+1/2}\dfrac{p_V(\phi_j^{n+1/2}) - p_V(\phi_{j+1}^{n+1/2})}{\phi_{j+1}^{n+1/2} - \phi_j^{n+1/2}} & \text{if } \phi_{j+1}^{n+1/2} \neq \phi_j^{n+1/2}, \\ 0 & \text{if } \phi_{j+1}^{n+1/2} = \phi_j^{n+1/2}, \end{cases}$$

$$D_{j-1/2}^{n+1/2} := \begin{cases} \lambda p_V(\phi_j^{n+1/2})\dfrac{(\boldsymbol{v}^{\max})^{\mathrm{T}}\big(\Phi_j^{n+1/2} - \Phi_{j-1}^{n+1/2}\big)}{\phi_j^{n+1/2} - \phi_{j-1}^{n+1/2}} & \text{if } \phi_j^{n+1/2} \neq \phi_{j-1}^{n+1/2}, \\ 0 & \text{if } \phi_j^{n+1/2} = \phi_{j-1}^{n+1/2}. \end{cases}$$

Since $p_V(\phi)$ is a non-increasing positive function we have $C_{j+1/2}^{n+1/2}, D_{j-1/2}^{n+1/2} \geqslant 0$. To ensure that $|C_{j+1/2}^{n+1/2}| \leqslant 1/2$ and $|D_{j-1/2}^{n+1/2}| \leqslant 1/2$ we impose the CFL condition

$$\lambda\phi_{\max}\max_{1\leqslant j\leqslant M}\big|p_V'(\phi_j^n)\big| \cdot \max_{1\leqslant i\leqslant N} v_i^{\max} \leqslant \frac{1}{2}, \quad \lambda \max_{1\leqslant j\leqslant M} p(\phi_j^n) \cdot \max_{1\leqslant i\leqslant N} v_i^{\max} \leqslant \frac{1}{2}. \tag{1.51}$$

Lemma 1.14. *Assume that*

$$\Phi_j^0 \in \mathcal{D} \quad \text{for } j = 1, \ldots, M. \tag{1.52}$$

Then $\Phi_j^n, \Phi_j^{n+1/2} \in \mathcal{D}$ *for* $j = 1, \ldots, M$.

Proof. We claim that

$$\begin{aligned} &\Phi_j^{n+1/2} \in \mathcal{D} \quad \text{for all } j = 1, \ldots, M \\ &\Rightarrow g_{V,j}^{n+1/2} \in [0, \alpha_V] \quad \text{for all } j = 1, \ldots, M. \end{aligned} \tag{1.53}$$

We consider first the case $\Phi_{j-1}^n = \mathbf{0}$. Then the result follows from the definition of the function $g_V(z)$ and (1.8). Suppose that $\Phi_{j-1}^n \neq \mathbf{0}$, summing over $i = 1, \ldots, N$ the first equation in (1.45) yields

$$\phi_j^{n+1/2} = \tilde{G}_V^{-1}\big(\phi_j^n - \lambda(\boldsymbol{v}^{\max})^{\mathrm{T}}\Phi_j^n g_{V,j+1}^{n+1/2}; \Phi_{j-1}^n\big).$$

Using (1.49) and (1.47) we find that

$$\phi_j^{n+1/2} - \lambda(\boldsymbol{v}^{\max})^{\mathrm{T}}\Phi_{j-1}^n g_{V,j}^{n+1/2} \in \tilde{G}_V\big(\phi_j^{n+1/2}; \Phi_{j-1}^n\big).$$

Thus, a straightforward case-by-case study and (1.49) prove that (1.53) is valid. The remainder of the proof is similar to the proof of Lemma 1.2. □

1.4 Numerical examples

We now present some numerical simulations to illustrate the behaviour of solutions to system (1.1) by using Algorithms 1.1 and 1.2 for the scalar and multiclass case, respectively. In the scalar case, we compare numerical approximations with those generated by the scheme (1.7) proposed by Towers in [90]. To this end we choose the discontinuous velocity function

$$V(\phi) = \begin{cases} 1 - \phi/\phi_{\max} & \text{for } 0 \leqslant \phi \leqslant \phi^*, \\ -w_{\mathrm{f}}(1 - \phi_{\max}/\phi) & \text{for } \phi^* < \phi \leqslant \phi_{\max}, \end{cases}$$

where $\phi^* = 0.5$, $w_{\mathrm{f}} = 0.2$, $\phi_{\max} = 1$, and $\alpha_V = 0.3$.

In all numerical experiments computations are performed on a finite interval $[-1, 1]$ that is subdivided into M subintervals of length $\Delta x = 2/M$, and the time step is computed by $\Delta t = \Delta x/2$ in the scalar case ($N = 1$) and $\Delta t = \Delta x/(2\max\{v_1^{\max}, \ldots, v_N^{\max}\})$ in the multiclass case $N \geqslant 2$. These choices ensure that the respective CFL conditions (1.21) and (1.51) are satisfied.

1.4.1 Example 1.1: scalar Riemann problem ($N = 1$).

We consider the Riemann problem for the scalar equation $\partial_t\phi + \partial_x(\phi V(\phi)) = 0$ with initial data

$$\phi_0(x) = \begin{cases} \phi_{\mathrm{L}} & \text{for } x < 0.2, \\ \phi_{\mathrm{R}} & \text{for } x \geqslant 0.2 \end{cases} \tag{1.54}$$

(no boundary conditions are involved). For $\phi_{\mathrm{L}} = 0.3$ and $\phi_{\mathrm{R}} = 0.9$, the solution consists of two shock waves with negative velocities of propagation, namely a shock wave connecting ϕ_{L} with ϕ^* that travels velocity $\sigma_1 = -0.55$ and another shock wave connecting ϕ^* with ϕ_{R} with velocity $\sigma_2 = -0.2$. Figure 1.3 (a) shows the numerical approximations to the solution of this problem computed with $M = 800$ for both schemes at simulated time $T = 1.8$.

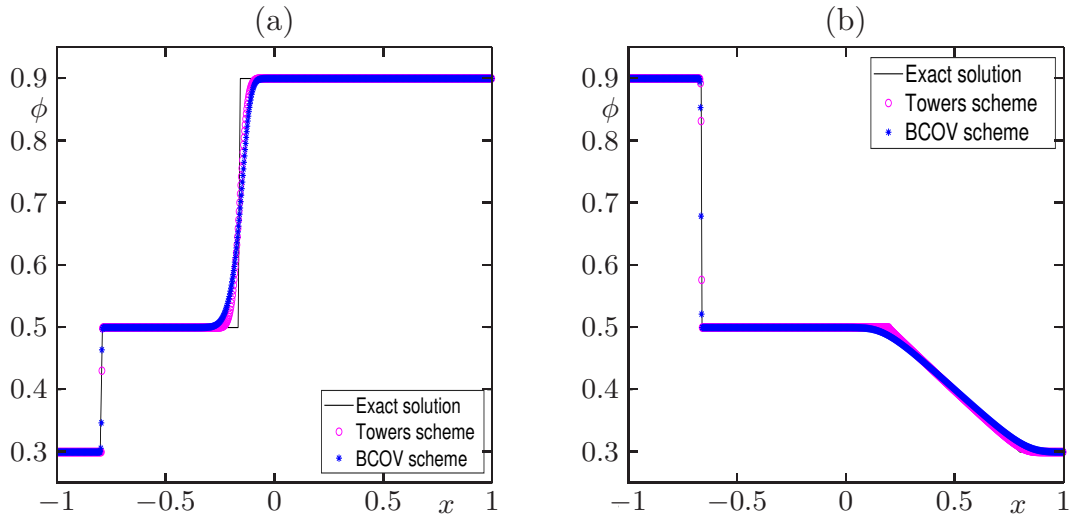

Figure 1.3: Example 1.1: numerical solution with $M = 800$ and comparison with the exact solution of the Riemann problem (a) with $\phi_{\rm L} = 0.3$ and $\phi_{\rm R} = 0.9$ at simulated time $T = 1.8$, (b) with $\phi_{\rm L} = 0.9$ and $\phi_{\rm R} = 0.3$ at simulated time $T = 1.5$. Here and in Figures 1.4 and 1.5 we label with 'Towers scheme' the scheme (1.7) proposed in [90] and by 'BCOV scheme' the scheme of Algorithm 1.1 advanced in the present work.

For $\phi_{\rm L} = 0.9$ and $\phi_{\rm R} = 0.3$, the solution consists of a shock wave connecting $\phi_{\rm L}$ with ϕ^* that travels at velocity $\sigma_1 = -0.575$ and a rarefaction wave connecting ϕ^* with $\phi_{\rm R}$. In Figure 1.3 (b) we display the numerical solutions computed with $M = 800$ for both schemes at simulated time $T = 1.5$. In both scenarios, all waves are approximated correctly by both schemes.

1.4.2 Example 1.2: scalar problem ($N = 1$), smooth initial datum

In this example we compare numerical approximations for equation (1.1) obtained by both schemes (Towers scheme (1.7) and Algorithm 1.1), starting from the initial function $\phi_0(x) = \exp(-(x + 0.2)^2/(0.04))$ for $x \in [-1, 1]$. Numerical approximations are computed at simulated times $T = 0.1$ and $T = 0.3$ with discretizations $M = 100 \times 2^l$, $l = 0, 1, \ldots, 4$. Table 1.1 displays the corresponding approximate L^1 errors obtained by utilizing a reference solution computed by the Towers scheme with $M_{\rm ref} = 12800$, We observe that the approximate L^1 errors decrease as the grid is refined. In Figure 1.4 where we display the numerical approximations for $M = 100$ and compared with the reference solution.

	$T = 0.1$		$T = 0.3$	
	Towers	BCOV	Towers	BCOV
M	$e_M(\phi^\Delta)$	$e_M(\phi^\Delta)$	$e_M(\phi^\Delta)$	$e_M(\phi^\Delta)$
100	1.32e-2	1.76e-2	1.63e-2	2.39e-2
200	6.55e-3	9.22e-3	8.59e-3	1.31e-2
400	3.29e-3	4.46e-3	4.25e-3	6.46e-3
800	1.72e-3	2.403-3	2.12e-3	3.31e-3
1600	8.00e-4	1.18e-3	9.29e-4	1.563-3

Table 1.1: Example 1.2: approximate L^1 errors $e_M(u)$ with $\Delta x = 2/M$.

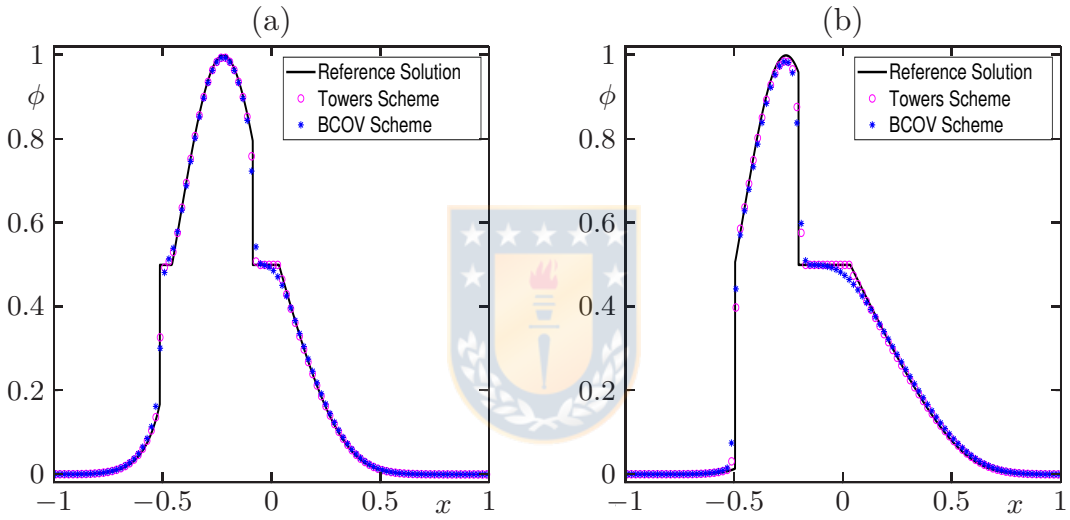

Figure 1.4: Example 1.2: numerical solutions for $M = 100$ at simulated times (a) $T = 0.1$, (b) $T = 0.3$.

1.4.3 Example 1.3: scalar problem ($N = 1$), non-standard boundary condition

This example comes from [90, Example 6.2] and is designed to illustrate that when $s(t^n) = \phi^*$, the solutions depend on the boundary condition $\mathcal{F}(t) \in \tilde{f}(\phi^*)$. For this example we consider the Riemann problem with initial data (1.54) with $\phi_{\rm L} = 1/4$ and $\phi_{\rm R} = 1/2$. We compute the solution twice, once using $\mathcal{G}(t) = \alpha_V$ (equivalently, $\mathcal{F}(t) = 1/2$), and the second time using $\mathcal{G}(t) = 0$ (equivalently, $\mathcal{F}(t) = 1/4$). As shown in Figure 1.5, in the first case the solution corresponds to a shock wave connecting $\phi_{\rm L}$ with $\phi_{\rm R}$ with speed of propagation $\sigma = 1$, and in the second case the solution corresponds to a stationary shock ($\sigma = 0$) connecting $\phi_{\rm L}$ with $\phi_{\rm R}$.

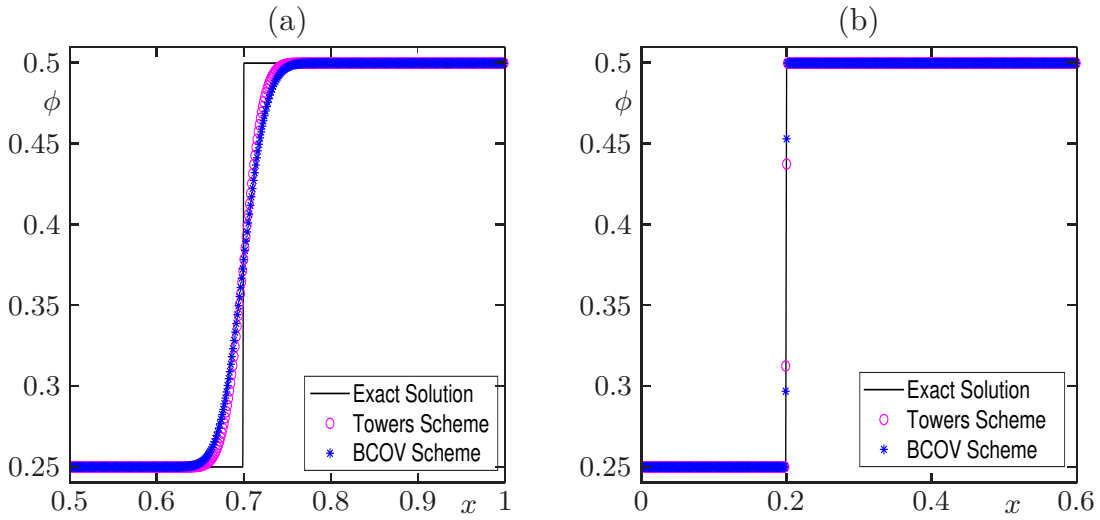

Figure 1.5: Example 1.3: numerical solutions depending on the boundary conditions $\mathcal{F}(t) \in \tilde{f}(\phi^*)$ with $M = 1600$ at simulated time $T = 0.5$, with (a) $\mathcal{F}(t) \in \tilde{f}(\phi^*-)$ (free flow), (b) $\mathcal{F}(t) \in \tilde{f}(\phi^*+)$ (congested flow).

1.4.4 Example 1.4: multiclass case ($N = 3$), preservation of invariant region

To illustrate the invariant region property of the proposed scheme (Lemma 1.14), we consider the case $N = 3$ and the Riemann initial data

$$\phi_0(x) = \begin{cases} (0.1, 0.1, 0.1)^{\mathrm{T}} & \text{for } x < 0.5, \\ (0.4, 0.5, 0.1)^{\mathrm{T}} & \text{for } x \geqslant 0.5, \end{cases}$$

with velocities $\boldsymbol{v}^{\max} = (1, 3, 10)^{\mathrm{T}}$. The solution consists of a stationary shock plus two shock waves that travel with negative velocities. The numerical simulation at three simulated times is displayed in Figure 1.6. The profile for each class and the total density are displayed in this figure. Furthermore we can see that the profile of the total density in Figure 1.6 looks like the profile of Figure 1.3 (a).

1.4.5 Example 1.5: multiclass case ($N = 3$), non-standard boundary condition

It is the purpose of this example to illustrate the boundary condition

$$g_{V,M+1}^{n+1/2} = \mathcal{G}\big(\phi_{M+1}^{n+1/2}\big), \tag{1.55}$$

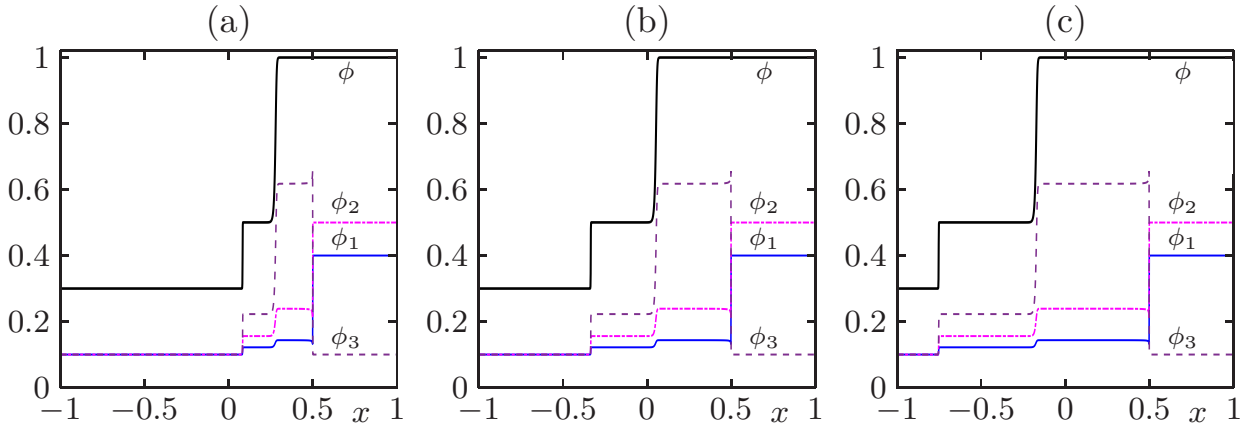

Figure 1.6: Example 1.4: density profiles simulated with $M = 1600$ at (a) $T = 0.2$, (b) $T = 0.4$, (c) $T = 0.6$.

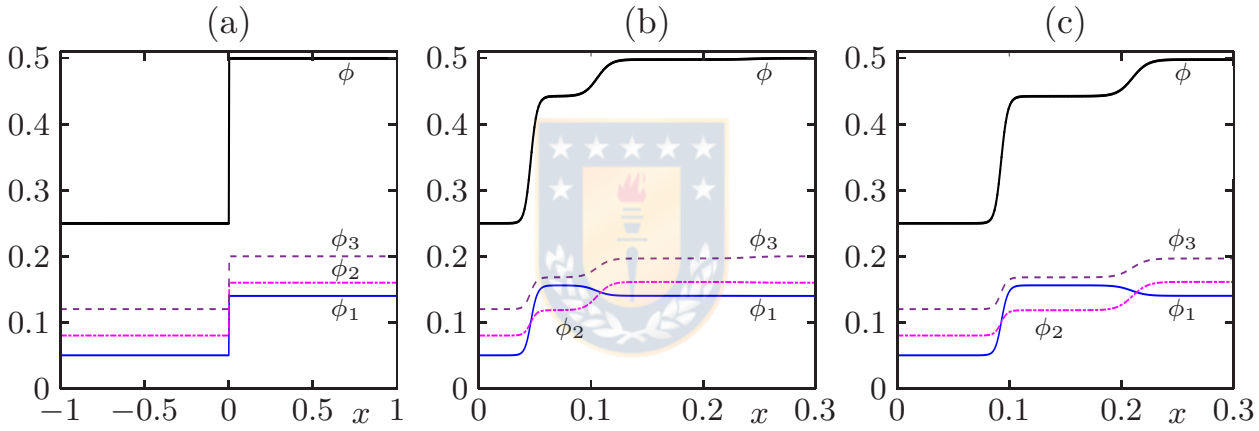

Figure 1.7: Example 1.5: numerical solution for a free-flow regime ($\mathcal{G}(t) = \alpha_V$): (a) initial condition, (b, c) density profiles with $M = 1600$ at simulated times (b) $T = 0.1$, (c) $T = 0.2$.

where $\mathcal{G}(\cdot)$ is specified in (1.10), that appears within Algorithm 1.2. To this end consider $N = 3$ and the velocities and Riemann initial data

$$\boldsymbol{v}^{\max} = (1, 3, 6)^{\mathrm{T}}, \quad \Phi(x, 0) = \Phi_0(x) = \begin{cases} \Phi_{\mathrm{L}} = (0.05, 0.08, 0.12)^{\mathrm{T}} & \text{for } x < 0, \\ \Phi_{\mathrm{R}} = (0.14, 0.16, 0.12)^{\mathrm{T}} & \text{for } x \geqslant 0. \end{cases}$$

Observe that $\phi_{\mathrm{R}} = \phi^* = s(t)$, where ϕ_{R} is the total density of the right state Φ_{R}.

As in Example 3 we show that the solution depends on the boundary condition $\boldsymbol{\mathcal{F}}(t) \in (\boldsymbol{v}^{\max})^{\mathrm{T}} \boldsymbol{s}(t) \tilde{V}(s(t))$. We start with the initial condition shown in Figure 1.7 (a) and compute the solution twice, once using $\mathcal{G}(t) = \alpha_V$, and the second time using $\mathcal{G}(t) = 0$. In Figures 1.7 (b) and (c) we display the profile for each class and total density for the first case $\mathcal{G}(t) = \alpha_V$ at two different simulated times. We can see that in this case a free-flow regime is produced, which is

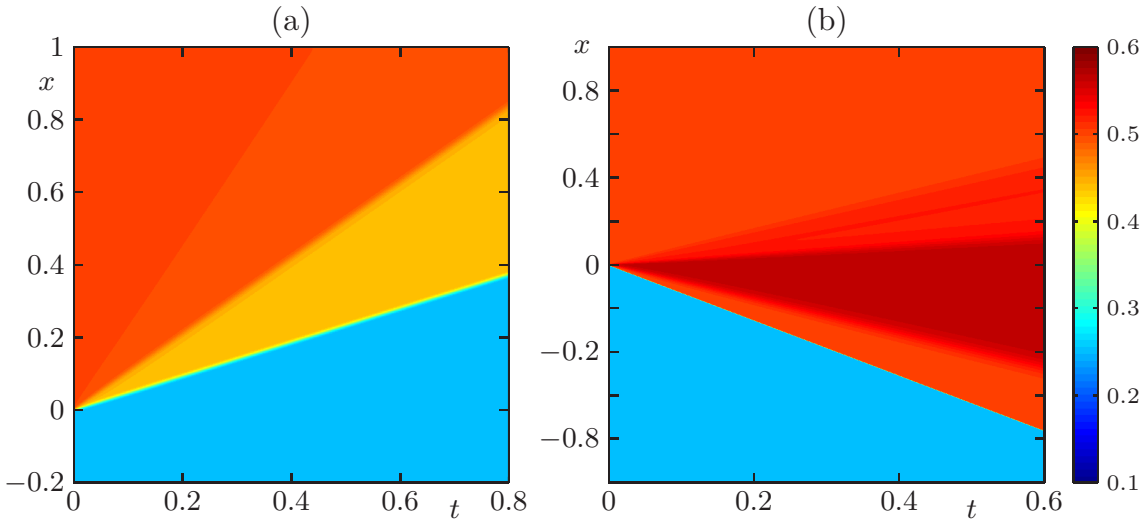

Figure 1.8: Example 1.5: simulated total density computed with BCOV scheme with $N = 3$ and $M = 1600$: (a) free flow ($\mathcal{G}(t) = \alpha_V$), (b) congested flow ($\mathcal{G}(t) = 0$).

	$T = 0.02$	$T = 0.12$
M	$e_M(\phi^\Delta)$	$e_M(\phi^\Delta)$
100	1.39e-2	3.87e-2
200	7.90e-3	2.47e-2
400	4.20e-3	1.55e-2
800	2.00e-3	9.20e-3
1600	1.00e-3	5.10e-3

Table 1.2: Example 1.6: approximate L^1 errors $e_M(u)$ with $\Delta x = 2/M$.

verified in Figure 1.8 (a). In Figure 1.9 we display the profiles for each class and total density for the second case $\mathcal{G}(t) = 0$ at two different simulation time. In contrast to the previous cases, a congested flow regime is produced, as is illustrated in Figure 1.8 (b).

1.4.6 Example 1.6: multiclass case ($N = 5$), smooth initial condition

In this example we consider $N = 5$, the velocities $\boldsymbol{v}^{\max} = (1, 2, 3, 4, 5)^{\mathrm{T}}$, and the initial condition

$$\Phi(x, 0) = \Phi_0(x) = (0.15, 0.2, 0.3, 0.2, 0.15)^{\mathrm{T}}\psi(x), \quad \psi(x) = \exp\big(-50(x + 2)^2/3\big).$$

We display in Figure 1.10 numerical approximation computed with $M = 1600$ at simulation times $T = 0.02$ and $T = 0.12$. We observe the dynamics of each individual densities ϕ_i and the total density ϕ, which exhibits a shock wave due to the discontinuity in the flux. This behaviour is similar to that presented in Figure 1.4. In Figure 1.11 we display the evolution of

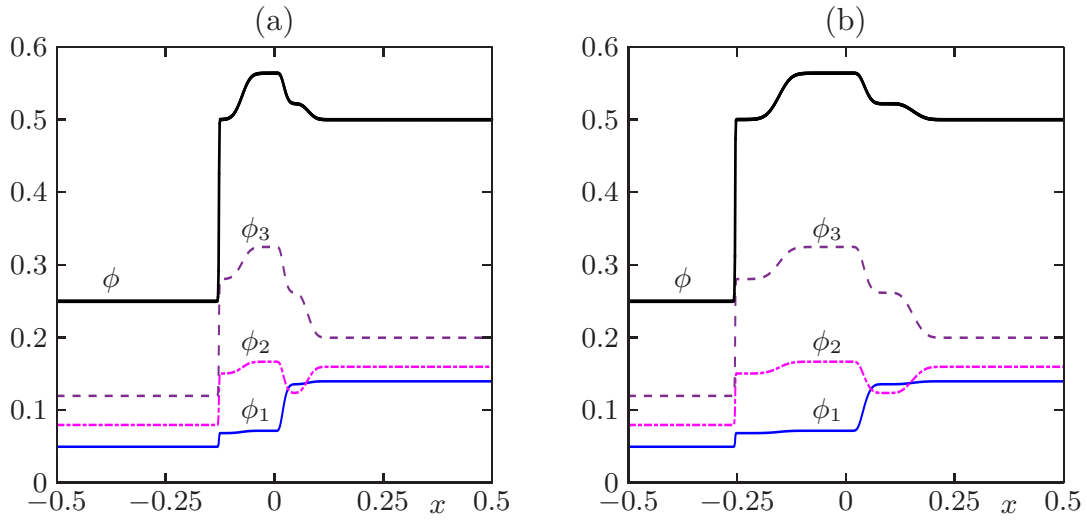

Figure 1.9: Example 1.5: numerical solution for a congested flow regime ($\mathcal{G}(t) = 0$): density profiles with $M = 1600$ at simulated times (a) $T = 0.1$, (b) $T = 0.2$. The initial condition is the same as in Figure 1.7 (a).

$\phi^{\Delta}(\cdot, t)$ for $t \in [0, 0.12]$, and we compare the solution with the approximation of the continuous problem (where $\alpha_V = 0$). For the discontinuous case the shock is more clearly observed than in the continuous case. In Figures 1.12 and 1.13 we compare the numerical approximation computed with $M = 100$, with a reference solution at simulated times $T = 0.02$ and $T = 0.12$. In Table 1.2, we compute the approximate L^1 error based on a reference solution obtained by the BCOV scheme with $M_{\text{ref}} = 12800$. We observe that the approximate L^1 errors decrease as the grid is refined.

1.4.7 Example 1.7: multiclass case ($N = 5$), bimodal smooth initial condition

In this example we consider $N = 5$, the velocity vector $\boldsymbol{v}^{\max} = (1, 1.5, 2, 6, 7)^{\mathrm{T}}$, and the initial condition

$$\Phi(x, 0) = \Phi_0(x) = (0.17, 0.17, 0.16, 0, 0)^{\mathrm{T}}\psi_1(x) + (0, 0, 0, 0.245, 0.245)^{\mathrm{T}}\psi_2(x),$$

where we define

$$\psi_1(x) = \exp\big(-10(x-2)^2\big), \quad \psi_2(x) = \exp\big(-50(x-1)^2/4\big)$$

for $x \in [0, 5]$. We compute numerical approximation at simulated times $T = 0.1$, $T = 0.2$ and $T = 0.3$ with different discretizations by using $M = 100 \times 2^l$ and $l = 0, 1, \ldots, 4$. In Table 1.3 we compute the L^1 error comparing with respect to a reference solution computed by the BCOV scheme with $M_{\text{ref}} = 12800$. We observe that the approximate L^1 errors decrease as the grid

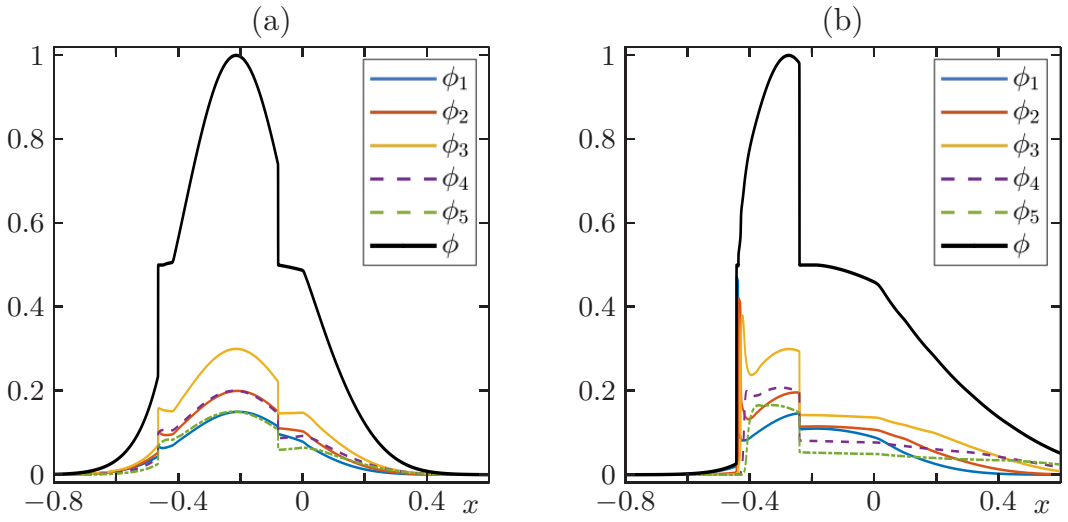

Figure 1.10: Example 1.6: numerical solutions obtained with BCOV scheme with $N = 5$ and $M = 1600$ at simulated times (a) $T = 0.02$, (b) $T = 0.12$.

is refined. Again, this behaviour is similar to that observed in Figure 1.4. Figure 1.15 shows results for $M = M_{\text{ref}} = 12800$. The numerical results of Figure 1.15 indicate that jumps in the total density ϕ only occur from smaller to higher values in an increasing x-direction. This phenomenon occurs because the speeds of the last two classes are greater than the first three. Furthermore, in Figure 1.14 we show the simulated total density computed by the BCOV scheme with $N = 5$ and $M = 1600$.

	$T = 0.1$	$T = 0.2$	$T = 0.3$
M	$e_M(\phi^\Delta)$	$e_M(\phi^\Delta)$	$e_M(\phi^\Delta)$
100	7.42e-2	9.50e-2	1.06e-1
200	4.12e-2	5.50e-2	6.49e-2
400	2.27e-2	3.34e-2	3.88e-2
800	1.24e-2	1.97-2	2.35e-2
1600	6.50e-3	1.10e-2	1.35e-2

Table 1.3: Example 1.7: Approximate L^1 errors $e_M(u)$ with $\Delta x = 5/M$.

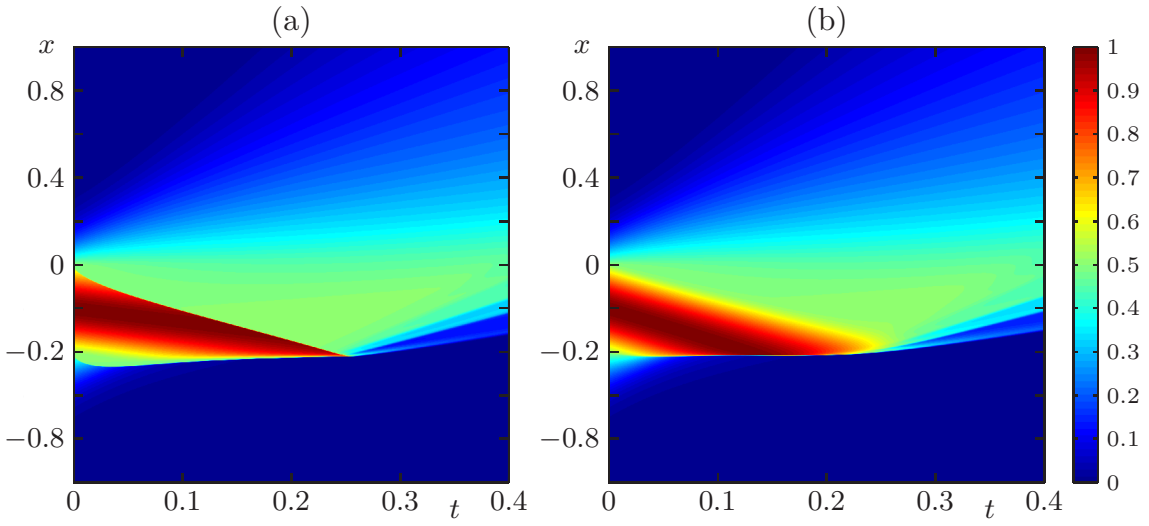

Figure 1.11: Example 1.6: simulated total density obtained with BCOV scheme with $N = 5$ and $M = 1600$: (a) discontinuous problem, (b) continuous problem.

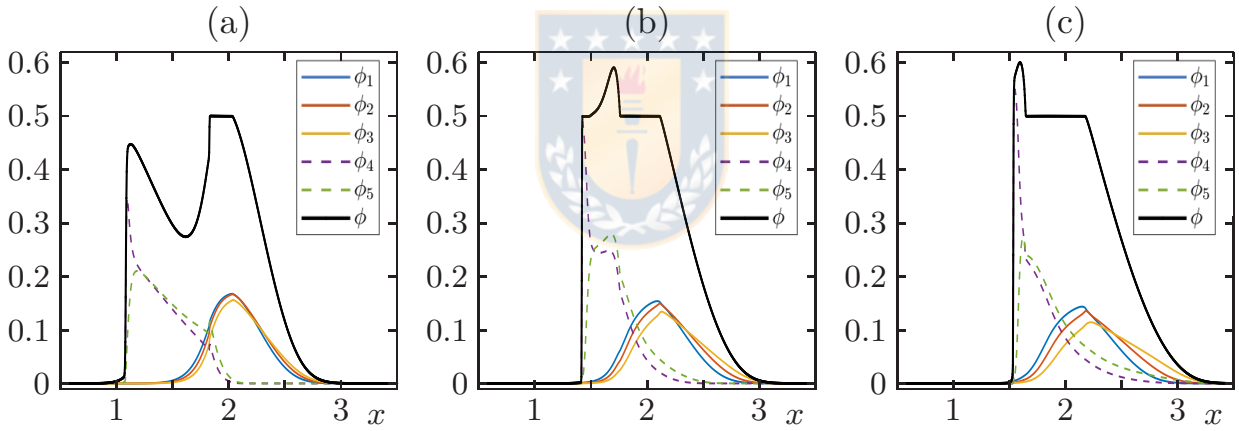

Figure 1.15: Example 1.7: numerical solution computed with BCOV scheme with $N = 5$ and $M = 12800$ at simulated times (a) $T = 0.1$, (b) $T = 0.2$ and (c) $T = 0.3$.

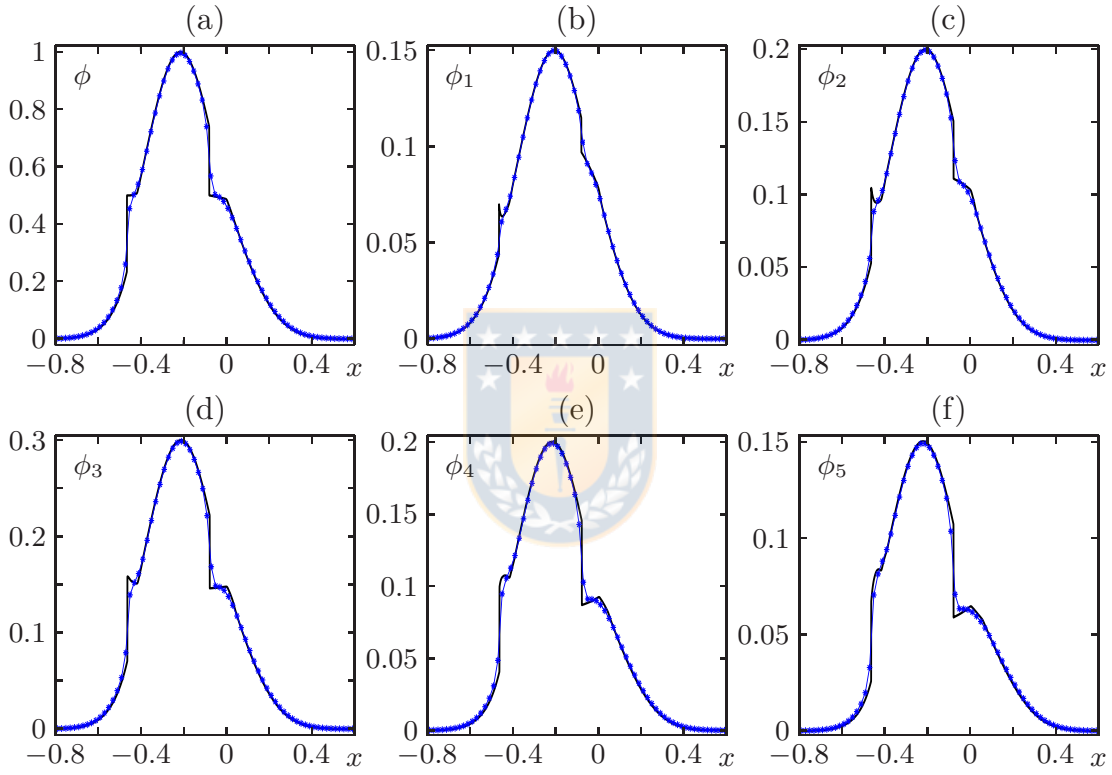

Figure 1.12: Example 1.6: comparison of reference solution ($M_{\text{ref}} = 12800$) with approximate solutions computed by BCOV scheme with $M = 100$ at simulated time $T = 0.02$.

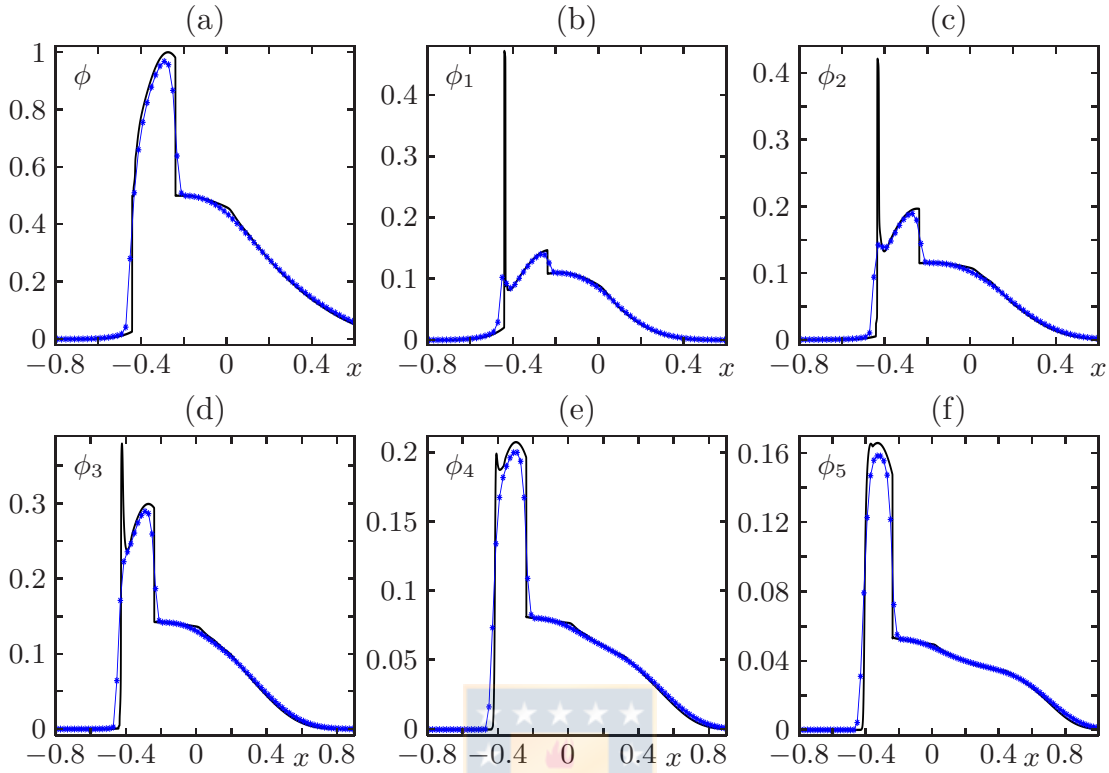

Figure 1.13: Example 1.6: comparison of reference solution ($M_{\text{ref}} = 12800$) with approximate solutions computed by BCOV scheme with $M = 100$ at simulated time $T = 0.12$.

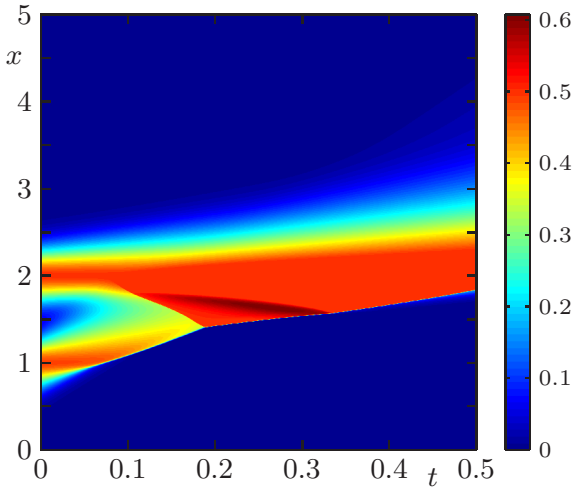

Figure 1.14: Example 1.7: simulated total density computed with BCOV scheme with $N = 5$ and $M = 1600$.

CHAPTER 2

Numerical analysis of a three-species chemotaxis model

2.1 Introduction

2.1.1 Scope

We consider a reaction-diffusion system describing three interacting species with respective density u_i, $i = 1, 2, 3$, in the Hastings-Powell (HP) food chain structure [52, 71], where each species secretes a chemical substance of corresponding concentration y_i, $i = 1, 2, 3$. Each biological species is able to orient its movement towards a higher concentration of a chemical (chemotaxis) or away from it (chemorepulsion). The resulting model is a strongly coupled nonlinear system of six PDEs with chemotactic terms, namely three parabolic equations describing the evolution of the densities u_i coupled with three elliptic equations for the concentrations y_i, $i = 1, 2, 3$:

$$\begin{aligned} \partial_t u_1 - D_1 \Delta u_1 + \chi_1 \operatorname{div}(u_1 \nabla y_2) &= F_1(\boldsymbol{u}), \\ \partial_t u_2 - D_2 \Delta u_2 + \chi_2 \operatorname{div}\big(u_2 \nabla (y_1 - y_3)\big) &= F_2(\boldsymbol{u}), \\ \partial_t u_3 - D_3 \Delta u_3 + \chi_3 \operatorname{div}(u_3 \nabla y_2) &= F_3(\boldsymbol{u}), \\ -\mathcal{D}_i \Delta y_i + \theta_i y_i = \delta_i u_i, \quad i = 1, 2, 3, \quad (\boldsymbol{x}, t) &\in \Omega \times (0, T], \end{aligned} \tag{2.1}$$

where $u_i(\boldsymbol{x}, t)$, $i = 1, 2, 3$ are the population densities of the species at the lowest level of the food chain (prey; $i = 1$), of the species that preys upon species 1 (predator, $i = 2$), and of species 3 that preys upon species 2 (super-predator, $i = 3$), and $\boldsymbol{u}(\boldsymbol{x}, t) \coloneqq (u_1(\boldsymbol{x}, t), u_2(\boldsymbol{x}, t), u_3(\boldsymbol{x}, t))^{\mathrm{T}}$. Moreover, $y_i(\boldsymbol{x}, t)$ denotes the concentration of the chemical substance secreted by species i at position $\boldsymbol{x}$ at time t, and $\boldsymbol{y}(\boldsymbol{x}, t) \coloneqq (y_1(\boldsymbol{x}, t), y_2(\boldsymbol{x}, t), y_3(\boldsymbol{x}, t))^{\mathrm{T}}$. The chemotactic movement of the species is due to chemical substances secreted by the other species, which is determined by the sign of the chemotactic coefficients χ_i for $i = 1, 2, 3$ [37]. In this work, we consider that the prey (species 1) moves in the direction of decreasing concentration of the chemical secreted by species 2 (trying to avoid that species), which means that $\chi_1 < 0$, while the super-predator (species 3) moves in the direction of increasing concentration of the chemical secreted

by species 2, which means that $\chi_3 > 0$. On the other hand, the predator (species 2) moves in the direction of increasing concentration of the chemical secreted by species 1 and in the direction of decreasing concentration of the chemical secreted by species 2, such that $\chi_2 > 0$.

The interaction due to the competition between the species is specified by the functional responses

$$\begin{aligned} F_1(\boldsymbol{u}) &:= \left(1 - \frac{u_1}{k}\right) u_1 - \frac{L_2 M_2 u_1 u_2}{R_0 + u_1}, \\ F_2(\boldsymbol{u}) &:= \frac{L_2 M_2 u_1 u_2}{R_0 + u_1} - L_2 u_2 - \frac{L_3 M_3 u_2 u_3}{C_0 + u_2}, \\ F_3(\boldsymbol{u}) &:= \frac{L_3 M_3 u_2 u_3}{C_0 + u_2} - L_3 u_3 \end{aligned} \tag{2.2}$$

(see [52, 71]). Here, the constant k is the carrying capacity of species 1, and R_0 and C_0 are the half-saturation densities of u_1 and u_2, respectively. Moreover, L_2 and L_3 are the mass-specific metabolic rates of species 2 and 3, respectively, M_2 is a measure of ingestion rate per unit metabolic rate of species 2, and M_3 denotes the ingestion rate for species 3 on prey. We impose, in addition, the zero-flux boundary conditions

$$\begin{gathered} \left(\chi_j u_j \nabla y_2 - D_j \nabla u_j\right) \cdot \boldsymbol{n}|_{\partial\Omega} = \left(\chi_2 u_2 \nabla (y_1 - y_3) - D_3 \nabla u_3\right) \cdot \boldsymbol{n}|_{\partial\Omega} = 0, \quad j = 1, 2, \\ \nabla y_i \cdot \boldsymbol{n}|_{\partial\Omega} = 0, \quad i = 1, 2, 3, \end{gathered} \tag{2.3}$$

where $\boldsymbol{n}$ stands for the outward unit normal vector to $\partial\Omega$, and the initial condition

$$u_i(\boldsymbol{x}, 0) = u_{i,0}(\boldsymbol{x}), \quad i = 1, 2, 3. \tag{2.4}$$

2.1.2 Related work

The classical Lotka–Volterra predator-prey model (cf., e.g., [72, vol. I]) only reflects population changes due to predation in a situation where predator and prey densities are not spatially dependent. Variants of the model have been applied to medicine [77], biology [73], ecology [8, 51, 70, 75, 92], mathematics [72, 91], and other fields. This model does not take into account that population is usually not homogeneously distributed, or that predators and prey naturally develop strategies for survival. Both considerations involve spatial biological movement that is usually described by diffusion. The resulting models can become complicated due to hierarchies of predator-prey dependence that cause complicated patterns of movement of populations. Such movements can be determined by the concentration of the same species (diffusion) or that of other species (cross–diffusion). However, systems of two interacting species can account for only a small number of the phenomena that are commonly exhibited in nature. This limitation is particularly significant in community studies where the essence of the behavior of a complex system may only be understood when the interactions among a large number of species are incorporated; of course, the increasing number of differential equations and the increasing dimensionality raises additional problems.

The dynamics of interacting population with chemotaxis has been investigated by numerous researchers. Lin et al. [62] construct energy functionals to investigate the asymptotic behavior of solutions under simple choices of parameter. Stability and asymptotic behavior of chemotactic systems with two biological species have been studied in [85, 87], where the stability of homogeneous steady states is obtained for one chemical substance secreted, while in [37, 74] the authors established the asymptotic behavior and the global existence of solutions for two secretions. In [4] a reaction-diffusion model for predator-prey interaction is analyzed, featuring both prey and predator taxis mediated by nonlocal sensing. The analysis is supported by some numerical experiments. On the other hand, Bürger et al. [21] propose and simulate a three-species spatio-temporal predator-prey system with infected prey where the biological movement is not directed by the gradient of a chemical, but rather by a non-local convolution of the density of infected prey that determines a convection term.

Mathematical developments also suggest that models which involve only two species may miss important ecological behavior. Results that are much more complicated than those seen in two-species models appeared in early theoretical studies of three species (e.g [81]) based on local stability analyses. Hastings and Powell [52] studied the three-species food chain, and among other results they found that there is a "tea-cup" attractor in the system. In [29] the effects of size of forest remnants on trophically linked communities of plants, leaf-mining insects, and their parasitoids were evaluated. The time evolution and spatiotemporal pattern in the Lotka-Volterra model of three interacting species with noise and time delay were investigated by stochastic simulation in [99]. Anaya et al. [5] proposed a convergent semi-implicit FV scheme to describe three interacting species in the food chain structure with nonlocal and cross diffusion. The global existence and boundedness of solutions of the system in bounded domains of arbitrary spatial dimension and small prey-taxis sensitivity coefficients are proved in [93]. The model considered in that work is a reaction-diffusion system with prey taxis that models a two-predator-one-prey ecosystem in which the predators collaboratively take advantage of the prey's strategy.

2.1.3 Outline

The remainder of this chapter is organized as follows. Section 2.2 is concerned to definition of the weak solution of (2.1). Before, we collect in Section 2.2.1 some preliminary material, including relevant notation and assumptions on the data problem, this section ends with definition of a weak solution of (2.1). Next, in Section 2.3, we specify the FV method, starting with recalling in Section 2.3.1 the standard notation of an admissible mesh from [45]. Then, in Section 2.3.2 we specify the FV scheme to discretize (2.1)–(2.4). Since the scheme is implicit and requires the solution of nonlinear algebraic equations in each time step, we need to demonstrate that the scheme is well defined, that is, that it admits a solution in each time step. This is done in Section 2.4.3, where we first prove (in Section 2.4.1) that any (discrete) solution produced by the FV scheme is non-negative, and then establish (in Section 2.4.2) certain a priori L^2

estimates on the discrete solutions. These results allow us to prove in Section 2.4.3 the existence and uniqueness of a solution for the FV scheme. Section 2.5 is concerned with the proof of convergence of the FV scheme as the mesh is refined. To this end, we prove in Section 2.5.1 compactness for discrete solutions (in an appropiate sense) and prove in Section 2.5.2 that the limit of discrete solutions constitutes a weak solution of (2.1)–(2.4). In Section 2.6, we provide three numerical examples. Example 1 shows that species interact with each other via chemical substance, while in Example 2 the prey do not interact by via chemical substance. Finally, Example 3 compares the dynamics of the spatio-temporal model (2.1)–(2.4) with that of the non-spatial model.

2.2 Weak solutions

2.2.1 Preliminaries

Let $\Omega \subset \mathbb{R}^d$, $d = 2$ or $d = 3$ be a bounded open domain with piecewise smooth boundary $\partial\Omega$. Namely we use standard Lebesgue and Sobolev spaces $W^{m,p}(\Omega)$, $H^m(\Omega) = W^{m,2}(\Omega)$ and $L^p(\Omega)$ (with their usual norms [1]) for all $m \in \mathbb{N}$ and $p \in [1, \infty]$. We define for $p \in [1, \infty)$ the spaces

$$\mathcal{W}^p := \{u \in W^{2,p}(\Omega) : \nabla u \cdot \boldsymbol{n} = 0\},$$
$$\big(L^p(\Omega)\big)^+ := \left\{ u : \Omega \longrightarrow \mathbb{R}_+ \text{ measurable and } \int_\Omega |u(\boldsymbol{x})|^p \, \mathrm{d}\boldsymbol{x} < \infty \right\}.$$

Furthermore, for later use, we recall the Sobolev inequalities (see e.g. [16]) $W^{1,p}(\Omega) \hookrightarrow L^\theta$ with $\theta \in (2, +\infty)$ if $d = 2$, $\theta = (2d)/(d-2) = 6$ if $d = 3$.

If X is a Banach space, $a < b$ and $p \in [1, \infty]$, then $L^p(a, b; X)$ denotes the space of all measurable functions $u : (a, b) \longrightarrow X$ such that $\|u(\cdot)\|_X \in L^p(a, b)$. Next , for $T > 0$ we define $\Omega_T := \Omega \times (0, T]$. We define

$$\boldsymbol{z} = \begin{pmatrix} z_1 \\ z_2 \\ z_3 \end{pmatrix} := \begin{pmatrix} y_2 \\ y_1 - y_3 \\ y_2 \end{pmatrix} = \boldsymbol{B}\boldsymbol{y}, \quad \text{where} \quad \boldsymbol{B} = \begin{bmatrix} \boldsymbol{b}_1^{\mathrm{T}} \\ \boldsymbol{b}_2^{\mathrm{T}} \\ \boldsymbol{b}_3^{\mathrm{T}} \end{bmatrix} = \begin{bmatrix} 0 & 1 & 0 \\ 1 & 0 & -1 \\ 0 & 1 & 0 \end{bmatrix}.$$

The system (2.1) can then be written as

$$\partial_t u_i - D_i \Delta u_i + \chi_i \operatorname{div}\big(u_i \nabla(\boldsymbol{b}_i^{\mathrm{T}} \boldsymbol{y})\big) = F_i(\boldsymbol{u}), \tag{2.5}$$
$$-\mathcal{D}_i \Delta y_i + \theta_i y_i = \delta_i u_i, \quad i = 1, 2, 3, \quad (\boldsymbol{x}, t) \in \Omega_T. \tag{2.6}$$

In matrix form, (2.5) and (2.6) can be written as

$$\partial_t \boldsymbol{u} - \mathbf{div}\big(\boldsymbol{D}_1 \nabla \boldsymbol{u} - \mathcal{A}(\boldsymbol{u}) \nabla(\boldsymbol{B}\boldsymbol{y}\boldsymbol{\chi}^{\mathrm{T}})\big) = \boldsymbol{F}(\boldsymbol{u}), \quad -\mathbf{div}(\boldsymbol{D}_2 \nabla \boldsymbol{y}) + \boldsymbol{\Pi}_1 \boldsymbol{y} = \boldsymbol{\Pi}_2 \boldsymbol{u},$$

where $\boldsymbol{D}_1 \coloneqq \operatorname{diag}(D_1, D_2, D_3)$, $\mathcal{A}(\boldsymbol{u}) \coloneqq \operatorname{diag}(u_1, u_2, u_3)$, $\boldsymbol{\chi} \coloneqq (\chi_1, \chi_2, \chi_3)^{\mathrm{T}}$, $\boldsymbol{F} \coloneqq (F_1, F_2, F_3)^{\mathrm{T}}$, $\boldsymbol{D}_2 \coloneqq \operatorname{diag}(\mathcal{D}_1, \mathcal{D}_2, \mathcal{D}_3)$, $\boldsymbol{\Pi}_1 \coloneqq \operatorname{diag}(\theta_1, \theta_2, \theta_3)$, and $\boldsymbol{\Pi}_2 \coloneqq \operatorname{diag}(\delta_1, \delta_2, \delta_3)$. Furthermore, we assume that $D_i > 0$, $\mathcal{D}_i > 0$, $\theta_i \geqslant 0$, and $\delta_i \geqslant 0$ for $i = 1, 2, 3$.

For later use we point out that the particular choice of the functions F_i allows us to write them as

$$F_i(\boldsymbol{u}) = \tilde{F}_i(\boldsymbol{u}) u_i \tag{2.7}$$

with bounded functions $\tilde{F}_i$, $i = 1, 2, 3$.

Next, we define what we mean by weak solutions of the system (2.1).

Definition 2.1. *A* weak solution *of* (2.1) *is a set of non-negative functions u_i, y_i belongs to $L^2(0, T; H^1(\Omega))$, for $i = 1, 2, 3$, such that for all test functions $\xi_i, \psi_i \in \mathcal{D}([0, T) \times \bar{\Omega})$, u_i and y_i satisfy the following identities for all $i = 1, 2, 3$:*

$$\begin{aligned} -\int_0^T u_i \partial_t \xi_i \,\mathrm{d}t + \int_{\Omega_T} \left(D_i \nabla u_i \cdot \nabla \xi_i - \chi_i u_i \nabla(\boldsymbol{b}_i^{\mathrm{T}} \boldsymbol{y}) \cdot \nabla \xi_i \right) \mathrm{d}\boldsymbol{x}\,\mathrm{d}t \\ - \int_\Omega u_{i,0}(\boldsymbol{x}) \xi_i(\boldsymbol{x}, 0) \,\mathrm{d}t = \int_{\Omega_T} F_i \cdot \xi_i \,\mathrm{d}\boldsymbol{x}\,\mathrm{d}t, \\ \mathcal{D}_i \int_{\Omega_T} \nabla y_i \cdot \nabla \psi_i \,\mathrm{d}\boldsymbol{x}\,\mathrm{d}t + \theta_i \int_{\Omega_T} y_i \cdot \psi_i \,\mathrm{d}\boldsymbol{x}\,\mathrm{d}t = \int_{\Omega_T} u_i \cdot \psi_i \,\mathrm{d}\boldsymbol{x}\,\mathrm{d}t. \end{aligned} \tag{2.8}$$

2.3 Finite volume scheme

In this section, we construct approximate solutions of problem (2.1). For this purpose, we introduce a notion of admissible finite volume mesh (see e.g. [45]).

2.3.1 Admissible mesh

Let $\Omega \subset \mathbb{R}^d$, $d = 2$ or $d = 3$ denote an open bounded polygonal connected domain with boundary $\partial\Omega$. An admissible FV mesh of Ω is given by a family $\mathscr{T}_h$ of control volumes (open and convex polygonal subsets of Ω), a family $\mathcal{E} \subset \bar{\Omega}$ of hyperplanes of $\mathbb{R}^d$ (edges in two-dimensional case or sides in three-dimensional) and a family of points $\mathcal{P} = (\boldsymbol{x}_K)_{K \in \mathscr{T}_h}$ that satisfy

$$\bar{\Omega} = \bigcup_{K \in \mathscr{T}_h} \bar{K}, \qquad \mathcal{E} = \bigcup_{K \in \mathscr{T}_h} \mathcal{E}_K, \qquad \partial K = \bigcup_{L \in \mathcal{N}(K)} \bar{\sigma}.$$

Let $K, L \in \mathscr{T}_h$ with $K \neq L$. If $\bar{K} \cap \bar{L} = \bar{\sigma}$ for some $\sigma \in \mathcal{E}$, then $\sigma = K|L$ (common edge). We introduce the set of interior (respectively boundary) edges denoted by $\mathcal{E}_{\mathrm{int}}$ (resp. $\mathcal{E}_{\mathrm{ext}}$), that is $\mathcal{E}_{\mathrm{int}} = \{\sigma \in \mathcal{E} \ : \ \sigma \not\subset \partial\Omega\}$ (resp. $\mathcal{E}_{\mathrm{ext}} = \{\sigma \in \mathcal{E} \ : \ \sigma \subset \partial\Omega\}$). The set of neighbours of K is given by $\mathcal{N}(K) = \{L \in \mathscr{T}_h \ : \ \exists \sigma \in \mathcal{E}, \bar{\sigma} = \bar{K} \cap \bar{L}\}$. The family $\mathcal{P}$ is such that for all $K \in \mathscr{T}_h$, $\boldsymbol{x}_K \in \bar{K}$, and, if $\sigma = K|L$, it is assumed that $\boldsymbol{x}_K \neq \boldsymbol{x}_L$, and that the segment $\overline{\boldsymbol{x}_K \boldsymbol{x}_L}$

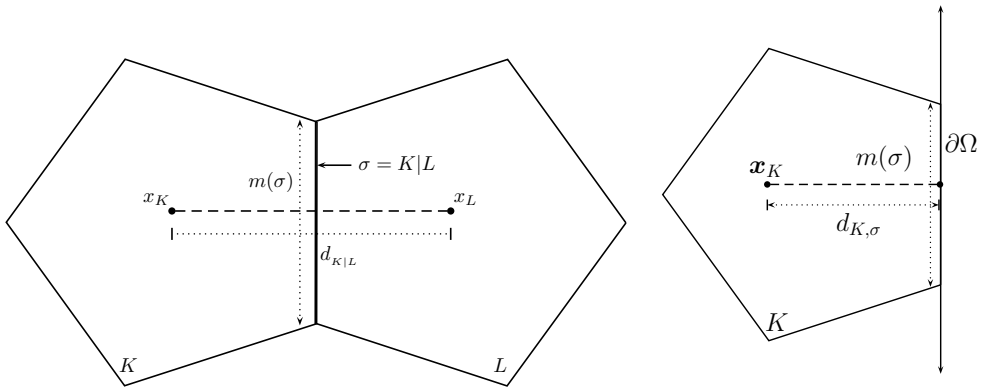

Figure 2.1: Admissible meshes.

is orthogonal to $\sigma = K|L$ (see Figure 2.1). Let $d_{K|L}$ denote the Euclidean distance between $\boldsymbol{x}_k$ and $\boldsymbol{x}_L$ and by $d_{K,\sigma}$ the distance from $\boldsymbol{x}_K$ to σ. The transmissibility through $\sigma \in \mathcal{E}_{\text{int}}$ is defined by $\tau_{K|L} = m(K|L)/d_{K|L} = m(\sigma)/d_\sigma$ and for $\sigma \in \mathcal{E}_{\text{ext}}$ by $\tau_{K,\sigma} = m(\sigma)/d_{K,\sigma}$. We require local regularity restrictions on the family of meshes $\mathscr{T}_h$; namely

$$\exists \gamma > 0 \; \forall h \; \forall K \in \mathscr{T}_h \; \forall L \in \mathcal{N}(K) : \quad \operatorname{diam}(K) + \operatorname{diam}(L) \leqslant \gamma d_{K,L} \tag{2.9}$$

$$\exists \gamma > 0 \; \forall h \; \forall K \in \mathscr{T}_h \; \forall L \in \mathcal{N}(K) : \quad m(K|L) d_{K,L} \leqslant \gamma m(K). \tag{2.10}$$

A discrete function on the mesh $\mathscr{T}_h$ is a set $(u_K)_{K \in \mathscr{T}_h}$. Whenever convenient, we identify it with the piecewise constant function $u_h \in \Omega$ such that $u_h|_K = u_K$. Finally, the discrete gradient $\nabla_h u_h$ of a constant per control volume function u_h is defined on $\bar{K} \cap \bar{L}$ by

$$\nabla_{K,L} u_{i,h} \coloneqq \frac{u_L - u_K}{d_{K|L}} \boldsymbol{n}_{K|L}. \tag{2.11}$$

2.3.2 Description of the finite volume (FV) scheme

To discretize (2.1) we choose an admissible discretization of Ω_T consisting of an admissible mesh $\mathscr{T}_h$ of Ω along with a time step $\Delta t_h > 0$; both Δt_h and the size $\max_{K \in \mathscr{T}} \operatorname{diam}(K)$ tend to zero as $h \to 0$.We define $N_h > 0$ as the smallest integer such that $(N_h + 1)\Delta t_h \geqslant T$, and set $t_n = n\Delta t_h$ for $n \in \{0, \dots, N_h\}$. Whenever Δt_h is fixed, we will drop the subscript h in the notation.

To formulate the resulting scheme, we introduce the terms

$$\mathcal{A}_{i,K,L}^{n+1} \coloneqq \min\big\{(u_{i,K}^{n+1})^+, (u_{i,L}^{n+1})^+\big\}, \quad F_{i,K}^{n+1} \coloneqq F_i\big((u_{1,K}^{n+1})^+, (u_{2,K}^{n+1})^+, (u_{3,K}^{n+1})^+\big), \quad i = 1, 2, 3. \tag{2.12}$$

The computation starts from the initial cell averages

$$u_{i,K}^0 \coloneqq \frac{1}{m(K)} \int_K u_{i,0}(\boldsymbol{x}) \, \mathrm{d}\boldsymbol{x}, \quad i = 1, 2, 3. \tag{2.13}$$

We state the FV scheme for (2.1) as follows: for all $K \in \mathscr{T}_h$ and $n \in \{0, 1, \ldots, N_h\}$, find $(u_{i,K}^{n+1})_{K\in\mathscr{T}_h}$, $i = 1, 2, 3$, such that

$$-\mathcal{D}_i \sum_{L\in\mathcal{N}(K)} \tau_{K|L}\big(y_{i,L}^{n+1} - y_{i,K}^{n+1}\big) + \theta_i m(K) y_{i,K}^{n+1} = \delta_i m(K) u_{i,K}^{n}, \quad i = 1, 2, 3, \tag{2.14a}$$

$$\begin{aligned} m(K)\frac{u_{i,K}^{n+1} - u_{i,K}^{n}}{\Delta t} - D_i \sum_{L\in\mathcal{N}(K)} \tau_{K|L}\big(u_{i,L}^{n+1} - u_{i,K}^{n+1}\big) \\ + \chi_i \sum_{L\in\mathcal{N}(K)} \tau_{K|L} \mathcal{A}_{i,K,L}^{n+1} \boldsymbol{b}_i^{\mathrm{T}}\big(\boldsymbol{y}_L^{n+1} - \boldsymbol{y}_K^{n+1}\big) = m(K) F_{i,K}^{n+1}, \quad i = 1, 2, 3 \end{aligned} \tag{2.14b}$$

As usual, homogeneous Neumann boundary conditions are taken into account implicitly. Indeed, the parts of ∂K that lie in $\partial\Omega$ do not contribute to the sums over $L \in \mathcal{N}(K)$ terms, which means that the flux is zero is imposed on the external edge of the mesh.

The sets of values $(u_{1,K}^{n+1}, u_{2,K}^{n+1}, u_{3,K}^{n+1})_{K\in\mathscr{T}_h, n\in\{0,1,\ldots,N_h\}}$ and $(y_{1,K}^{n+1}, y_{2,K}^{n+1}, y_{3,K}^{n+1})_{K\in\mathscr{T}_h, n\in\{0,1,\ldots,N_h\}}$ satisfying (2.14) will be called a discrete solution. We associate a discrete solution of the scheme at $t = t_{n+1}$ with the triplets $\boldsymbol{u}_h^{n+1} = (u_{1,h}^{n+1}, u_{2,h}^{n+1}, u_{3,h}^{n+1})^{\mathrm{T}}$ and $\boldsymbol{y}_h^{n+1} = (y_{1,h}^{n+1}, y_{2,h}^{n+1}, y_{3,h}^{n+1})^{\mathrm{T}}$ of the piecewise constant on Ω functions given by

$$u_{y,h}^{n+1}|_K = u_{i,K}^{n+1}, \quad y_{i,h}^{n+1}|_K = y_{i,K}^{n+1}, \quad \text{for all } K \in \mathscr{T}_h, \text{ all } n \in \{0, 1, \ldots, N_h - 1\} \text{ and all } i = 1, 2, 3.$$

Furthermore, we define the piecewise constant function

$$\boldsymbol{u}_h(\boldsymbol{x}, t) = \big(u_{1,h}(\boldsymbol{x}, t), u_{2,h}(\boldsymbol{x}, t), u_{3,h}(\boldsymbol{x}, t)\big)^{\mathrm{T}} := \sum_{\substack{K\in\mathscr{T}_h \\ n\in\{0,1,\ldots,N_h\}}} \boldsymbol{u}_h^{n+1} \mathbb{1}_{(t_n, t_{n+1}]\times K}.$$

Herein, the expression $\mathbb{1}_{(t_n,t_{n+1}]\times K}$ denotes the characteristic function of set $(t_n, t_{n+1}] \times K$, in similar way we define the piecewise constant function $\boldsymbol{y}_h(\boldsymbol{x}, t)$. Finally, it is assumed that Δt satisfies the mild restriction

$$\Delta t < \max\left\{\frac{1}{2}, \frac{1}{2L_2M_2}, \frac{1}{2L_3M_3}\right\}, \tag{2.15}$$

which will be used to prove the existence of solution to the scheme.

2.4 Existence of a solution for the finite volume scheme

In this section, we assume that any solution $(y_{1,K}^{n+1}, y_{2,K}^{n+1}, y_{3,K}^{n+1})^{\mathrm{T}}$, $K \in \mathscr{T}_h$, $n \in \{0, 1, \ldots, N_h\}$ of (2.14a) is non-negative. This property will be stated in Theorem 2.1 at the end of this section.

2.4.1 Non-negativity

The non-negativity of any (discrete) solution produced by the FV scheme (2.14b) is given in the following lemma.

Lemma 2.1. *Any solution* $\boldsymbol{u}^{n+1} = (u_{1,K}^{n+1}, u_{2,K}^{n+1}, u_{3,K}^{n+1})^{\mathrm{T}}$, $K \in \mathscr{T}_h$, $n \in \{0, 1, \dots, N_h\}$ *of* (2.14) *is non-negative.*

Proof. We fix $i \in \{1, 2, 3\}$ and prove by induction that $\min\{u_{i,K}^{n+1} : K \in \mathscr{T}_h\} \geqslant 0$ for all $n \in \{0, 1, \dots, N_h\}$. To this end, we recall that $u_{i,K}^0 \geqslant 0$ for all $K \in \mathscr{T}_h$. For $n \geqslant 0$, we fix $K \in \mathscr{T}_h$ such that $u_{i,K}^{n+1} \coloneqq \min\{u_L^{n+1} : L \in \mathscr{T}_h\}$. Multiplying (2.14b) by $-\Delta t (u_{i,K}^{n+1})^-$, we deduce

$$m(K)\big(u_{i,K}^{n+1} - u_{i,K}^n\big)(u_{i,K}^{n+1})^- = S_1 + S_2 + S_3, \tag{2.16}$$

where we define

$$S_1 \coloneqq \Delta t D_i \sum_{L \in \mathcal{N}(K)} \tau_{K|L}\big(u_{i,L}^{n+1} - u_{i,K}^{n+1}\big)(u_{i,K}^{n+1})^-, \quad S_3 \coloneqq \Delta t\, m(K) F_{i,K}^{n+1}(u_{i,K}^{n+1})^-,$$
$$S_2 \coloneqq \Delta t \chi_i \sum_{L \in \mathcal{N}(K)} \tau_{K|L} \mathcal{A}_{i,K,L}^{n+1} \boldsymbol{b}_i^{\mathrm{T}}\big(\boldsymbol{y}_K^{n+1} - \boldsymbol{y}_L^{n+1}\big)(u_{i,K}^{n+1})^-.$$

By the choice of K, we have $S_1 \geqslant 0$, and the choice (2.12) of $\mathcal{A}_{i,K,L}^{n+1}$ implies that $S_2 = 0$. Similarly, by the definition of $F_{i,K}^{n+1}$, we obtain

$$S_3 = \Delta t\, m(K) \tilde{F}_i\big((\boldsymbol{u}_K^{n+1})^+\big)(u_{i,K}^{n+1})^+(u_{i,K}^{n+1})^- = 0.$$

Since $m(K) > 0$, (2.16) now means that

$$\big(u_{i,K}^{n+1} - u_{i,K}^n\big)(u_{i,K}^{n+1})^- \geqslant 0. \tag{2.17}$$

By definition, $(u_{i,K}^{n+1})^- \geqslant 0$. Since $u_{i,K}^n \geqslant 0$, (2.17) cannot be satisfied for $(u_{i,K}^{n+1})^- > 0$ (and therefore $u_{i,K}^{n+1} < 0$). We conclude that $(u_{i,K}^{n+1})^- = 0$, hence $u_{i,K}^{n+1} \geqslant 0$. By induction on n, we infer that $u_{i,L}^{n+1} \geqslant 0$ for all $n \in \{0, 1, \dots, N_h\}$ and $L \in \mathscr{T}$. □

2.4.2 A priori estimates

In this section we employ an argument similar to those of [11, 30, 33] in order to establish the a priori estimates necessary to prove later the existence of a solution to the discrete problem.

Lemma 2.2. *Let* $(\boldsymbol{u}_K^{n+1})_{K \in \mathscr{T}_h, n \in \{0,1,\dots,N_h\}}$ *be a solution of* (2.14b). *Then there are constants* $C_i > 0$, $i = 1, 2, 3$ *depending on* Ω, T, $\|u_{i,0}\|_{L^2(\Omega)}$ *for* $i = 1, 2, 3$, L_j, M_j *for* $j = 2, 3$, R_0, *and* C_0 *such that*

$$\sum_{i=1}^{3} \left(\max_{n \in \{0,1,\dots,N_h\}} \sum_{K \in \mathscr{T}_h} m(K)\big(u_{i,K}^{n+1}\big)^2 \right) \leqslant C_1, \tag{2.18}$$

$$\frac{1}{2} \sum_{n=0}^{N_h} \Delta t \sum_{K \in \mathscr{T}_h} \sum_{L \in \mathcal{N}(K)} \tau_{K|L} \sum_{i=1}^{3} D_i\big(u_{i,L}^{n+1} - u_{i,K}^{n+1}\big)^2 \leqslant C_2, \tag{2.19}$$

$$\frac{1}{2} \sum_{n=0}^{N_h} \Delta t \sum_{K \in \mathscr{T}_h} \sum_{L \in \mathcal{N}(K)} \tau_{K|L} \sum_{i=1}^{3} |\chi_i| \boldsymbol{p}_i^{\mathrm{T}} \boldsymbol{y}_K^{n+1}\big(u_{i,L}^{n+1} - u_{i,K}^{n+1}\big)^2 \leqslant C_3. \tag{2.20}$$

Here we define the vectors $\boldsymbol{p}_1^{\mathrm{T}} = \boldsymbol{p}_3^{\mathrm{T}} = (0,1,0)$ and $\boldsymbol{p}_2^{\mathrm{T}} = (1,0,1)$.

Proof. We multiply (2.14b) by $\Delta t u_{i,K}^{n+1}$ and sum the result over $i = 1,2,3$, $K \in \mathscr{T}_h$, and $n \in \{0,1\ldots,N_h\}$. This yields an identity $T_1 + T_2 + T_3 + T_4 = 0$, where

$$
\begin{aligned}
T_1 &:= \sum_{n=0}^{N_h} \sum_{K\in\mathscr{T}_h} m(K) \sum_{i=1}^{3} \big(u_{i,K}^{n+1} - u_{i,K}^{n}\big) u_{i,K}^{n+1},\\
T_2 &:= -\Delta t \sum_{n=0}^{N_h} \sum_{K\in\mathscr{T}_h} \sum_{L\in\mathcal{N}(K)} \tau_{K|L} \sum_{i=1}^{3} D_i \big(u_{i,L}^{n+1} - u_{i,K}^{n+1}\big) u_{i,K}^{n+1},\\
T_3 &:= \Delta t \sum_{n=0}^{N_h} \sum_{K\in\mathscr{T}_h} \sum_{L\in\mathcal{N}(K)} \tau_{K|L} \sum_{i=1}^{3} \chi_i \mathcal{A}_{i,K,L}^{n+1} \boldsymbol{b}_i^{\mathrm{T}} \big(\boldsymbol{y}_L^{n+1} - \boldsymbol{y}_K^{n+1}\big) u_{i,K}^{n+1},\\
T_4 &= -\Delta t \sum_{n=0}^{N_h} \sum_{K\in\mathscr{T}_h} m(K) \sum_{i=1}^{3} F_{i,K}^{n+1} u_{i,K}^{n+1}.
\end{aligned}
$$

Using the inequality $a(a-b) \geqslant \frac{1}{2}(a^2 - b^2)$ for $a, b \in \mathbb{R}$, we obtain

$$
T_1 \geqslant \frac{1}{2} \sum_{n=0}^{N_h} \sum_{K\in\mathscr{T}_h} m(K) \sum_{i=1}^{3} \big(\big(u_{i,K}^{n+1}\big)^2 - \big(u_{i,K}^{n}\big)^2\big) = \frac{1}{2} \sum_{K\in\mathscr{T}_h} m(K) \sum_{i=1}^{3} \big(\big(u_{i,K}^{N_h+1}\big)^2 - \big(u_{i,K}^{0}\big)^2\big).
$$

Gathering by edges, we can write

$$
T_2 = \frac{\Delta t}{2} \sum_{n=0}^{N_h} \sum_{K\in\mathscr{T}_h} \sum_{L\in\mathcal{N}(K)} \tau_{K|L} \sum_{i=1}^{3} D_i \big(u_{i,L}^{n+1} - u_{i,K}^{n+1}\big)^2.
$$

Next, in order to find a low bound for T_3, we must carefully handle the expression $\boldsymbol{b}_i^{\mathrm{T}}(\boldsymbol{y}_L^{n+1} - \boldsymbol{y}_K^{n+1})$. First, we consider $i = 1$. Then using summation by parts and the definition of $\mathcal{A}_{1,K,L}^{n+1}$ in (2.12), we get

$$
\begin{aligned}
&\Delta t \sum_{n=0}^{N_h} \sum_{K\in\mathscr{T}_h} \sum_{L\in\mathcal{N}(K)} \tau_{K|L} \chi_1 \mathcal{A}_{1,K,L}^{n+1} \boldsymbol{b}_1^{\mathrm{T}} \big(\boldsymbol{y}_L^{n+1} - \boldsymbol{y}_K^{n+1}\big) u_{1,K}^{n+1}\\
&= -\frac{\Delta t}{2} \sum_{n=0}^{N_h} \sum_{K\in\mathscr{T}_h} \sum_{L\in\mathcal{N}(K)} \tau_{K|L} \chi_1 \mathcal{A}_{1,K,L}^{n+1} \big(y_{2,L}^{n+1} - y_{2,K}^{n+1}\big)\big(u_{1,L}^{n+1} - u_{1,K}^{n+1}\big)\\
&\geqslant -\frac{\Delta t}{2} \sum_{n=0}^{N_h} \sum_{K\in\mathscr{T}_h} \sum_{L\in\mathcal{N}(K)} \tau_{K|L} |\chi_1| \mathcal{A}_{1,K,L}^{n+1} \big(y_{2,L}^{n+1} - y_{2,K}^{n+1}\big)\big(u_{1,L}^{n+1} - u_{1,K}^{n+1}\big) \qquad (2.21)\\
&\geqslant -\Delta t \sum_{n=0}^{N_h} \sum_{K\in\mathscr{T}_h} \sum_{L\in\mathcal{N}(K)} \tau_{K|L} |\chi_1| y_{2,K}^{n+1} u_{1,L}^{n+1} \big(u_{1,K}^{n+1} - u_{1,L}^{n+1}\big)\\
&= \frac{\Delta t}{2} \sum_{n=0}^{N_h} \sum_{K\in\mathscr{T}_h} \sum_{L\in\mathcal{N}(K)} \tau_{K|L} |\chi_i| y_{2,K}^{n+1} \big(u_{1,L}^{n+1} - u_{1,K}^{n+1}\big)^2.
\end{aligned}
$$

Using a similar argument for $i = 3$ yields

$$\begin{aligned}&\Delta t\sum_{n=0}^{N_h}\sum_{K\in\mathscr{T}_h}\sum_{L\in\mathcal{N}(K)}\tau_{K|L}\chi_2\mathcal{A}_{3,K,L}^{n+1}\boldsymbol{b}_3^{\mathrm{T}}\big(\boldsymbol{y}_L^{n+1}-\boldsymbol{y}_K^{n+1}\big)u_{3,K}^{n+1}\\&\geqslant\frac{\Delta t}{2}\sum_{n=0}^{N_h}\sum_{K\in\mathscr{T}_h}\sum_{L\in\mathcal{N}(K)}\tau_{K|L}|\chi_2|y_{2,k}^{n+1}\big(u_{3,L}^{n+1}-u_{3,K}^{n+1}\big)^2.\end{aligned}\tag{2.22}$$

For $i = 2$ we obtain

$$\begin{aligned}&\Delta t\sum_{n=0}^{N_h}\sum_{K\in\mathscr{T}_h}\sum_{L\in\mathcal{N}(K)}\tau_{K|L}\chi_2\mathcal{A}_{2,K,L}^{n+1}\boldsymbol{b}_2^{\mathrm{T}}\big(\boldsymbol{y}_L^{n+1}-\boldsymbol{y}_K^{n+1}\big)u_{2,K}^{n+1}\\&=\Delta t\sum_{n=0}^{N_h}\sum_{K\in\mathscr{T}_h}\sum_{L\in\mathcal{N}(K)}\tau_{K|L}\chi_2\mathcal{A}_{2,K,L}^{n+1}\big(y_{1,L}^{n+1}-y_{1,K}^{n+1}\big)u_{2,K}^{n+1}\\&\quad-\Delta t\sum_{n=0}^{N_h}\sum_{K\in\mathscr{T}_h}\sum_{L\in\mathcal{N}(K)}\tau_{K|L}\chi_2\mathcal{A}_{2,K,L}^{n+1}\big(y_{3,L}^{n+1}-y_{3,K}^{n+1}\big)u_{2,K}^{n+1}.\end{aligned}$$

Again, reasoning in the same way as in (2.21) yields

$$\begin{aligned}&\Delta t\sum_{n=0}^{N_h}\sum_{K\in\mathscr{T}_h}\sum_{L\in\mathcal{N}(K)}\tau_{K|L}\chi_2\mathcal{A}_{2,K,L}^{n+1}\boldsymbol{b}_2^{\mathrm{T}}\big(\boldsymbol{y}_L^{n+1}-\boldsymbol{y}_K^{n+1}\big)u_{2,K}^{n+1}\\&\geqslant\frac{\Delta t}{2}\sum_{n=0}^{N_h}\sum_{K\in\mathscr{T}_h}\sum_{L\in\mathcal{N}(K)}\tau_{K|L}|\chi_2|\big(y_{1,K}^{n+1}\big(u_{2,L}^{n+1}-u_{2,K}^{n+1}\big)^2+y_{3,k}^{n+1}\big(u_{2,L}^{n+1}-u_{2,K}^{n+1}\big)^2\big).\end{aligned}\tag{2.23}$$

Thus, from (2.21)–(2.23) we get

$$T_3\geqslant\frac{\Delta t}{2}\sum_{n=0}^{N_h}\sum_{K\in\mathscr{T}_h}\sum_{L\in\mathcal{N}(K)}\tau_{K|L}\sum_{i=1}^{3}|\chi_i|\boldsymbol{p}_i^{\mathrm{T}}\boldsymbol{y}_K^{n+1}\big(u_{i,L}^{n+1}-u_{i,K}^{n+1}\big)^2.$$

Finally, the non-negativity of $u_{i,K}^{n+1}$ implies that

$$\begin{aligned}T_4&=-\Delta t\sum_{n=0}^{N_h}\sum_{K\in\mathscr{T}_h}m(K)\Bigg\{\Bigg(\Bigg(1-\frac{u_{1,K}^{n+1}}{k}\Bigg)u_{1,K}^{n+1}-\frac{L_2M_2u_{1,K}^{n+1}u_{2,K}^{n+1}}{R_0+u_{1,K}^{n+1}}\Bigg)u_{1,K}^{n+1}\\&\quad+\Bigg(\frac{L_2M_2u_{1,K}^{n+1}u_{2,K}^{n+1}}{R_0+u_{1,K}^{n+1}}-L_2u_{2,K}^{n+1}-\frac{L_3M_3u_{2,K}^{n+1}u_{3,K}^{n+1}}{C_0+u_{2,K}^{n+1}}\Bigg)u_{2,K}^{n+1}\\&\quad+\Bigg(\frac{L_3M_3u_{2,K}^{n+1}u_{3,K}^{n+1}}{C_0+u_{2,K}^{n+1}}-L_3u_{3,K}^{n+1}\Bigg)u_{3,K}^{n+1}\Bigg\}\\&\geqslant-\Delta t\sum_{n=0}^{N_h}\sum_{K\in\mathscr{T}_h}m(K)\Big(\big(u_{1,K}^{n+1}\big)^2+L_2M_2(u_{2,K}^{n+1})^2+L_3M_3\big(u_{3,K}^{n+1}\big)^2\Big).\end{aligned}$$

Collecting the previous inequalities we obtain

$$\begin{aligned}
&\frac{1}{2}\sum_{K\in\mathscr{T}_h} m(K)\sum_{i=1}^{3}\Big(\big(u_{i,K}^{N_h+1}\big)^2-\big(u_{i,K}^{0}\big)^2\Big)+\frac{\Delta t}{2}\sum_{n=0}^{N_h}\sum_{K\in\mathscr{T}_h}\sum_{L\in\mathcal{N}(K)}\tau_{K|L}\sum_{i=1}^{3}D_i\big(u_{i,L}^{n+1}-u_{i,K}^{n+1}\big)^2\\
&+\frac{\Delta t}{2}\sum_{n=0}^{N_h}\sum_{K\in\mathscr{T}_h}\sum_{L\in\mathcal{N}(K)}\tau_{K|L}\sum_{i=1}^{3}|\chi_i|\boldsymbol{p}_i^{\mathrm{T}}\boldsymbol{y}_K^{n+1}\big(u_{i,L}^{n+1}-u_{i,K}^{n+1}\big)^2 \qquad (2.24)\\
&\leqslant \Delta t\sum_{n=0}^{N_h}\sum_{K\in\mathscr{T}_h} m(K)\Big(\big(u_{1,K}^{n+1}\big)^2+L_2M_2(u_{2,K}^{n+1})^2+L_3M_3\big(u_{3,K}^{n+1}\big)^2\Big).
\end{aligned}$$

In view of the discrete Gronwall inequality, (2.18) follows from (2.24). Consequently, (2.24) entails the estimates (2.19) and (2.20). This concludes the proof. □

Remark 2.1. *For the proof of Lemma 2.2 we have used the non-negativity of* $(y_{i,K})_{K\in\mathscr{T},n\in[0,\dots,N_h]}$. *Moreover, this implies that in* (2.24) *we have* $\boldsymbol{p}_i^{\mathrm{T}}\boldsymbol{y}_K^{n+1}>0$ *for all* $i=1,2,3$.

Lemma 2.3. *Let* $(\boldsymbol{y}_K^{n+1})_{K\in\mathscr{T}_h,n\in\{0,1,\dots,N_h\}}$ *be a solution of* (2.14a). *Then, there are constants* $C_4,C_5>0$ *depending on* Ω, T, $\|u_{i,0}\|_{L^2(\Omega)}$ *for* $i=1,2,3$, L_j, M_j *for* $j=2,3$, R_0, *and* C_0 *such that*

$$\sum_{i=1}^{3}\left(\max_{n\in\{0,1,\dots,N_h\}}\sum_{K\in\mathscr{T}_h} m(K)\big(y_{i,K}^{n+1}\big)^2\right)\leqslant C_4, \qquad (2.25)$$

$$\frac{1}{2}\sum_{n=0}^{N_h}\Delta t\sum_{K\in\mathscr{T}_h}\sum_{L\in\mathcal{N}(K)}\tau_{K|L}\sum_{i=1}^{3}\mathcal{D}_i\big(y_{i,L}^{n+1}-y_{i,K}^{n+1}\big)^2\leqslant C_5. \qquad (2.26)$$

Proof. We fix $i\in\{1,2,3\}$, multiply (2.14a) by $y_{i,K}^{n+1}$, and sum the result over $K\in\mathscr{T}_h$ to obtain

$$-\mathcal{D}_i\sum_{K\in\mathscr{T}_h}\sum_{L\in\mathcal{N}(K)}\tau_{K|L}\big(y_{i,L}^{n+1}-y_{i,K}^{n+1}\big)y_{i,K}^{n+1}+\theta_i\sum_{K\in\mathscr{T}_h} m(K)\big(y_{i,K}^{n+1}\big)^2=\delta_i\sum_{K\in\mathscr{T}_h} m(K)u_{i,K}^{n}y_{i,K}^{n+1}. \qquad (2.27)$$

Using the Cauchy-Schwarz inequality, we obtain

$$\begin{aligned}
&\frac{1}{2}\sum_{K\in\mathscr{T}_h}\sum_{L\in\mathcal{N}(K)}\tau_{K|L}\mathcal{D}_i\big(y_{i,L}^{n+1}-y_{i,K}^{n+1}\big)^2+\theta_i\sum_{K\in\mathscr{T}_h} m(K)\big(y_{i,K}^{n+1}\big)^2\\
&\leqslant\delta_i\left(\sum_{K\in\mathscr{T}_h} m(K)\big(u_{i,K}^{n}\big)^2\right)^{1/2}\left(\sum_{K\in\mathscr{T}_h} m(K)\big(y_{i,K}^{n+1}\big)^2\right)^{1/2}.
\end{aligned} \qquad (2.28)$$

From (2.28) we deduce

$$\delta_i\sum_{K\in\mathscr{T}_h} m(K)\big(y_{i,K}^{n+1}\big)^2\leqslant\delta_i\left(\sum_{K\in\mathscr{T}_h} m(K)\big(u_{i,K}^{n}\big)^2\right)^{1/2}\left(\sum_{K\in\mathscr{T}_h} m(K)\big(y_{i,K}^{n+1}\big)^2\right)^{1/2}.$$

Considering the estimates for all $i = 1, 2, 3$, we may deduce (2.25) from (2.18). To get the discrete $L^2(\Omega)$ estimate for $\nabla_h y_{i,h}$ we use the generalized Young inequality and gathering by edges in (2.27) to obtain

$$\begin{aligned}&\frac{1}{2}\sum_{K\in\mathscr{T}_h}\sum_{L\in\mathcal{N}(K)}\tau_{K|L}\mathcal{D}_i\big(y_{i,L}^{n+1}-y_{i,K}^{n+1}\big)^2+\theta_i\sum_{K\in\mathscr{T}_h}m(K)\big(y_{i,K}^{n+1}\big)^2\\&\leqslant\delta_i\left(C(\varepsilon)\sum_{K\in\mathscr{T}_h}m(K)\big(u_{i,K}^{n}\big)^2+\varepsilon\sum_{K\in\mathscr{T}_h}m(K)\big(y_{i,K}^{n+1}\big)^2\right)\end{aligned}$$

for all $\varepsilon > 0$. Taking $\varepsilon = \theta_i/\delta_i$ we have

$$\frac{1}{2}\sum_{K\in\mathscr{T}_h}\sum_{L\in\mathcal{N}(K)}\tau_{K|L}\mathcal{D}_i\big(y_{i,L}^{n+1}-y_{i,K}^{n+1}\big)^2\leqslant\delta_i C(\varepsilon)\sum_{K\in\mathscr{T}_h}m(K)\big(u_{i,K}^{n}\big)^2.$$

Again, considering the estimates for all $i = 1, 2, 3$ we may deduce (2.26) from (2.18). □

2.4.3 Existence of a solution for the finite volume scheme

The following theorem shows that the scheme (2.14a) is well defined, and we prove the non-negativity of $y_{i,K}^{n+1}$ for $i = 1, 2, 3$.

Theorem 2.1. *Let $\mathcal{T}$ be an admissible discretization of Ω_T and the initial data (2.13). Then there exists a unique non-negative solution $\boldsymbol{y}_K^{n+1} = (y_{1,K}^{n+1}, y_{2,K}^{n+1}, y_{3,K}^{n+1})^{\mathrm{T}}$ for all $K \in \mathscr{T}_h$ and $n \in \{0, 1, \ldots, N_h\}$ to (2.14a).*

Proof. Utilizing an argument similar to that of [14, Section 3], we rewrite (2.14a) as the linear system

$$\boldsymbol{A}_i^{n+1}\boldsymbol{y}_i^{n+1}=\boldsymbol{R}_i\boldsymbol{u}_i^n,\quad\text{where }\boldsymbol{y}_i^n\coloneqq(y_{i,K}^n)_{K\in\mathscr{T}_h}\text{ and }\boldsymbol{u}_i^n\coloneqq(u_{i,K}^n)_{K\in\mathscr{T}_h},\ i=1,2,3,$$

and

$$\boldsymbol{A}_i^{n+1}\coloneqq(a_{i,K,L}^{n+1})_{K,L\in\mathscr{T}_h}=\begin{cases}\theta_i m(K)+\sum_{L\in\mathcal{N}(K)}\mathcal{D}_i\tau_{K|L} & \text{for } K=L,\\ -\mathcal{D}_i\tau_{K|L} & \text{for } K\neq L,\end{cases},$$

$$\boldsymbol{R}_i\coloneqq(r_{i,K,L})_{K,L\in\mathscr{T}_h}=\begin{cases}\delta_i m(K) & \text{for } K=L,\\ 0 & \text{for } K\neq L,\end{cases}\quad i=1,2,3.$$

Since for all $L \in \mathscr{T}_h$ and $i = 1, 2, 3$,

$$\big|a_{i,L,L}^{n+1}\big|-\sum_{K\neq L}\big|a_{i,K,L}^{n+1}\big|=\theta_i m(L)+\sum_{L\in\mathcal{N}(K)}\mathcal{D}_i\tau_{K|L}-\sum_{L\in\mathcal{N}(K)}\mathcal{D}_i\tau_{K|L}=\theta_i m(L)>0,$$

the matrix $\boldsymbol{A}_i^{n+1}$ is strictly dominant with respect to the columns and hence $(\boldsymbol{A}_i^{n+1})^{-1}$ is positive. Finally, under the assumption $u_i^0 > 0$ for $i = 1, 2, 3$ we obtain $y_{i,K}^n \geqslant 0$ for $i = 1, 2, 3$ and all $n \in \mathbb{N}$. □

Theorem 2.1 shows the existence and uniqueness of discrete solution of the FV scheme (2.14a). The following theorem shows the existence for (2.14b).

Theorem 2.2. *Let $\mathcal{T}$ be admissible discretization of Ω. Then the discrete problem (2.14b) admits at least one solution $(u_{i,K}^{n+1})_{K\in\mathscr{T}_h,n\in\{0,1,\dots,N_h\}}$ for $i=1,2,3$.*

Proof. We introduce the Hilbert space $H_h := X_h\times X_h\times X_h$ of triples $\boldsymbol{u}_h^{n+1}=(u_{1,h}^{n+1},u_{2,h}^{n+1},u_{3,h}^{n+1})^{\mathrm{T}}$ of discrete functions on Ω. Here, we denote by $X_h\subset L^2(\Omega)$ the space of functions which are piecewise constant on each control volume K. We define the norm

$$\|\boldsymbol{u}_h^{n+1}\|_{H_h}^2 := \sum_{i=1}^{3}\left(|u_{i,h}^{n+1}|_{X_h}^2+\|u_{i,h}^{n+1}\|_{L^2(\Omega)}^2\right),$$

where the squared discrete seminorm $|\cdot|_{X_h}^2$ is given by

$$|w_h|_{X_h}^2 := \frac{1}{2}\sum_{K\in\mathscr{T}_h}\sum_{L\in\mathcal{N}(K)} m(K|L)d_{K,L}\left|\frac{w_L-w_K}{d_{K,L}}\right|^2$$

We introduce the discrete operator $\boldsymbol{G}_h : H_h\to H_h$ defined by $\boldsymbol{G}_h(\boldsymbol{u}_h):=\boldsymbol{y}_h$, and let $\boldsymbol{\Psi}_h=(\psi_{1,h},\psi_{2,h},\psi_{3,h})^{\mathrm{T}}$. Multiplying (2.14b) by $\psi_{i,h}$ and summing the result over $K\in\mathscr{T}_h$ we obtain

$$\begin{aligned}&\frac{1}{\Delta t}\big(\boldsymbol{B}_h(\boldsymbol{u}_h^{n+1},\boldsymbol{\Psi}_h^{n+1})-\boldsymbol{B}_h\,(\boldsymbol{u}_h^{n},\boldsymbol{\Psi}_h^{n+1})\big)\\&+\boldsymbol{a}_{1,h}(\boldsymbol{u}_h^{n+1},\boldsymbol{\Psi}_h^{n+1})+\boldsymbol{a}_{2,h}\big(\boldsymbol{G}_h(\boldsymbol{u}_h^{n+1}),\boldsymbol{\Phi}_h^{n+1}\big)-\boldsymbol{B}_h(\boldsymbol{F}_h(\boldsymbol{u}_h^{n+1}),\boldsymbol{\Psi}_h^{n+1})=0,\end{aligned}$$

where the discrete bilinear forms are given by

$$\begin{aligned}\boldsymbol{B}_h(\boldsymbol{u}_h^{n+1},\boldsymbol{\Psi}_h^{n+1}) &:= \sum_{K\in\mathscr{T}_h} m(K)\sum_{i=1}^{3}u_{i,K}^{n+1}\psi_{i,K}^{n+1}\\
\boldsymbol{a}_{1,h}(\boldsymbol{u}_h^{n+1},\boldsymbol{\Psi}_h^{n+1}) &:= \frac{1}{2}\sum_{K\in\mathscr{T}_h}\sum_{L\in\mathcal{N}(K)}\tau_{K|L}\sum_{i=1}^{3}D_i(u_{i,L}^{n+1}-u_{i,K}^{n+1})(\psi_{i,L}^{n+1}-\psi_{i,K}^{n+1})\\
\boldsymbol{a}_{2,h}\big(\boldsymbol{G}_h(\boldsymbol{u}_h^{n+1}),\boldsymbol{\Psi}_h^{n+1}\big) &:= -\frac{1}{2}\sum_{K\in\mathscr{T}_h}\sum_{L\in\mathcal{N}(K)}\tau_{K|L}\sum_{i=1}^{3}\chi_i\mathcal{A}_{i,K,L}^{n+1}\boldsymbol{b}_i^{\mathrm{T}}\big(\boldsymbol{y}_L^{n+1}-\boldsymbol{y}_K^{n+1}\big)(\psi_{i,L}^{n+1}-\psi_{i,K}^{n+1}).\end{aligned}$$

Now, we define, by duality, the mapping $\mathbb{P}$ from H_h into itself: for all $\boldsymbol{\Phi}_h\in H_h$

$$\begin{aligned}[\mathbb{P}(\boldsymbol{u}_h^{n+1}),\boldsymbol{\Phi}_h^{n+1}] = &\frac{1}{\Delta t}\big(\boldsymbol{B}_h(\boldsymbol{u}_h^{n+1},\boldsymbol{\Phi}_h^{n+1})-\boldsymbol{B}_h(\boldsymbol{u}_h^{n},\boldsymbol{\Phi}_h^{n+1})\big)+\boldsymbol{a}_{1,h}(\boldsymbol{u}_h^{n+1},\boldsymbol{\Phi}_h^{n+1})\\&+\boldsymbol{a}_{2,h}\big(\boldsymbol{G}_h(\boldsymbol{u}_h^{n+1}),\boldsymbol{\Psi}_h^{n+1}\big)-\boldsymbol{B}_h(\boldsymbol{F}_h^{n+1},\boldsymbol{\Phi}_h^{n+1}),\end{aligned}$$

where $\boldsymbol{F}_h^{n+1}:=(F_{i,h}^{n+1},F_{2,h}^{n+1},F_{3,h}^{n+1})^{\mathrm{T}}$. The continuity of $\mathbb{P}$ follows from that of the nonlinearities $\boldsymbol{F}_h^{n+1}$, $\mathcal{A}_h^{n+1}$ and of $a_{1,h}(\cdot,\cdot)$, $a_{2,h}(\cdot,\cdot)$ and $\boldsymbol{B}_h(\cdot,\cdot)$.

Now, using the definition of $F_{i,K}^{n+1}$, for $i=1,2,3$ and the Young's inequality we deduce

$$
\begin{aligned}
&[\mathbb{P}(\boldsymbol{u}_h^{n+1}),\boldsymbol{u}_h^{n+1}]\\
&\geqslant \frac{1}{\Delta t}\sum_{K\in\mathscr{T}_h} m(K)\sum_{i=1}^{3}(u_{i,K}^{n+1})^2-\frac{1}{\Delta t}\sum_{K\in\mathscr{T}_h} m(K)\sum_{i=1}^{3}u_{i,K}^{n}u_{i,K}^{n+1}\\
&\quad+\frac{1}{2}\sum_{K\in\mathscr{T}_h}\sum_{L\in\mathcal{N}(K)}\tau_{K|L}\sum_{i=1}^{3}D_i(u_{i,L}^{n+1}-u_{i,K}^{n+1})^2+\frac{1}{2}\sum_{K\in\mathscr{T}_h}\sum_{L\in\mathcal{N}(K)}\tau_{K|L}\sum_{i=1}^{3}|\chi_i|\boldsymbol{p}_i^{\mathrm{T}}\boldsymbol{y}_K^{n+1}(u_{i,L}^{n+1}-u_{i,K}^{n+1})^2\\
&\quad-\sum_{K\in\mathscr{T}_h} m(K)\sum_{i=1}^{3}\big((u_{1,K}^{n+1})^2+L_2M_2(u_{2,K}^{n+1})^2+L_3M_3(u_{3,K}^{n+1})^2\big)\\
&\geqslant \frac{1}{2\Delta t}\sum_{K\in\mathscr{T}_h} m(K)\sum_{i=1}^{3}(u_{i,K}^{n+1})^2-\frac{1}{2\Delta t}\sum_{K\in\mathscr{T}_h} m(K)\sum_{i=1}^{3}(u_{i,K}^{n})^2\\
&\quad+\frac{1}{2}\sum_{K\in\mathscr{T}_h}\sum_{L\in\mathcal{N}(K)}\tau_{K|L}\sum_{i=1}^{3}D_i(u_{i,L}^{n+1}-u_{i,K}^{n+1})^2\\
&\quad-\sum_{K\in\mathscr{T}_h} m(K)\sum_{i=1}^{3}\big((u_{1,K}^{n+1})^2+L_2M_2(u_{2,K}^{n+1})^2+L_3M_3(u_{3,K}^{n+1})^2\big)\\
&=\left(\frac{1}{2\Delta t}-1\right)\|u_{1,h}^{n+1}\|_{L^2(\Omega)}^2+D_1|u_{1,h}^{n+1}|_{X_h}+\left(\frac{1}{2\Delta t}-L_2M_2\right)\|u_{2,h}^{n+1}\|_{L^2(\Omega)}^2+D_2|u_{2,h}^{n+1}|_{X_h}\\
&\quad+\left(\frac{1}{2\Delta t}-L_3M_3\right)\|u_{3,h}^{n+1}\|_{L^2(\Omega)}^2+D_3|u_{3,h}^{n+1}|_{X_h}-C_1(\Delta t,\boldsymbol{u}_h^n)\\
&\geqslant C_2\left(\|\boldsymbol{u}_h^{n+1}\|_{H_h}^2\right)-C_1(\Delta t,\boldsymbol{u}_h^n).
\end{aligned}
$$

The constant C_2 depends on D_i, L_j, M_j, and Δt, for $i=1,2,3$ and $j=2,3$, Moreover, due to (2.15), $C_2>0$. This implies that $[\mathbb{P}(\boldsymbol{u}_h^{n+1}),\boldsymbol{u}_h^{n+1}]>0$ whenever $\|\boldsymbol{u}_h^{n+1}\|_{H_h}=r$, where $r>C_1/C_2$. By induction on n, we deduce (see for e.g [35, 63]) the existence of at least one solution to the discrete problem. □

2.5 Convergence

In this section we prove that the solution approximated by the finite volume scheme constitutes a weak solution of (2.1). We start giving compactness argument for the family $\boldsymbol{y}_h$, then we will prove that the family of the discrete solutions $\boldsymbol{u}_h$ is relatively compact in $L^1(\Omega_T)$.

2.5.1 Compactness argument

First, observe that (2.25) and (2.26) imply that the family of discrete solutions $y_{i,h}$ is bounded in $L^2(0,T;H^1(\Omega))$. This ensures the existence of a subsequence, which is not labeled, such that

for all $i = 1, 2, 3$ there holds

$$y_{i,h} \to y_i, \qquad \nabla_h y_{i,h} \to \nabla y_i \quad \text{weakly in } L^2(\Omega_T) \tag{2.29}$$

Next, we use the following lemma proven in [6, Appendix A] to prove that the family of discrete solutions $u_{i,h}$ are relatively compact in $L^1(\Omega_T)$.

Lemma 2.4. *Let Ω be an open bounded polygonal subset of $\mathbb{R}^d$, $T > 0$, and $\Omega_T := \Omega \times (0, T)$. Let $(\mathscr{T}^h)_h$ be an admissible family of meshes on Ω satisfying (2.9); let $(\Delta t_h)_h$ be the associated time steps. For all $h > 0$, assume that the discrete functions (u_h^{n+1}), (f_h^{n+1}) and discrete fields $(\boldsymbol{\mathcal{F}}_h^{n+1})$ for $n \in \{0, 1, \dots, N_h\}$ satisfy the discrete evolution equations*

$$\frac{u_h^{n+1} - u_h^n}{\Delta t} = \operatorname{div}_h[\boldsymbol{\mathcal{F}}_h^{n+1}] + f_h^{n+1} \quad \text{for } n \in \{0, 1, \dots, N_h\} \tag{2.30}$$

with a family $(u_h^0)_h$ of initial data. Assume that for all $\Omega' \subseteq \Omega$, there exists a constant $M(\Omega')$ such that

$$\sum_{n=0}^{N_h} \Delta t \|u_h^{n+1}\|_{L^1(\Omega')} + \sum_{n=0}^{N_h} \Delta t \|f_h^{n+1}\|_{L^1(\Omega')} + \sum_{n=0}^{N_h} \Delta t \|\boldsymbol{\mathcal{F}}_h^{n+1}\|_{L^1(\Omega')} \leqslant M(\Omega'), \tag{2.31}$$

and, moreover,

$$\sum_{n=0}^{N_h} \Delta t \|\nabla_h u_h^{n+1}\|_{L^1(\Omega')} \leqslant M(\Omega'). \tag{2.32}$$

Assume that the family $(u_0^h)_h$ is bounded in $L^1_{\mathrm{loc}}(\Omega)$. Then there exists a measurable function u on Ω_T such that, along a subsequence,

$$\sum_{n=0}^{N_h} \sum_{K \in \mathscr{T}_h} u_k^{n+1} \mathbb{1}_{(t_n, t_{n+1}] \times K} \to u \quad \text{in } L^1_{\mathrm{loc}}(\Omega \times [0, T]) \text{ as } h \to 0.$$

We have the following convergence results along a subsequence.

Lemma 2.5. *There exists $\boldsymbol{u} \in [L^r(\Omega_T)]^3 \cap [L^2(0, T; H^1(\Omega))]^3$ with $r \in (0, 4)$ if d=2, and $r \in (0, 10/3)$ if $d = 3$, and subsequences of $\boldsymbol{u}_h = (u_{1,h}, u_{2,h}, u_{3,h})^{\mathrm{T}}$ not labeled, such that for $i = 1, 2, 3$ and as $h \to 0$,*

(i) $u_{i,h} \to u_i$ *in* $L^1(\Omega_T)$, *a.e in* Ω_T,

(ii) $\nabla_h u_{i,h} \to \nabla u_i$ *weakly in* $[L^2(\Omega_T)]^{2d}$,

(iii) $\mathcal{A}_{i,h} \nabla_h (\boldsymbol{b}_i^T \boldsymbol{y}_h) \to u_i \nabla (\boldsymbol{b}_i^T \boldsymbol{y})$ *weakly in* $[L^1(\Omega_T)]^{2d}$,

(iv) $F_i(\boldsymbol{u}_h) \to F_i(\boldsymbol{u})$ *weakly in* $L^1(\Omega_T)$.

Proof. We fix $i \in \{1,2,3\}$. The evolution of the i-th component $(\boldsymbol{u}_h^{n+1})$ of the solution is governed by the system of discrete equations

$$\frac{u_{i,K}^{n+1}-u_{i,K}^{n}}{\Delta t} = \frac{1}{m(K)} \sum_{L\in\mathcal{N}(K)} |\sigma_{K,L}| \boldsymbol{\mathcal{F}}_{i,K,L}^{n+1} \cdot \boldsymbol{n}_{K,L} + F_{i,K}^{n+1}, \tag{2.33}$$

where $F_{i,K}^{n+1} \coloneqq F_i(u_{1,K}^{n+1}, u_{2,K}^{n+1}, u_{3,K}^{n+1})$ and

$$\begin{aligned}\boldsymbol{\mathcal{F}}_{i,K,L}^{n+1} \cdot \boldsymbol{n}_{K,L} &\coloneqq D_i \frac{u_{i,L}^{n+1}-u_{i,K}^{n+1}}{d_{K,L}} \boldsymbol{n}_{K,L} - \chi_i \mathcal{A}_{i,K,L}^{n+1} \frac{\boldsymbol{b}_i^{\mathrm{T}}\left(\boldsymbol{y}_L^{n+1}-\boldsymbol{y}_K^{n+1}\right)}{d_{K,L}} \boldsymbol{n}_{K,L} \\ &= \nabla_{K,L} u_{i,h}^{n+1} - \chi_i \mathcal{A}_{i,K,L}^{n+1} \nabla_{K,L}\left(\boldsymbol{b}_i^{\mathrm{T}} \boldsymbol{y}_K^{n+1}\right).\end{aligned}$$

Equations (2.33) have the form (2.30) required in Lemma 2.4.

It remains to check that the local L^1 bounds (2.31), (2.32) are satisfied. In fact, we have the global $L^1(\Omega_T)$ uniform estimates on the families

$$u_{i,h} \coloneqq \sum_{\substack{K\in\mathscr{T}_h \\ n\in\{0,1,\dots,N_h\}}} u_{i,K}^{n+1} \mathbb{1}_{(t_n,t_{n+1}]\times K}, \quad \boldsymbol{\mathcal{F}}_{i,h} \coloneqq \frac{1}{2}\sum_{n=0}^{N_h} \sum_{K\in\mathscr{T}_h} \sum_{L\in\mathcal{N}(K)} \boldsymbol{\mathcal{F}}_{i,K,L}^{n+1} \mathbb{1}_{(t_n,t_{n+1}]\times K},$$

$$F_{i,h} \coloneqq \sum_{\substack{K\in\mathscr{T}_h \\ n\in\{0,1,\dots,N_h\}}} F_{i,K}^{n+1} \mathbb{1}_{(t_n,t_{n+1}]\times K}, \quad \nabla_h u_{i,h} \coloneqq \frac{1}{2}\sum_{n=0}^{N_h} \sum_{K\in\mathscr{T}_h} \sum_{L\in\mathcal{N}(K)} \nabla_{K,L} u_{i,h}^{n+1} \mathbb{1}_{(t_n,t_{n+1}]\times K}$$

Indeed, the non-negativity of the discrete solutions, the assumption (2.7) and the Cauchy-Schwarz inequality ensure, for $i = 1,2,3$, the existence of $M_1(\Omega_T), M_2(\Omega_T) > 0$ such that $\|F_{i,h}\|_{L^1(\Omega_T)} \leqslant M_1(\Omega_T)$ and

$$\|u_{i,h}\|_{L^1(\Omega_T)} \leqslant \left(\sum_{n=0}^{N_h} \Delta t \sum_{K\in\mathscr{T}_h} m(K)|u_{i,K}^{n+1}|^2\right)^{1/2} \left(\sum_{n=0}^{N_h} \Delta t \sum_{K\in\mathscr{T}_h} m(K)\right)^{1/2} \leqslant M_2(\Omega_T).$$

The estimate (2.19) and the restriction (2.10) guarantee the existence of $M_3(\Omega_T) > 0$ satisfying

$$\begin{aligned}&\|\nabla_h u_{i,h}\|_{L^1(\Omega_T)} \\ &= \frac{1}{2}\sum_{n=0}^{N_h} \Delta t \sum_{K\in\mathscr{T}_h} \sum_{L\in\mathcal{N}(K)} m(K|L)|u_{i,L}^{n+1} - u_{i,K}^{n+1}| \\ &= \frac{1}{2}\sum_{n=0}^{N_h} \Delta t \sum_{K\in\mathscr{T}_h} \sum_{L\in\mathcal{N}(K)} \sqrt{m(K|L)d_{K|L}}\sqrt{m(K|L)}\frac{|u_{i,L}^{n+1}-u_{i,K}^{n+1}|}{\sqrt{d_{K|L}}} \\ &\leqslant \left(\frac{1}{2}\sum_{n=0}^{N_h} \Delta t \sum_{K\in\mathscr{T}_h} \sum_{L\in\mathcal{N}(K)} \tau_{K|L}(u_{i,L}^{n+1}-u_{i,K}^{n+1})^2\right)^{1/2} \times \\ &\quad \left(\frac{1}{2}\sum_{n=0}^{N_h} \Delta t \sum_{K\in\mathscr{T}_h} \sum_{L\in\mathcal{N}(K)} \gamma m(K)\right)^{1/2} \\ &\leqslant M_3(\Omega_T).\end{aligned} \tag{2.34}$$

Using the critical discrete Sobolev embedding (see [6, Appendix B, Prop. B.1]) and the interpolation between $L^{p_t}(0,T;L^{p_x}(\Omega))$ spaces, from the $L^\infty(0,T;L^2(\Omega))$ estimate (2.18) and the discrete $L^2(0,T;H^1(\Omega))$ estimate (2.19) we get a uniform $L^r(\Omega_T)$ bound on $u_{i,h}$, and uniform $L^1(\Omega_T)$ bound on $\mathcal{A}_{i,h}$ (moreover, they are uniformly integrable). The quantity

$$\mathcal{A}_{i,h} \coloneqq \frac{1}{2}\sum_{n=0}^{N_h}\sum_{K\in\mathscr{T}_h}\sum_{L\in\mathcal{N}(K)}\mathcal{A}_{i,K,L}^{n+1}\mathbb{1}_{(t_n,t_{n+1}]\times K}$$

satisfies the estimate

$$\begin{aligned}
\|\mathcal{A}_{i,h}\nabla_h\big(\boldsymbol{b}_i^{\mathrm{T}}\boldsymbol{y}_h\big)\|_{L^1(\Omega_T)} &= \frac{1}{2}\sum_{n=0}^{N_h}\Delta t\sum_{K\in\mathscr{T}_h}\sum_{L\in\mathcal{N}(K)} m(K|L)\mathcal{A}_{i,K,L}^{n+1}|\boldsymbol{b}_i^{\mathrm{T}}\big(\boldsymbol{y}_L^{n+1}-\boldsymbol{y}_K^{n+1}\big)| \\
&\leqslant \frac{1}{2}\sum_{n=0}^{N_h}\Delta t\sum_{K\in\mathscr{T}_h}\sum_{L\in\mathcal{N}(K)} m(K|L)u_{i,K}^{n+1}|\boldsymbol{b}_i^{\mathrm{T}}\big(\boldsymbol{y}_L^{n+1}-\boldsymbol{y}_K^{n+1}\big)| \\
&\leqslant \left(\frac{1}{2}\sum_{n=0}^{N_h}\Delta t\sum_{K\in\mathscr{T}_h}\sum_{L\in\mathcal{N}(K)}\tau_{K|L}\big(\boldsymbol{b}_i^{\mathrm{T}}(\boldsymbol{y}_L^{n+1}-\boldsymbol{y}_K^{n+1})\big)^2\right)^{1/2} \\
&\quad\times\left(\frac{1}{2}\sum_{n=0}^{N_h}\Delta t\sum_{K\in\mathscr{T}_h}\sum_{L\in\mathcal{N}(K)}\gamma m(K)(u_K^{n+1})^2\right)^{1/2}\leqslant M_4(\Omega_T).
\end{aligned} \tag{2.35}$$

Since we can write

$$\boldsymbol{\mathcal{F}}_{i,h} = \nabla_h u_{i,h} - \chi_i\mathcal{A}_{i,h}^{n+1}\nabla_h\big(\boldsymbol{b}_i^{\mathrm{T}}\boldsymbol{y}_h\big),$$

we deduce an $L^1(\Omega_T)$ bound on $\boldsymbol{\mathcal{F}}_h$ from (2.34) and (2.35). Thus (2.31) and (2.32) are satisfied; the uniform $L^1(\Omega)$ bound on the initial data $u_{0,h}$ is also clear from (2.13), and Lemma 2.4 can be applied to derive the $L^1(\Omega_T)$ compactness of $(\boldsymbol{u}_h)_h$. Thus we can define the limits $\boldsymbol{u}=(u_1,u_2,u_3)$ of $\boldsymbol{u}_h$ and from this obtain the claim (i). Furthermore, to deduce the claim (ii), we use (2.19) to bound $\nabla_h u_{i,h}$ in $L^2(\Omega_T)$. Upon extraction of a further subsequence, we have e.g. $u_{i,h}\to u_i\in L^2(\Omega_T)$ and $\nabla_h u_{i,h}\to\zeta_i$ in $[L^2(\Omega_T)]^d$. Let us show (as in [46]) that $u_i\in L^2(0,T;H^1(\Omega))$ and $\zeta_i=\nabla u_i$ for $i=1,2,3$. Let $\Psi_i\in C_{\mathrm{c}}^\infty([0,T)\times\bar\Omega))$ be given and

$$T_{i,1} \coloneqq \int_0^T\int_\Omega \nabla_h u_{i,h}(\boldsymbol{x},t)\Psi_i(\boldsymbol{x},t)\,\mathrm{d}\boldsymbol{x}\,\mathrm{d}t = -\frac{1}{2}\sum_{n=0}^{N_h}\Delta t\sum_{K\in\mathscr{T}_h}\sum_{L\in\mathcal{N}(K)}\tau_{K|L}(u_{i,L}^{n+1}-u_{i,K}^{n+1})\cdot\Psi_{i,K}^{n+1},$$

$$T_{i,2} \coloneqq \frac{1}{2}\sum_{n=0}^{N_h}\Delta t\sum_{K\in\mathscr{T}_h}\sum_{L\in\mathcal{N}(K)} m(K|L)(u_{i,L}^{n+1}-u_{i,K}^{n+1})\boldsymbol{n}_{K|L}\cdot\Psi_{i,K|L}^{n+1},$$

where $\boldsymbol{n}_{K|L}$ denotes the unit normal vector to $K|L$ outward to K and we define

$$\Psi_{i,K}^{n+1} \coloneqq \frac{1}{m(K)}\int_K\Psi_i(x,t_{n+1})\,\mathrm{d}\boldsymbol{x}\,\mathrm{d}t,\quad\text{and}\quad \Psi_{i,K|L}^{n+1} \coloneqq \frac{1}{m(K|L)}\int_{\sigma_{K|L}}\Psi_i(x,t_{n+1})\,\mathrm{d}\gamma(\boldsymbol{x}).$$

Applying summation by parts and the Cauchy-Schwarz inequality, we get

$$
\begin{aligned}
&|T_{i,1} - T_{i,2}| \\
&= \left| \frac{1}{2} \sum_{n=0}^{N_h} \Delta t \sum_{K \in \mathscr{T}_h} \sum_{L \in \mathcal{N}(K)} m(K|L) \big(u_{i,L}^{n+1} - u_{i,K}^{n+1}\big) \big(\boldsymbol{n}_{K|L} \cdot \big(\Psi_{i,K}^{n+1} - \Psi_{i,K|L}^{n+1}\big)\big) \right| \\
&\leqslant \left(\frac{1}{2} \sum_{n=0}^{N_h} \Delta t \sum_{K \in \mathscr{T}_h} \sum_{L \in \mathcal{N}(K)} \tau_{K|L} |u_{i,L}^{n+1} - u_{i,K}^{n+1}|^2 \right)^{1/2} \times \\
&\quad \left(\frac{1}{2} \sum_{n=0}^{N_h} \Delta t \sum_{K \in \mathscr{T}_h} \sum_{L \in \mathcal{N}(K)} m(K|L) d_{K|L} (R_{i,K|L})^2 \right)^{1/2},
\end{aligned}
$$

where we define $R_{i,K|L} \coloneqq \Psi_{i,K}^{n+1} - \Psi_{i,K|L}^{n+1}$. Regularity properties of the function Ψ_i give the existence of $C_{i,\Psi_i} > 0$ only depending on Ψ_i, such that $|R_{i,K|L}| \leqslant C_{i,\Psi_i} h$. Therefore,

$$
\frac{1}{2} \sum_{n=0}^{N_h} \Delta t \sum_{K \in \mathscr{T}_h} \sum_{L \in \mathcal{N}(K)} m(K|L) d_{K|L} \leqslant d m(\Omega_T)
$$

and the estimate (2.19) imply that $T_{i,1} - T_{i,2} \to 0$ as $h \to 0$. Applying summation by parts yields

$$
T_{i,2} = -\frac{1}{2} \sum_{n=0}^{N_h} \Delta t \sum_{K \in \mathscr{T}_h} \sum_{L \in \mathcal{N}(K)} m(K|L) u_{i,K}^{n+1} \boldsymbol{n}_{K|L} \cdot \Psi_{i,K|L}^{n+1} = - \int_0^T \int_\Omega u_{i,h}(\boldsymbol{x}, t) \operatorname{div}\big(\Psi_i(\boldsymbol{x}, t)\big) \, \mathrm{d}\boldsymbol{x} \, \mathrm{d}t,
$$

such that

$$
T_{i,1} \longrightarrow - \int_0^T \int_\Omega u_i(\boldsymbol{x}, t) \operatorname{div}\big(\Psi_i(\boldsymbol{x}, t)\big) \, \mathrm{d}\boldsymbol{x} \, \mathrm{d}t \quad \text{as } h \to 0.
$$

This proves that $u_i \in L^2(0, T; H^1(\Omega_T))$ and the function $\zeta_i \in [L^2(\Omega_T)]^d$ is almost everywhere equal to ∇u_i for $i = 1, 2, 3$ in Ω_T, and the uniqueness of the limit implies that the whole family $\nabla_h u_{i,h}$ weakly convergence in $[L^2(\Omega_T)]^d$ to ∇u_i as $h \to 0$. Now, from the a.e convergence of $u_{i,h}$ to u_i and the Vitali theorem one has $\mathcal{A}_{i,h}$ weakly converge to u_i. Then, we using (2.29) and pass the limit to obtain (iii).

To prove (iv), we use the uniform $L^2(\Omega_T)$ estimation of $u_{i,h}$ and the assumption (2.7) of F_i to prove that the family $(F_i(\boldsymbol{u}_h))_h$ is uniformly integrable. Finally, using the a.e. convergence of $\boldsymbol{u}_h$ to $\boldsymbol{u}$ and by the Vitali theorem we get the a.e. convergence of $F_i(\boldsymbol{u}_h)$ to $F_i(\boldsymbol{u})$ in $L^1(\Omega_T)$ and from this we get (iv). □

2.5.2 Convergence analysis

Our final goal is to show that the limit functions $\boldsymbol{u}$ constructed in Lemma (2.5.1) and the limit $\boldsymbol{y}$ given in (2.29) constitute a weak solution of system (2.1). We start by passing the limit (keep in mind that $i = 1, 2, 3$) in (2.14b) to get the first equation in (2.8).

Let $\psi_i \in \mathcal{D}([0,T)\times\bar{\Omega})$. Set $\psi_{i,K}^n := \psi_i(\boldsymbol{x}_K, t_n)$ for all $K \in \mathscr{T}_h$ and $n \in [0, N_h+1]$. Then multiply the discrete equation (2.14b) by $\Delta t \psi_{i,K}^{n+1}$ and summing the result over $K \in \mathscr{T}_h$ and $n \in \{0,1,\dots,N_h\}$.

$$T_{i,h}^1 + T_{i,h}^2 + T_{i,h}^3 = T_{i,h}^4,$$

where

$$\begin{aligned}
T_{i,h}^1 &= \sum_{n=0}^{N_h} \sum_{K\in\mathscr{T}_h} m(K)(u_{i,K}^{n+1} - u_{i,K}^n)\psi_{i,K}^{n+1},\\
T_{i,h}^2 &= -D_i \sum_{n=0}^{N_h} \Delta t \sum_{K\in\mathscr{T}_h} \sum_{L\in\mathcal{N}(K)} \tau_{K|L}(u_{i,L}^{n+1} - u_{i,K}^{n+1})\psi_{i,K}^{n+1},\\
T_{i,h}^3 &= \chi_i \sum_{n=0}^{N_h} \Delta t \sum_{K\in\mathscr{T}_h} \sum_{L\in\mathcal{N}(K)} \tau_{K|L}\mathcal{A}_{i,K,L}^{n+1}\boldsymbol{b}_i^{\mathrm{T}}\big(\boldsymbol{y}_L^{n+1} - \boldsymbol{y}_K^{n+1}\big)\psi_{i,K}^{n+1},\\
T_{i,h}^4 &= \sum_{n=0}^{N_h} \Delta t \sum_{K\in\mathscr{T}_h} m(K) F_{i,K}^{n+1}\psi_{i,K}^{n+1}.
\end{aligned}$$

Item (iv) of Lemma 2.5 implies that

$$T_{i,h}^4 \longrightarrow \int_0^T \int_\Omega F_i(\boldsymbol{u})\psi_i \,\mathrm{d}\boldsymbol{x}\,\mathrm{d}t \quad \text{as } h \to 0.$$

By a summation by parts in time and keeping in mind that $\psi^{N_h+1} = 0$ we get

$$\begin{aligned}
T_{i,h}^1 &= -\sum_{n=0}^{N_h} \sum_{K\in\mathscr{T}_h} m(K)u_{i,K}^{n+1}(\psi_{i,K}^{n+1} - \psi_{i,K}^n) - \sum_{K\in\mathscr{T}_h} m(K)u_{i,K}^0\psi_{i,K}^0\\
&= -\sum_{n=0}^{N_h} \sum_{K\in\mathscr{T}_h} \int_{t_n}^{t_{n+1}} \int_K u_{i,K}^{n+1}\partial_t\psi_i(\boldsymbol{x}_K,t)\,\mathrm{d}\boldsymbol{x}\,\mathrm{d}t - \sum_{K\in\mathscr{T}_h}\int_K u_{i,K}^0\psi_{i,K}^0\,\mathrm{d}\boldsymbol{x} =: -T_{i,h}^{1,1} - T_{i,h}^{1,2}.
\end{aligned}$$

We compare $T_{i,h}^1$ with

$$\tilde{T}_{i,h}^1 := -\sum_{n=0}^{N_h} \sum_{K\in\mathscr{T}_h} \int_{t_n}^{t_{n+1}} \int_K u_{i,h}(\boldsymbol{x},t)\partial_t(\psi_i(\boldsymbol{x},t)\,\mathrm{d}\boldsymbol{x}\,\mathrm{d}t - \int_\Omega u_{i,0}(\boldsymbol{x})\psi_i(\boldsymbol{x},0)\,\mathrm{d}\boldsymbol{x} = -\tilde{T}_{i,h}^{1,1} - \tilde{T}_{i,h}^{1,2}$$

to obtain

$$\begin{aligned}
\big|T_{i,h}^{1,2} - \tilde{T}_{i,h}^{1,2}\big| &= \left|\int_\Omega u_{i,0}(\boldsymbol{x})\psi_i(x,0)\,\mathrm{d}\boldsymbol{x} - \sum_{K\in\mathscr{T}_h} m(K)u_{i,K}^0\psi_{i,K}^0 -\right|\\
&= \left|\int_\Omega u_{i,0}(\boldsymbol{x})\left(\sum_{K\in\mathscr{T}_h}(\psi_i(\boldsymbol{x},0) - \psi_i(\boldsymbol{x}_K,0))\right)\mathrm{d}\boldsymbol{x}\right|\\
&\leqslant \left(\int_\Omega |u_{i,0}|^2\,\mathrm{d}\boldsymbol{x}\right)^{1/2}\left(\sum_{K\in\mathscr{T}_h}\int_K |\psi_i(\boldsymbol{x},0) - \psi_i(\boldsymbol{x}_K,0)|^2\,\mathrm{d}\boldsymbol{x}\right)^{1/2} \leqslant C_{i,1}h
\end{aligned}$$

due to the Lipschitz continuity of ψ_i. Using the regularity properties of $\partial_t\psi_i$ and the estimates (2.18) we get

$$\begin{aligned}
&|T^{1,1}_{i,h} - \tilde{T}^{1,1}_{i,h}| \\
&= \left| \sum_{n=0}^{N_h} \sum_{K\in\mathscr{T}_h} \int_{t_n}^{t_{n+1}} \int_K u_{i,h}(\boldsymbol{x},t)\partial_t\psi_i(\boldsymbol{x},t)\,\mathrm{d}\boldsymbol{x}\,\mathrm{d}t - \sum_{n=0}^{N_h} \sum_{K\in\mathscr{T}_h} \int_{t_n}^{t_{n+1}} \int_K u^{n+1}_{i,K}\partial_t\psi_i(\boldsymbol{x}_K,t)\,\mathrm{d}\boldsymbol{x}\,\mathrm{d}t \right| \\
&\leqslant \left| \sum_{n=0}^{N_h} \Delta t \sum_{K\in\mathscr{T}_h} m(K) u^{n+1}_{i,K} \int_{t_n}^{t_{n+1}} \int_K (\partial_t\psi_i(\boldsymbol{x},t) - \partial_t\psi_i(\boldsymbol{x}_K,t))\,\mathrm{d}\boldsymbol{x}\,\mathrm{d}t \right| \\
&\leqslant C_2 h \left(\sum_{n=0}^{N_h} \Delta t \sum_{K\in\mathscr{T}_h} m(K)|u^{n+1}_{i,K}|^2 \right)^{1/2} \leqslant C_3 h.
\end{aligned}$$

Thus $T^{1,1}_{i,h} \to \tilde{T}^{1,1}_{i,h}$ and $T^{1,2}_{i,h} \to \tilde{T}^{1,2}_{i,h}$ as $h \to 0$, which proves that

$$T^1_{i,h} \longrightarrow -\int_0^T \int_\Omega u(\boldsymbol{x},t)\partial_t\psi(\boldsymbol{x},t)\,\mathrm{d}\boldsymbol{x}\,\mathrm{d}t - \int_\Omega u_0(\boldsymbol{x})\partial_t\psi(x,0)\,\mathrm{d}\boldsymbol{x}\,\mathrm{d}t \quad \text{as } h \to 0.$$

Next, we deal with $T_{2,h}$ and $T_{3,h}$. Gathering by edges and using the definition (2.11) of $\nabla_h u_h$, we get

$$\begin{aligned}
T^2_{i,h} &= \frac{D_i}{2} \sum_{n=0}^{N_h} \Delta t \sum_{K\in\mathscr{T}_h} \sum_{L\in\mathcal{N}(K)} \tau_{K|L}(u^{n+1}_{i,L} - u^{n+1}_{i,K})(\psi^{n+1}_{i,L} - \psi^{n+1}_{i,K}) \\
&= \frac{D_i}{2} \sum_{n=0}^{N_h} \Delta t \sum_{K\in\mathscr{T}_h} \sum_{L\in\mathcal{N}(K)} m(K|L) d_{K|L} \frac{u^{n+1}_{i,L} - u^{n+1}_{i,K}}{d_{K|L}} \frac{\psi^{n+1}_{i,L} - \psi^{n+1}_{i,K}}{d_{K|L}} \\
&= \frac{D_i}{2} \sum_{n=0}^{N_h} \Delta t \sum_{K\in\mathscr{T}_h} \sum_{L\in\mathcal{N}(K)} m(K|L) d_{K|L} (\nabla_{K|L} u^{n+1}_{i,h} \cdot \boldsymbol{n}_{K,L})(\nabla_{K|L}\psi_i(\overline{\boldsymbol{x}_{K,L}}, t_{n+1}\cdot\boldsymbol{n}_{K,L}),
\end{aligned}$$

and

$$\begin{aligned}
T^3_{i,h} &= -\frac{\chi_i}{2} \sum_{n=0}^{N_h} \Delta t \sum_{K\in\mathscr{T}_h} \sum_{L\in\mathcal{N}(K)} \tau_{K|L} \mathcal{A}^{n+1}_{i,K,L} \boldsymbol{b}_i^{\mathrm{T}} (\boldsymbol{y}^{n+1}_L - \boldsymbol{y}^{n+1}_K)(\psi^{n+1}_{i,L} - \psi^{n+1}_{i,K}) \\
&= -\frac{\chi_i}{2} \sum_{n=0}^{N_h} \Delta t \sum_{K\in\mathscr{T}_h} \sum_{L\in\mathcal{N}(K)} m(K|L) d_{K|L} \mathcal{A}^{n+1}_{i,K,L} \frac{\boldsymbol{b}_i^{\mathrm{T}} (\boldsymbol{y}^{n+1}_L - \boldsymbol{y}^{n+1}_K)}{d_{K|L}} \frac{(\psi^{n+1}_{i,L} - \psi^{n+1}_{i,K})}{d_{K|L}} \\
&= -\frac{\chi_i}{2} \sum_{n=0}^{N_h} \Delta t \sum_{K\in\mathscr{T}_h} \sum_{L\in\mathcal{N}(K)} m(K|L) d_{K|L} \mathcal{A}^{n+1}_{i,K,L} (\nabla_{K|L}(\boldsymbol{b}_i^{\mathrm{T}} \boldsymbol{y}^{n+1}_h) \cdot \boldsymbol{n}_{K,L})(\nabla_{K|L}\psi_i(\overline{\boldsymbol{x}_{K,L}}, t_{n+1}\cdot\boldsymbol{n}_{K,L}),
\end{aligned}$$

where $\overline{\boldsymbol{x}_{K,L}}$ is some point on the segment with the endpoints $\boldsymbol{x}_K$, $\boldsymbol{x}_L$. Since the values $\nabla_{K,L}$ are aligned with $\boldsymbol{n}_{K,L}$, we have

$$\begin{aligned}
(\nabla_{K|L} u^{n+1}_h \cdot \boldsymbol{n}_{K,L})(\nabla_{K|L}\psi(\overline{\boldsymbol{x}_{K,L}}, t_{n+1})\cdot\boldsymbol{n}_{K,L}) &\equiv (\nabla_{K|L} u^{n+1}_h) \cdot (\nabla_{K|L}\psi(\overline{\boldsymbol{x}_{K,L}}, t_{n+1})) \\
(\nabla_{K|L}(\boldsymbol{b}_i^{\mathrm{T}} \boldsymbol{y}^{n+1}_h) \cdot \boldsymbol{n}_{K,L})(\nabla_{K|L}\psi(\overline{\boldsymbol{x}_{K,L}}, t_{n+1})\cdot\boldsymbol{n}_{K,L}) &\equiv (\nabla_{K|L}(\boldsymbol{b}_i^{\mathrm{T}} \boldsymbol{y}^{n+1}_h)) \cdot (\nabla_{K|L}\psi(\overline{\boldsymbol{x}_{K,L}}, t_{n+1})),
\end{aligned}$$

Then

$$T^2_{i,h} = D_i \int_0^T \int_\Omega \nabla_h u_h (\nabla\psi)_h \,\mathrm{d}\boldsymbol{x}\,\mathrm{d}t, \quad T^3_{i,h} = -\chi_i \int_0^T \int_\Omega \mathcal{A}_{i,h} \nabla_{K|L}(\boldsymbol{b}_i^{\mathrm{T}} \boldsymbol{y}_h^{n+1})(\nabla\psi)_h \,\mathrm{d}\boldsymbol{x}\,\mathrm{d}t,$$

where $(\nabla\psi_i)_h|_{(t_n,t_{n+1})\times K} \coloneqq \nabla\psi_i(\overline{\boldsymbol{x}_K\boldsymbol{x}_L}, t_{n+1})$. Here the construction of the diamond $T_{K,L}$ from the neighboring centers $\boldsymbol{x}_K$ and $\boldsymbol{x}_L$ and the interface $\sigma = K|L$ (see e.g [5, 6]) has been used.

From the continuity of $\nabla\psi$ we get $(\nabla\psi_i)_h \to \nabla\psi_i$ in $L^\infty(\Omega_T)$. Hence using the weak L^2 convergence of $\nabla_h u_{i,h}$ to ∇u_i, and the weak L^1 convergence of $\mathcal{A}_{i,h}\nabla_h(\boldsymbol{b}_i^{\mathrm{T}}\boldsymbol{y}_h)$ to $u_i\nabla(\boldsymbol{b}_i^{\mathrm{T}}\boldsymbol{y}_h)$, we obtain

$$T^2_{i,h} \to D_i \int_0^T \int_\Omega \nabla u \nabla\psi \,\mathrm{d}\boldsymbol{x}\,\mathrm{d}t, \quad T^3_{i,h} \to -\chi_i \int_0^T \int_\Omega u_i \nabla(\boldsymbol{b}_i^{\mathrm{T}}\boldsymbol{y})\nabla\psi \,\mathrm{d}\boldsymbol{x}\,\mathrm{d}t \quad \text{as } h \to 0.$$

Gathering the results obtained, we can justify first equation in (2.8). Finally, we use (2.29) and reasoning in the same way as above, we pass to the limit in (2.14a) to prove that second equation in (2.8). This concludes the proof of the following theorem.

Theorem 2.3. *Assume that $u_{i,0} \in (L^2(\Omega))^+$ for $i = 1, 2, 3$. Let $\boldsymbol{u}_h = (u_{1,h}, u_{2,h}, u_{3,h})^{\mathrm{T}}$ be the discrete solution generated by the finite volume scheme (2.14) on a family of meshes satisfying (2.9) and (2.10). Then, as $h \to 0$, $\boldsymbol{u}_h$ converges (along a subsequence) a.e on Ω_T to a limit $\boldsymbol{u} = (u_1, u_2, u_3)^{\mathrm{T}}$ that is a weak solution of the system (2.1), (2.2).*

2.6 Numerical examples

We present in this section some numerical results obtained by the finite volume scheme (2.14). To obtain the numerical test, we will reduce the number of the parameters in the model (2.1), (2.2). For this reason we non-dimensionalize the system following [52]. We choose $U_i = u_i/k$ for $i = 1, 2, 3$. Making the substitution and simplifying, we obtain

$$\begin{aligned}
F_1(\boldsymbol{U}) &= (1 - U_1)U_1 - \frac{a_1 U_1}{1 + b_1 U_1} U_2, \\
F_2(\boldsymbol{U}) &= \frac{a_1 U_1}{1 + b_1 U_1} U_2 - \frac{a_2 U_2}{1 + b_2 U_2} U_3 - e_1 U_2, \\
F_3(\boldsymbol{U}) &= \frac{a_2 U_2}{1 + b_2 U_2} U_3 - e_2 U_3.
\end{aligned}$$

On the domain $\Omega \coloneqq (-2, 2) \times (-2, 2)$ we define a uniform Cartesian grid

$$\mathscr{T}_h = \{K_{ij} \subseteq \Omega \ : \ K_{ij} = ((i-1)N_x, iN_x) \times ((j-1)N_x, jN_x)\}$$

with $N_x \times N_y$ control volumes. For the simulations, we choose $N_x = N_y = 256$ and we take the parameters

$$a_1 = 5.0, \qquad a_2 = 0.1, \qquad b_1 = 2.0, \qquad b_2 = 2.0, \qquad e_1 = 0.4, \qquad e_2 = 0.01$$

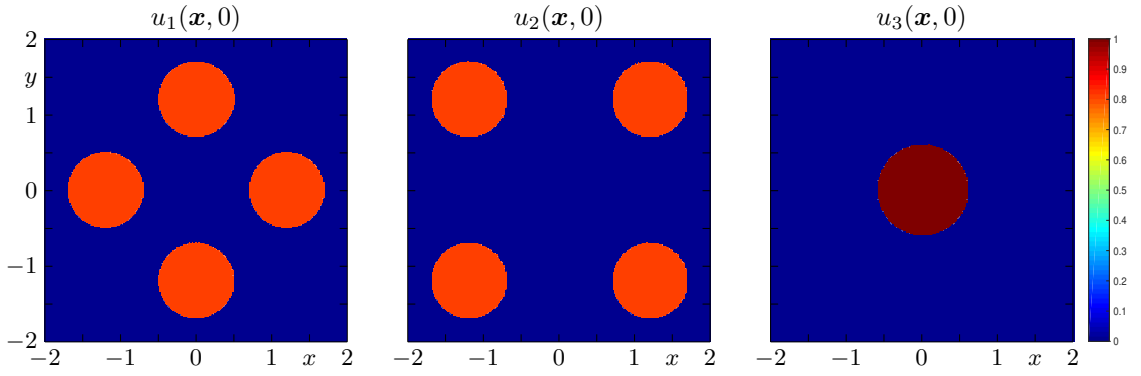

Figure 2.2: Example 1: initial condition for the u_1, u_2 and u_3 species.

used in [52]. The corresponding diffusion coefficients are given by $D_i = \mathcal{D}_i = \theta_i = 1$, for $i = 1, 2, 3$. The sensitivity chemotactic parameters are chosen by

$$\delta_1 = 100, \qquad \delta_2 = 20, \qquad \delta_3 = 10.$$

The initial distribution for u_1, u_2 and u_3 species correspond to a constant $u_{1,0} = u_{2,0} = 0.8$ and $u_{3,0} = 1$.

In order to illustrate the convergence of the numerical scheme and due to the lack of exact solutions for each example, we compute approximate errors in different norms using a numerical solution on an extremely fine mesh as reference. To measure errors between such a reference solution u_{ref} and an approximate solution u_h at time t^n, we will use the L^2-error

$$e_2^n(u) = \|u_{\text{ref}}^n - u_h^n\|_2 = \left(\sum_{K \in \mathcal{T}_h} \frac{1}{m(K)} |u_{\text{ref},K}^n - u_{h,K}^n|^2 \right)^{1/2}.$$

Here, $u_{\text{ref},K}^n$ stands for the projection of the reference solution onto control volume K. For solving the corresponding nonlinear system arising from the implicit finite FV, we use the Newton method, where at each time step, only a few iterations are required to achieve convergence. In addition, the linear systems involved in Newton method are solved by the GMRES method.

2.6.1 Example 2.1 (species interacting via chemical substance)

For this numerical test, the chemotactic coefficients are $\chi_1 = -0.8$, $\chi_2 = 0.8$ and $\chi_3 = 2$, where $\chi_1 < 0$ means that movement of the prey is against the presence of the predator. For the initial condition, the super-predators are concentrated in small pockets at a one spatial point while de predators and preys are concentrated in small pockets at four spatial points (see Figure 2.2).

In Figure 2.3, we display the numerical solution for each species at three different simulated times. Initially, at simulated time $t = 0.02$ (Figure 2.3, top), we can observe the effect of

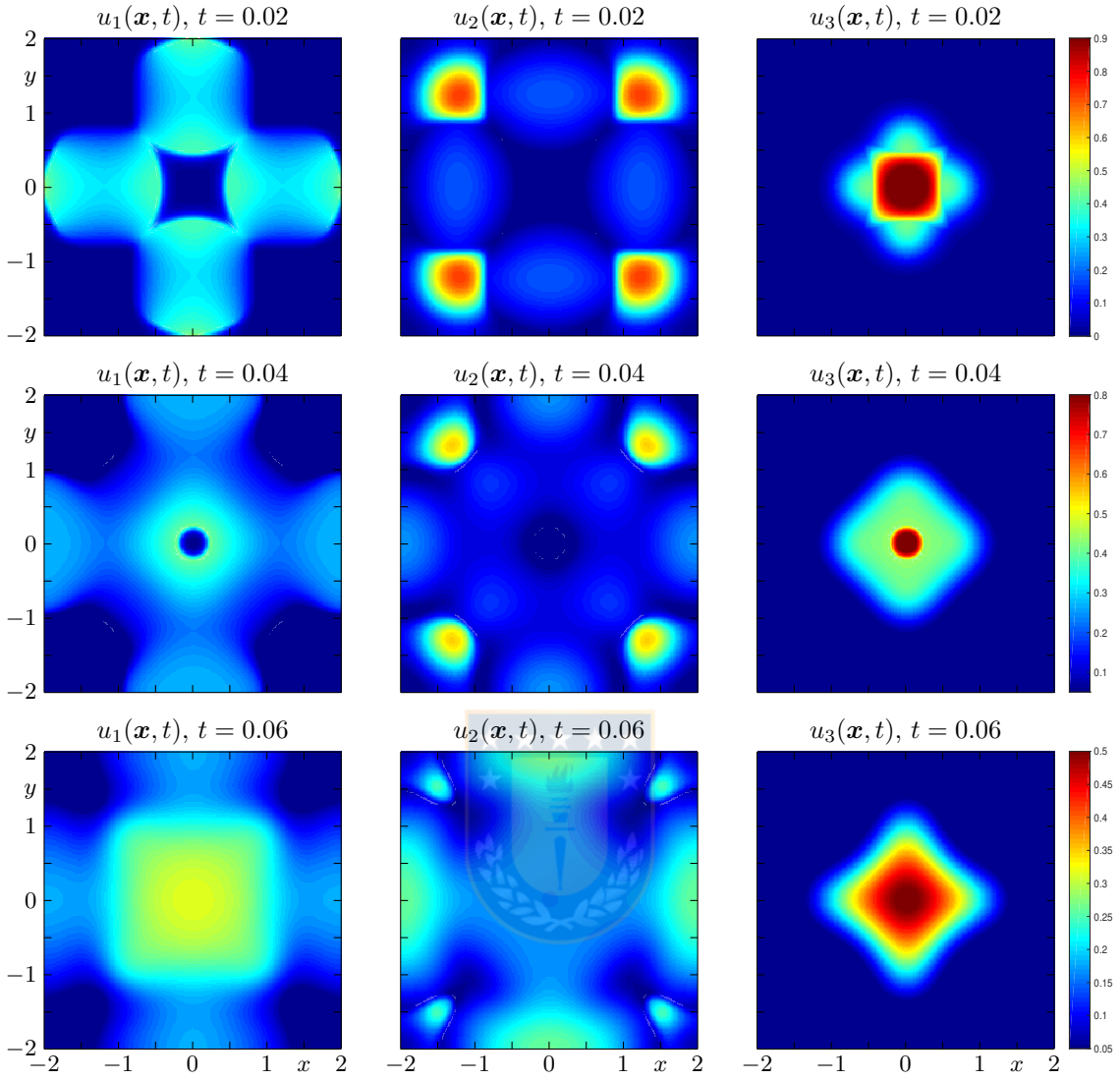

Figure 2.3: Example 1.1: interaction of the three species at different times $t = 0.02,\ 0.04,\ 0.06$.

the chemotaxis for the super-predators (u_3) and predators (u_2) feeling their respective preys, and the preys feeling the presence of the predator. At simulation time $t = 0.04$ (Figure 2.3, middle). We notice the rapid movement of the super-predators towards the regions occupied by the predators and at the same time predators spread out to the areas where the prey (u_1) are located, but it does not move towards the area occupied by the predator. The prey move to the regions where the predator is not located. At $t = 0.06$ (Figure 2.3, bottom), we can see that the super-predators continue moving towards the area occupied by the predators, the predators occupy almost the entire area, except the region where the super-predators are located while the prey move toward (running away) the area where the predators are not located. In Table 2.1 we show the L^2-error for each species at simulated time $t = 0.02$, we observe convergence of the numerical scheme.

$N_x \times N_y$	h	$e_2^n(u_1)$	$e_2^n(u_2)$	$e_2^n(u_3)$
32×32	1.25e-1	1.33e-03	3.09e-03	4.97e-04
64×64	6.25e-2	2.82e-04	6.61e-04	2.09e-04
128×128	3.12e-2	4.41e-05	1.16e-04	3.39e-05
256×256	1.56e-2	1.07e-05	3.20e-05	8.00e-06

Table 2.1: Example 1.1: approximate L^2-errors for each species at simulated time $t = 0.02$.

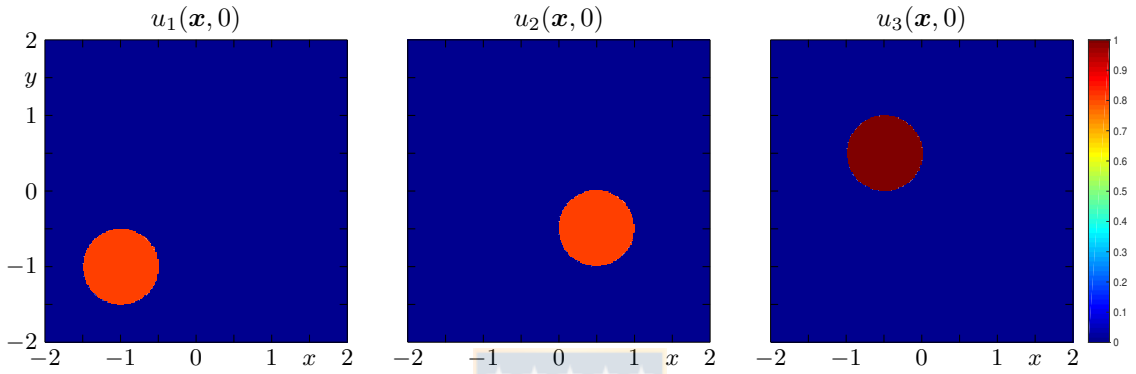

Figure 2.4: Example 2.2: initial condition for the u_1, u_2 and u_3 species.

2.6.2 Example 2.2 (prey do not interact via chemical substances)

In Example 2, we choose $\chi_1 = 0$, $\chi_2 = 0.8$ and $\chi_3 = 2$. In this case we do not consider chemotactic movement of the prey. The initial distribution is as in Example 1, but the super-predators, predators, and prey are concentrated in small pockets at a one spatial point (see Figure 2.4). We display in Figure 2.5 the numerical solution for each species at three different simulations time. We notice the rapid movement of the super-predators towards the regions occupied by the predators and at the same time predators spread out to the areas where the preys are located, while the prey present isotropic and homogeneous diffusion (due to the choice of the chemotactic coefficients $\chi_1 = 0$). In Table 2.2 we show the L^2-error for each species at simulated time $t = 0.04$, we observe the convergence of the numerical scheme.

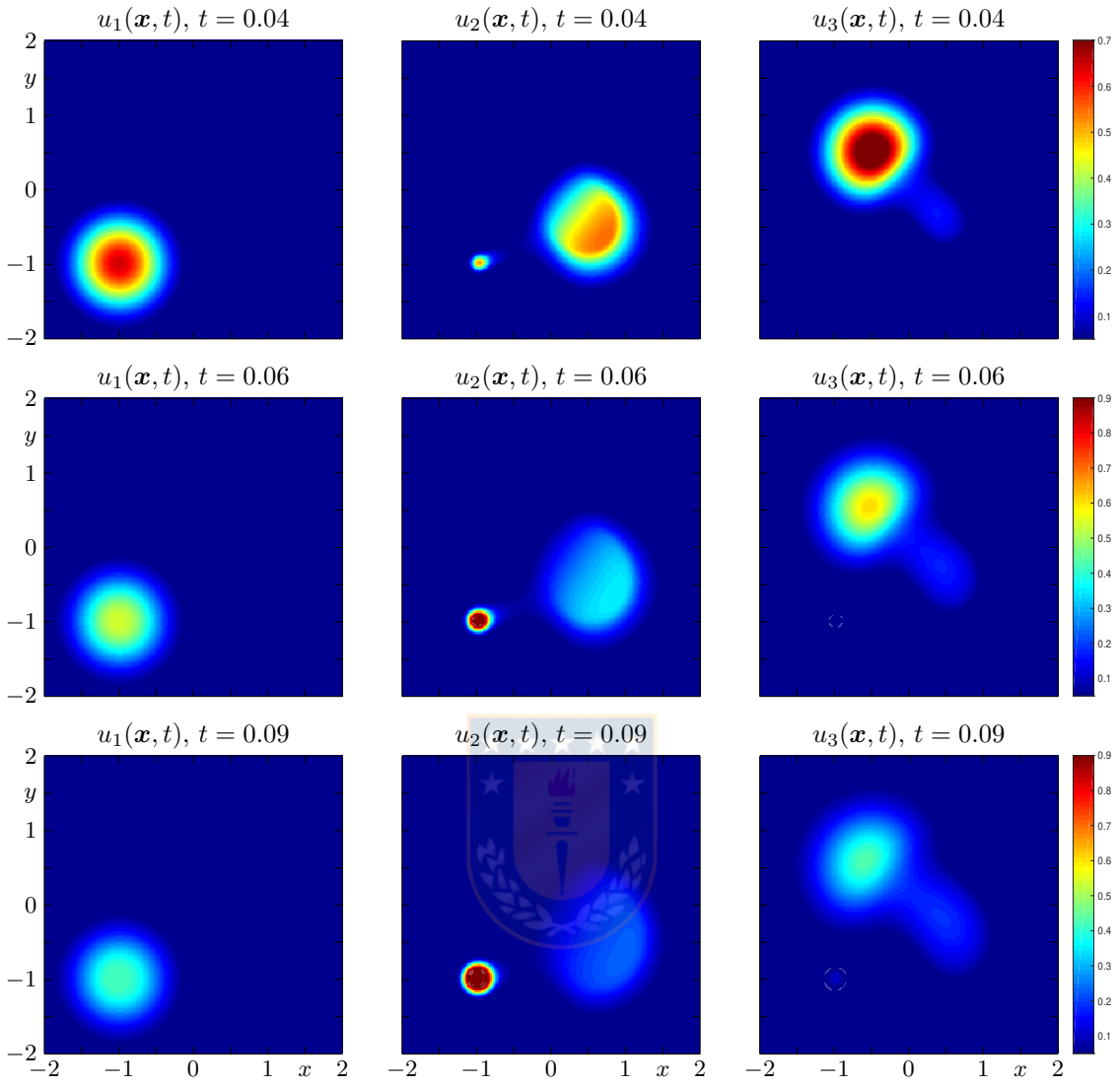

Figure 2.5: Example 2.2: interaction of the three species at different times $t = 0.04,\ 0.06,\ 0.09$.

2.6.3 Example 2.3: spatio-temporal model versus non-spatial ODE model

In this numerical example, we wish to compare the dynamics of the spatio-temporal model (2.1)–(2.4), with that of the non-spatial model

$$\frac{\mathrm{d}u_i}{\mathrm{d}t} = F_i\big(u_1(t), u_2(t), u_3(t)\big), \quad i = 1, 2, 3, \tag{2.36}$$

$N_x \times N_y$	h	$e_2^n(u_1)$	$e_2^n(u_2)$	$e_2^n(u_3)$
32×32	1.25e-1	1.13e-3	1.60e-3	1.56e-3
64×64	6.25e-2	5.47e-4	8.09e-4	7.56e-4
128×128	3.12e-2	2.74e-4	4.09e-4	3.71e-4
256×256	1.56e-2	1.36e-4	2.08e-4	1.84e-4

Table 2.2: Example 2.2: approximate L^2-errors for each species at simulated time $t = 0.04$.

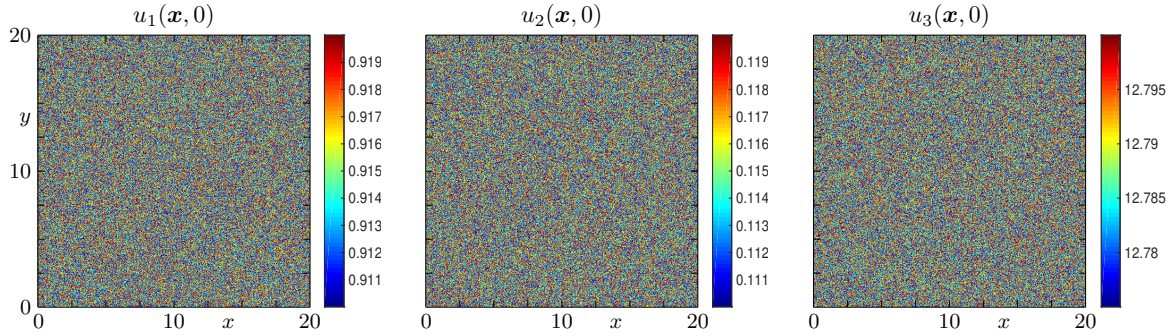

Figure 2.6: Example 2.3: initial conditions for species u_1, u_2 and u_3.

where the diffusion and chemotaxis movement are not present. To this end we determine for each species i at simulated time t_n the quantities

$$\mathcal{I}(u_i, t_n) := \sum_{K \in \mathcal{T}_h} m(K) u_{i,K}^n \approx \int_\Omega u_i(\boldsymbol{x}, t_n) \, \mathrm{d}\boldsymbol{x},$$

which represents the approximate total number in Ω of individuals of compartment u at time t_n and

$$u_{i,\max}^n := \max_{K \in \mathcal{T}_h} u_K^n, \quad u_{i,\min}^n := \min_{K \in \mathcal{T}_h} u_K^n.$$

We consider the diffusion coefficients $D_1 = 0.02$, $D_2 = 0.5$ and $D_3 = 5$, the sensitivity chemotactic parameters are chosen by $\delta_1 = 6$, $\delta_2 = 4$ and $\delta_3 = 2$ and the chemotactic coefficients $\chi_1 = -2$, $\chi_2 = 4$ and $\chi_3 = 6$. The other parameters are the same as in Examples 1 and 2. The initial condition for $i = 1, 2, 3$ is a spatially distributed random perturbation of the respective values $u_1 = 0.9$, $u_2 = 0.1$ and $u_3 = 12.75$, which is displayed in Figure 2.6. The "random" initial datum has been chosen to test whether small perturbations would give rise to large-scale regular structures akin to the well-known mechanism of pattern formation, or rather, the small fluctuations in the initial datum would simply be smoothed out. In Figure 2.7 we display the numerical solution at four different times. It turns out that each species aggregates in a kind of groups structure which forming zones of different densities. This structure varies with time (not show here), moreover in Figure 2.8 we can observe that the quantities $\mathcal{I}(u_i, t)$ and the solution u_i of ODE problem (2.36) have the same behavior even when the total variation of

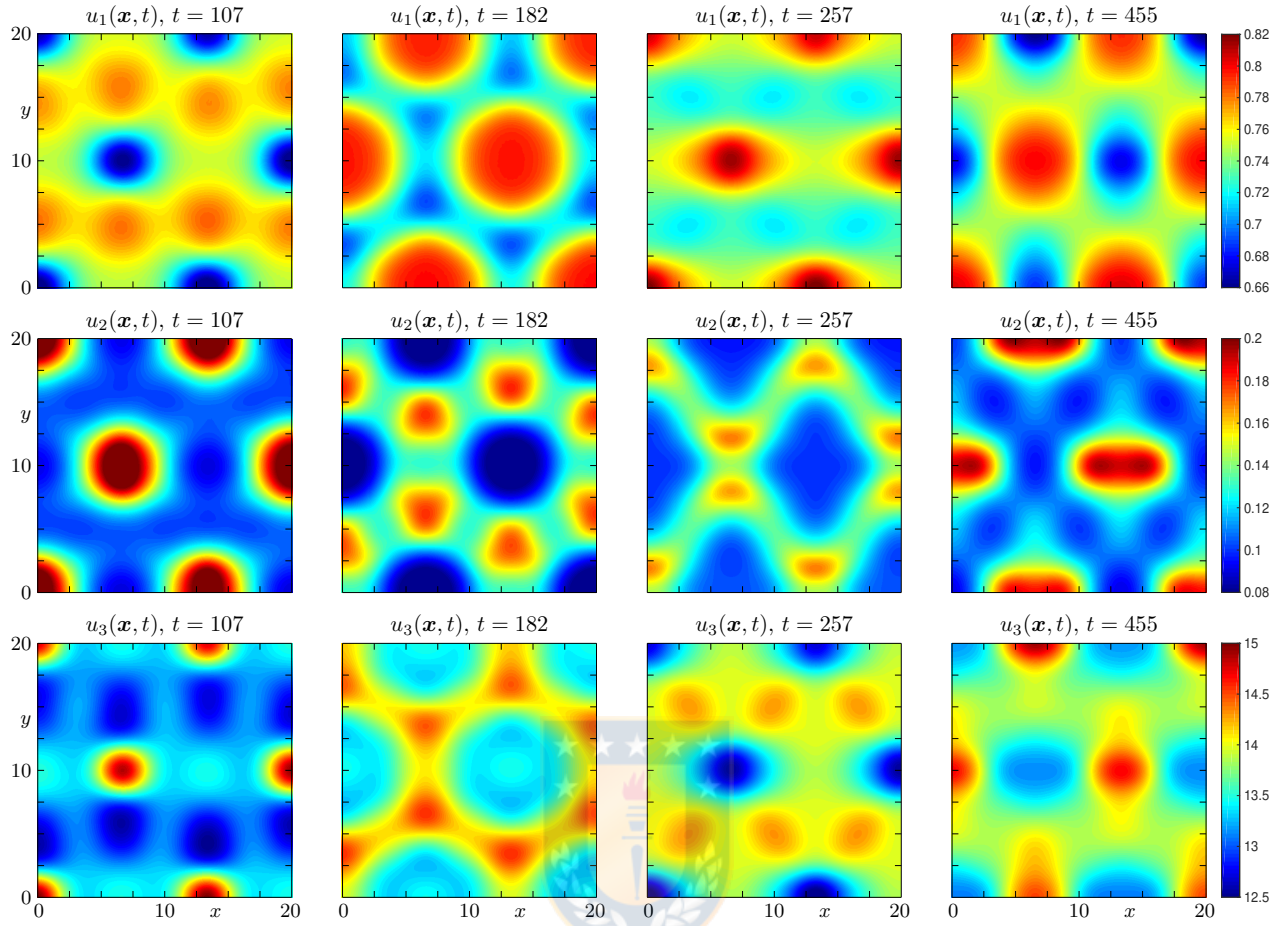

Figure 2.7: Example 2.3: numerical solution at four different times.

each species $u_{i,\max} - u_{i,\min}$ have a oscillatory behavior and remains bounded along the time, which lends further support to the conjecture that this model (at least with the parameters chosen) exhibits spatial-temporal oscillatory behavior.

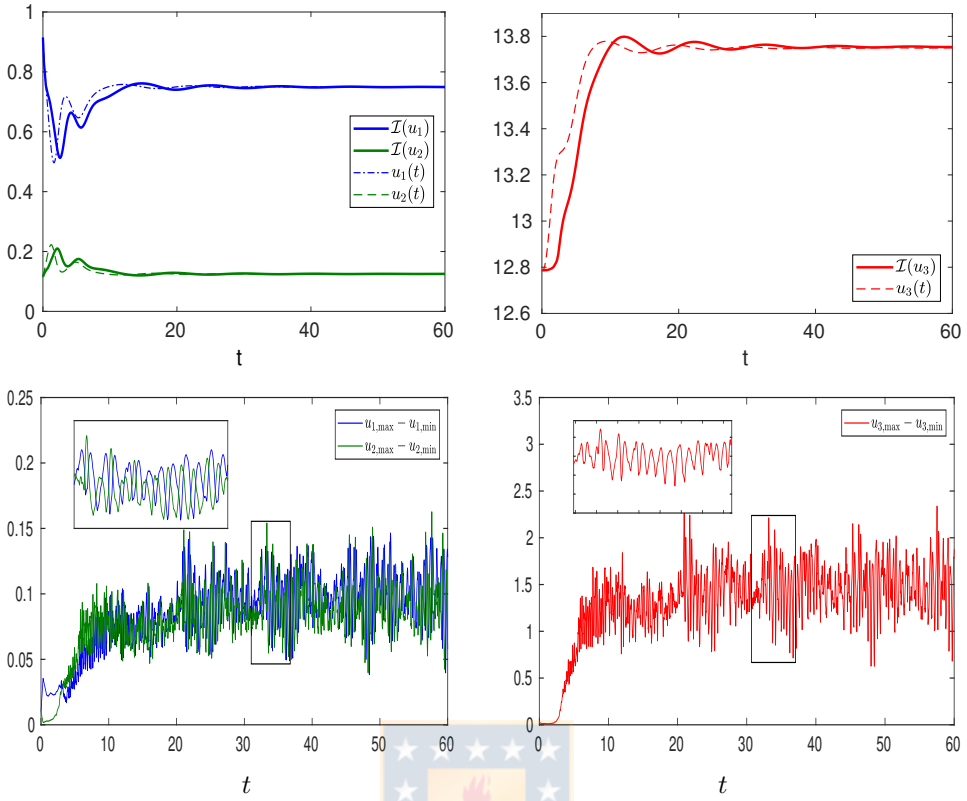

Figure 2.8: Example 2.3: spatial-temporal model versus non-spatial ODE model and time evolution of the total variation for each species.

CHAPTER 3

Global existence in a food chain model with two competitive preys, one predator and chemotaxis

3.1 Introduction

3.1.1 Scope

We consider a reaction-diffusion system describing three interacting species with respective density u_i, $i = 1, 2, 3$, in a food chain model on the basis of the following system [65, 97], where each species secretes a chemical substance of corresponding concentration y_i, $i = 1, 2, 3$. The resulting model is a strongly coupled nonlinear system of six PDEs with chemotactic terms, namely three parabolic equations describing the evolution of the densities u_i coupled with three elliptic equations for the concentrations y_i, $i = 1, 2, 3$:

$$\begin{aligned}
\partial_t u_1 - D_1 \Delta u_1 - \chi_1 \mathrm{div}(u_1 \nabla y_3) &= F_1(\boldsymbol{u}), \\
\partial_t u_2 - D_2 \Delta u_2 - \chi_2 \mathrm{div}(u_2 \nabla y_3) &= F_2(\boldsymbol{u}), \\
\partial_t u_3 - D_3 \Delta u_3 + \chi_3 \mathrm{div}(u_3 \nabla (y_1 + y_2)) &= F_3(\boldsymbol{u}), \\
-\mathcal{D}_1 \Delta y_1 + \theta_1 y_1 &= \delta_1 u_1, \\
-\mathcal{D}_2 \Delta y_2 + \theta_2 y_2 &= \delta_2 u_2, \\
-\mathcal{D}_3 \Delta y_3 + \theta_3 y_3 &= \delta_3 u_3, \quad (\boldsymbol{x}, t) \in \Omega \times (0, T],
\end{aligned} \tag{3.1}$$

where $u_i(\boldsymbol{x}, t)$, $i = 1, 2, 3$ are the population densities of the species at position $\boldsymbol{x}$ at time t. At the lowest level of the food chain we find the prey ($i = 1, 2$), while species 3, the predator preys upon species 1 and 2. Moreover, $y_i(\boldsymbol{x}, t)$ denotes the concentration of the chemical substance secreted by species i at position $\boldsymbol{x}$ at time t, and $\boldsymbol{y}(\boldsymbol{x}, t) := (y_1(\boldsymbol{x}, t), y_2(\boldsymbol{x}, t), y_3(\boldsymbol{x}, t))^{\mathrm{T}}$.

The chemotactic movement of the species is due to chemical substances secreted by the other species. Its direction is determined by the sign of the chemotactic coefficients χ_i [37] for $i = 1, 2, 3$. In this work, we consider that the prey (species 1 and 2) move in the direction of

decreasing concentration of the chemical secreted by species 3 (trying to avoid that species), while the predator (species 3) moves in the direction of increasing concentration of the chemical secreted by species 1 and 2. Notice that the equations for the chemical substances of the preys and predator are elliptic, rather than parabolic. This is justified in cases where the diffusion of the chemical substances occurs on a much faster time scale than the movement of individuals, which is reasonable in a variety of ecological settings.

The Holling-type II functional responses F_i, $i = 1, 2, 3$ are given by

$$\begin{aligned} F_1(\boldsymbol{u}) &:= r_1 u_1\Big(1 - \frac{u_1}{k_1}\Big) - \sigma_1 u_1 u_2 - \frac{M_1 u_1}{A_1 + u_1} u_3, \\ F_2(\boldsymbol{u}) &:= r_2 u_2\Big(1 - \frac{u_2}{k_2}\Big) - \sigma_2 u_1 u_2 - \frac{M_2 u_2}{A_2 + u_2} u_3, \\ F_3(\boldsymbol{u}) &:= \gamma_1 \frac{M_1 u_1}{A_1 + u_1} u_3 + \gamma_2 \frac{M_2 u_2}{A_2 + u_2} u_3 - L u_3 - H u_3^2, \end{aligned} \tag{3.2}$$

where r_1 and r_2 are biotic potentials, k_1 and k_2 are environmental carrying capacities of two prey species, σ_1 and σ_2 are coefficients of inter-specific competition between two prey species, M_1 and M_2 are predation coefficients, γ_1 and γ_2 are conversion factors, A_1 and A_2 are half-saturation constants, L is the natural death rate of predator, and H is the intra-specific competition among predator. We assume Neumman boundary conditions

$$\frac{\partial u_i}{\partial \boldsymbol{\nu}} = \frac{\partial y_i}{\partial \boldsymbol{\nu}} = 0, \qquad i = 1, 2, 3, \tag{3.3}$$

and the initial condition

$$u_i(\boldsymbol{x}, 0) = u_{i,0}(\boldsymbol{x}), \quad i = 1, 2, 3. \tag{3.4}$$

3.2 Preliminaries

Let $\Omega \subset \mathbb{R}^n$, $n = 2$ be a bounded open domain with piecewise smooth boundary $\partial\Omega$. We use standard Lebesgue and Sobolev spaces $W^{m,p}(\Omega)$, $H^m(\Omega) = W^{m,2}(\Omega)$ and $L^p(\Omega)$ (with their usual norms [1]) for all $m \in \mathbb{N}$ and $p \in [1, \infty]$. If X is a Banach space, $a < b$ and $p \in [1, \infty]$, then $L^p(a, b; X)$ denotes the space of all measurable functions $u : (a, b) \longrightarrow X$ such that $\|u(\cdot)\|_X \in L^p(a, b)$. Next, for $T > 0$ we define $\Omega_T := \Omega \times (0, T]$.

Let

$$\boldsymbol{z} = \begin{pmatrix} z_1 \\ z_2 \\ z_3 \end{pmatrix} := \begin{pmatrix} -y_3 \\ -y_3 \\ y_1 + y_2 \end{pmatrix} = \boldsymbol{B}\boldsymbol{y}, \quad \text{where} \quad \boldsymbol{B} = \begin{bmatrix} \boldsymbol{b}_1^{\mathrm{T}} \\ \boldsymbol{b}_2^{\mathrm{T}} \\ \boldsymbol{b}_3^{\mathrm{T}} \end{bmatrix} = \begin{bmatrix} 0 & 0 & -1 \\ 0 & 0 & -1 \\ 1 & 1 & 0 \end{bmatrix}.$$

Then the system (3.1) can then be written as

$$\partial_t u_i - D_i \Delta u_i + \chi_i \operatorname{div}\big(u_i \nabla(\boldsymbol{b}_i^{\mathrm{T}} \boldsymbol{y})\big) = F_i(\boldsymbol{u}), \tag{3.5}$$

$$-\mathcal{D}_i \Delta y_i + \theta_i y_i = \delta_i u_i, \quad i = 1, 2, 3, \quad (\boldsymbol{x}, t) \in \Omega_T. \tag{3.6}$$

Our basic requirements are the following: The functional responses F_i are locally Lipschitz continuous and L_i denote a Lipschitz constant for F_i for all $i = 1, 2, 3$.
$D_i > 0$, $\mathcal{D}_i > 0$, $\theta_i \geqslant 0$, and $\delta_i \geqslant 0$ for $i = 1, 2, 3$.
$\gamma_1 M_1 + \gamma_2 M_2 - L > 0$.
Next, we collect some tools that will frequently be used in this work.

Lemma 3.1. *Let u_1, u_2 and u_3 be a nonnegative functions. Then there exists a constant $C > 0$ such that*

$$\sum_{i=1}^{3} \|F_i\|_{L^\infty(\Omega)} \leqslant C \tag{3.7}$$

Proof. Due the nonnegativity of the functions u_i and (3.2) we get

$$\begin{aligned}
|F_1(\boldsymbol{u})| &\leqslant r_1 u_1\Big(1 - \frac{u_1}{k_1}\Big) \leqslant \frac{1}{4} r_1 k_1,\\
|F_2(\boldsymbol{u})| &\leqslant r_2 u_2\Big(1 - \frac{u_2}{k_2}\Big) \leqslant \frac{1}{4} r_2 k_2,\\
|F_3(\boldsymbol{u})| &\leqslant (\gamma_1 M_1 + \gamma_2 M_2 - L)u_3 - H u_3^2 \leqslant \frac{(\gamma_1 M_1 + \gamma_2 M_2 - L)^2}{4H}.
\end{aligned}$$

Taking the supreme in each of the previous inequalities and summing the results yields (3.7). □

We shall need the following consequence of the Gagliardo-Nirenberg interpolation inequality in two dimensions (see e.g. [17, 76])

$$\int_\Omega \xi^{\alpha+1} \, \mathrm{d}\boldsymbol{x} \leqslant C(\omega, \alpha)\|\xi\|_{L^1(\Omega)} \int_\Omega |\nabla \xi^{\alpha/2}|^2 \, \mathrm{d}\boldsymbol{x} \tag{3.8}$$

and elliptic regularity in the L^p sense (cf. [50]): the linear equation

$$-\Delta v + v = u \quad \text{in } \Omega, \qquad \frac{\partial v}{\partial \boldsymbol{\nu}} = 0 \quad \text{on } \partial\Omega,$$

admits a unique solution v satisfying

$$\|v\|_{W^{2,p}(\Omega)} \leqslant C\|u\|_{L^p(\Omega)}. \tag{3.9}$$

For the proof of the L^α integrability property, we shall require the two following lemmas (see [3, Apendix A])

Lemma 3.2 (ODE comparison)**.** *Assume Y and X are non-negative absolutely continuous functions in $[0, T]$ and such that for every $t > 0$:*

$$\begin{aligned}
Y'(t) + aY^\alpha(t) &\geqslant b + \delta + c\Big(1 + \frac{1}{t^\gamma}\Big) \sup_{\tau(t)\leqslant s\leqslant t} Y^{\alpha_0}(s),\\
X'(t) + aX^\alpha(t) &\leqslant b + c\Big(1 + \frac{1}{t^\gamma}\Big) \sup_{\tau(t)\leqslant s\leqslant t} X^{\alpha_0}(s),
\end{aligned}$$

for some continuous mapping $t \to \tau(t) \in [0,t]$ *and constants* $b \geqslant 0$, $c \geqslant 0$, $a > 0$, $\delta > 0$, $\alpha > \alpha_0 \geqslant 0$, $\gamma \geqslant 0$. *If* $Y(0) > X(0)$ *then* $Y \geqslant X$ *in* $[0,T]$. *In particular, if* $\gamma = 0$*:*

$$\sup_{t\in[0,T]} X(t) \leqslant \max\{X(0), C\},$$

where the constant $C > 0$ *depends on all parameters but* $\tau(\cdot)$, δ *and* T.

Lemma 3.3. *Assume* X *be an absolutely continuous functions in* $[0,T]$ *and such that*

$$X'(t) + aX^{\alpha}(t) \leqslant b + c\left(1 + \frac{1}{t^{\gamma}}\right) \sup_{\frac{t}{2}\leqslant s\leqslant t} X^{\alpha_0}(s),$$

with $b \geqslant 0$, $c \geqslant 0$, $a > 0$, $\alpha > \alpha_0 \geqslant 0$, $\gamma \geqslant 0$. *Then*

$$X(t) \leqslant C\left(1 + \frac{1}{t^{\beta}}\right), \quad \beta = \max\left\{\frac{1}{\alpha - 1}, \frac{\gamma}{\alpha - \alpha_0}\right\}.$$

where the constant $C > 0$ *depends on all parameters but it is independent of* T.

For $p \in (1,\infty)$, let $A := A_p$ denote the sectorial operator defined by

$$A_p u := -\Delta u, \quad \text{for} \quad u \in D(A_p) := \left\{\psi \in W^{2,p}(\Omega) : \frac{\partial \psi}{\partial \boldsymbol{\nu}} = 0\right\}. \tag{3.10}$$

Then we define the operators $\exp(-tA)$ by

$$\big(\exp(-tA)f\big)(x) = \int_{\Omega} G(x,y,t) f(y)\, \mathrm{d}y,$$

where G represent the Green's function and the family $(\exp(-tA))_{t\geqslant 0}$ denotes the Neumann heat semigroup. We use the following property of the Neumann heat semigroup

$$\|\exp(-tA)w\|_{L^p(\Omega)} \leqslant Ct^{-\frac{n}{2}\left(\frac{1}{q}-\frac{1}{p}\right)} \|w\|_{L^q(\Omega)}, \tag{3.11}$$

to prove the existence global classical solution. We refer to [95, Lemma 1.3] for another properties of Neumann heat semigroup.

Furthermore, the fact to that the spectrum of A is a p-independent countable set of positive real numbers, namely

$$0 = \mu_0 < \mu_1 < \mu_2 < \cdots,$$

entails the following consequence.
The operator $A+1$ possesses fractional powers $(A+1)^{\beta}$, $\beta \geqslant 0$, whose domains have the embedding properties (see [53, Theorem 1.6.1])

$$D((A_p+1)^{\beta}) \hookrightarrow C^{\delta}(\overline{\Omega}) \qquad \text{if } 2\beta - \frac{n}{p} > \delta \geqslant 0. \tag{3.12}$$

Moreover, it can easily be seen ([55, Lemma 2.1]) that for $t > 0$ the operator $(A+1)^{\beta}\exp(-tA)\,\mathrm{div}(\cdot)$ possesses a unique extension from $C_0^{\infty}(\Omega)$ to $L^p(\Omega)$ that satisfies the following lemma.

Lemma 3.4. *Let $\beta \geqslant 0$ and $p \in (1,\infty)$. Then for all $\epsilon > 0$ there exists $c(\epsilon) > 0$ such that for all $w \in C_0^\infty$ we have*

$$\begin{aligned} \|(A+1)^\beta \exp(-tA)\,\mathrm{div}(x)\|_{L^p(\Omega)} &\leqslant c(\epsilon)t^{-\beta-\frac{1}{2}-\epsilon}\exp(-\mu t)\|w\|_{L^p(\Omega)} \\ &\leqslant c(\epsilon)t^{-\beta-\frac{1}{2}-\epsilon}\|w\|_{L^p(\Omega)} \qquad \forall t>0, \end{aligned} \tag{3.13}$$

for some $\mu > 0$.

3.3 Global Classical Solutions

The goal of this section is to guarantee the global existence of solution to the system (3.1). In order to achieve this, first we show the local existence of a nonnegative solution. Then we prove some a priori estimates and finally we establish the global existence. The local existence proof is valid for $n \geqslant 2$.

3.3.1 Local existence

This subsection is devoted to proving local existence of a nonnegative solution to the system (3.1). The proof is based on Banach fixed-point theorem.

Lemma 3.5. *Suppose that the functions $u_{i,0} \in C^0(\overline{\Omega})$ for all $i = 1,2,3$ are nonnegative. Then there exists $T_{\max} \in (0,\infty]$ and an unique classical solution $(\boldsymbol{u},\boldsymbol{y})$ of (3.5) which is nonnegative and each u_i, y_i belongs to $C^0\big(\overline{\Omega}\times[0,T_{max})\big)\cap C^{2,1}\big(\overline{\Omega}\times(0,T_{\max})\big)$ Furthermore, we have the following extensibility criterion:*

$$T_{\max} = \infty \qquad \text{or} \lim_{t\nearrow T_{\max}} \Big(\sum_{i=1}^{3}\|u_i\|_{L^\infty(\Omega)}\Big) = \infty. \tag{3.14}$$

Proof. We claim that for all $R > 0$ there exists $T = T(R) > 0$ such that if in addition to the above assumptions we have $\|u_{i,0}\|_{L^\infty(\Omega)} \leqslant R$ for all $i = 1,2,3$. Furthermore, $L_i(R) > 0$ denote a Lipschitz constant for F_i on $(-R,R)$.
For a small $T \in (0,1)$, we introduce the Banach space

$$X := [C^0\big([0,T];C^0(\bar{\Omega})\big)]^3$$

along with its closed subset

$$S := \{(u_1,u_2,u_3)^{\mathrm{T}} \in X \ : \ \|u_i\|_{L^\infty((0,T);L^\infty(\Omega))} \leqslant 2R,\ i=1,2,3\},$$

where $R = \max_{i=1,2,3}\|u_{i,0}\|_\infty$.

For $\boldsymbol{u} \coloneqq (u_1, u_2, u_3)^{\mathrm{T}} \in S$ and $t \in [0, T]$, we introduce a mapping Φ on S by

$$\Phi(\boldsymbol{u}) \coloneqq \big(\Phi_1(u_1), \Phi_2(u_2), \Phi_3(u_3)\big)^{\mathrm{T}},$$

where, for all $i = 1, 2, 3$, $\Phi_i(u_i)$ is defined by

$$\Phi_i(u_i) \coloneqq \exp(-D_i t A)u_{i,0} - \chi_i \int_0^t \exp(-D_i(t-s)A)\operatorname{div}\big(u_i \nabla(\boldsymbol{b}_i^{\mathrm{T}}\boldsymbol{y})\big)\mathrm{d}s + \int_0^t \exp(-D_i(t-s)A)F_i\big(\boldsymbol{u}(s)\big)\mathrm{d}s.$$

Let $y_i \in \bigcap_{1<p<\infty} L^\infty((0,T); W^{2,p}(\Omega))$ denote the (weak) solution of

$$\begin{aligned} -\mathcal{D}_i \Delta y_i + \theta_i y_i &= \delta_i u_i, && \text{on } \Omega, \\ \frac{\partial y_i}{\partial \boldsymbol{\nu}} &= 0, && \text{on } \partial\Omega. \end{aligned} \tag{3.15}$$

Then, for all $i = 1, 2, 3$ we have

$$\|\Phi_i(u_i)\|_{L^\infty(\Omega)} \leqslant I_1 + I_2 + I_3, \tag{3.16}$$

where we define

$$I_1 \coloneqq \|\exp(-D_i t A)u_{i,0}\|_{L^\infty(\Omega)}, \quad I_2 \coloneqq \chi_i \int_0^t \|\exp(-D_i(t-s)A)\operatorname{div}\big(u_i(s)\nabla(\boldsymbol{b}_i^{\mathrm{T}}\boldsymbol{y}(s))\big)\|_{L^\infty(\Omega)}\,\mathrm{d}s,$$

$$I_3 \coloneqq \int_0^t \|\exp(-D_i(t-s)A)F_i(\boldsymbol{u}(s))\|_{L^\infty(\Omega)}\,\mathrm{d}s.$$

It is clear that for all $t \in (0, T)$,

$$I_1 \leqslant \|u_{i,0}\|_{L^\infty(\Omega)} \leqslant R. \tag{3.17}$$

Using (3.7), we get

$$I_3 \leqslant \int_0^t \|F_i(\boldsymbol{u}(s))\|_{L^\infty(\Omega)}\,\mathrm{d}s \leqslant \|F_i\|_{L^\infty((-R,R))} \cdot T, \tag{3.18}$$

for all $t \in (0, T)$.

Now, in order to control the second member of (3.16), we fix $p \in (1, \infty)$ with $p > n$. Let $\beta \in (\frac{n}{2p}, \frac{1}{2})$ and $\varepsilon \in (0, \frac{1}{2} - \beta)$. Then, by Lemma 3.4

$$\begin{aligned} I_2 &\leqslant C \int_0^t \|(A+1)^\beta \exp(-D_i(t-s)A)\operatorname{div}\big(u_i(s)\nabla(\boldsymbol{b}_i^{\mathrm{T}}\boldsymbol{y}(s))\big)\|_{L^p(\Omega)}\,\mathrm{d}s \\ &\leqslant C \int_0^t (t-s)^{-(\beta+\frac{1}{2}+\varepsilon)} \|u_i(s)\nabla(\boldsymbol{b}_i^{\mathrm{T}}\boldsymbol{y}(s))\|_{L^p(\Omega)}\,\mathrm{d}s \\ &\leqslant C \int_0^t (t-s)^{-(\beta+\frac{1}{2}+\varepsilon)} \|u_i(s)\|_{L^\infty(\Omega)} \|\boldsymbol{b}_i^{\mathrm{T}}\boldsymbol{y}(s)\|_{W^{1,p}(\Omega)}\,\mathrm{d}s \\ &\leqslant C \int_0^t (t-s)^{-(\beta+\frac{1}{2}+\varepsilon)} \|u_i(s)\|_{L^\infty(\Omega)} \|\boldsymbol{b}_i^{\mathrm{T}}\boldsymbol{y}(s)\|_{W^{2,p}(\Omega)}\,\mathrm{d}s \\ &\leqslant C(R) \int_0^t (t-s)^{-(\beta+\frac{1}{2}+\varepsilon)}\,\mathrm{d}s \\ &\leqslant C(R) T^{-(\beta+\varepsilon)+\frac{1}{2}} \end{aligned} \tag{3.19}$$

for all $t \in (0,T)$, were have used that $T < 1$, elliptic regularity (cf. 3.9) for (3.15), and that $\|\exp(\tau A)\mathrm{div} w\|_{L^p\Omega} \leqslant c(\varepsilon)t^{-(\beta+\frac{1}{2}+\varepsilon)}\|w\|_{L^p}$ for all $w \in L^p$ (see Lemma 3.4). From (3.17),(3.18),(3.19) and $1/2 - \beta - \epsilon > 0$, it follows that if we choose T small enough, then Φ maps S into itself.

Now, let $\boldsymbol{u}, \tilde{\boldsymbol{u}} \in S$, then for all $i = 1,2,3$ we estimate

$$\|\Phi_i(u_i)(t) - \Phi_i(\tilde{u}_i)(t)\|_{L^\infty(\Omega)} \leqslant J_1 + J_2,$$

where we define

$$J_1 \coloneqq \chi_i \int_0^t \|\exp(-D_i(t-s)A)\,\mathrm{div}\big(u_i(s)\nabla(\boldsymbol{b}_i^{\mathrm{T}}\boldsymbol{y}(s)) - \tilde{u}_i(s)\nabla(\boldsymbol{b}_i^{\mathrm{T}}\tilde{\boldsymbol{y}}(s))\big)\|_{L^\infty(\Omega)}\,\mathrm{d}s,$$
$$J_2 \coloneqq \int_0^t \|\exp(-D_i(t-s)A)(F_i(\boldsymbol{u}) - F_i(\tilde{\boldsymbol{u}}))\|_{L^\infty(\Omega)}\,\mathrm{d}s.$$

The fact of the functional responses F_i are locally Lipschitz continuous implies

$$J_2 \leqslant \int_0^t \|F_i(\boldsymbol{u}) - F_i(\tilde{\boldsymbol{u}})\|_{L^\infty(\Omega)}\,\mathrm{d}s \leqslant L_i(R)\int_0^t \|\boldsymbol{u} - \tilde{\boldsymbol{u}}\|_X\,\mathrm{d}s \leqslant T\cdot L_i(R)\|\boldsymbol{u} - \tilde{\boldsymbol{u}}\|_X$$

Using the properties of the operator $A+1$ we find that

$$\begin{aligned}
J_1 &\leqslant C\int_0^t \|(A+1)^\beta \exp(-D_i(t-s)A)\,\mathrm{div}\big(u_i(s)\nabla(\boldsymbol{b}_i^{\mathrm{T}}\boldsymbol{y}(s)) - \tilde{u}_i(s)\nabla(\boldsymbol{b}_i^{\mathrm{T}}\tilde{\boldsymbol{y}}(s))\big)\,\|_{L^p(\Omega)}\,\mathrm{d}s \\
&\leqslant C\int_0^t (t-s)^{-(\beta+\frac{1}{2}+\varepsilon)}\|\big(u_i(s)\nabla(\boldsymbol{b}_i^{\mathrm{T}}\boldsymbol{y}(s)) - \tilde{u}_i(s)\nabla(\boldsymbol{b}_i^{\mathrm{T}}\tilde{\boldsymbol{y}}(s))\big)\,\|_{L^p(\Omega)}\mathrm{d}s \\
&\leqslant C\int_0^t (t-s)^{-(\beta+\frac{1}{2}+\varepsilon)}\Big(\|\big(u_i(s)\big(\nabla(\boldsymbol{b}_i^{\mathrm{T}}(\boldsymbol{y}(s) - \tilde{\boldsymbol{y}}(s))\big)\|_{L^p(\Omega)} \\
&\quad + \|\nabla\big(\boldsymbol{b}_i^{\mathrm{T}}\tilde{\boldsymbol{y}}(s)\big)(u_i(s) - \tilde{u}_i(s))\,\|_{L^p(\Omega)}\Big)\,\mathrm{d}s.
\end{aligned}$$

Now, using elliptic regularity (cf. 3.9) and keeping in mind that Equation (3.15) is linear we get

$$\|\boldsymbol{b}_i^{\mathrm{T}}\tilde{\boldsymbol{y}}(s)\|_{W^{1,p}(\Omega)} \leqslant C\|\boldsymbol{b}_i^{\mathrm{T}}\tilde{\boldsymbol{y}}(s)\|_{W^{2,p}(\Omega)} \leqslant C\|\boldsymbol{b}_i^{\mathrm{T}}\tilde{\boldsymbol{u}}(s)\|_{L^p(\Omega)} \leqslant C\|\boldsymbol{b}_i^{\mathrm{T}}\tilde{\boldsymbol{u}}(s)\|_{L^\infty(\Omega)},$$

and

$$\begin{aligned}
\|\boldsymbol{b}_i^{\mathrm{T}}(\boldsymbol{y}(s) - \tilde{\boldsymbol{y}}(s))\|_{W^{1,p}(\Omega)} &\leqslant C\|\boldsymbol{b}_i^{\mathrm{T}}(\boldsymbol{y}(s) - \tilde{\boldsymbol{y}}(s))\|_{W^{2,p}(\Omega)} \\
&\leqslant C\|\boldsymbol{b}_i^{\mathrm{T}}(\boldsymbol{u}(s) - \tilde{\boldsymbol{u}}(s))\|_{L^p(\Omega)} \\
&\leqslant C\|\boldsymbol{b}_i^{\mathrm{T}}(\boldsymbol{u}(s) - \tilde{\boldsymbol{u}}(s))\|_{L^\infty(\Omega)}.
\end{aligned}$$

Thus

$$\begin{aligned}
J_1 &\leqslant C\int_0^t (t-s)^{-(\beta+\frac{1}{2}+\varepsilon)}\Big(\|u_i(s)\|_{L^\infty(\Omega)}\|\boldsymbol{b}_i^{\mathrm{T}}(\boldsymbol{u}(s) - \tilde{\boldsymbol{u}}(s))\|_{L^\infty(\Omega)} \\
&\quad + \|u_i(s) - \tilde{u}_i(s)\|_{L^\infty(\Omega)}\|\boldsymbol{b}_i^{\mathrm{T}}\tilde{\boldsymbol{u}}(s)\|_{L^\infty(\Omega)}\Big)\,\mathrm{d}s \\
&\leqslant C(R)T^{-(\beta+\frac{1}{2}+\varepsilon)}\|\boldsymbol{u} - \tilde{\boldsymbol{u}}\|_X.
\end{aligned}$$

Therefore collecting the previous inequalities we get

$$\|\Phi_i(u_i)(t) - \Phi_i(\tilde{u}_i)(t)\|_{L^\infty(\Omega)} \leqslant C(R)T^{-(\beta+\frac{1}{2}+\varepsilon)}\|\boldsymbol{u} - \tilde{\boldsymbol{u}}\|_X + T \cdot L_i(R)\|\boldsymbol{u} - \tilde{\boldsymbol{u}}\|_X$$

for all $t \in (0, T)$, which shows that if T is chosen sufficiently small, then Φ acts as a contraction on S. Accordingly, the Banach fixed point theorem asserts the existence of some $\boldsymbol{u} \in S$ such that $\Phi(\boldsymbol{u}) = \boldsymbol{u}$, along with the existence of y_1, y_2 and y_3 as is obtained from (3.15).
Since the above choice of T depends only on $\|u_{i,0}\|_{L^\infty}$, the existence of maximal time $T_{\max}$, that satisfies (3.14) can be ensured by [79, Proposition 16.1]. Relying on this, the inclusions $u_1, u_2, u_3 \in C^{2,1}(\overline{\Omega} \times (0, T_{\max})$ result from straightforward regularity arguments including standard semigroup techniques and parabolic Schauder estimates ([60, Theorem IV.5.3]). Again by standard regularity arguments, we are able to establish the regularity of y_1, y_2 and y_3.

An application of the strong maximum principle applied to (3.5) implies the claim concerning the positivity of u_1, u_2 and u_3. Hence u_1, u_2 and u_3 is positive in $\overline{\Omega} \times (0, T_{\max})$ and the strong elliptic maximum principle applied to (3.6) yields positivity also of y_1, y_2 and y_3.

Let us finally prove uniqueness of solutions in the indicated class, without loss of generality, we assume that $D_i = 1$ for all $i = 1, 2, 3$. Assume that $T > 0$ and two classical solutions of the system (3.1) $(\boldsymbol{u}, \boldsymbol{y})$ and $(\tilde{\boldsymbol{u}}, \tilde{\boldsymbol{y}})$ in $\Omega \times (0, T)$ are given. We fix $T_0 \in (0, T)$, and define $w_i = u_i - \tilde{u}_i$ and $z = y_i - \tilde{y}_i$. The system for these differences is given by

$$\begin{aligned} \partial_t w_i - D_i\Delta w_i + \chi_i \operatorname{div}\big(w_i\nabla(\boldsymbol{b}_i^{\mathrm{T}}\tilde{\boldsymbol{y}})\big) + \chi_i \operatorname{div}\big(u_i\nabla(\boldsymbol{b}_i^{\mathrm{T}}\boldsymbol{z})\big) &= F_i(\boldsymbol{u}) - F_i(\tilde{\boldsymbol{u}}), \\ -\mathcal{D}_i\Delta z_i + \theta_i z_i = \delta_i w_i, \quad i = 1, 2, 3, \quad (\boldsymbol{x}, t) &\in \Omega_T. \end{aligned} \tag{3.20}$$

Multiplying (3.20) by w_i and integrating the result in space, we get

$$\begin{aligned} \frac{1}{2}\frac{\mathrm{d}}{\mathrm{d}t}\int_\Omega |w_i|^2 \,\mathrm{d}\boldsymbol{x} + D_i\int_\Omega |\nabla w_i|^2 \,\mathrm{d}\boldsymbol{x} &= \chi_i \int_\Omega \big(u_i\nabla(\boldsymbol{b}_i^{\mathrm{T}}\boldsymbol{y}) - \tilde{u}_i\nabla(\boldsymbol{b}_i^{\mathrm{T}}\tilde{y})\big)\nabla w_i \,\mathrm{d}\boldsymbol{x} \\ &\quad + \int_\Omega (F_i(\boldsymbol{u}) - F_i(\tilde{\boldsymbol{u}}))w_i \,\mathrm{d}\boldsymbol{x} \\ &= \chi_i \int_\Omega u_i\nabla(\boldsymbol{b}_i^{\mathrm{T}}\boldsymbol{z})\nabla w_i \,\mathrm{d}\boldsymbol{x} + \chi_i \int_\Omega w_i\nabla(\boldsymbol{b}_i^{\mathrm{T}}\tilde{y}))\nabla w_i \,\mathrm{d}\boldsymbol{x} \\ &\quad + \int_\Omega (F_i(\boldsymbol{u}) - F_i(\tilde{\boldsymbol{u}}))w_i \,\mathrm{d}\boldsymbol{x}, \end{aligned} \tag{3.21}$$

for all $t \in (0, T)$. By Hölder's, Gagliardo-Nirenberg and Young's inequalities,

$$\begin{aligned} \chi_i \int_\Omega w_i\nabla(\boldsymbol{b}_i^{\mathrm{T}}\tilde{\boldsymbol{y}})\nabla w_i \,\mathrm{d}\boldsymbol{x} &\leqslant |\chi_i\|\nabla w_i\|_{L^2(\Omega)}\|\nabla(\boldsymbol{b}_i^{\mathrm{T}}\tilde{\boldsymbol{y}})\|_{L^p(\Omega)}\|w_i\|_{L^{2p/(p-2)}(\Omega)} \\ &\leqslant C\|\nabla w_i\|_{L^2(\Omega)}\|\nabla(\boldsymbol{b}_i^{\mathrm{T}}\tilde{\boldsymbol{y}})\|_{L^p(\Omega)}\|\nabla w_i\|_{L^2(\Omega)}^{n/p}\|w_i\|_{L^2(\Omega)}^{(p-n)/p} \\ &\leqslant C\|\nabla w_i\|_{L^2(\Omega)}\|\nabla(\boldsymbol{b}_i^{\mathrm{T}}\tilde{\boldsymbol{y}})\|_{L^p(\Omega)}\|\nabla w_i\|_{L^2(\Omega)}^{n/p}\|w_i\|_{L^2(\Omega)}^{(p-n)/p} \\ &\leqslant C\|\nabla w_i\|_{L^2(\Omega)}^{(p+n)/p}\|\nabla(\boldsymbol{b}_i^{\mathrm{T}}\tilde{\boldsymbol{y}})\|_{L^p(\Omega)}\|w_i\|_{L^2(\Omega)}^{(p-n)/p} \\ &\leqslant \frac{1}{2}\|\nabla w_i\|_{L^2(\Omega)}^2 + C\|w_i\|_{L^2(\Omega)}^2, \end{aligned} \tag{3.22}$$

were we have used that $\|\nabla(\boldsymbol{b}_i^{\mathrm{T}}\tilde{\boldsymbol{y}})\|_{L^p(\Omega)} \leqslant C$ for $t \in (0,T_0)$, and that $p > n \geqslant 2$. Furthermore, in view of the boundedness of u_i and $\tilde{u}_i$ in $\Omega \times (0,T_0)$ and the Lipshitz continuity of F_i, we obtain

$$\chi_i \int_\Omega u_i \nabla(\boldsymbol{b}_i^{\mathrm{T}}\boldsymbol{z})\nabla w_i \,\mathrm{d}\boldsymbol{x} \leqslant \frac{1}{2}\|\nabla w_i\|^2_{L^2(\Omega)} + C\|\nabla(\boldsymbol{b}_i^{\mathrm{T}}\boldsymbol{z})\|^2_{L^2(\Omega)}$$

and

$$\int_\Omega (F_i(\boldsymbol{u}) - F_i(\tilde{\boldsymbol{u}})w_i \,\mathrm{d}\boldsymbol{x} \leqslant C\|w_i\|^2_{L^2(\Omega)}.$$

We conclude upon (3.21) that

$$\frac{\mathrm{d}}{\mathrm{d}t}\int_\Omega |w_i|^2 \,\mathrm{d}\boldsymbol{x} \leqslant C\|w_i\|^2_{L^2(\Omega)} \qquad \text{for all } t \in (0,T_0).$$

The Gronwall inequality clearly implies uniqueness in $\Omega \times (0,T_0)$ and hence the uniqueness in $\Omega \times (0,T)$ because $T_0 \in (0,T)$ was arbitrary. □

3.3.2 Global solutions

In this subsection, we prove global solution to the system (3.1). That is we prove $T_{\max} = \infty$ which implies that $u_1, u_2, u_3, y_1, y_2, y_3$ belongs to $C^0\big(\overline{\Omega} \times [0,\infty)\big) \cap C^{2,1}\big(\overline{\Omega} \times (0,\infty)\big)$. First, we will prove the L^1-integrability.

Lemma 3.6. *Let $(\boldsymbol{u},\boldsymbol{y})$ be sufficiently smooth non-negative solutions of the system (3.1) with the boundary conditions (3.3). Then there exists a constant M depending on $\gamma_1, \gamma_2, |\Omega|, \|u_{i,0}\|_{L^1(\Omega)}$ but not on t, such that for all $t > 0$,*

$$\int_\Omega (u_1 + u_2 + u_3) \,\mathrm{d}\boldsymbol{x} \leqslant \mathcal{M}. \tag{3.23}$$

Proof. Integrating the first, second and third equations of (3.1) and using the Neumann boundary conditions we find

$$\frac{\mathrm{d}}{\mathrm{d}t}\int_\Omega (\gamma_1 u_1 + \gamma_2 u_2 + u_3) \,\mathrm{d}\boldsymbol{x} \leqslant r_1\gamma_1 \int_\Omega u_1\Big(1 - \frac{u_1}{k}\Big) \,\mathrm{d}\boldsymbol{x} + r_2\gamma_2 \int_\Omega u_1\Big(1 - \frac{u_1}{k}\Big) \,\mathrm{d}\boldsymbol{x} - L\int_\Omega u_3 \,\mathrm{d}\boldsymbol{x},$$

for all $t \in (0, T_{\max})$. From the inequality

$$r_i u_i\Big(1 - \frac{u_i}{k_i}\Big) \leqslant \frac{k_i(r_i+1)^2}{4r_i} - u_i$$

we get

$$\begin{aligned}\frac{\mathrm{d}}{\mathrm{d}t}\int_\Omega (\gamma_1 u_1 + \gamma_2 u_2 + u_3) \,\mathrm{d}\boldsymbol{x} &\leqslant \gamma_1\frac{k_1(r_1+1)^2}{4r_1}\int_\Omega \mathrm{d}\boldsymbol{x} - \gamma_1\int_\Omega u_1 \,\mathrm{d}\boldsymbol{x} + \gamma_2\frac{k_2(r_2+1)^2}{4r_2}\int_\Omega \mathrm{d}\boldsymbol{x} \\ &\quad - \gamma_2\int_\Omega u_2 \,\mathrm{d}\boldsymbol{x} - L\int_\Omega u_3 \,\mathrm{d}\boldsymbol{x} \\ &\leqslant C|\Omega| - \int_\Omega (\gamma_1 u_1 + \gamma_2 u_2 + u_3) \,\mathrm{d}\boldsymbol{x}.\end{aligned}$$

If we take $A(t) = \gamma_1 u_1 + \gamma_2 u_2 + u_3$, then have result $\frac{d}{dt}A(t) + A(t) \leqslant C|\Omega|$ which implies

$$A(t) \leqslant e^{-t}A(0) + (1 - e^{-t})C|\Omega|.$$

The conclusion of the lemma readily follows. □

Our main ingredient for the proof of global existence is the following a priori estimate which asserts that if $u_{i,0} \in L^\alpha(\Omega)$, then u_i is uniformly bounded in L^α for some $\alpha > 1$. We adapt the proof shown in [4, Proposition 3.2] to our context.

Lemma 3.7. *Assume that $(\boldsymbol{u}, \boldsymbol{y})$ is a pair of vectors of sufficiently smooth non-negative solutions of the system (3.1) with the boundary conditions (3.3) and integrable initial data. Let $t > 0$ be arbitrary. Then, for any $\alpha \in (1, \infty)$, we have the estimate*

$$\sum_{i=1}^{3} \|u_i\|_\alpha \leqslant C(\alpha, \mathcal{M})\left(1 + \frac{1}{t^{\alpha-1}}\right). \tag{3.24}$$

Moreover, if $u_{i,0} \in L^\alpha(\Omega)$ for $i = 1, 2, 3$, then the following bound is an effect:

$$\sum_{i=1}^{3} \|u_i\|_\alpha \leqslant C(\alpha, \mathcal{M}, \|u_{1,0}\|_\alpha, \|u_{2,0}\|_\alpha, \|u_{3,0}\|_\alpha). \tag{3.25}$$

Proof. For simplicity we put $\|\cdot\|_{L^\alpha(\Omega)} = \|\cdot\|_\alpha$. Multiplying the first equation in (3.1) by $u_1^{\alpha-1}$ and integrating by parts we obtain

$$\frac{1}{\alpha}\frac{\mathrm{d}}{\mathrm{d}t}\|u_1\|_\alpha^\alpha + D_1(\alpha - 1)\int_\Omega u_1^{\alpha-2}|\nabla u_1|^2 \,\mathrm{d}\boldsymbol{x} + \frac{\chi_1(\alpha-1)}{\alpha}\int_\Omega \nabla y_3 \nabla u_1^\alpha \,\mathrm{d}\boldsymbol{x} = \int_\Omega F_1(\boldsymbol{u})u_1^{\alpha-1} \,\mathrm{d}\boldsymbol{x}. \tag{3.26}$$

Next, we multiply the equation $-\mathcal{D}_3\Delta y_3 + \theta_3 y_3 = \delta_3 u_3$ by u_1^α to obtain

$$-\int_\Omega \nabla y_3 \nabla u_1^\alpha \,\mathrm{d}\boldsymbol{x} \leqslant \frac{\theta_3}{\mathcal{D}_3}\int_\Omega y_3 u_1^\alpha \,\mathrm{d}\boldsymbol{x}. \tag{3.27}$$

Then using the equality

$$\int_\Omega w^{\alpha-2}|\nabla w|^2 \,\mathrm{d}\boldsymbol{x} = \frac{4}{\alpha^2}\int |\nabla w^{\alpha/2}|^2 \,\mathrm{d}\boldsymbol{x}$$

and

$$\int_\Omega F_1(\boldsymbol{u})u_1^{\alpha-1} \,\mathrm{d}\boldsymbol{x} \leqslant r_1 \int_\Omega u_1^\alpha \,\mathrm{d}\boldsymbol{x},$$

we get,

$$\frac{\mathrm{d}}{\mathrm{d}t}\|u_1\|_\alpha^\alpha + 4\frac{D_1(\alpha-1)}{\alpha}\|\nabla u_1^{\alpha/2}\|_2^2 \leqslant \frac{(\alpha-1)\chi_1\delta_3}{\mathcal{D}_3}\int_\Omega y_3 u_1^\alpha \,\mathrm{d}\boldsymbol{x} + r_1\alpha\int_\Omega u_1^\alpha \,\mathrm{d}\boldsymbol{x}. \tag{3.28}$$

In order to estimate the right-hand side of (3.28). Take $\epsilon > 0$ (to be specified later). We use the following consequence of Young's inequality:

$$y_3 u_1^\alpha \leqslant \epsilon u_1^{\alpha+1} + \epsilon^{-\alpha} y_3^{\alpha+1}, \tag{3.29}$$

and also the inequality

$$\int_\Omega u_1^\alpha \, \mathrm{d}\boldsymbol{x} \leqslant \|u_1\|_1^{\frac{1}{\alpha^2}} \|u_1\|_{\alpha+1}^{\frac{\alpha^2-1}{\alpha}} \leqslant C_1'(\mathcal{M}, \epsilon, \alpha) + \epsilon \|u_1\|_{\alpha+1}^{\alpha+1}.$$

Therefore, for some constant $C_1' = C_1'(\mathcal{M}, \epsilon, \alpha, \delta_3, \chi_1, \mathcal{D}_3)$ we have

$$\frac{(\alpha-1)\chi_1\delta_3}{\mathcal{D}_3} \int_\Omega y_3 u_1^\alpha \, \mathrm{d}\boldsymbol{x} + r_1 \alpha \int_\Omega u_1^\alpha \, \mathrm{d}\boldsymbol{x} \leqslant C_1' + C_1' \epsilon \|u_1\|_{\alpha+1}^{\alpha+1} + C_1' \|y_3\|_{\alpha+1}^{\alpha+1}.$$

The last inequality together (3.28) yields

$$\frac{\mathrm{d}}{\mathrm{d}t}\|u_1\|_\alpha^\alpha + 4\frac{D_1(\alpha-1)}{\alpha}\|\nabla u_1^{\alpha/2}\|_2^2 \leqslant C_1' + C_1' \epsilon \|u_1\|_{\alpha+1}^{\alpha+1} + C_1' \|y_3\|_{\alpha+1}^{\alpha+1}.$$

From the Gagliardo-Nirenberg-Sobolev inequality (3.8) and for ϵ small enough we get

$$\frac{\mathrm{d}}{\mathrm{d}t}\|u_1\|_\alpha^\alpha + C_1' \|u_1\|_{\alpha+1}^{\alpha+1} \leqslant C_1' + C_1' \|u_1\|_\alpha^\alpha + C_1' \|y_3\|_{\alpha+1}^{\alpha+1}, \tag{3.30}$$

for some C_1' depending on the $\alpha, \mathcal{M}$.

Now we deal with the last term in the right-hand side of (3.30). First we multiply the six equations in (3.1) by $y_3^{\alpha-1}$ to get

$$\int_\Omega |\nabla y_3^{\alpha/2}|^2 \, \mathrm{d}\boldsymbol{x} \leqslant \frac{\delta_3}{\mathcal{D}_3} \int_\Omega u_3 y_3^{\alpha-1} \, \mathrm{d}\boldsymbol{x} \leqslant C_1'' \int_\Omega u_3^\alpha \, \mathrm{d}\boldsymbol{x} + C_1'' \int_\Omega y_3^\alpha \, \mathrm{d}\boldsymbol{x}. \tag{3.31}$$

Then from (3.8) and (3.31) we deduce that

$$\|y_3\|_{\alpha+1}^{\alpha+1} \leqslant C_1'' \|u_3\|_\alpha^\alpha + C_1'' \|y_3\|_\alpha^\alpha \leqslant C_1'' + C_1'' \|u_3\|_\alpha^\alpha + C_1'' \epsilon \|y_3\|_{\alpha+1}^{\alpha+1}.$$

Taking ϵ small enough yields

$$\|y_3\|_{\alpha+1}^{\alpha+1} \leqslant C_1'' + C_1'' \|u_3\|_\alpha^\alpha. \tag{3.32}$$

In view of (3.32), the estimates (3.30) become

$$\frac{\mathrm{d}}{\mathrm{d}t}\|u_1\|_\alpha^\alpha + C_1 \|u_1\|_{\alpha+1}^{\alpha+1} \leqslant C_1 + C_1 \|u_3\|_\alpha^\alpha, \tag{3.33}$$

for some C_1 depending on the $\alpha, \mathcal{M}$, the GNS constant and the parameters of the system.

Reasoning in the same way for the second equation of (3.1), we obtain

$$\frac{\mathrm{d}}{\mathrm{d}t}\|u_2\|_\alpha^\alpha + C_1 \|u_2\|_{\alpha+1}^{\alpha+1} \leqslant C_1 + C_1 \|u_3\|_\alpha^\alpha. \tag{3.34}$$

Performing very similar computations to those of (3.28), we get

$$\begin{aligned}\frac{\mathrm{d}}{\mathrm{d}t}\|u_3\|_\beta^\beta + 4\frac{D_3(\beta-1)}{\beta}\|\nabla u_3^{\beta/2}\|_2^2 \leqslant (\beta-1)\chi_3\left(\frac{\delta_1}{\mathcal{D}_1}\int_\Omega u_1 u_3^\beta \,\mathrm{d}\boldsymbol{x} + \frac{\delta_2}{\mathcal{D}_2}\int_\Omega u_2 u_3^\beta \,\mathrm{d}\boldsymbol{x}\right)\\ + (\gamma_1 M_1 + \gamma_2 M_2 - L)\int_\Omega u_3^\beta \,\mathrm{d}\boldsymbol{x}.\end{aligned} \tag{3.35}$$

Therefore, using (3.29) we find that for $\epsilon_1 > 0$ (to be specified later) there exists a constant $C_2 = C_2(\mathcal{M}, \epsilon_1, \beta, \delta_1, \delta_2\chi_3, \mathcal{D}_1, \mathcal{D}_2)$ such that

$$\frac{\mathrm{d}}{\mathrm{d}t}\|u_3\|_\beta^\beta + 4\frac{D_3(\beta-1)}{\beta}\|\nabla u_3^{\beta/2}\|_2^2 \leqslant C_2 + C_2\epsilon_1\|u_3\|_{\beta+1}^{\beta+1} + C_2\|u_1\|_{\beta+1}^{\beta+1} + C_2\|u_2\|_{L^{\beta+1}(\Omega)}^{\beta+1}. \tag{3.36}$$

Again, from Gagliardo-Nirenberg-Sobolev inequality and choosing ϵ_1 sufficiently small we get

$$\frac{\mathrm{d}}{\mathrm{d}t}\|u_3\|_\beta^\beta + C_2\|u_3\|_{\beta+1}^{\beta+1} \leqslant C_2 + C_2\|u_1\|_{\beta+1}^{\beta+1} + C_2\|u_2\|_{\beta+1}^{\beta+1}. \tag{3.37}$$

In light of (3.34), (3.35) and (3.37) we obtain

$$\frac{\mathrm{d}}{\mathrm{d}t}\big(\|u_1\|_\alpha^\alpha + \|u_2\|_\alpha^\alpha + \|u_3\|_\beta^\beta\big) + C\big(\|u_1\|_{\alpha+1}^{\alpha+1} + \|u_2\|_{\alpha+1}^{\alpha+1} + \|u_3\|_{\beta+1}^{\beta+1}\big) \leqslant C + CU_1 + CU_2 + CU_3,$$

for some constant C depending on α, β and $\mathcal{M}$, where we define

$$U_1 \coloneqq \|u_1\|_{\beta+1}^{\beta+1}, \quad U_2 \coloneqq \|u_2\|_{\beta+1}^{\beta+1}, \quad U_3 \coloneqq \|u_3\|_\alpha^\alpha.$$

In order to obtain a conveniently bound the terms on the right-hand side using the left-hand side, we take $\beta < \alpha < \beta + 1$.

Now, due the interpolation inequalities

$$\begin{aligned}\|u_i\|_{\beta+1} &\leqslant \|u_i\|_1^{1-\theta_1}\|u_i\|_{\alpha+1}^{\theta_1}, \quad \theta_1 = \frac{\beta(\alpha+1)}{\alpha(\beta+1)} \in (0,1), \quad i = 1,2,\\ \|u_3\|_\alpha &\leqslant \|u_3\|_1^{1-\theta_2}\|u_i\|_{\beta+1}^{\theta_2}, \quad \theta_2 = \frac{(\beta+1)(\alpha-1)}{\alpha\beta} \in (0,1),\end{aligned}$$

and (3.23) we have

$$\frac{\mathrm{d}}{\mathrm{d}t}\big(\|u_1\|_\alpha^\alpha + \|u_2\|_\alpha^\alpha + \|u_3\|_\beta^\beta\big) + C\big(\|u_1\|_{\alpha+1}^{\alpha+1} + \|u_2\|_{\alpha+1}^{\alpha+1} + \|u_3\|_{\beta+1}^{\beta+1}\big) \leqslant C + C\big(S_1 + S_2 + S_3\big).$$

for some constant C depending on α, β and $\mathcal{M}$, where we define

$$S_1 \coloneqq \|u_1\|_{\alpha+1}^{\theta_1(\beta+1)}, \quad S_2 \coloneqq \|u_2\|_{\alpha+1}^{\theta_1(\beta+1)}, \quad S_3 \coloneqq \|u_3\|_{\beta+1}^{\theta_2\alpha}.$$

We observe that $\theta_1(\beta+1) < \alpha+1$ and $\theta_2\alpha < \beta+1$, so using Young's inequality with a sufficiently small ϵ allows the terms on the right-hand side to be absorbed into the left-hand side. This gives

$$\frac{\mathrm{d}}{\mathrm{d}t}\big(\|u_1\|_\alpha^\alpha + \|u_2\|_\alpha^\alpha + \|u_3\|_\beta^\beta\big) + C\big(\|u_1\|_{\alpha+1}^{\alpha+1} + \|u_2\|_{\alpha+1}^{\alpha+1} + \|u_3\|_{\beta+1}^{\beta+1}\big) \leqslant C,$$

for some constant C depending on α, β and $\mathcal{M}$. Applying the interpolation inequality

$$\|w\|_\alpha \leqslant \|w\|_1^{1-\xi}\|w\|_{\alpha+1}^{\xi}, \qquad \xi = \frac{\alpha^2-1}{\alpha^2} \in (0,1),$$

we get

$$\frac{\mathrm{d}}{\mathrm{d}t}\big(\|u_1\|_\alpha^\alpha + \|u_2\|_\alpha^\alpha + \|u_3\|_\beta^\beta\big) + C\big((\|u_1\|_\alpha^\alpha)^{\frac{\alpha}{\alpha-1}} + (\|u_2\|_\alpha^\alpha)^{\frac{\alpha}{\alpha-1}} + (\|u_3\|_\beta^\beta)^{\frac{\beta}{\beta-1}}\big) \leqslant C$$

and so, from $(\|u_3\|_\beta^\beta)^{\frac{\alpha}{\alpha-1}} \leqslant (\|u_3\|_\beta^\beta)^{\frac{\beta}{\beta-1}}$ and the convexity of the function $x \mapsto a^x$, we find, setting

$$Z(t) \coloneqq \|u_1\|_\alpha^\alpha + \|u_2\|_\alpha^\alpha + \|u_3\|_\beta^\beta$$

that

$$\frac{\mathrm{d}}{\mathrm{d}t}Z(t) + CZ(t)^{\frac{\alpha}{\alpha-1}} \leqslant C.$$

Now use the ODE comparison (3.3) to conclude

$$Z(t) \leqslant C\left(1 + \frac{1}{t^{\alpha-1}}\right).$$

Furthermore, by invoking (3.2) we obtain the estimate (3.25). □

The following lemma contain a general statement on extensibility and regularity of solutions that are known to be bounded in $L^\infty((0,T_{\max});L^p(\Omega))$ for some $p>1$, it will be used to prove global existence and boundedness. We adapt the methods used in the proof of [10, Lemma 3.2] and [7, Lemma 2.6] to our context for its proof.

Lemma 3.8. *Let $p>1$ such that $u_{i,0} \in L^p(\Omega)$. Then, $T_{\max}=\infty$ and*

$$\sup\left(\sum_{i=1}^{3}\|u_i(\cdot,t)\|_{L^\infty(\Omega)}\right) < \infty.$$

Proof. For each $T \in (0,T_{\max})$, we have

$$M(T) \coloneqq \sup_{t\in(0,T)}\left(\sum_{i=1}^{3}\|u_i\|_{L^\infty(\Omega)}\right) < \infty.$$

To estimate $M(T)$ adequately, we fix an arbitrary $t \in (0,T)$. Let $t_0 \coloneqq \max\{t-1,0\}$, by the variation of constants formula,

$$\|u_i(\cdot,t)\|_{L^\infty(\Omega)} \leqslant K_1 + K_2 + K_3,$$

where we define

$$K_1 \coloneqq \|\exp(-D_i(t-t_0)A)u_i(\cdot,t_0)\|_{L^\infty(\Omega)}, \quad K_2 \coloneqq \int_{t_0}^{t}\|\exp(-D_i(t-s)A)F_i(\boldsymbol{u}(s))\|_{L^\infty(\Omega)}\,\mathrm{d}s,$$

$$K_3 \coloneqq \chi_i\int_{t_0}^{t}\|\exp(-D_i(t-s)A)\operatorname{div}\big(u_i(s)\nabla(\boldsymbol{b}_i^{\mathrm{T}}\boldsymbol{y}(s))\big)\|_{L^\infty(\Omega)}\,\mathrm{d}s$$

Here, if $t \leqslant 1$, then $t_0 = 0$, we use the comparison principle to see

$$K_1 \leqslant \|u_{i,0}\|_{L^\infty(\Omega)}, \tag{3.38}$$

whereas in the case $t > 1$, we invoke (3.11) and (3.23) to estimate

$$K_1 \leqslant C(t - t_0)^{-1}\|u_i(\cdot, t_0)\|_{L^1(\Omega)} \leqslant C_1\mathcal{M}. \tag{3.39}$$

Again using parabolic maximum principle and (3.7) we get

$$K_2 \leqslant \int_{t_0}^{t} \|F_i(\boldsymbol{u}(s))\|_{L^\infty(\Omega)}\, ds \leqslant \|F_i\|_{L^\infty(\Omega)}. \tag{3.40}$$

Now, let $p > 2$. $\beta \in (\frac{1}{p}, \frac{1}{2})$ and $\varepsilon \in (0, \frac{1}{2} - \beta)$. Then

$$\begin{aligned} K_3 &\leqslant C_2 \int_{t_0}^{t} \|(A+1)^\beta \exp(-D_i(t-s)A)\, \mathrm{div}\big(u_i(s)\nabla(\boldsymbol{b}_i^{\mathrm{T}}\boldsymbol{y}(s))\big)\|_{L^p(\Omega)}\, \mathrm{d}s \\ &\leqslant C_2 \int_{t_0}^{t} (t-s)^{-(\beta+\frac{1}{2}+\varepsilon)}\|u_i(s)\nabla(\boldsymbol{b}_i^{\mathrm{T}}\boldsymbol{y}(s))\|_{L^p(\Omega)}\, \mathrm{d}s \qquad \forall t \in (0, T_{\max}) \end{aligned}$$

By Lemma 3.7, $\|u_i(t)\|_{L^\alpha(\Omega)} \leqslant C'$ holds for any $\alpha > 1$, $t > 0$ and $i = 1, 2, 3$ with $C' > 0$ depending on $\alpha, \|u_{1,0}\|_{L^\alpha(\Omega)}, \|u_{2,0}\|_{L^\alpha(\Omega)}, \|u_{3,0}\|_{L^\alpha(\Omega)}$ and $\mathcal{M}$ but not on t. Thus elliptic regularity theory applied to (3.6) tells us that also $\|\nabla y_i(t)\|_{L^\alpha(\Omega)} \leqslant C_3$ holds for any $\alpha > 1$ and $t > 0$. In particular, $\|u_i(s)\nabla(\boldsymbol{b}_i^{\mathrm{T}}\boldsymbol{y}(s))\|_{L^p(\Omega)} \leqslant C_3$ for any $s \in (0, T_{\max})$ with $C_3 > 0$ depending on $p, \|u_{1,0}\|_{L^p(\Omega)}, \|u_{2,0}\|_{L^p(\Omega)}, \|u_{3,0}\|_{L^p(\Omega)}$ and $\mathcal{M}$ but not on t. Consequently, using Lemma 3.4, arrive at

$$\begin{aligned} K_3 &\leqslant C_2 \int_{t_0}^{t} (t-s)^{-(\beta+\frac{1}{2}+\varepsilon)}\|u_i(s)\nabla(\boldsymbol{b}_i^{\mathrm{T}}\boldsymbol{y}(s)\|_{L^p(\Omega)}\, \mathrm{d}s \\ &\leqslant C_3 \int_{t_0}^{t} (t-s)^{-(\beta+\frac{1}{2}+\varepsilon)}\, \mathrm{d}s := C_4 \quad \text{for all } t \in (0, T), \end{aligned} \tag{3.41}$$

where C_4 is independent of t. Collecting (3.38)–(3.41) we conclude that

$$\|u_i(\cdot, t)\|_{L^\infty(\Omega)} \leqslant C_5 \qquad \text{for all } t \in (0, T).$$

Herein the constant $C_5 > 0$ is independent of t. Thus, we obtain $T_{\max} = \infty$ in view of (3.14) □

The last lemma entails the main result of this section, namely the existence and uniqueness of the global classical solution to the system (3.1).

Theorem 3.1. *Let $u_{i,0} \in C^0(\overline{\Omega}) \cap L^p(\Omega)$ nonnegative for some $p > 2$ with $i = 1, 2, 3$. Then (3.1) possesses a unique global classical solution $(\boldsymbol{u}, \boldsymbol{y})$ for which both u_i and y_i are nonnegative and each $u_1, u_2, u_3, y_1, y_2, y_3$ belongs to $C^0\big(\overline{\Omega} \times [0, \infty)\big) \cap C^{2,1}\big(\overline{\Omega} \times (0, \infty)\big)$.*

3.4 Weak Solutions

Our goal in this section is to construct the existence of a weak solution as the limit of global classical solutions of appropriately regularized problems.

Definition 3.1. *A* weak solution *of* (3.1) *in the time interval* $(0,T)$ *is a set of non-negative functions* $(\boldsymbol{u},\boldsymbol{y})$ *such that for all* $i=1,2,3$

$$u_i, y_i \in L^2(0,T;H^1(\Omega)), \qquad \partial_t u_i \in L^2(0,T;\big(W^{1,\infty}(\Omega)\big)^*),$$

and for all test functions $\xi_i,\psi_i \in L^2(0,T;W^{1,\infty}(\Omega))$, u_i *and* y_i *satisfy the following identities for all* $i=1,2,3$*:*

$$\begin{aligned} -\int_0^T u_i\partial_t\xi_i \,\mathrm{d}t + \int_{\Omega_T}\left(D_i\nabla u_i\cdot\nabla\xi_i - \chi_i u_i\nabla(\boldsymbol{b}_i^{\mathrm{T}}\boldsymbol{y})\cdot\nabla\xi_i\right)\mathrm{d}\boldsymbol{x}\,\mathrm{d}t \\ -\int_\Omega u_{i,0}(\boldsymbol{x})\xi_i(\boldsymbol{x},0)\,\mathrm{d}t = \int_{\Omega_T} F_i\cdot\xi_i\,\mathrm{d}\boldsymbol{x}\,\mathrm{d}t, \qquad (3.42)\\ \mathcal{D}_i\int_{\Omega_T}\nabla y_i\cdot\nabla\psi_i\,\mathrm{d}\boldsymbol{x}\,\mathrm{d}t + \theta_i\int_{\Omega_T} y_i\cdot\psi_i\,\mathrm{d}\boldsymbol{x}\,\mathrm{d}t = \int_{\Omega_T} u_i\cdot\psi_i\,\mathrm{d}\boldsymbol{x}\,\mathrm{d}t. \end{aligned}$$

Theorem 3.2. *Fix an arbitrary* $T>0$*. Then for all nonnegative* $u_{i,0}\in L^4(\Omega)$ *there exists a unique weak solution to the system* (3.1) *in the sense of Definition 2.8.*

We postpone the proof of the Theorem to the end of the section, and prove now the auxiliary results needed. The first is a stability result for the classical solutions of (3.1) obtained in Theorem 3.1.

Lemma 3.9. *Let* $p>2$ *and* $u_{i,0}^a$, $u_{i,0}^b\in C^0(\overline{\Omega})\cap L^p(\Omega)$ *be two sets of nonnegative initial data with* $i=1,2,3$*. Then, the respective classical solutions* $(\boldsymbol{u}^a,\boldsymbol{y}^a)$ *and* $(\boldsymbol{u}^b,\boldsymbol{y}^b)$ *obtained in Theorem 3.1 are stable in the sense that there exists a constant* $C>0$ *depending only on the* L^p *norms of the initial data, on* Ω*, and on the constants appearing in* (3.1) *such that*

$$\sum_{i=1}^3 \|u_i^a(t)-u_i^b(t)\|_{L^2(\Omega)} \le \sum_{i=1}^3 \|u_{i,0}^a-u_{i,0}^b\|_{L^2(\Omega)}\ \exp(Ct). \qquad (3.43)$$

Proof. Let $\overline{u}_i := u_i^a - u_i^b$, for $i=1,2,3$, and similarly for y_i. The equations for $\overline{u}_i$ read

$$\partial_t\overline{u}_i - D_i\Delta\overline{u}_i - \chi_i\,\mathrm{div}(\overline{u}_i\nabla y_3^a) - \chi_i\,\mathrm{div}(u_i^b\nabla\overline{y}_3) = F_i(\boldsymbol{u}^a)-F_i(\boldsymbol{u}^b), \qquad (3.44)$$

if $i=1,2$, and for $i=3$,

$$\partial_t\overline{u}_3 - D_3\Delta\overline{u}_3 - \chi_3\,\mathrm{div}\left(\overline{u}_3\nabla(y_1^a+y_2^a)\right) - \chi_3\,\mathrm{div}\left(u_3^b\nabla(\overline{y}_1+\overline{y}_2)\right) = F_3(\boldsymbol{u}^a)-F_3(\boldsymbol{u}^b). \qquad (3.45)$$

Multiplying (3.44) by $\overline{u}_i$ and integrating in Ω, we find

$$\frac{1}{2}\frac{\mathrm{d}}{\mathrm{d}t}\int_\Omega|\overline{u}_i|^2\,\mathrm{d}\boldsymbol{x} + D_i\int_\Omega|\nabla\overline{u}_i|^2\,\mathrm{d}\boldsymbol{x} = -T_1-T_2+T_3, \qquad (3.46)$$

where we define

$$T_1 = \chi_i \int_\Omega \overline{u}_i \nabla y_3^a \cdot \nabla \overline{u}_i \,\mathrm{d}\boldsymbol{x}, \qquad T_2 = \chi_i \int_\Omega u_i^b \nabla \overline{y}_3 \cdot \nabla \overline{u}_i \,\mathrm{d}\boldsymbol{x}, \qquad T_3 = \int_\Omega \big(F_i(\boldsymbol{u}^a) - F_i(\boldsymbol{u}^b)\big)\overline{u}_i \,\mathrm{d}\boldsymbol{x}.$$

First note that since $n = 2$, we find from Sobolev embedding, elliptic regularity and the estimate (3.25) that

$$\|\nabla y_3^a\|_{L^\infty(\Omega)} \le C\|y_3^a\|_{W^{2,p}} \le C\|u_3^a\|_{L^p(\Omega)} \le C(\|u_{i,0}^a\|_{L^p(\Omega)}). \tag{3.47}$$

Thus we can write, using an appropriate Young's inequality,

$$\begin{aligned} T_1 &\le \chi_i \|\nabla y_3^a\|_{L^\infty(\Omega)} \int_\Omega |\overline{u}_i \nabla \overline{u}_i| \,\mathrm{d}\boldsymbol{x} \\ &\le C(\|u_{i,0}^a\|_{L^p(\Omega)}) \int_\Omega |\overline{u}_i|^2 \,\mathrm{d}\boldsymbol{x} + \frac{D_i}{2} \int_\Omega |\nabla \overline{u}_i|^2 \,\mathrm{d}\boldsymbol{x}, \end{aligned}$$

where $C(\|u_{i,0}^a\|_{L^p(\Omega)})$ depends also on the constants appearing in (3.1). For the second term in the right-hand side of (3.46), we find

$$\begin{aligned} T_2 &\le \frac{D_i}{2} \int_\Omega |\nabla \overline{u}_i|^2 \,\mathrm{d}\boldsymbol{x} + C\|u_i^b\|_{L^\infty(\Omega)}^2 \int_\Omega |\nabla \overline{y}_3|^2 \,\mathrm{d}\boldsymbol{x} \\ &\le \frac{D_i}{2} \int_\Omega |\nabla \overline{u}_i|^2 \,\mathrm{d}\boldsymbol{x} + C(\|u_{i,0}^b\|_{L^p(\Omega)})\|\overline{u}_3\|_2^2, \end{aligned}$$

where we used Lemma 3.8 and elliptic regularity. Finally, from the locally Lipschitz property of F_i, and the L^∞ estimate of Lemma 3.8, we find that

$$T_3 \le L \sum_{i=1}^3 \|\overline{u}_i\|_{L^2(\Omega)}^2$$

for some constant $L > 0$. Putting these estimates together in (3.46) gives for $i = 1, 2$,

$$\frac{\mathrm{d}}{\mathrm{d}t}\|\overline{u}_i\|_2^2 \le C \sum_{j=1}^3 \|\overline{u}_j\|_{L^2(\Omega)}^2.$$

For the third equation of (3.1), similar calculations yields

$$\frac{\mathrm{d}}{\mathrm{d}t}\|\overline{u}_3\|_2^2 \le C \sum_{j=1}^3 \|\overline{u}_j\|_{L^2(\Omega)}^2.$$

Therefore, with $\zeta(t) = \sum_{j=1}^3 \|\overline{u}_j\|_2^2$, we find $\zeta'(t) \le C\zeta(t)$ and so $\zeta(t) \le \zeta(0)\exp(Ct)$, which is (3.43). □

Now we take a sequence of smoothed initial data $u_{i,0}^k \in C^0(\overline{\Omega}) \cap L^4(\Omega)$ such that $u_{i,0}^k \to u_{i,0}$ in $L^4(\Omega)$. We consider, for $k \in \mathbb{N}$, the classical solution $(\boldsymbol{u}^k, \boldsymbol{y}^k) \in C^0\big(\overline{\Omega}\times[0,\infty)\big) \cap C^{2,1}\big(\overline{\Omega}\times(0,\infty)\big)$

of the system

$$\begin{aligned}
\partial_t u_1^k - D_1\Delta u_1^k - \chi_1 \operatorname{div}\big(u_1^k\nabla(y_3^k)\big) &= F_1(\boldsymbol{u}^k),\\
\partial_t u_2^k - D_2\Delta u_2^k - \chi_2 \operatorname{div}\big(u_2^k\nabla(y_3^k)\big) &= F_2(\boldsymbol{u}^k)\\
\partial_t u_3^k - D_3\Delta u_3^k + \chi_3 \operatorname{div}\big(u_3^k\nabla(y_1^k + y_2^k)\big) &= F_3(\boldsymbol{u}^k)\\
-\mathcal{D}_i\Delta y_i^k + \theta_i y_i^k = \delta_i u_i^k, \quad i = 1,2,3, \quad (\boldsymbol{x},t) &\in \Omega_T,
\end{aligned} \tag{3.48}$$

which is given by Theorem 3.1. The next Lemma provides the remaining estimates needed to obtain a weak solution.

Lemma 3.10. *Let $(\boldsymbol{u}^k, \boldsymbol{y}^k)$ be the sequence of classical solutions of the system (3.1) described above. Fix an arbitrary $T > 0$. Then there exist constants $C_1, C_2, C_3, C_4, C_5 > 0$ not depending on k such that for $i = 1, 2, 3$ we get*

$$\|u_i^k\|_{L^\infty(0,T;L^2(\Omega))} + \|y_i^k\|_{L^\infty(0,T;L^2(\Omega))} \leqslant C_1, \tag{3.49}$$

$$\|F_i(u^k)\|_{L^2(\Omega_T)} \leqslant C_2 \tag{3.50}$$

$$\|\nabla u_i^k\|_{L^2(\Omega_T)} + \|\nabla y_i^k\|_{L^2(\Omega_T)} \leqslant C_3. \tag{3.51}$$

$$\|u_i^k \nabla(b_i^T \boldsymbol{y}^k)\|_{L^2(\Omega_T)} \leqslant C_4. \tag{3.52}$$

$$\|\partial_t u_i^k\|_{L^2(0,T;(H^1(\Omega))^*)} \leqslant C_5. \tag{3.53}$$

Proof. Multiplying the first equation in (3.48) by u_1^k and integrating by parts yields

$$\frac{1}{2}\frac{\mathrm{d}}{\mathrm{d}t}\|u_1^k\|^2_{L^2(\Omega)} + D_1\|\nabla u_1^k\|^2_{L^2(\Omega)} + \chi_1\int_\Omega u_1^k\nabla y_3^k\cdot\nabla u_1^k\,\mathrm{d}\boldsymbol{x} \leqslant r_1\|u_1^k\|^2_{L^2(\Omega)}. \tag{3.54}$$

We have

$$\chi_1\int_\Omega |u_1^k||\nabla y_3^k||\nabla u_1^k|\,\mathrm{d}\boldsymbol{x} \leq \|\nabla y_3^k\|_{L^\infty(\Omega)}\chi_1\int_\Omega |u_1^k||\nabla u_1^k|\,\mathrm{d}\boldsymbol{x}$$

and, by (3.47), $\|\nabla y_3^k\|_{L^\infty(\Omega)} \leq C(\|u_{i,0}^k\|_{L^4(\Omega)})$. Since $u_{i,0}^k \to u_{i,0}$ in $L^4(\Omega)$, $\|u_{i,0}^k\|_{L^4(\Omega)}$ is bounded uniformly in k. Therefore, $\|\nabla y_3^k\|_{L^\infty(\Omega)} \leq C$ and we get

$$\|\nabla y_3^k\|_{L^\infty(\Omega)}\chi_1\int_\Omega |u_1^k||\nabla u_1^k|\,\mathrm{d}\boldsymbol{x} \leq C\int_\Omega |u_1^k||\nabla u_1^k|\,\mathrm{d}\boldsymbol{x} \leq \frac{D_1}{2}\int_\Omega |\nabla u_1^k|^2\,\mathrm{d}\boldsymbol{x} + C\int_\Omega |u_1^k|^2\,\mathrm{d}\boldsymbol{x}$$

for some appropriate constant C. Thus

$$\frac{1}{2}\frac{\mathrm{d}}{\mathrm{d}t}\|u_1^k\|^2_{L^2(\Omega)} + \frac{D_1}{2}\|\nabla u_1^k\|^2_{L^2(\Omega)} \leqslant C\|u_1^k\|^2_{L^2(\Omega)}. \tag{3.55}$$

In view of Gronwalls inequality it follows from (3.54) that

$$\sup_{(0,T)} \|u_1^k\|_{L^2(\Omega)} \leqslant C_1'. \tag{3.56}$$

Now, we apply elliptic regularity theory and (3.56) to find

$$\sup_{(0,T)} \|y_1^k\|_{L^2(\Omega)} \leqslant C_1', \tag{3.57}$$

for some constant $C_1' > 0$. The treatment of the second species u_2^k is exactly the same, and we obtain

$$\sup_{(0,T)} \|u_2^k\|_{L^2(\Omega)} \leqslant C_2' \text{ and } \sup_{(0,T)} \|y_2^k\|_{L^2(\Omega)} \leqslant C_2', \tag{3.58}$$

for some constant $C_2' > 0$.

For the third species, the procedure is still the same, except that we need to bound $\|\nabla(y_1^k + y_2^k)\|_{L^\infty(\Omega)}$ instead of $\|\nabla y_3^k\|_{L^\infty(\Omega)}$. But in a similar way, we find that

$$\|\nabla(y_1^k + y_2^k)\|_{L^\infty(\Omega)} \leq C_3',$$

where C_3' depends on $\|u_{i,0}^k\|_{L^4(\Omega)}$, which is uniformly bounded in k. We thus get

$$\sup_{(0,T)} \|u_3^k\|_{L^2(\Omega)} \leqslant C_3' \text{ and } \sup_{(0,T)} \|y_3^k\|_{L^2(\Omega)} \leqslant C_3'. \tag{3.59}$$

for some constant $C_3' > 0$. Then (3.49) it follows from (3.56), (3.57), (3.58) and (3.59).

The quadratic growth of F_i and the $L^\infty(0,T;L^4(\Omega))$ estimates on the solutions u_i^k, ensure the $L^2(\Omega_T)$ bound for F_i, (3.50).

Now from (3.55) and (3.49) we obtain (3.51).

To obtain (3.52), we observe that

$$\int_0^T \|u_i^k \nabla(b_i^T \boldsymbol{y}^k)\|_{L^2(\Omega)} \leqslant \sup_{(0,T)} \|\nabla(b_i^T \boldsymbol{y}^k)\|_{L^\infty(\Omega)} \int_0^T \|u_i^k\|_{L^2(\Omega)}. \tag{3.60}$$

By (3.47) and (3.25), we have that $\sup_{(0,T)} \|\nabla y_i^k\|_{L^\infty(\Omega)} \leq C(\|u_{i,0}^k\|_{L^4(\Omega)}) \leq C$ uniformly in k. Therefore, using (3.49), we get

$$\int_0^T \|u_i^k \nabla(b_i^T \boldsymbol{y}^k)\|_{L^2(\Omega)} \leqslant C_4',$$

which is (3.52).

Finally, we deduce from (3.50), (3.51) and (3.52): for all $\phi \in L^2(0,T;H^1(\Omega))$,

$$\begin{aligned}
\left|\int_0^T \int_\Omega \langle \partial_t u_i^k, \phi\rangle\right| &\leqslant \left|-D_i \int_0^T \int_\Omega \nabla u_i^k \cdot \nabla\phi + \chi_i \int_0^T \int_\Omega u_i^k \nabla(b_i^T \boldsymbol{y}^k)\cdot\nabla\phi + \int_0^T \int_\Omega F_i(\boldsymbol{u}^k)\phi\right| \\
&\leqslant D_i \|\nabla u_i^k\|_{L^2(\Omega_T)} \|\nabla\phi\|_{L^2(\Omega_T)} + |\chi_i| \|u_i^k \nabla(b_i^T \boldsymbol{y}^k)\|_{L^2(\Omega_T)} \|\nabla\phi\|_{L^2(\Omega_T)} \\
&\quad + \|F_i(u^k)\|_{L^2(\Omega_T)} \|\phi\|_{L^2(\Omega_T)} \\
&\leqslant C_5 \|\phi\|_{L^2(0,T;H^1(\Omega))},
\end{aligned}$$

for some constant C_5 independent of k. From this we deduce the bound (3.53). This completes the proof of Lemma 3.10. □

We are now ready to prove the well-posedness result of Theorem 3.2.

Proof of Theorem 3.2. For $k, l \in \mathbb{N}$, consider the Cauchy differences

$$Z_{k,l}(t) = \sum_{i=1}^{3} \|u_i^k(t) - u_i^l(t)\|_{L^2(\Omega)}$$

constructed from the smooth solutions in Lemma 3.10. From the stability result in Lemma 3.9, we see that

$$Z_{k,l}(t) \leq Z_{k,l}(0) \exp(Ct),$$

with C independent of the indices k, l. Therefore, the sequences $(u_i^k)_k$ are Cauchy sequences in $L^\infty(0,T;L^2(\Omega))$. As a consequence, there exist $u_i \in L^\infty(0,T;L^2(\Omega))$ with

$$u_i^k \to u_i \quad \text{in } L^\infty(0,T;L^2(\Omega)).$$

From the equations for y_i^k we easily deduce (for instance with $i = 1$) that

$$\|y_1^k(t) - y_1^l(t)\|_{H^1}^2 \leq C\|u_3^k - u_3^l\|_{L^2}^2 \to 0,$$

and so $(y_i^k)_k$ are Cauchy sequences in $L^\infty(0,T;H^1(\Omega))$. Therefore we have

$$y_i^k \to y_i \quad \text{in } L^\infty(0,T;H^1(\Omega)).$$

From the estimates (3.51) and (3.53)we deduce also that

$$\begin{aligned} u_i^k &\rightharpoonup u_i && \text{weakly in } L^2(0,T;H^1(\Omega)), \\ \partial_t u_i^k &\rightharpoonup \partial_t u_i && \text{weakly in } L^2(0,T;(H^1(\Omega))^*). \end{aligned}$$

As a consequence of the previous estimates we find, in addition, that

$$\begin{aligned} u_i^k \nabla(b_i^T \boldsymbol{y}^k) &\to u_i \nabla(b_i^T \boldsymbol{y}) && \text{in } L^1((0,T)\times\Omega), \\ F_i(u_i^k) &\to F_i(u_i) && \text{in } L^\infty(0,T;L^2(\Omega)). \end{aligned}$$

The above convergences, along with a time continuity property in $L^2((0,T)\times\Omega)$ (which is a consequence of the Aubin-Lions lemma [88, Theorem 2.1]), ensure that for each $\xi \in C^\infty\big([0,T)\times\Omega\big)$ we can pass to the limit on each term of

$$\begin{aligned} -\int_0^T u_i^k \partial_t \xi \, \mathrm{d}t + \int_{\Omega_T} \left(D_i \nabla u_i^k \cdot \nabla \xi - \chi_i u_i^k \nabla(\boldsymbol{b}_i^{\mathrm{T}} \boldsymbol{y}^k) \cdot \nabla \xi\right) \mathrm{d}\boldsymbol{x}\,\mathrm{d}t \\ - \int_\Omega u_{i,0}(\boldsymbol{x})\xi(\boldsymbol{x},0)\,\mathrm{d}t = \int_{\Omega_T} F_i \xi \,\mathrm{d}\boldsymbol{x}\,\mathrm{d}t, \\ \mathcal{D}_i \int_{\Omega_T} \nabla y_i^k \cdot \nabla \xi \,\mathrm{d}\boldsymbol{x}\,\mathrm{d}t + \theta_i \int_{\Omega_T} y_i^k \xi \,\mathrm{d}\boldsymbol{x}\,\mathrm{d}t = \int_{\Omega_T} u_i^k \xi \,\mathrm{d}\boldsymbol{x}\,\mathrm{d}t \end{aligned}$$

to obtain a weak solution according to Definition 2.8. The uniqueness follows from the fact that the stability property in Lemma 3.9 holds, by approximation, for weak solutions as well. This completes the proof of Theorem 3.2. □

3.5 Finite Volume Scheme

In this section, we construct approximate solutions of problem (3.1). For this purpose, we introduce a notion of admissible finite volume mesh (see e.g. [45]). This notion its was mentioned in Section 2.3.1, in fact is the same definition.

3.5.1 Admissible mesh

Let $\Omega \subset \mathbb{R}^n$, $n = 2$ denote an open bounded polygonal connected domain with boundary $\partial\Omega$. An admissible FV mesh of Ω is given by a family $\mathscr{T}_h$ of control volumes (open and convex polygonal subsets of Ω), a family $\mathcal{E} \subset \bar{\Omega}$ of hyperplanes of $\mathbb{R}^d$ (edges in two-dimensional case or sides in three-dimensional) and a family of points $\mathcal{P} = (\boldsymbol{x}_K)_{K\in\mathscr{T}_h}$ that satisfy

$$\bar{\Omega} = \bigcup_{K\in\mathscr{T}_h} \bar{K}, \qquad \mathcal{E} = \bigcup_{K\in\mathscr{T}_h} \mathcal{E}_K, \qquad \partial K = \bigcup_{L\in\mathcal{N}(K)} \bar{\sigma}.$$

Let $K, L \in \mathscr{T}_h$ with $K \neq L$. If $\bar{K} \cap \bar{L} = \bar{\sigma}$ for some $\sigma \in \mathcal{E}$, then $\sigma = K|L$ (common edge). We introduce the set of interior (respectively boundary) edges denoted by $\mathcal{E}_{\text{int}}$ (resp. $\mathcal{E}_{\text{ext}}$), that is $\mathcal{E}_{\text{int}} = \{\sigma \in \mathcal{E} \ : \ \sigma \not\subset \partial\Omega\}$ (resp. $\mathcal{E}_{\text{ext}} = \{\sigma \in \mathcal{E} \ : \ \sigma \subset \partial\Omega\}$). The set of neighbours of K is given by $\mathcal{N}(K) = \{L \in \mathscr{T}_h \ : \ \exists\sigma \in \mathcal{E}, \bar{\sigma} = \bar{K} \cap \bar{L}\}$. The family $\mathcal{P}$ is such that for all $K \in \mathscr{T}_h$, $\boldsymbol{x}_K \in \bar{K}$, and, if $\sigma = K|L$, it is assumed that $\boldsymbol{x}_K \neq \boldsymbol{x}_L$, and that the segment $\overline{\boldsymbol{x}_K\boldsymbol{x}_L}$ is orthogonal to $\sigma = K|L$ Let $d_{K|L}$ denote the Euclidean distance between $\boldsymbol{x}_k$ and $\boldsymbol{x}_L$ and by $d_{K,\sigma}$ the distance from $\boldsymbol{x}_K$ to σ. The transmissibility through $\sigma \in \mathcal{E}_{\text{int}}$ is defined by $\tau_{K|L} = m(K|L)/d_{K|L} = m(\sigma)/d_\sigma$ and for $\sigma \in \mathcal{E}_{\text{ext}}$ by $\tau_{K,\sigma} = m(\sigma)/d_{K,\sigma}$. We require local regularity restrictions on the family of meshes $\mathscr{T}_h$; namely

$$\exists\gamma > 0\ \forall h\ \forall K \in \mathscr{T}_h\ \forall L \in \mathcal{N}(K) : \quad \operatorname{diam}(K) + \operatorname{diam}(L) \leqslant \gamma d_{K,L} \tag{3.61}$$

$$\exists\gamma > 0\ \forall h\ \forall K \in \mathscr{T}_h\ \forall L \in \mathcal{N}(K) : \quad m(K|L)d_{K,L} \leqslant \gamma m(K). \tag{3.62}$$

A discrete function on the mesh $\mathscr{T}_h$ is a set $(u_K)_{K\in\mathscr{T}_h}$. Whenever convenient, we identify it with the piecewise constant function $u_h \in \Omega$ such that $u_h|_K = u_K$. Finally, the discrete gradient $\nabla_h u_h$ of a constant per control volume function u_h is defined on $\bar{K} \cap \bar{L}$ by

$$\nabla_{K,L} u_{i,h} \coloneqq \frac{u_L - u_K}{d_{K|L}} \boldsymbol{n}_{K|L}. \tag{3.63}$$

3.5.2 Description of the finite volume (FV) scheme

We adapt the finite volume scheme given in Chapter 2 our context, and we recall that the convergence to the weak solution of FV scheme was proved.

To discretize (3.1) we choose an admissible discretization of Ω_T consisting of an admissible mesh $\mathscr{T}_h$ of Ω along with a time step $\Delta t_h > 0$; both Δt_h and the size $\max_{K\in\mathscr{T}} \operatorname{diam}(K)$ tend

to zero as $h \to 0$.We define $N_h > 0$ as the smallest integer such that $(N_h + 1)\Delta t_h \geqslant T$, and set $t_n = n\Delta t_h$ for $n \in \{0, \dots, N_h\}$. Whenever Δt_h is fixed, we will drop the subscript h in the notation.

To formulate the resulting scheme, we introduce the terms

$$\mathcal{A}_{i,K,L}^{n+1} \coloneqq \min\big\{(u_{i,K}^{n+1})^+, (u_{i,L}^{n+1})^+\big\}, \quad F_{i,K}^{n+1} \coloneqq F_i\big((u_{1,K}^{n+1})^+, (u_{2,K}^{n+1})^+, (u_{3,K}^{n+1})^+\big), \quad i = 1, 2, 3.$$

The computation starts from the initial cell averages

$$u_{i,K}^0 \coloneqq \frac{1}{m(K)} \int_K u_{i,0}(\boldsymbol{x})\, \mathrm{d}\boldsymbol{x}, \quad i = 1, 2, 3. \tag{3.64}$$

We state the FV scheme for (2.1) as follows: for all $K \in \mathscr{T}_h$ and $n \in \{0, 1, \dots, N_h\}$, find $(u_{i,K}^{n+1})_{K \in \mathscr{T}_h}$, $i = 1, 2, 3$, such that

$$-\mathcal{D}_i \sum_{L \in \mathcal{N}(K)} \tau_{K|L}\big(y_{i,L}^{n+1} - y_{i,K}^{n+1}\big) + \theta_i m(K) y_{i,K}^{n+1} = \delta_i m(K) u_{i,K}^n, \quad i = 1, 2, 3, \tag{3.65a}$$

$$\begin{aligned} m(K)\frac{u_{i,K}^{n+1} - u_{i,K}^n}{\Delta t} - D_i \sum_{L \in \mathcal{N}(K)} \tau_{K|L}\big(u_{i,L}^{n+1} - u_{i,K}^{n+1}\big) \\ + \chi_i \sum_{L \in \mathcal{N}(K)} \tau_{K|L} \mathcal{A}_{i,K,L}^{n+1} \boldsymbol{b}_i^{\mathrm{T}}\big(\boldsymbol{y}_L^{n+1} - \boldsymbol{y}_K^{n+1}\big) = m(K) F_{i,K}^{n+1}, \quad i = 1, 2, 3 \end{aligned} \tag{3.65b}$$

As usual, homogeneous Neumann boundary conditions are taken into account implicitly. Indeed, the parts of ∂K that lie in $\partial\Omega$ do not contribute to the sums over $L \in \mathcal{N}(K)$ terms, which means that the flux is zero is imposed on the external edge of the mesh.

The sets of values $(u_{1,K}^{n+1}, u_{2,K}^{n+1}, u_{3,K}^{n+1})_{K \in \mathscr{T}_h, n \in \{0,1,\dots,N_h\}}$ and $(y_{1,K}^{n+1}, y_{2,K}^{n+1}, y_{3,K}^{n+1})_{K \in \mathscr{T}_h, n \in \{0,1,\dots,N_h\}}$ satisfying (3.65) will be called a discrete solution. We associate a discrete solution of the scheme at $t = t_{n+1}$ with the triplets $\boldsymbol{u}_h^{n+1} = (u_{1,h}^{n+1}, u_{2,h}^{n+1}, u_{3,h}^{n+1})^{\mathrm{T}}$ and $\boldsymbol{y}_h^{n+1} = (y_{1,h}^{n+1}, y_{2,h}^{n+1}, y_{3,h}^{n+1})^{\mathrm{T}}$ of the piecewise constant on Ω functions given by

$$u_{y,h}^{n+1}|_K = u_{i,K}^{n+1}, \quad y_{i,h}^{n+1}|_K = y_{i,K}^{n+1}, \quad \text{for all } K \in \mathscr{T}_h, \text{ all } n \in \{0, 1, \dots, N_h - 1\} \text{ and all } i = 1, 2, 3.$$

Furthermore, we define the piecewise constant function

$$\boldsymbol{u}_h(\boldsymbol{x}, t) = \big(u_{1,h}(\boldsymbol{x}, t), u_{2,h}(\boldsymbol{x}, t), u_{3,h}(\boldsymbol{x}, t)\big)^{\mathrm{T}} \coloneqq \sum_{\substack{K \in \mathscr{T}_h \\ n \in \{0,1,\dots,N_h\}}} \boldsymbol{u}_h^{n+1} \mathbb{1}_{(t_n, t_{n+1}] \times K}.$$

Herein, the expression $\mathbb{1}_{(t_n, t_{n+1}] \times K}$ denotes the characteristic function of set $(t_n, t_{n+1}] \times K$, in similar way we define the piecewise constant function $\boldsymbol{y}_h(\boldsymbol{x}, t)$.

3.6 Numerical Examples

We present in this section some numerical results obtained by the finite volume scheme (3.65). To obtain the numerical test, we will reduce the number of the parameters in the model (3.1),

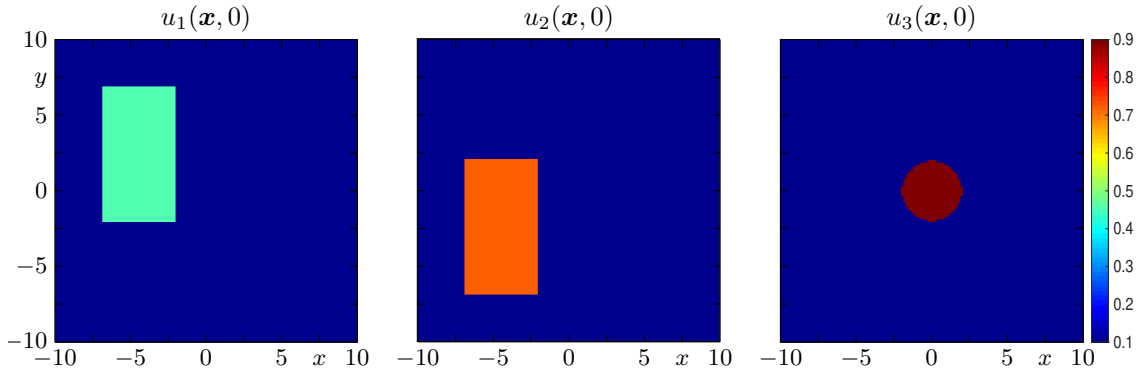

Figure 3.1: Example 1: initial condition for species u_1, u_2 and u_3.

(3.2). For this reason we non-dimensionalize the system following [2]. We choose

$$U_1 = \frac{u_1}{k_1}, \quad U_2 = \frac{M_1 A_1 u_2}{k_1 A_2 M_2}, \quad U_3 = \frac{\gamma_1 K_1}{u_3}, \quad t = r_1 t.$$

Making the substitution and simplifying, we obtain

$$\begin{aligned} F_1(\boldsymbol{U}) &= U_1(1-U_1) - c_1 U_1 U_2 - \frac{a_1 U_1}{b_1 + U_1} U_3, \\ F_2(\boldsymbol{U}) &= r U_1(k - U_1) - c_2 U_1 U_2 - \frac{a_2 U_2}{b_2 + U_2} U_2, \\ F_3(\boldsymbol{U}) &= \frac{a_1 U_1}{b_1 + U_1} U_3 + \frac{a_3 U_2}{b_2 + U_2} U_3 - d U_3 - f U_3^2. \end{aligned}$$

On the domain $\Omega := (-10, 10) \times (-10, 10)$ we define a uniform Cartesian grid

$$\mathscr{T}_h = \{K_{ij} \subseteq \Omega \ : \ K_{ij} = ((i-1)N_x, iN_x) \times ((j-1)N_x, jN_x)\}$$

with $N_x \times N_y$ control volumes. For the simulations, we choose $N_x = N_y = 128$. The corresponding diffusion coefficients are given by

$$D_1 = D_2 = 5, \qquad D_3 = 1, \qquad \mathcal{D}_1 = \mathcal{D}_2 = 1, \qquad \mathcal{D}_3 = 10,$$

and the sensitivity chemotactic parameters are chosen by

$$\delta_1 = 20, \qquad \delta_2 = 20, \qquad \delta_3 = 2, \qquad \theta_1 = \theta_2 = 10, \qquad \theta_3 = 1.$$

The initial distribution for u_1, u_2 and u_3 species correspond to a constant $u_{1,0} = 0.5$, $u_{2,0} = 0.8$ and $u_{3,0} = 1$.

3.6.1 Example 1 (species the interacting via chemical substance)

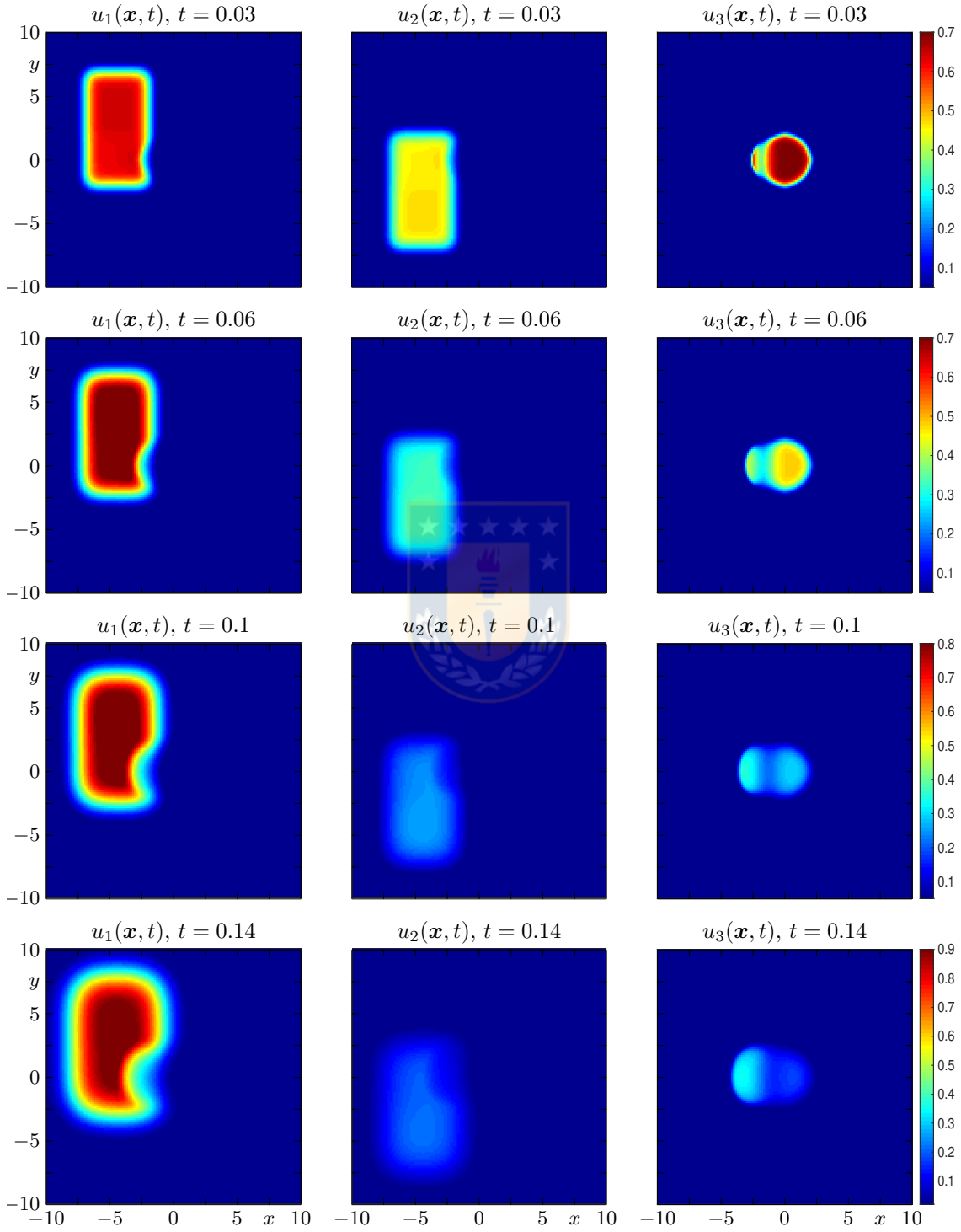

Figure 3.2: Example 1:interaction of the three species at different times $t = 0.03,\ 0.06,\ 0.1$ and 0.14.

For this numerical test, the chemotactic coefficients are $\chi_1 = 5,\ \chi_2 = 5$ and $\chi_3 = 10$. For the initial condition we consider the uniform spatial distribution for the preys and predator (see Figure 3.1).

In Figure 3.2, we display the numerical solution for each species at different simulated times. Initially, at simulated time $t = 0.03$ we can see that the predator begins to chase its preys and its preys feeling the presence of the predator. This characteristic is preserved, the predator continue movement towards regions occupied by the preys.

Conclusions and future works

Conclusions

Here we present a summary with the main contributions and conclusions of the thesis.

In **Chapter** 1, we propose a numerical scheme for a multiclass Lighthill-Whitham-Richards model with a velocity function that is discontinuous in the solution variable. The treatment is motivated and in part based on the numerical scheme proposed by Towers [90]. Recall that this model interests us because it present a phase transitions between free and congested traffic flow regimes. However, in contrast to that approach have assume that the discontinuity is present in the velocity function (not in the flux); this observation makes it possible to construct an alternative scheme based on Scheme 4 of [23]. Furthermore, we have seen that our scheme easily can be extended to the multiclass case. We prove for the scalar case that the numerical approximations convergence to a weak solution and for the multiclass case that the scheme preserves an invariant region. Examples 1 to 3 indicate that the scheme converges to the same weak solution as that of [90], and all numerical examples indicate that our scheme converges in both the scalar and multiclass cases. The present analysis and numerical method can be extended in several directions. Concerning the model itself, at the moment a certain shortcoming is the limitation to the initial-boundary value problem on a fixed road segment. This is due to the particular boundary condition (1.5). It seems desirable to obtain a formulation for a closed road with periodic boundary conditions (a configuration that is commonly studied in traffic modeling to analyze, say, the formation of stop-and-go waves; cf., e.g., [20,26]). However, it is not obvious whether the way the boundary condition is posed allows "gluing together" the ends of the computational domain to create a "seamless" closed circuit. Open issues also include the incorporation of discontinuities in spatial position (akin to the treatment in [24]), and the discussion of the notion of entropicity. In fact, the issue of convergence to an entropy solution is an open problem even in the scalar case for both the scheme advanced in [90] as well as the present approach. Likewise, we recall that for general N the MCLWR model with a Lipschitz continuous function V admits a separable entropy function (see [12, 13]) that can be utilized, for instance, to construct entropy stable schemes [28].

In **Chapter** 2 we proved the existence of a weak solution of a reaction-diffusion system that describes three interacting species with in the Hastings-Powell (HP) food chain structure

with chemotaxis produced by three chemicals. For this purpose, we have used a finite volume (FV) discretization of equations (2.1)–(2.4), then a priori L^2-estimates on the discrete solutions have been established. We have proved, in an appropriate sense, compactness for the discrete solutions and that the limit of discrete solutions constitutes a weak solution. All numerical experiments show that the behavior of species is guided by high concentrations of the chemicals produced by themselves. In particular in Figure 2.7 we can see that each species aggregates in a kind of groups structure which forming zones of different densities. This structure varies with time (which not show here), moreover in Figure 2.8 we can observe that the discrete solution our FV scheme and the solution u_i of ODE problem have the same behavior even when the total variation of each species have a oscillatory behavior and remains bounded along the time, which lends further support to the conjecture that this model (at least with the parameters chosen) exhibits spatial-temporal oscillatory behavior.

In **Chapter** 3 we extend the theoretical background to the model of Chapter 2 in the sense that in this chapter we discuss the existence of a solution from analytical point of view. To this end, we consider a mathematical model for the spatio-temporal evolution of three biological species in a food chain model consisting of two competitive preys and one predator with intra-specific competition. The global boundedness classical solution is proved and after defining appropriate approximate problems we prove the existence of the weak solution.

Future work

The methods developed and the results obtained in this thesis have motivated several ongoing andfuture projects. Some of them are described below:

1. We are interested in exploring whether the notion of entropicity is meaningful for the MCLWR model with a discontinuous velocity function V. That is, to study the convergence to an entropy weak solution

2. It is clear that the numerical method presented in the **Chapter** 1 is formally first-order accurate and can possibly improved by known techniques (e.g., weighted essentially non-oscillatory (WENO) reconstructions in combination with higher-order time integrators).

3. To use the numerical method presented in the **Chapter** 1 to predict the vehicle trajectories. That is, given the traffic density field as $\phi(x,t)$, we can generate a vehicle trajectory starting from any point, by solving

$$\frac{\mathrm{d}x(t)}{\mathrm{d}t} = V(\phi(t,x(t))),$$

where V is the velocity function which is given by

$$V(\phi) = \begin{cases} 1-\phi/\phi_{\max} & \text{for } 0 \leqslant \phi \leqslant \phi^*, \\ -w_{\mathrm{f}}(1-\phi_{\max}/\phi) & \text{for } \phi^* < \phi \leqslant \phi_{\max}. \end{cases}$$

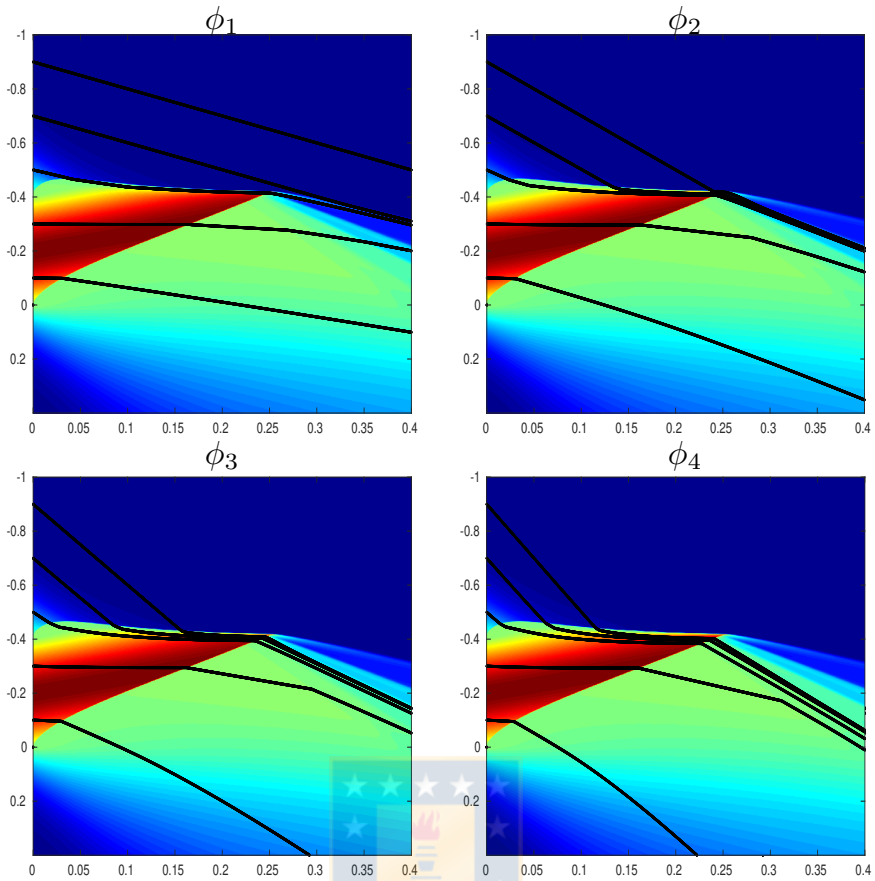

Figure 3.3: Vehicle trajectories at simulation time $t = 0.4$ with $N = 4$.

As a first idea of the vehicle trajectories, in Fig 3.3 we display the vehicle trajectories starting from $x_0 = -0.9 + 0.2(i-1)$ with $i = 1, 2, 3, 4, 5$. This numerical simulation is based in [27, Example 6] (multiclass case ($N = 5$), smooth initial condition), we realize the numerical simulation for $N = 4$ with the following parameters $\phi^* = 0.5$, $w_{\mathrm{f}} = 0.2$, $\phi_{\max} = 1$ the other parameters are the same that in the mentioned example.

4. To extend the results and techniques of **Chapter** 1 to study a multiclass Lighthill-Whitham-Richards (MCLWR) model with discontinuous velocity function, which the velocity function for each classes are not the same. That is, the model is given by the following system of conservation laws in one space dimension, where the sought unknowns are the densities $\phi_i = \phi_i(x,t)$ of vehicles of class i, $i = 1, \ldots, N$, as a function of distance x and time t:

$$\partial_t \phi_i + \partial_x\big(\phi_i v_i(\phi)\big) = 0, \quad i = 1, \ldots, N. \tag{3.66}$$

Where we denote by $\phi = \phi_1 + \cdots + \phi_N$ the total density of vehicles and the velocity function v_i is assumed to depend on ϕ, where we assume that

$$v_i(\phi) = \begin{cases} V_i^{\max} & 0 \leqslant \phi \leqslant \phi^* \\ -\omega_i \left(1 - \frac{\phi_{\max}}{\phi}\right), & \phi^* \leqslant \phi \leqslant \phi_{\max} \end{cases} \quad i = 1, \ldots, N, \tag{3.67}$$

we asume that

$$-\omega_i \left(1 - \frac{\phi_{\max}}{\phi}\right) \neq V_i^{\max}.$$

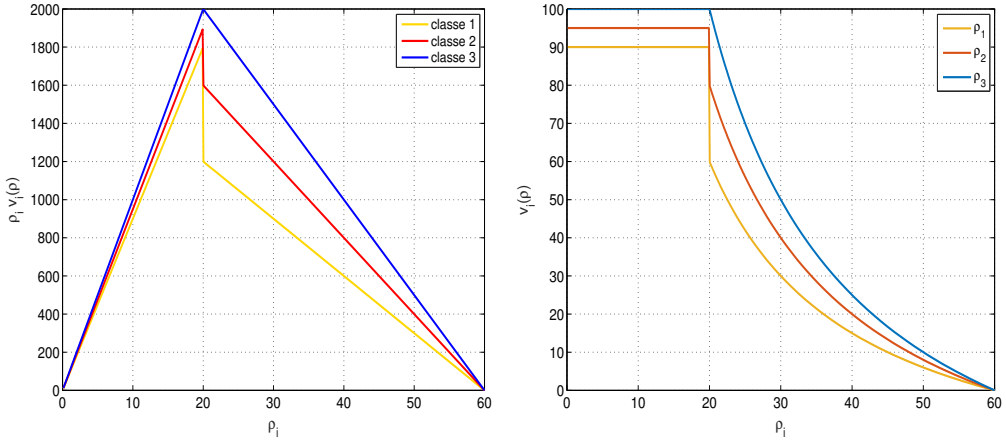

Figure 3.4: (left) discontinuous flux, (Right) discontinuous velocities.

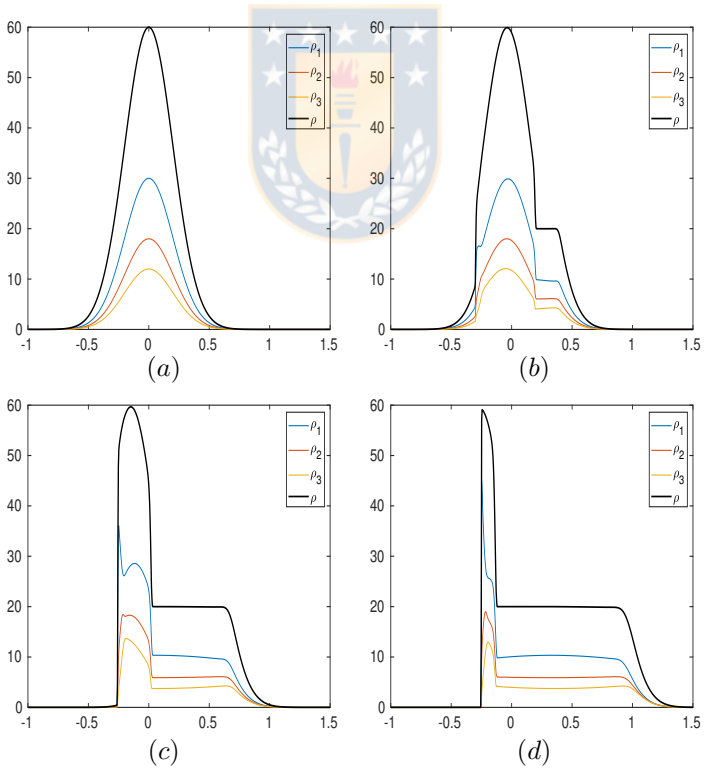

Figure 3.5: Numerical simulation of (3.66) with velocity function v_i given by (3.67) at different time. (a) initial condition $t = 0$. (b) $t = 0.001$. (c) $t = 0.004$. (d) $t = 0.007$. With $\phi^* = 20$, $\phi_{\max} = 60$, $\boldsymbol{\omega} = (30, 40, 50)^T$, $\boldsymbol{V}^{\max} = (90, 95, 100)^T$.

5. To finish the numerical example of **Chapter** 3.

6. we are interested in studying some kind of pattern formation mechanism for the models presented in **Chapter** 2 y 3, but the main difficulty is that we have a three parabolic equations and three elliptic the equations this leads to consider in the first instance a characteristic polynomial of degree three which makes that the calculus is very complicated.

Bibliography

[1] R. A. Adams and J. F. Fournier, *Sobolev Spaces*, Elsevier, 2003.

[2] N. Ali and S. Chakravarty, *Stability analysis of a food chain model consisting of two competitive preys and one predator*, Nonli Dyna, 82 (2015), pp. 1303–1316.

[3] R. Alonso, P. Amorim, and T. Goudon, *Analysis of a chemotaxis system modeling ant foraging*, Math. Models Methods Appl. Sci, 26 (2016), pp. 1785–1824.

[4] P. Amorim, B. Telch, and L. M. Villada, *A reaction-diffusion predator-prey model with pursuit, evasion, and nonlocal sensing*, Math. Biosci. Eng, 16 (2019), pp. 5114–5145.

[5] V. Anaya, M. Bendahmane, and M. Sepúlveda, *Numerical analysis for a three interacting species model with nonlocal and cross diffusion*, Math. Model. Numer. Anal, 49 (2015), pp. 171–192.

[6] B. Andreianov, M. Bendahmane, and R. Ruiz-Baier, *Analysis of a finite volume method for a cross-diffusion model in population dynamics*, Math. Model. Meth. Appl. Sci, 21 (2011), pp. 307–344.

[7] X. Bai and M. Winkler, *Equilibration in a fully parabolic two-species chemotaxis system with competitive kinetics*, Indiana University Math. J., (2016), pp. 553–583.

[8] J. Bascompte and R. V. Solé, *Modeling Spatiotemporal Dynamics in Ecology*, Springer-Verlag, 1998.

[9] N. Bellomo, A. Bellouquid, J. J.Ñieto, and J. Soler, *Multiscale biological tissue models and flux-limited chemotaxis for multicellular growing systems*, Math. Models Methods Appl. Sci, 20 (2010), pp. 1179–1207.

[10] N. Bellomo, A. Bellouquid, Y. Tao, and M. Winkler, *Toward a mathematical theory of Keller–Segel models of pattern formation in biological tissues*, Math. Models Methods Appl. Sci., 25 (2015), pp. 1663–1763.

[11] M. Bendahmane, Z. Khalil, and M. Saad, *Convergence of a finite volume scheme for gas–water flow in a multi-dimensional porous medium*, Math. Models. Methods Appl. Sci, 24 (2014), pp. 145–185.

[12] S. Benzoni-Gavage and R. M. Colombo, *An n-populations model for traffic flow*, Eur. J. Appl. Math, 13 (2003), pp. 587–612.

[13] S. Benzoni-Gavage, R. M. Colombo, and P. Gwiazda, *Measure valued solutions to conservation laws motivated by traffic modelling*, Proc. Royal Soc. A, 462 (2006), pp. 1791–1803.

[14] M. Bessemoulin-Chatard and A. Jüngel, *A finite volume scheme for a Keller-Segel model with additional cross-diffusion*, IMA J. Numer. Anal, 34 (2013), pp. 96–122.

[15] W. Bo, H. Jin, D. Kim, X. Liu, H. Lee, N. Pestieau, Y. Yu, J. Glimm, and J. W. Grove, *Compressible multi species multiphase flow models*, Phys. Rev. E, (2007).

[16] H. Brézis, *Functional Analysis, Sobolev Spaces and Partial Differential Equations*, Springer, 2011.

[17] H. Brézis and W. A. Strauss, *Semi-linear second-order elliptic equations in l1*, J. Math. Soc. Japan, 25 (1973), pp. 565–590.

[18] M. Bulíček, P. Gwiazda, J. Málek, and A. Świerczewska–Gwiazda, *On scalar hyperbolic conservation laws with a discontinuous flux*, Math. Models Meth. Appl. Sci, 21 (2011), pp. 89–113.

[19] M. Bulíček, P. Gwiazda, and A. Świerczewska–Gwiazda, *Multi-dimensional scalar conservation laws with fluxes discontinuous in the unknown and the spatial variable*, Math. Models Methods Appl. Sci, 23 (2013), pp. 407–439.

[20] R. Bürger, C. Chalons, and L. M. Villada, *Anti-diffusive and random-sampling lagrangian-remap schemes for the multi-class Lighthill-Whitham-Richards traffic model*, SIAM J. Sci. Comput, 35 (2013), pp. B1341–B1368.

[21] R. Bürger, G. Chowell, E. Gavilán, P. Mulet, and L. M. Villada, *Numerical solution of a spatio-temporal predator-prey model with infected prey*, Math. Biosci. Eng, 16 (2019), pp. 438–473.

[22] R. Bürger, A. García, K. H. Karlsen, and J. D. Towers, *Difference schemes, entropy solutions, and speedup impulse for an inhomogeneous kinematic traffic flow model*, Netw. Heterog. Media, 3 (2008), pp. 1–41.

[23] ——, *A family of numerical schemes for kinematic flows with discontinuous flux*, J. Eng. Math, 60 (2008), pp. 387–425.

[24] R. Bürger, K. Karlsen, and J. Towers, *On some difference schemes and entropy conditions for a class of multi-species kinematic flow models with discontinuous flux*, Netw. Heterog. Media, 5 (2010), pp. 461–485.

[25] R. Bürger, K. H. Karlsen, H. Torres, and J. D. Towers, *Second-order schemes for conservation laws with discontinuous flux modelling clarifier-thickener units*, Numer. Math, 116 (2010), pp. 579–617.

[26] R. Bürger, P. Mulet, and L. M. Villada, *A diffusively corrected multiclass Lighthill-Whitham-Richards traffic model with anticipation lengths and reaction times*, Adv. Appl. Math. Mech, 5 (2013), pp. 728–758.

[27] R. Bürger, R. Ordoñez, M. Sepulveda, and L. Villada, *Numerical analysis of a three-species chemotaxis model*, Comput. Math. Appl, 80 (2020), pp. 183–203.

[28] R. Bürger, H. Torres, and C. A. Vega, *An entropy stable scheme for the multiclass Lighthill-Whitham-Richards traffic model*, Adv. Appl. Math. Mech, 11 (2019), pp. 1022–1047.

[29] L. Cagnolo, G. Valladares, S. Adriana, M. Cabido, and M. Zak, *Habitat fragmentation and species loss across three interacting trophic levels: effects of life-history and food-web traits*, Conservation Biology, 23 (2009), pp. 1167–1175.

[30] C. Cancès, M. Ibrahim, and M. Saad, *Positive nonlinear CVFE scheme for degenerate anisotropic Keller-Segel system*, SMAI J. Comput. Math, 3 (2017), pp. 1–28.

[31] J. Carrillo, *Conservation law with discontinuous flux function and boundary condition*, J. Evol. Equ, 3 (2003), pp. 283–301.

[32] C. Chalons and P. Goatin, *Godunov scheme and sampling technique for computing phase transitions in traffic flow modeling*, Interf. Free Bound, 10 (2008), pp. 197–221.

[33] G. Chamoun, M. Saad, and R. Talhouk, *Monotone combined edge finite volume-finite element scheme for anisotropic keller-segel model*, Numer. Meth. Part. Diff. Equat, 30 (2014), pp. 1030–1065.

[34] W. Chen and J. D. Olden, *Evaluating transferability of flow–ecology relationships across space, time and taxonomy*, Freshwater Biology, 63 (2018), pp. 817–830.

[35] P. G. Ciarlet, *Linear and Nonlinear Functional Analysis with Applications*, SIAM, 2013.

[36] R. M. Colombo, *Hyperbolic phase transitions in traffic flow*, SIAM J. Appl. Math, 63 (2002), pp. 708–721.

[37] E. Cruz, M. Negreanu, and J. Tello, *Asymptotic behavior and global existence of solutions to a two-species chemotaxis system with two chemicals*, Z. Angew. Math. Phys, 69 (2018), p. 107.

[38] C. C. D'Aloia, R. M. Daigle, I. M. Côté, J. M. Curtis, F. Guichard, and M. J. Fortin, *A multiple-species framework for integrating movement processes across life stages into the design of marine protected areas*, Biological Conservation, 216 (2017), pp. 93–100.

[39] J. P. Dias and M. Figueira, *On the Riemann problem for some discontinuous systems of conservation laws describing phase transitions*, Commun. Pure Appl. Anal, 3 (2004), pp. 53–58.

[40] ——, *On the approximation of the solutions of the Riemann problem for a discontinuous conservation law*, Bull. Braz. Math. Soc. New Ser, 36 (2015), pp. 115–125.

[41] J. P. Dias, M. Figueira, and J. F. Rodrigues, *Solutions to a scalar discontinuous conservation law in a limit case of phase transitions*, J. Math. Fluid Mech, 7 (2005), pp. 153–163.

[42] S. Diehl, *A conservation law with point source and discontinuous flux function*, SIAM J. Math. Anal, 56 (1996), pp. 388–419.

[43] R. Donat and P. Mulet, *Characteristic-based schemes for multi-class Lighthill-Whitham-Richards traffic models*, J. Sci. Comput, 37 (2008), pp. 233–250.

[44] ——, *A secular equation for the Jacobian matrix of certain multi-species kinematic flow models*, Numer. Meth. Part. Diff. Equat, 26 (2010), pp. 159–175.

[45] R. Eymard, T. Gallouët, and R. Herbin, *Finite Volume Methods, Handbook of Numerical Analysis vol. VII*, North-Holland, 2000.

[46] ——, *Discretisation of heterogeneous and anisotropic diffusion problems on general non-conforming meshes. sushi: A scheme using stabilization and hybrid interfaces*, IMA J. Numer. Anal, 30 (2010), pp. 1009–1043.

[47] T. Gimse, *Conservation laws with discontinuous flux functions*, SIAM J. Numer. Anal, 24 (1993), pp. 279–289.

[48] T. Gimse and N. H. Risebro, *Solution to the Cauchy problem for a conservation law with a discontinuous flux function*, SIAM J. Math. Anal, 23 (1992), pp. 635–648.

[49] D. N. Grigoryev, S. F. Ma, R. A. Irizarry, S. Q. Ye, J. Quackenbush, and J. G. Garcia, *Orthologous gene-expression profiling in multi-species models: search for candidate genes*, Genome Biology, 5 (2004), p. R34.

[50] P. Grisvard, *Elliptic problems in nonsmooth domains*, SIAM, 2011.

[51] M. Hassell, *The Dynamics of Arthopod Predator-Prey Systems*, Princeton University Press, 2020.

[52] A. Hastings and T. Powell, *Chaos in a three-species food chain*, Ecology, 72 (1991), pp. 896–903.

[53] D. Henry, *Geometric theory of semilinear parabolic equations*, vol. 840, Springer, 2006.

[54] H. Holden and N. H. Risebro, *Front Tracking for Hyperbolic Conservation Laws*, Springer, 2015.

[55] D. Horstmann and M. Winkler, *Boundedness vs. blow-up in a chemotaxis system*, J. Diff. Equat, 215 (2005), pp. 52–107.

[56] S. A. Hosseini, N. Darabiha, and D. Thévenin, *Mass-conserving advection–diffusion lattice boltzmann model for multi-species reacting flows*, Physica A: Stat. Mech. Appl, 499 (2018), pp. 40–57.

[57] C. Izzo, Z. A. Doubleday, G. L. Grammer, T. C. Barnes, S. Delean, G. J. Ferguson, Q. Ye, and B. M. Gillanders, *Multi-species response to rapid environmental change in a large estuary system: A biochronological approach*, Eco. Indi, 69 (2016), pp. 739–748.

[58] Y. Kim, J. Son, Y. S. Lee, M. Lee, J. Hong, and K. Cho, *Integration of an individual-oriented model into a system dynamics model: An application to a multi-species system*, Envi. Modelling & Software, 112 (2019), pp. 23–35.

[59] G. N. S. Kumar and N. K. Maheshwari, *Viscous multi-species lattice boltzmann solver for simulating shock-wave structure*, Computers & Fluids, (2020), p. 104539.

[60] O. Ladyzhenskaia, V. Solonnikov, and N. Ural'tseva, *Linear and quasi-linear equations of parabolic type*, vol. 23, American Mathematical Soc., 1968.

[61] M. J. Lighthill and G. B. Whitham, *On kinematic waves: II. a theory of traffic flow on long crowded roads*, Proc. Royal Soc. A, 229 (1955), pp. 317–345.

[62] K. Lin, C. Mu, and H. Zhong, *A new approach toward stabilization in a two-species chemotaxis model with logistic source*, Comput. Math. Appl, 75 (2018), pp. 837–849.

[63] J. L. Lions, *Quelques Méthodes de Résolution des Problèmes Aux Limites Non Linéaires*, Dunod, 1969.

[64] Y. Lu, S. Wong, M. Zhang, and C.-W. Shu, *The entropy solutions for the Lighthill-Whitham-Richards traffic flow model with a discontinuous flow-density relationship*, Transp. Sci, 43 (2009), pp. 511–530.

[65] S. Lv and M. Zhao, *The dynamic complexity of a three species food chain model*, Chaos Solit. Fractals, 37 (2008), pp. 1469–1480.

[66] P. K. Maini, D. S. McElwain, and D. I. Leavesley, *Traveling wave model to interpret a wound-healing cell migration assay for human peritoneal mesothelial cells*, Tissue Eng, 10 (2004), pp. 475–482.

[67] R. R. Marrotte, J. Bowman, M. G. Brown, C. Cordes, K. Morris, M. B. Prentice, and P. J. Wilson, *Multi-species genetic connectivity in a terrestrial habitat network*, Movement Ecology, 5 (2017), p. 21.

[68] S. Martin and J. Vovelle, *Convergence of the finite volume method for scalar conservation law with discontinuous flux function*, ESAIM: Math. Model. Numer. Anal, 42 (2008), pp. 699–727.

[69] E. Masi, J. Bellan, K. G. Harstad, and N. A. Okong'o, *Multi-species turbulent mixing under supercritical-pressure conditions: modelling, direct numerical simulation and analysis revealing species spinodal decomposition*, Journal of Fluid Mechanics, 721 (2013), pp. 578–626.

[70] R. M. May, *Stability and complexity in model ecosystems*, Princeton University Press, 1973.

[71] W. W. Murdoch and A. Oaten, *Predation and population stability*, Adv. Eco. Res, 9 (1975), pp. 1–131.

[72] J. D. Murray, *Mathematical Biology: I. An Introduction*, Springer, 2002.

[73] D. Neal, *Introduction to Population Biology*, Cambridge University Press, 2018.

[74] M. Negreanu and J. I. Tello, *Global existence and asymptotic behavior of solutions to a predator-prey chemotaxis system with two chemicals*, J. Math. Anal. Appl, 474 (2019), pp. 1116–1131.

[75] L. R. Nie and D. C. Mei, *Noise and time delay: suppressed population explosion of the mutualism system*, Europhysics Lett, 79 (2007), p. 20005.

[76] B. Perthame, *Transport Equations in Biology*, Springer Science & Business Media, 2006.

[77] G. J. Pettet, D. L. S. McElwain, and J. Norbury, *Lotka-Volterra equations with chemotaxis: walls, barriers and travelling waves*, Math. Med. Biol, 17 (2000), pp. 395–413.

[78] A. V. Praseeja and N. Sajikumar, *A review on the study of immiscible fluid flow in unsaturated porous media: Modeling and remediation*, J. Porous Media, 22 (2019).

[79] P. Quittner and P. Souplet, *Superlinear Parabolic Problems: Blow-up, Global Existence and Steady States*, Springer, 2019.

[80] P. I. Richards, *Shock waves on the highway*, Oper. Res, 4 (1956), pp. 42–51.

[81] M. L. Rosenzweig, *Exploitation in three trophic levels*, Am. Nat, 107 (1973), pp. 275–294.

[82] P. Sivasankar and G. S. Kumar, *Modelling the influence of interaction between injection and formation brine salinities on in-situ microbial enhanced oil recovery processes by coupling of multiple-ion exchange transport model with multiphase fluid flow and multi-species reactive transport models*, J. Petrol. Sci. and Eng, 163 (2018), pp. 435–452.

[83] S. Soleimanikutanaei, C. X. Lin, and D. Wang, *Modeling and simulation of cross-flow transport membrane condenser heat exchangers*, Int. Commun. Heat and Mass Trans, 95 (2018), pp. 92–97.

[84] ——, *Numerical modeling and analysis of transport membrane condensers for waste heat and water recovery from flue gas*, Int. J. Thermal Sci, 136 (2019), pp. 96–106.

[85] C. Stinner, J. I. Tello, and M. Winkler, *Competitive exclusion in a two-species chemotaxis model*, J. Math. Biol, 68 (2014), pp. 1607–1626.

[86] J. I. Tello and M. Winkler, *A chemotaxis system with logistic source*, Commun. Part. Diff. Equat, 32 (2007), pp. 849–877.

[87] J. I. Tello and M. Winkler, *Stabilization in a two-species chemotaxis system with a logistic source*, Nonlinearity, 25 (2012), pp. 1413–1425.

[88] R. Temam, *Navier-Stokes Equations. Theory and Numerical Analysis*. Studies in Mathematics and Its Applications, Amsterdam: North-Holland, 1997.

[89] O. Teşileanu, A. Mignone, and S. Massaglia, *Simulating radiative astrophysical flows with the PLUTO code: a non-equilibrium, multi-species cooling function*, Astronomy & Astrophysics, 488 (2008), pp. 429–440.

[90] J. D. Towers, *A splitting algorithm for LWR traffic models with flux discontinuities in the unknown*, J. Comput. Phys, 421 (2020), p. 109722 (30pp).

[91] S. D. Tuljapurkar and J. S. Semura, *Stability of lotka-volterra systems*, Nature, 257 (1975), pp. 388–389.

[92] M. Turelli, *Does environmental variability limit niche overlap?*, Proc. Nat. Acad. Sci, 75 (1978), pp. 5085–5089.

[93] J. Wang and X. Guo, *Dynamics and pattern formation in a three-species predator-prey model with two prey-taxis*, J. Math. Anal. Appl, 475 (2019), pp. 1054–1072.

[94] J. K. Wiens, J. M. Stockie, and J. F. Williams, *Riemann solver for a kinematic wave traffic model with discontinuous flux*, J. Comput. Phys, 242 (2013), pp. 1–23.

[95] M. Winkler, *Aggregation vs. global diffusive behavior in the higher-dimensional Keller–Segel model*, J. Diff. Equat, 248 (2010), pp. 2889–2905.

[96] G. C. K. Wong and S. C. Wong, *A multi-class traffic flow model—an extension of LWR model with heterogeneous drivers*, Transp. Res. A, 36 (2002), pp. 827–841.

[97] C. Xu, P. Li, and Y. Shao, *Existence and global attractivity of positive periodic solutions for a Holling II two-prey one-predator system*, Adv. Diff. Equat, 2012 (2012), p. 84.

[98] Y. Yang and G. Park, *Analysis of catalytic heat transfer for a multi-species gas mixture*, Int. J. Heat and Mass Trans, 137 (2019), pp. 1088–1102.

[99] S. Yi-Jian and M. Dong-Cheng, *Effects of time delay on three interacting species system with noise*, Int. J. Theor. Phys, 47 (2008), pp. 2409–2414.

[100] M. Zhang, C. W. Shu, G. C. K. Wong, and S. C. Wong, *A weighted essentially non-oscillatory numerical scheme for a multi-class Lighthill-Whitham-Richards traffic flow model*, J. Comput. Phys, 191 (2003), pp. 639–659.

[101] P. Zhang, R. X. Liu, S. C. Wong, and S. Q. Dai, *Hyperbolicity and kinematic waves of a class of multi-population partial differential equations*, Eur. J. Appl. Math, 17 (2006), pp. 171–200.

[102] P. Zhang, S. C. Wong, and S. Q. Dai, *A note on the weighted essentially non-oscillatory numerical scheme for a multi-class Lighthill-Whitham-Richards traffic flow model*, Commun. Numer. Meth. Eng, 25 (2009), pp. 1120–1126.

[103] P. Zhang, S. C. Wong, and C. W. Shu, *A weighted essentially non-oscillatory numerical scheme for a multi-class traffic flow model on an inhomogeneous highway*, J. Comput. Phys, 212 (2006), pp. 739–756.

[104] P. Zhang, S. C. Wong, and Z. Xu, *A hybrid scheme for solving a multi-class traffic flow model with complex wave breaking*, Comput. Meth. Appl. Mech. Eng, 197 (2008), pp. 3816–3827.

[105] S. Zheng, J. Hwang, R. Manchanda, and M. M. Sharma, *An integrated model for non-isothermal multi-phase flow, geomechanics and fracture propagation*, J. Petrol. Sci. Eng, 196 (2020), p. 107716.